Determinants for the subcellular localization of the inner and outer spore coat hubs in *Bacillus subtilis*

Filipa Nunes

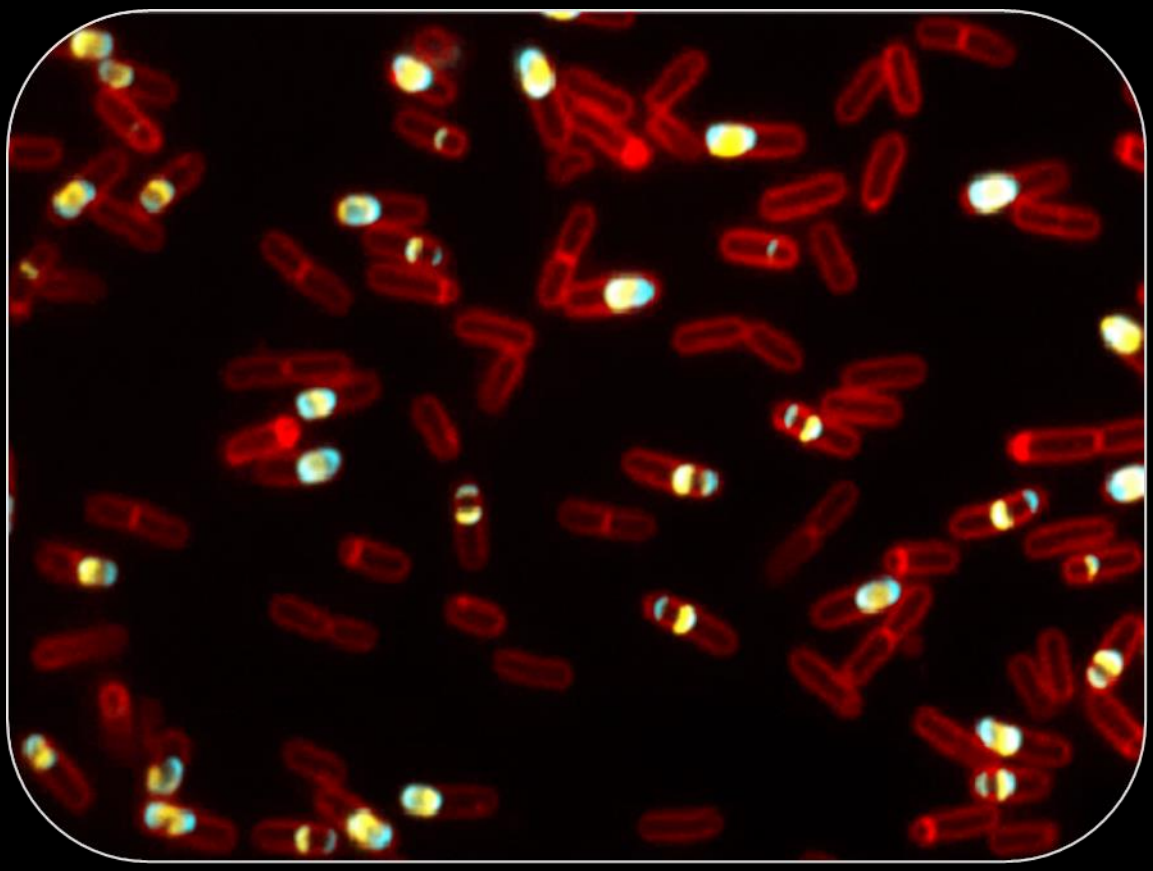

Dissertation presented to obtain the Ph.D degree in Biology

Instituto de Tecnologia Química e Biológica António Xavier | Universidade Nova de Lisboa

Oeiras,
June, 2015

INSTITUTO
DE TECNOLOGIA
QUÍMICA E BIOLÓGICA
ANTÓNIO XAVIER /UNL

Knowledge Creation

Determinants for the subcellular localization of the inner and outer spore coat hubs in *Bacillus subtilis*

Filipa Nunes

Dissertation presented to obtain the Ph.D degree in Biology

Instituto de Tecnologia Química e Biológica António Xavier | Universidade Nova de Lisboa

Oeiras, June, 2015

INSTITUTO
DE TECNOLOGIA
QUÍMICA E BIOLÓGICA
ANTÓNIO XAVIER /UNL

Knowledge Creation

Financial support from *Fundação para a Ciência e a Tecnologia* and *Fundação Luso-Americana para o Desenvolvimento* through grants SFRH/BD/64470/2009 and 2014/CON3/CAN34 awarded to Filipa Nunes

From left to right: Prof. Dr. Adriano O. Henriques (supervisor), Dr. Mónica Serrano (co-supervisor), Dr. Federico Herrera and Prof. Dr. Carlos São-José (examiners), Filipa Nunes (PhD candidate), Prof. Dr. Isabel Sá-Nogueira and Dr. José Pereira-Leal (examiners), and Prof. Dr. Miguel Teixeira (president of the jury).

This thesis is dedicated to my parents,
who taught me the importance of education
and always encouraged me to pursue my dreams

ACKNOWLEDGMENTS

To Instituto de Tecnologia Química e Biológica António Xavier (**ITQB-AX**) of the Universidade Nova de Lisboa, for receiving me as a PhD student and for providing all the working conditions and the great scientific environment for the execution of this work.

To Fundação para a Ciência e a Tecnologia (**FCT**) for awarding me with a PhD fellowship. To Fundação Luso-Americana para o Desenvolvimento (**FLAD**), whose financial support allowed me to perform part of my work at Prof. Eichenberger's lab.

To my supervisor **Prof. Adriano O. Henriques** and my co-supervisor **Dr. Mónica Serrano**, without whom this work would have never been possible. For the opportunity to work with them, for all the knowledge they shared with me, and for the guidance and encouragement along this journey, specially is those moments in which the results were not the expected.

To my present and former **lab colleagues**, for creating a good atmosphere in the lab and for the great times out of it. To **Catarina Fernandes** and **Fátima Pereira**, for the direct contributions to this work and the helpful suggestions. To **Anabela Isidro** and **Lia Domingues**, that started the studies on the LysM domain of SafA and on the cysteine residues of SpoVID. To **Ana Paiva**, **Ana Rita Tomé**, **Cláudia Serra**, **Fátima Pereira**, **Patrícia Amaral** and **Teresa Costa**, who more than lab colleagues, are my friends. Thank you for your constant willingness to help, useful suggestions, scientific and non-scientific discussions, and specially, for your support during good and bad moments. To **Teresa Silva**, who made my life so much easier in the lab.

To **Prof. Patrick Eichenberger**, for welcoming me in his lab, for the excellent working conditions, and for making me feel as part of the team.

Thank you for your constant interest in this work and helpful contributions, and for the opportunity to give a talk at NYBIG. To all the members of his lab, specially **Tim Chu**, **Bentley Shuster** and **Giana D'Aleo**, for all the support in the lab and for showing me a little bit of the New York culture. To **Marina Raguse**, for her friendship and for those wonderful weeks in the lab and exploring New York City.

To **Prof. Aida Duarte**, my former supervisor, who introduced me into the scientific research world. Thank you for sharing with me your passion for science, and for all the teaching and support during my first years in a lab.

To my colleagues of the **ITQB PhD Program** and the **InTeraQB**, for the good times at ITQB and out of it. To **Leiria Toastmasters** and **Young Entrepreneur Toastmasters** Clubs, for giving me confidence to speak in public.

To my dear friends outside the lab that helped me so much along this journey. A special thank to **Catarina Dourado**, **Rita Aires**, **Isabel Guerreiro**, **Dina Marques**, **Célia Rodrigues**, **Marta Pizzighella**, **Manuela Gomes**, **Igor Murta**, **Sara Focaccia** and **Marija Vranic** for their support and friendship.

To my dear **family**, for all the love and care during all these years. To my parents, **David** and **Lina Leitão**, and to my brother, **Diogo Nunes**, for your unconditional love, advice and support. You will always be an inspiration to me, and without you by my side I would never had the strength to complete this PhD. Finally, to **Fabio Silva**, for your love, help and constant support. Thank you for pushing me not to give up on my dreams, and for remembering me that after all, life is to be enjoyed.

TABLE OF CONTENTS

LIST OF ABBREVIATIONS

DSM: Difco sporulation medium

DTT: dithiothreitol

EDTA: ethylenediamine tetraacetic acid

g: gram

GlcNAc: N-Acetylglucosamine

H: hour

IPTG: isopropyl β-D-1-thiogalactopyranoside

L: liter

LB media: Luria-Bertani medium

M: molar

MALDI-TOF: matrix assisted laser desorption ionization – time of flight

MCD pole: mother cell distal pole

MCP pole: mother cell proximal pole

MS: mass spectrometry

MurNAc: N-Acetylmuramic acid

PBS(-T): phosphate buffered saline(-tween)

PMSF: phenylmethanesulfonylfluoride

PVDF: polyvinylidene difluoride

SDS: sodium dodecyl sulfate

SDS-PAGE: sodium dodecyl sulfate polyacrylamide gel electrophoresis

SM: sporulation medium

TBS-T: tris-buffered saline- tween

TSDS-PAGE: tricine-sodium dodecyl sulfate polyacrylamide gel electrophoresis

ABSTRACT

Endospores, or spores for simplicity, are a highly resistant cell type produced by some bacterial species under adverse conditions. Two main protective layers contribute to the resilience of spores: the cortex, composed of peptidoglycan, and the outermost proteinaceous coat. In *Bacillus subtilis*, the coat comprises up to 80 different proteins, organized into four sublayers: the basement layer, the inner coat, the outer coat and the crust. These proteins are synthesized at different times during sporulation and deposited at the spore surface in multiple coordinated waves. Central to coat formation is a group of morphogenetic proteins that guide the assembly of the coat components. Targeting of the coat proteins to the surface of the developing spore is mainly controlled by the SpoIVA morphogenetic ATPase. In a second stage, the coat proteins fully encircle the spore, a process termed encasement that requires the morphogenetic protein SpoVID. Assembly of the inner coat requires SafA, whereas formation of the outer coat and the crust requires CotE. SafA interacts directly with the N terminus of SpoVID.

In Chapter 2, we started by demonstrating that a stretch of 12 residues at the N-terminal domain of SpoVID, that we named region E, is required for spore encasement by all the coat sublayers. We identified specific residues within this region that are important for binding and encasement by CotE, linking encasement by the outer coat to a specific protein-protein interaction. Encasement is presumably facilitated by the oligomerization of SpoVID at the spore surface, and we showed that SpoVID oligomers contain disulfide bonds. Finally, we addressed some structural features of SpoVID, and we proposed an updated model for coat assembly that incorporates the interactions between the major coat morphogenetic proteins.

In Chapter 3, we focus on the interaction between SpoVID and SafA. We found single amino acid substitutions in region E of SpoVID that cause

mislocalization of SafA and prevent its binding to SpoVID, showing that encasement by both the inner and the outer coat modules require specific interactions of their hubs (SafA and CotE) with the same region of SpoVID. Our results also suggest that region E facilitates binding of SafA and CotE to a second surface in SpoVID. Furthermore, two residues within region E are required for encasement by both SafA and CotE hubs, and consequently, by inner and outer coat/crust components, having a major role in coat integrity. As the substitution of one of them do not preclude binding of CotE to SpoVID and mislocalization of CotE is suppressed by the deletion of *safA*, we conclude that a mislocalized inner coat acts as an attractor for CotE. This reveals a tight connection between assembly of the inner and the outer coat modules.

In Chapter 4, we analysed the role of the peptidoglycan-binding LysM domain of SafA on the subcellular localization and function of the protein. Within this domain, we identified five conserved, surface-exposed residues that are required for SafA-YFP localization and peptidoglycan recognition *in vitro*. Of those, two are important for earlier SafA-YFP deposition, whereas the other three are involved in late localization, at a time where the cortex is already present in the spore. Late localization of SafA-YFP also requires the cortex, reinforcing that cortex and coat morphogenesis are linked. Finally, we provide evidence that the LysM module of SpoVID does not recognize peptidoglycan in our experimental conditions. Altogether, we propose a model for SafA localization that includes the interactions with SpoIVA and SpoVID (via region A), as well as peptidoglycan recognition (via LysM).

Overall, our work expands the current model for coat assembly, and highlights the role of protein-protein interactions during coat morphogenesis.

RESUMO

Endósporos, ou simplesmente esporos, são um tipo celular extremamente resistente produzido por algumas espécies bacterianas em resposta a condições adversas. Duas camadas protetoras contribuem para a resiliência destas estruturas: o cortex, composto por peptidoglicano, e mais externamente o manto, de natureza proteica. Em *Bacillus subtilis*, o manto é composto por mais de 80 proteínas diferentes, organizadas em quatro subcamadas: a camada basal, o manto interno, o manto externo e a crosta. Estas proteínas são sintetizadas em diferentes etapas da esporulação e depositam-se à superfície do esporo de uma forma coordenada, através de múltiplas ondas. As proteínas morfogenéticas tem um papel central na formação do manto, guiando a deposição dos seus componentes. A localização das proteínas à superfície do esporo em desenvolvimento é essencialmente controlada pela ATPase morfogenética SpoIVA. Numa segunda fase, as proteínas do manto rodeiam completamente o esporo, num processo designado por envolvimento que requer a proteína morfogenética SpoVID. A montagem do manto interno depende de SafA, enquanto que as do manto externo e da crosta necessitam de CotE. SafA interage diretamente com o N-terminal de SpoVID.

No Capítulo 2, começámos por demonstrar que uma região de 12 resíduos no domínio N-terminal de SpoVID, a que chamámos região E, é essencial para o envolvimento do esporo pelas quatro subcamadas do manto. Nesta região, identificámos resíduos específicos importantes para a interação com CotE e para a sua migração em redor do esporo, estabelecendo uma relação entre o envolvimento pelo manto externo a uma interação proteína-proteína específica. Presume-se que o envolvimento seja facilitado pela oligomerização de SpoVID à superfície do esporo, e nós demostrámos que os oligomeros de SpoVID contêm pontes dissulfídicas. Finalmente, determinámos algumas características estruturais de SpoVID e propusemos

um modelo atualizado para a montagem do manto que incorpora as interações entre as proteínas morfogenéticas mais importantes.

No Capítulo 3, focámo-nos na interação entre SpoVID e SafA. Identificámos substituições de aminoácidos na região E de SpoVID que levam à deslocalização de SafA e previnem a sua ligação a SpoVID, demostrando que o envolvimento do esporo pelos mantos interno e externo requer interações específicas das suas proteínas *hub* (SafA e CotE) com a mesma região de SpoVID. Os nossos resultados sugerem ainda que a região E facilita a ligação de SafA e CotE a uma segunda superfície em SpoVID. Além disso, dois dos resíduos da região E são importantes para o envolvimento do esporo tanto por SafA como por CotE, e consequentemente, pelos componentes dos mantos interno e externo e da crosta, tendo um papel determinante na integridade do manto. Tendo em conta que a substituição de um desses resíduos não compromete a ligação de CotE a SpoVID e que a deslocalização de CotE é suprimida pela deleção de *safA*, concluímos que a deslocalização do manto interno leva à deslocalização de CotE. Assim, concluímos que existe uma estreita ligação entre a montagem destas subcamadas do manto.

No Capítulo 4, analisámos o papel do domínio de ligação a peptidoglicano de SafA, LysM, na localização e função desta proteína. Identificámos cinco resíduos conservados expostos à superfície do domínio que são importantes para a localização de SafA-YFP e para o reconhecimento de peptidoglicano *in vitro*. Destes, dois são necessários para a deposição inicial de SafA-YFP, enquanto os outros três estão envolvidos na sua localização tardia, quando o cortex já está presente no esporo. A localização tardia de SafA-YFP também requer a presença do cortex, reforçando que as morfogéneses do cortex e do manto estão intimamente ligadas. Finalmente, mostrámos que o domínio LysM de SpoVID não reconhece peptidoglicano nas nossas condições experimentais. Deste modo, propusemos um modelo para a localização de SafA que inclui as interações com SpoIVA e SpoVID (*via*

região A), assim como o reconhecimento do peptidoglicano presente no esporo (*via* LysM).

Em suma, o nosso trabalho aprofunda o modelo atual da morfogénese do manto, enfatizando a importância das interações proteína-proteína durante o processo.

Chapter 1

General introduction

THE MODEL ORGANISM *BACILLUS SUBTILIS*

Bacillus subtilis is a Gram-positive, rod-shaped bacterium that is both a soil organism and a gut commensal of several animals, including humans (Nicholson, 2002; Tam *et al.*, 2006; Hong *et al.*, 2009). This facultative aerobe (Hoffmann *et al.*, 1995; Nakano and Zuber, 1998) is able to differentiate highly resistant dormant cells named endospores, or spores for simplicity, that contribute for its persistence under unfavorable conditions. *B. subtilis* is an important model for studies of cell differentiation and one of the best-characterized organisms. The main advantages of its use are the natural competence, easy manipulation and maintenance, high growth rates and non-pathogenicity, as well as the availability of its whole genome for almost 20 years (Kunst *et al.*, 1997). These features, together with the spore properties and the capacity to secrete high concentrations of several products directly into the culture medium, makes *B. subtilis* well suited for applications in industry, biotechnology and biomedicine (see below in "*Applications of spores*").

Spore-forming bacteria are diverse and ubiquitous. They include several *Bacillus* and *Clostridium* species that form spores through an evolutionary conserved mechanism, such as the pathogens *B. cereus*, *B. anthracis* and *C. difficile* (de Hoon *et al.*, 2010; Galperin *et al.*, 2012; Abecasis *et al.*, 2013). Sporeformers have been isolated, for example, from fresh and saline water, hot springs, arctic sediments, gastro-intestinal tracts of mammals and insects and soil (Nazina *et al.*, 2004; Yukimura *et al.*, 2009; Maughan and Van der Auwera, 2011), Their capacity to colonize such a diversity of ecological niches is in part due to the resilience of their spores.

The discovery of *B. subtilis* and of bacterial spores

Although infections by sporeformers were reported in ancient literature thousands of years ago (Torred *et al.*, 2012), the first known descriptions of spores are only dated from the 19th century. In 1852, Maximilian Perty observed light-refractile bodies in bacteria. Almost 20 years later (1870), Luis Pasteur confirmed these observations and correlated the presence of spores to a greater resistance to injurious agents (as cited in Morrison and Rettger, 1930). At that time, Henry Charlton Bastian showed that some bacteria could regrow in organic fluids after boiling them in sealed flasks (Bastian, 1872; in Torred *et al.*, 2012), and Ferdinand Cohn proposed that it may be due to a special developmental stage of some bacteria that survive high temperatures (as cited in Torred *et al.*, 2012). Cohn found that the bacteria growing in boiled cheese infusions was not the typical putrefactive *Bacterium termo*, but rather bacillus rods he renamed *Bacillus subtilis* (Cohn, 1872; in Torred *et al.*, 2012). This organism was described 40 years earlier and baptized *Vibrio subtilis* (Ehrenberg, 1833–1835; in Rasmussen *et al*., 2009). Cohn also observed the formation of spores in *B. subtilis* and proved that they survive strong heat and germinate to form new bacilli, justifying the microbial growth in boiled organics infusions (Cohn, 1876; in Torred *et al.*, 2012 and Rasmussen *et al.*, 2009). In the same year, Koch relied on Cohn's observations in his work on *B. anthracis* (Koch, 1876; in Torred *et al.*, 2012). Their independent experiments marked the beginning of the field of spore research.

THE SPORE

Spores are a highly resistant dormant cell-type produced via a differentiation process known as sporulation. They are one of the most resilient living structures, remaining viable under a wide variety of physical

stresses that kill other cells. These include extreme heat, freeze, high pressure, ionizing radiation, noxious chemicals — oxidizing agents, acids, bases and organic solvents — exogenous lytic enzymes and digestion by predators (Nicholson *et al.*, 2000; Nicholson *et al.*, 2002; Klobutcher *et al.*, 2006; Setlow, 2006).

In laboratory cultures, most of the strains initiate sporulation in response to adverse conditions. First, the bacterial cell divides asymmetrically and the larger compartment, named mother cell, encases the smaller one. Then, the smaller compartment differentiates into a mature spore, assisted by the mother cell. Finally, the mother cell lyses and the mature spore is released into the environment (Errington, 2003), where it can persist for long periods of time, perhaps even for millions of years (Nicholson *et al.*, 2000; Vreeland *et al.*, 2000).

Morphology and properties of the spore

Spores exhibit a conserved concentric, multilayered architecture that largely contributes to their resistance (de Hoon *et al.*, 2010). In those produced by *B. subtilis*, thin-section transmission electron microscopy revealed three main concentric compartments: the core, the cortex and the coat (Fig. 1.1). Species such as *B. cereus* and *B. anthracis* also have an additional outer layer, named exosporium (Driks, 1999; Henriques and Moran, 2007).

The core is the innermost compartment of the spore, and houses the chromosome. It has a reduced water content, which is important for spore dormancy and resistance to wet heat. The presence of dipicolinic acid, presumably chelated with divalent cations (predominantly Ca^{2+}), contributes to dehydration, protection of the DNA and spore resistance. This compartment also contains small acid-soluble proteins of the α/β-type that saturate the DNA, protecting it from a wide range of damaging agents, such as dry heat, desiccation, chemicals and radiation (Gerhardt and Marquis,

1989; Setlow, 2006). The core is delimitated by the inner forespore membrane, with similar composition to the plasma membrane. This membrane is a strong permeability barrier to noxious chemicals and contributes for the reduced water content in the core. Additionally, it becomes the membrane of the new vegetative cell that results from spore germination (Nicholson *et al.*, 2000; Cortezzo *et al.*, 2004; Setlow, 2006).

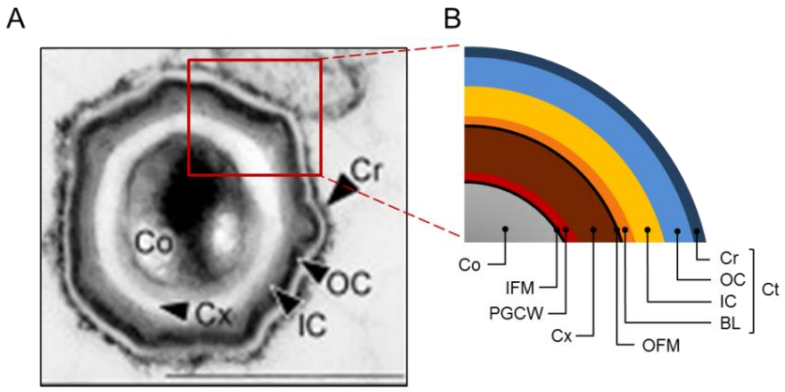

Figure 1.1 – Structure of the *B. subtilis* spore. **A)** Thin-section transmission electron micrograph of a *B. subtilis* spore fixed and stained with ruthenium red. Scale bar: 500nm (*in* McKenney *et al.*, 2010); **B)** Schematic representation of the structure of *B. subtilis* spores. Co: core, IFM: inner forespore membrane, PGCW: primordial germ cell wall, Cx: cortex, OFM: outer forespore membrane, Ct: coat, BL: basement layer, IC: inner coat, OC: outer coat, Cr: crust.

Two layers of peptidoglycan surround the inner forespore membrane: the primordial germ cell wall, in immediate contact with this membrane, and the cortex. The primordial germ cell wall has an identical composition to the vegetative cell peptidoglycan and, upon germination, gives rise to the cell wall of the vegetative cell. The cortex is composed of peptidoglycan with several spore-specific modifications, namely the presence of muramic δ-lactam residues, the reduced number of peptide side chains and the absence of teichoic acids (see more details on Chapter 4). As a result, the cortex peptidoglycan shows reduced cross-linking of the glycan strands. This structure is important for maintenance of the dehydrated state

of the core, spore mineralization, dormancy, and also for protection against organic solvents and heat (Popham, 2002; Setlow, 2006; Higgins and Dworkin, 2012). At least during the initial steps of spore development, the cortex is surrounded by the outer forespore membrane. This membrane is essential during spore formation, but may be absent from mature spores (Piggot and Hilbert, 2004; Setlow, 2006).

The next protective structure is the proteinaceous coat, arranged into several layers. From the inside to the outside, the *B. subtilis* spore coat comprises the basement layer, the inner coat, the outer coat and the crust (Fig. 1.1). The coat prevents access of peptidoglycan lytic enzymes, such as lysozyme, to the cortex and confers resistance to noxious chemicals, ionizing radiation and predation. Moreover, it has a major role in spore adhesion, infection by pathogenic sporeformers and in germination. In some species, including *B. subtilis*, the coat is the outermost layer of the spore, mediating the interaction with the surrounding environment. Thus, as an adaptation to distinct ecological niches, the coat composition differs among species (Nicholson *et al.*, 2000; Riesenman and Nicholson, 2000; Klobutcher *et al.*, 2006; Setlow, 2006). In organisms such as *B. cereus*, *B. anthracis* and some Clostridia, the spore coat is encased by an exosporium. This additional protective layer is loose-fitting, with a paracrystalline basal layer and an external hair-like nap, and is separated from the outer coat by an interspace (Henriques and Moran, 2007; Higgins and Dworkin, 2012).

The spore protective surface layers — the cortex, the coat and the exosporium — are flexible and elastic. This allows spore expansion or retraction according to environmental conditions, such as relative humidity (Westphal *et al.*, 2003).

Applications of spores

Bacterial spores, especially those produced by *B. subtilis*, have been widely used in industry, biotechnology and biomedicine. Spores have been

commercialized as probiotic preparations for animal and human consumption (Barbosa *et al.*, 2004; Cartman and La Ragione, 2004), or as biocontrol agents in agriculture, promoting plant growth or preventing plant diseases (Nicholson, 2002). Some of their applications exploit the capacity to display bioactive molecules at the surface by genetic manipulation. This way, they can be vehicles for vaccine delivery, biosensors for specific compounds, or display systems for proteins or peptides of biotechnological interest (Isticato *et al.*, 2001; Ferreira and Schumann, 2012). In addition to their resistance properties, they are easy and cheap to produce in larger scales and can remain stored at room temperature for long periods without losing viability. Understanding the mechanism of sporulation in *B. subtilis* is not only important in fundamental research, but also in the development of products of interest in industry and healthcare.

AN OVERVIEW OF SPORULATION

Endospore formation is an ancient, conserved process. The basic sequence of steps along this developmental program is essentially maintained in Bacilli and Clostridia species studied so far (de Hoon *et al.*, 2010). Sporulation is regulated by a program of gene expression, directed by specific RNA polymerase sigma factors and additional transcription regulators (Piggot, 2002; Errington, 2003; Hilbert and Piggot, 2004; Higgins and Dworkin, 2012; Robleto *et al.*, 2012). Cell-cell signaling pathways that operate between the developing spore and the mother cell is also a hallmark of the process. The genetic program dictates a series of morphological changes that culminate in the formation of a mature spore. Spore development represents a considerable investment of energy and time. Laboratory cultures of *B. subtilis* take about 8-10 hours to complete the process.

The morphological stages of sporulation

The basic sequence of morphologic changes along sporulation was elucidated by electron microscopy. Although this is a continuous process, several stages were considered for convenience (Ryter, 1965; Piggot and Coote, 1976) (Fig. 1.2). Vegetative growth is known as stage 0. Stage I corresponds to entry in sporulation, after a round of DNA replication. At this stage, the two sister chromosomes rearrange into an axial filament that stretches along the longitudinal plan of the cell. Then, an asymmetric septum is formed by membrane invagination, resulting in two compartments with different sizes and cell fates (stage II). The smaller compartment is the prespore that differentiates into a mature spore. The larger one is the mother cell, which participates in spore formation and ultimately lyse (Ryter, 1965; Piggot and Coote, 1976).

After asymmetrical division, the septum bulges into the cytoplasm and the membranes migrate around the prespore in a process similar to phagocytosis, named engulfment. This results in a double-membrane free protoplast, termed forespore, within the mother cell (stage III). During stage IV, the primordial germ cell wall and the cortex deposit between the two forespore membranes. Almost in parallel, the coat becomes visible around the surface of the forespore, corresponding to stage V. Forespores, previously phase-dark, become gradually phase-bright. Stage VI designates the maturation of the spore and acquisition of resistant properties (Ryter, 1965; Piggot and Coote, 1976).

In stage VII, the mother cell lyses through programed cell death and the mature spore is released. The spore has the ability to remain dormant for long periods of time in the absence of nutrients, and can be transported to different, more favorable, locations. Even in a dormant state, it constantly monitors the surrounding environment conditions through receptors in the inner forespore membrane. As soon as the environmental conditions become satisfactory to support vegetative growth, in particular the levels of amino

acids and sugars, the spore exits the dormant state and germinates (Ryter, 1965; Piggot and Coote, 1976).

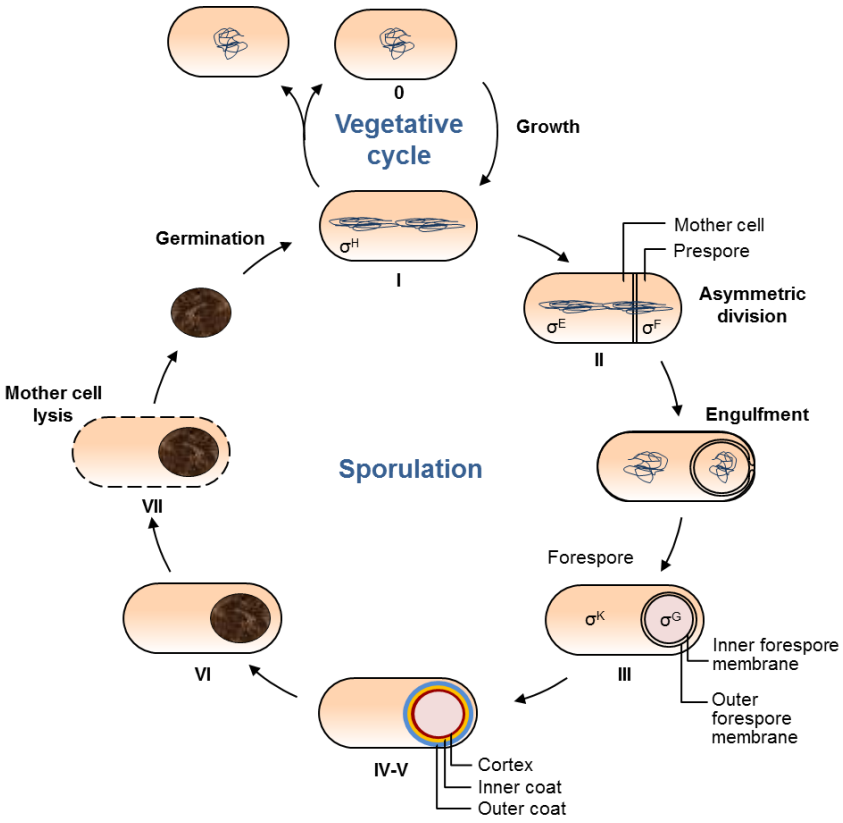

Figure 1.2 – The vegetative and sporulation cycles in *B. subtilis*. The key morphological stages during sporulation (I-VII) are represented. 0: vegetative growth; I: chromosomal replication and formation of the axial filament; II: asymmetric division, followed by engulfment; III: engulfment completion; IV-V: cortex and coat deposition; VI: spores maturation; VII: mother cell lysis, releasing the spore that then germinates and returns vegetative growth or sporulation cycles. The RNA polymerase sigma factors are indicated in the stages were they become active.

Entry into sporulation in *B. subtilis*

The decision-making apparatus that regulates entry into sporulation is precisely regulated and responds to a series of internal and external signals (Errington, 2003; de Hoon *et al.*, 2010). In domesticated strains of *B. subtilis*, sporulation is induced in laboratory by starvation for a carbon,

nitrogen or phosphate source, although high population density is also important (Piggot and Coote, 1976; Sonenshein, 2000; Piggot and Hilbert, 2004). These factors led to activation of Spo0A, the key transcription factor for triggering sporulation. Spo0A is activated by phosphorylation through an expanded two-component signal transduction system known as phosphorelay (Burbulys *et al.*, 1991; Jiang *et al.*, 2000; Sonenshein, 2000; Fujita and Losick, 2005; Chastanet *et al.*, 2010). The levels of phosphorylated Spo0A (Spo0A~P) are negatively regulated by specific phosphatases that dephosphorylate Spo0A~P or other components of the phosphorelay system (Perego *et al.*, 1996; Bongiorni *et al.*, 2007; Smits *et al.*, 2007). Spo0A~P controls the expression of more than 120 genes directly and 520 indirectly, including several genes coding for transcription factors (Fawcett *et al.*, 2000; Molle *et al.*, 2003). The concentration of Spo0A~P defines the physiological outcome in the cell. High cellular levels of Spo0A~P led to sporulation by activation of the transcription of genes coding for the first sporulation-specific regulators (σ^F and σ^E), as well as of genes required for the formation of the axial filament and asymmetric division of the cell (Fujita *et al.*, 2005; Chastanet *et al.*, 2010; Robleto *et al.*, 2012). However, in moderate levels, Spo0A~P triggers other less energy consuming stress responses, such as biofilm formation, sessile behavior, cannibalism, antibiotic production, or competence (Fujita *et al.*, 2005; Robleto *et al.*, 2012).

Another important positive regulator for entry into sporulation is the RNA polymerase sigma factor σ^H, whose regulatory pathways are interconnected with those leading to the production of Spo0A~P. σ^H regulates transcription in the predivisional cell, controls the expression of several genes involved in the phosphorelay, including *spo0A*, and is essential for asymmetric division (Britton *et al.*, 2002; Molle *et al.*, 2003; Hilbert and Piggot, 2004).

Asymmetric septum formation is initiated by redirecting the division machinery to near the cell pole (Errington, 2003). Consequently, when

finishing the asymmetrical division, only 1/3 of the chromosome is trapped in the prespore (Fig 1.2, stage II). Thus, a DNA translocase is required for translocation of the remaining chromosome (Wu and Errington, 1997).

Compartmentalized gene expression in *B. subtilis*

Immediately after asymmetric division, two parallel programs of gene expression start in each daughter cell, directed by different, sporulation-specific, RNA polymerase sigma factors. The first sigma factor to become active is σ^F in the prespore, followed by σ^E in the mother cell; after engulfment, they are replaced by σ^G and σ^K, respectively (Piggot and Hilbert, 2004).

σ^F is synthesized before asymmetric division and held inactive by association with an anti-σ factor. This association is untied by interaction with an anti-anti-σ factor, activating σ^F. The anti-anti-σ factor is regulated by phosphorylation and dephosphorylation cycles that involve a phosphatase present in higher levels in the prespore. This contributes to restrict σ^F activity to this compartment (Min *et al.*, 1993; Arigoni *et al.*, 1996; Decatur and Losick, 1996; Duncan *et al.*, 1996). Another factor that regulates σ^F activity is the transient chromosomal asymmetry generated during the asymmetrical division. Since the gene encoding anti-σ is one of the latest being translocated into the prespore, there is a time gap where it is not expressed in that compartment, allowing the presence of non-associated, active σ^F (Errington, 2003). The products of genes controlled by σ^F mediate activation of σ^E in the mother cell, DNA repair and communication with the mother cell compartment. Also, σ^F directs the transcription of genes encoding σ^G and germination receptors (Robleto *et al.*, 2012).

Soon after σ^F activation in the prespore, σ^E becomes active in the mother cell. σ^E is produced as an inactive precursor, pro-σ^E, that is activated via proteolytic processing by a protease under σ^F control (Jonas *et al.*, 1988; Karow *et al.*, 1995; Hofmeister, 1998). σ^E regulates the expression of genes

whose products are involved in engulfment, mother cell metabolism and cortex and coat formation. It also directs activation of σ^G and synthesis and activation of σ^K and the transcription factors SpoIIID and GerR. These two regulators act together with σ^E to activate or repress the expression of several genes involved in sporulation and germination (Robleto *et al.*, 2012).

About 1 h after asymmetric division, the prespore is engulfed by the mother cell. Membrane migration around the prespore only occurs if the septal peptidoglycan is hydrolyzed by several σ^E-dependent enzymes (Guinand *et al.*, 1974; Abanes-De Mello *et al.*, 2002; Morlot *et al.*, 2010). Engulfment also requires a channel composed by proteins synthesized in both compartments that may function as a feeding tube to nurture the forespore or may drive the membrane movements around it (de Hoon *et al.*, 2010; Higgins and Dworkin, 2012; Crawshaw *et al.*, 2014). After engulfment completion, σ^G is activated in the forespore to direct the final stages of spore development, together with σ^K in the mother cell. The gene coding for an inactive form of σ^G is transcribed only in the forespore under σ^F control, and its synthesis and activation require signals from the two compartments (Sun *et al.*, 1989). σ^G activation also involves at least one component of the channel mentioned above. Thus, either the channel is required to import specific regulatory factors to activate σ^G, or its assembly is an engulfment checkpoint (Errington, 2003; Blaylock *et al.*, 2004; Meisner *et al.*, 2008; de Hoon *et al.*, 2010). A third factor that regulates activity of σ^G is an anti-σ factor that prevents pre-engulfment activation and avoids a rapid increase of its levels in the forespore (Serrano *et al.*, 2011). σ^G-dependent genes encode important factors for σ^K activation, cortex morphogenesis, acquisition of the spore resistance properties and germination (Robleto *et al.*, 2012).

σ^K is the last sporulation-specific sigma factor being activated, and its activity is regulated both at transcriptional and post-translational levels. The DNA element coding for σ^K is interrupted by an integrated prophage-like element that has to be excised by a mother cell-specific, σ^E and SpoIIID-

dependent recombinase (Stragier *et al.*, 1989; Sato *et al.*, 1990). Also, σ^K is transcribed as an inactive precursor, and is proteolytically activated by a protease that requires σ^E and σ^G-dependent elements (Dong and Cutting, 2003). σ^K directs the expression of factors involved in coat formation, germination and mother cell autolysis. It is also required for activation of the transcription factor GerE, which activates and represses the expression of several genes under σ^K control (Robleto *et al.*, 2012).

THE SPORE COAT IN *B. SUBTILIS*

Morphogenesis of the spore coat in *B. subtilis* is a model system to study the formation of supramolecular structures at specific subcellular sites, in coordination with gene expression cascades, during a cell differentiation pathway. Understanding these mechanisms is a major goal in developmental biology, since all organisms share the challenge of directing the assembly of a vast number of proteins into functional molecular machines. Viral capsids (Dokland *et al.*, 1997), bacterial flagellum (McCarter, 2006), the divisome (Goehring and Beckwith, 2005) or the clathrin-coated vesicles in eukaryotic cells (Kaksonen *et al.*, 2005) are a few examples. Despite the diversification of these supramolecular machines in terms of structure and function, their assembly follows the same basic rules.

Structure of the coat

In mature spores of *B. subtilis*, the coat commonly varies between 60 and 250 nm width, appearing thicker at the spore poles (Driks, 1999; Henriques and Moran, 2007). This structure is composed of more than 80 different proteins, whose main features are referred in Table A1 of the Appendices. Transmission electron microscopy revealed that the *B. subtilis* spore coat is organized into at least the four sublayers previously mentioned:

the basement layer or undercoat, the inner coat, the outer coat and the crust (Fig. 1.1). The basement layer, with an amorphous appearance, is the innermost one. It contains proteins involved in initial steps of coat assembly and is presumably important to bridge the cortex and the coat (Driks, 1999; Henriques and Moran, 2007; McKenney *et al.*, 2013). Surrounding the basement layer, there is the lightly staining, lamellar inner coat, delimited by the electron-dense, striated outer coat. Together, these two substructures fill most of the coat volume (Driks, 1999; Henriques and Moran, 2007; McKenney *et al.*, 2013). The outermost layer is the crust, which was identified by staining the spores with ruthenium red before electron microscopy (Waller *et al.*, 2004). This compound marks acid polysaccharides, indicating that the crust comprises glycosylated components. As this is a characteristic of the exosporium of other sporeformers, the crust may represent a rudimentary exosporium in *B. subtilis* (Waller *et al.*, 2004; McKenney *et al.*, 2010; McKenney *et al.*, 2013). The existence of these four spatially distinct coat sublayers is supported by fluorescence microscopy coupled with high-resolution image analysis. By mapping the subcellular localization of several coat proteins fused to GFP or its derivatives and determining their genetic dependencies, coat components were grouped in four substructures that correspond to the layers described before (Imamura *et al.*, 2010; McKenney *et al.*, 2010).

Recently, *B. subtilis* mutant spores missing some important proteins for coat assembly were examined by high-resolution atomic force microscopy. This study supports the existence of the four coat layers previously reported and add others not identified before. According to the authors, the coat is organized into the basement layer or undercoat, a multilayer structure that possibly corresponds to the inner coat, a layer of ''nanodot'' particles that may be CotE molecules, a fibrous/granulous layer that likely corresponds to the outer coat, a honeycomb layer, a rodlet layer and an outermost amorphous crust (Plomp *et al.*, 2014).

Coat composition

About 70% of the *B. subtilis* coat proteins can be solubilized and extracted from purified spores by alkali treatment or using detergents and reducing agents. Proteins within this soluble fraction can then be resolved by SDS-PAGE, individually extracted from the gel and partially sequenced (Henriques and Moran, 2007; Aronson, 2012). This approach, coupled with reverse genetics, led to the identification of the first coat proteins. Nowadays, mass spectrometry, fluorescence microscopy and global transcriptional profiling of the mother cell compartment have been used to find additional coat components (van Ooij *et al.*, 2004; Kim *et al.*, 2006). Coupling fluorescence microscopy with high-resolution image analysis, it is possible not only to identify proteins that compose the coat, but also to assign them to a particular sublayer (Imamura *et al.*, 2010; McKenney *et al.*, 2010).

Most of the identified coat proteins are structural components, although there are also enzymes with important roles, such as post-translational modifications, spore resistance and germination (Table A1 of Appendices). For example, Tgl is a transglutaminase that cross-links several coat proteins (Zilhao *et al.*, 2005), SodA is a superoxide dismutase that provides protection against toxic oxidative compounds (Henriques *et al.*, 1998), and CwlJ is a cortex lytic enzyme essential for germination (Ragkousi *et al.*, 2003).

As mentioned before, the composition of the coat varies between species, reflecting the physical and nutritional conditions where the spores developed and persist (Nicholson *et al.*, 2000; Riesenman and Nicholson, 2000; Klobutcher *et al.*, 2006; Setlow, 2006; Aronson, 2012). Thus, most coat proteins are not conserved among sporeformers. Genome sequence comparison suggests that only about half of the known *B. subtilis* coat proteins have orthologous in other *Bacillus*, and the number is even lower if comparing to *Clostridium* species (Henriques and Moran, 2007; Permpoonpattana *et al.*, 2011; Abecasis *et al.*, 2013; Abhyankar *et al.*, 2013;

McKenney *et al.*, 2013) (Table A1 of Appendices). However, some species-specific coat proteins have functional analogues in other sporeformers. For example, SpoVID is a *Bacillus* protein essential for migration of the coat components around the spore (Beall *et al.*, 1993; Wang *et al.*, 2009), and SipL is its functional analogous in *Clostridium difficile* (Putnam *et al.*, 2013). SpoVID and SipL have a high degree of divergence, but both interact with SpoIVA (that directly recruits SpoVID to the surface of the spore) and their absence result in similar phenotypes in sporulating cells (Beall *et al.*, 1993; Wang *et al.*, 2009; Putnam *et al.*, 2013). This is a case where two organisms developed different structural solutions for the same biological challenge. In opposition, SpoIVA is one of the most conserved coat proteins in *Bacillus* and *Clostridium* species, but while in *B. subtilis* it has a role in both cortex and coat assembly, it is not required for cortex formation in *C. difficile* (Roels *et al.*, 1992; Henriques and Moran, 2007; Putnam *et al.*, 2013).

Regulation of coat assembly

Coat assembly begins as soon as the asymmetric septum starts to curve and proceeds even after spore release into the environment. Along the time, coat proteins are synthesized in the mother cell and deposit at the surface of the developing spore. Initially, they accumulate at the mother cell-proximal (MCP) pole and then they encircle the spore in successive waves (Henriques and Moran, 2000; Errington, 2003; Henriques and Moran, 2007; McKenney and Eichenberger, 2012; McKenney *et al.*, 2013). Coat morphogenesis is regulated at three levels: the time and localization of synthesis of coat components, the guiding role of a small group of coat proteins named morphogenetic proteins (see below) and the post-translational modifications of the coat components (Henriques and Moran, 2007).

The genes coding for coat proteins are organized in four regulons under control of σ^E, σ^K, SpoIIID, GerR and GerE. These regulators are

expressed in a hierarchical cascade, forming feed forward loops in which one of the regulators is required for synthesis of a second one, and together they control the expression of several target genes. This assures that coat proteins are synthesized in a specific order and in the right compartment (Driks, 1999; Henriques and Moran, 2000; Eichenberger *et al.*, 2004; Steil *et al.*, 2005). Genes within the first regulon are expressed under control of σ^E just before the asymmetric septum begins to curve. They include *spoVM*, *spoIVA*, *spoVID*, *safA* and *cotE*, which encode essential proteins for initiation of coat assembly. This regulon also comprises the genes coding for GerR, SpoIIID and σ^K. GerR represses the transcription of some genes under control of σ^E, while SpoIIID acts as a positive or negative regulator of the expression of several σ^E-dependent genes. σ^K, whose activation requires the concerted action of σ^E and SpoIIID, promotes the transcription of a large group of genes coding for coat proteins, as well as of *gerE*. In turn, GerE represses the expression of several σ^E-dependent genes, and together with σ^K, activates transcription of the genes that compose the last regulon (Driks, 1999; Henriques and Moran, 2000; Eichenberger *et al.*, 2004; Steil *et al.*, 2005; Henriques and Moran, 2007).

As the coat components are synthesized, they are guided to their specific subcellular sites by morphogenetic proteins (see below) and the coat is gradually formed. Protein-protein interactions, cross-linking, proteolytic processing, glycosylation and other post-translational modifications contribute to the assembly process (Henriques and Moran, 2007; Aronson, 2012). For instance, in the final stages of coat morphogenesis, several proteins are cross-linked by enzymes, such as Tgl and probably SodA, or via disulfide bridges. Tgl-dependent cross-linking in fact occurs mainly following spore release through lysis of the mother cell; hence, the released spore has an unfinished coat whose maturation path will depend on the environmental conditions (Henriques and Moran, 2007; Aronson, 2012).

The role of morphogenetic proteins in coat assembly

Morphogenetic proteins are a small subset of coat proteins whose function is to guide coat assembly. They localize at the surface of the prespore at earlier stages and direct the other coat components to their specific cellular sites. The role of these proteins is exclusively in protein localization, not interfering with their synthesis. In *B. subtilis*, the most important morphogenetic proteins are SpoVM, SpoIVA, SpoVID, SafA and CotE. The absence of each of these proteins results in spores missing the coat or exhibiting a coat with severe defects (Driks *et al.*, 1994; Henriques and Moran, 2000, 2007; McKenney *et al.*, 2013).

SpoVM:

SpoVM is among the first proteins assembling at the surface of the prespore. The transcription of its gene initiates 2 hours after the onset of sporulation, and the protein starts localizing at the asymmetric division septum shortly after it begins to curve. Then, SpoVM tracks along the engulfing membrane, surrounding the forespore (Levin *et al.*, 1993; van Ooij and Losick, 2003; Le and Schumann, 2008).

This morphogenetic protein is important for assembly of both the cortex and the coat. In a *spoVM* null mutant, spores exhibit an incipient cortex and the coat is thin, disorganized and loosely attached. Fluorescence microscopy experiments using 40 coat proteins-GFP fusions showed that in the absence of SpoVM, most coat proteins are recruited to the MCP pole of the spore, but fail to encircle it. As a result, mutant spores are sensitive to heat, organic solvents and lysozyme (Levin *et al.*, 1993; Wang *et al.*, 2009).

SpoVM is a 3 kDa, 26 residues peptide that folds into an amphipathic α-helix in the presence of lipids. This helix recognizes the positive curvature of the outer forespore membrane and localizes at its surface according to a specific orientation. The cytosolic side of the helix contains six positive charged residues, while all but three hydrophobic residues lie on the

opposite face, buried in the phospholipid bilayer (Levin *et al.*, 1993; Prajapati *et al.*, 2000; van Ooij and Losick, 2003; Ramamurthi *et al.*, 2006; Le and Schumann, 2008; Ramamurthi *et al.*, 2009) (Fig. 1.3 A). The three hydrophobic residues on the cytosolic side of the helix (F3, I6 and P9) localize at the N terminus and are essential for SpoVM localization and function. Localization of SpoVM also requires SpoIVA to restrict it to the spore surface, and residue I6 is involved in a direct interaction between these proteins (Prajapati *et al.*, 2000; van Ooij and Losick, 2003; Ramamurthi *et al.*, 2006). Moreover, residue I15 is essential for cortex formation, but not for SpoVM localization or for initiation of coat assembly (Ebmeier *et al.*, 2012).

SpoIVA:

SpoIVA is present in all sporeformers examined to date, which is a strong indication of its importance. It starts localizing earlier at the MCP pole of the prespore and then encircles it (Roels *et al.*, 1992; Driks *et al.*, 1994; Price and Losick, 1999; Henriques and Moran, 2007). As SpoVM, SpoIVA is involved in both cortex and coat formation. *spoIVA* null mutant spores miss the cortex, and coat proteins fail to assemble at the spore surface, forming swirls dispersed at the mother cell cytoplasm (Roels *et al.*, 1992; Stevens *et al.*, 1992). These swirls are composed by partially structured material, supporting that coat components are able to self-assemble (Aronson and Fitz-James, 1971; Aronson *et al.*, 1992).

SpoIVA has 492 residues and comprises an N and a C-terminal conserved domains (Price and Losick, 1999) (Fig 1.3 B). The N-terminal domain, corresponding to the first 240 residues, has the characteristic fold of GTPases. It includes a highly conserved Walker A motif between residues 24 and 31 that is responsible for ATP binding and hydrolysis. This motif is essential for SpoIVA self-assembly into cable-like structures in an ATP-dependent manner, a mechanism presumably required for the formation of a SpoIVA basal layer around the spore that serves as a platform for coat

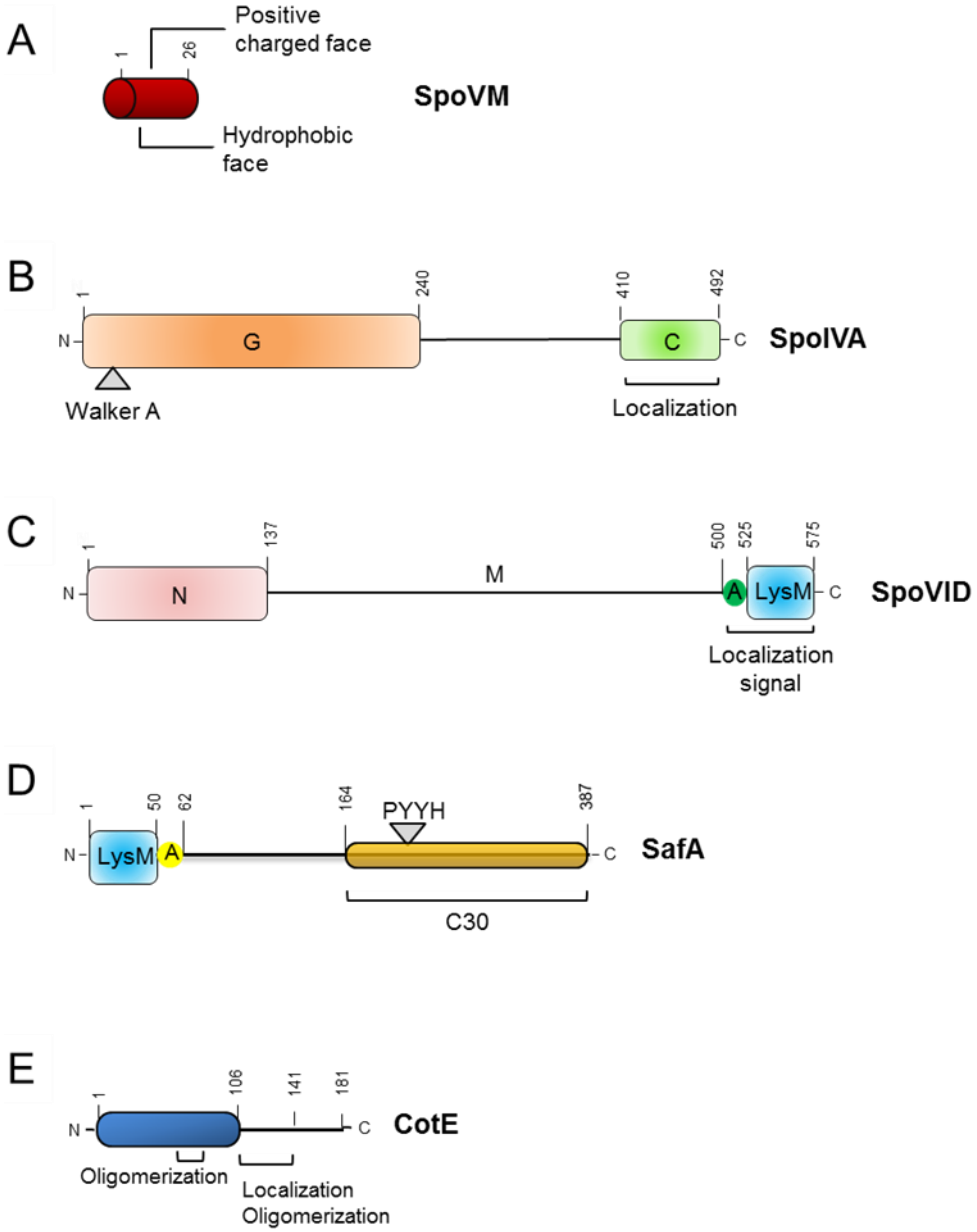

Figure 1.3 – Schematic representation of the main morphogenetic proteins in *B. subtilis* spore coat. **A)** The amphipathic α-helix SpoVM, with its hydrophobic and positive charged faces; **B)** SpoIVA, comprising the GTPase N-terminal domain (G), with the Walker A motif, and the C-terminal localization region (C); **C)** SpoVID consists of an N-terminal domain (N), a middle extended region (M) and a C-terminal targeting region composed by region A and the LysM domain; **D)** SafA has a LysM domain at the N terminus, followed by region A, essential for interaction with SpoVID. The region that composes the $SafA_{C30}$ form is represented in dark yellow, with the PYYH motif highlighted; **E)** CotE, composed of an N-terminal domain involved in oligomerization and a localization region also important for oligomer formation.

assembly. Furthermore, the Walker A motif, in particular residue K30, is involved in SpoIVA localization, indicating that the ATPase activity may be important for its targeting at the spore surface (Ramamurthi and Losick, 2008; Mullerova *et al.*, 2009; Castaing *et al.*, 2013). The SpoIVA C-terminal domain comprises the last 82 residues and interacts with SpoVM. These two morphogenetic proteins are co-dependent for localization: SpoIVA requires SpoVM to encircle the spore, and in turn SpoIVA helps restricting SpoVM to the spore surface (Price and Losick, 1999; Ramamurthi *et al.*, 2006). SpoIVA is also essential for subcellular localization of three others morphogenetic proteins: SpoVID, SafA and CotE (Driks *et al.*, 1994; Ozin *et al.*, 2001b; Wang *et al.*, 2009). Direct interactions of SpoIVA with SpoVID and SafA were already demonstrated *in vitro* (Mullerova *et al.*, 2009; Wang *et al.*, 2009; Qiao *et al.*, 2012).

SpoVID:

SpoVID is synthesized 2 hours after asymmetrical division and encircles the spore in a SpoVM-dependent manner. In the absence of this protein, sporulating cells exhibit a phenotype reminiscent of the *spoIVA* null mutant, in the sense that coat proteins also accumulate in the mother cell cytoplasm in partially structured swirls (Beall *et al.*, 1993; Driks *et al.*, 1994). Fusions of coat proteins to GFP localize at the MCP pole in *spoVID* null mutant spores, but fail to encircle them, similarly to what happens in cell missing SpoVM (Wang *et al.*, 2009). However, contrarily to *spoVM* and *spoIVA* null mutants, the cortex is not affected. As a result, *spoVID* mutant spores are susceptible to lysozyme, but not to high temperatures, and are deficient in germination (Beall *et al.*, 1993; Driks *et al.*, 1994).

This 575 residues long, highly acidic protein is composed by a N-terminal domain, a middle domain with an extended coiled-coil conformation and a C-terminal region comprising the 24 residues region A and a LysM domain (Beall *et al.*, 1993; Ozin *et al.*, 2000; Buist *et al.*, 2008; Wang *et al.*,

2009) (Fig. 1.3C). The N-terminal domain has 137 residues, resembles the phage-capsid protein PP7, and is essential for the morphogenetic function of SpoVID. In particular, a small region at the end of this domain (residues 86-136) is required for migration of coat components around the developing spore (Wang *et al.*, 2009) (see Chapters 2 and 3). The N-terminus of SpoVID interacts directly with the morphogenetic protein for the inner coat assembly, SafA (Costa *et al.*, 2006).

The C-terminal region of SpoVID is required for the assembly at the spore surface. Both region A, via interaction with SpoIVA, and the LysM domain are essential for SpoVID localization, although it seems that the major contribution comes from region A. (Mullerova *et al.*, 2009; Wang *et al.*, 2009). Since LysM motifs are commonly glycan-binding modules, it has been suggested that its role in SpoVID localization might implicate spore peptidoglycan recognition (see Chapter 4). However, it remains to be explained how the LysM domain binds to the spore peptidoglycan in the presence of the outer forespore membrane.

SpoVID oligomerizes *in vitro* (Ozin *et al.*, 2000; Mullerova *et al.*, 2009), and oligomerization may be important for the encasement process. Disulfide bridges may be involved, as SpoVID has five cysteine residues, two of them in the N-terminal domain. The homologous phage-capsid protein PP7 also has two cysteines that are responsible for oligomerization during assembly of the viral capsid (Tars *et al.*, 2000; Caldeira and Peabody, 2007).

SafA:

SafA, also known as YrbA, localizes at the cortex/coat interface and is essential for inner coat morphogenesis. *safA* null mutant spores exhibit a reduced inner coat and a loosely attached outer coat that tends to peel off. These spores are sensitive to lysozyme and deficient in germination (Takamatsu *et al.*, 1999; Ozin *et al.*, 2000). Moreover, at least CotG is absent from their outer coat, showing that although the role of SafA is mainly in

inner coat assembly, it also makes important contributions for outer coat formation (Ozin *et al.*, 2000).

SafA is a proline-rich protein that has at least three forms in sporulating cells: the 45 kDa full-length form, comprising 387 residues, a 30 kDa form named $SafA_{C30}$ that results from alternative internal translation starting from M164 (Fig. 1.3 D), and a 21 kDa N-terminal form termed $SafA_{N21}$ (Ozin *et al.*, 2000; Takamatsu *et al.*, 2000b; Ozin *et al.*, 2001a). The full-length form starts accumulating earlier, as the asymmetric septum begins to curve (Ozin *et al.*, 2000; Takamatsu *et al.*, 2000a), and has the morphogenetic role in coat assembly (Ozin *et al.*, 2001a). In contrast, neither $SafA_{N21}$ nor $SafA_{C30}$ are essential for coat formation. $SafA_{C30}$ requires the full-length form of SafA for localization, and interacts with the full length protein *in vitro* (Ozin *et al.*, 2001b).

SafA has a LysM domain at its N-terminal end, followed by a conserved region A (residues 51-63) that interacts directly with SpoVID (Fig. 1.3 D). This interaction is essential for SafA localization and function, and consequently for proper coat assembly. At the C-terminal half of SafA there is another region of interaction with SpoVID, named region B or PYYH motif (residues 203 and 206). Region B is important for formation of the SpoVID-SafA complex and its deletion causes deficient formation of the coat (Ozin *et al.*, 2000; Ozin *et al.*, 2001b; Costa *et al.*, 2006).

SafA requires SpoVID to encircle the spore, yet its initial localization at the MCP pole depends on SpoIVA (Ozin *et al.*, 2001b; Wang *et al.*, 2009). SafA establishes a direct interaction with this protein, but it appears weaker than the interaction with SpoVID (Mullerova *et al.*, 2009; Qiao *et al.*, 2012). It has been suggested that the LysM domain may also have a role in SafA localization via spore peptidoglycan binding, but again it is not clear how the LysM crosses the outer forespore membrane to reach it (Ozin *et al.*, 2000; Ozin *et al.*, 2001b) (see Chapter 4).

Since SafA appears to exhibit an elongated conformation, with

exception of the N-terminal region, it is possible that it extends radially from the cortex until reaching the outer coat. The LysM domain would be buried into the peptidoglycan layer, while the C-terminal region interacts with other coat proteins. The $SafA_{C30}$ form may contribute to increase the surface available for interactions with coat components (Ozin *et al.*, 2000; Ozin *et al.*, 2001b).

CotE:

CotE is essential for assembly of the outer coat and the crust. Proteins that constitute these layers fail to localize properly in *cotE* null mutants, resulting in germination-deficient spores with susceptibility to lysozyme (Zheng *et al.*, 1988; Kim *et al.*, 2006). However, likewise the major morphogenetic protein for inner coat formation, SafA, has a role in outer coat integrity, CotE also contributes to inner coat morphogenesis. It is important for the retention of at least some inner coat proteins, such as OxdD, at the spore surface and may be involved in a direct interaction with some of them (Zheng *et al.*, 1988; Kim *et al.*, 2006; Henriques and Moran, 2007).

Production of CotE is regulated at the transcription level by two tandem promotors. At first, *cotE* is expressed from promotor P1, controlled by σ^E, while in a second stage it requires promotor P2, initially regulated under jointed control of σ^E and SpoIIID and that remains active under control of σ^K (Costa *et al.*, 2007). CotE starts localizing at a 75 nm distance from the surface of the forespore, forming a ring that may be the basal layer for assembly of the outer coat. The gap between the basement layer and this ring, whose composition is unknown, is called matrix or precoat and defines the place for inner coat assembly after engulfment (Driks *et al.*, 1994; Henriques and Moran, 2007).

CotE, with 181 residues, has a modular design. The N-terminal domain and the C-terminal region (residues 1-106 and 153-181, respectively) are important to direct the assembly of coat proteins. Residues

107-141 are involved in CotE localization and, together with a second region in the N-terminal half of the protein (residues 58-75), in oligomerization (Fig. 1.3 E). The ability to form oligomers may facilitate the formation of the CotE ring around the spore (Bauer *et al.*, 1999; Little and Driks, 2001; Krajcikova *et al.*, 2009).

CotE depends on SpoIVA to localize at the surface of the prespore and on SpoVID to encircle it (Driks *et al.*, 1994; Wang *et al.*, 2009). In turn, CotE is essential for the localization of CotH and CotO, two other morphogenetic proteins with roles in assembly of small subsets of coat proteins, in germination and in lysozyme resistance (Naclerio *et al.*, 1996; Zilhao *et al.*, 1999; Eichenberger *et al.*, 2003; McPherson *et al.*, 2005).

Moreover, CotE is required for assembly of CotW, CotX and CotZ, which are important in crust morphogenesis. This outermost layer is mainly composed by proteins synthesized at later stages. Most of them are cysteine-rich and highly cross-linked, being part of the coat insoluble fraction. In the absence of the crust, spores show altered surface properties, specially hydrophobicity, and increased accessibility to germinants (Zhang *et al.*, 1994; Kim *et al.*, 2006; Henriques and Moran, 2007; Krajcikova *et al.*, 2009; McKenney *et al.*, 2010; Imamura *et al.*, 2011).

The coat genetic interaction network

Subcellular localization, genetic dependencies and direct interactions between coat proteins provide us clues on the mechanisms governing their recruitment and assembly at specific subcellular sites. SpoVM, SpoIVA and SpoVID are required for formation of all the coat sublayers (Roels *et al.*, 1992; Stevens *et al.*, 1992; Beall *et al.*, 1993; Levin *et al.*, 1993; Wang *et al.*, 2009). SpoVM and SpoIVA interact directly and are co-dependent for localization, while SpoVID depends on both to localize and binds at least SpoIVA (Price and Losick, 1999; Ramamurthi *et al.*, 2006; Mullerova *et al.*, 2009; Wang *et al.*, 2009; Qiao *et al.*, 2012). SafA and CotE are essential for

assembly of the inner coat and the outer coat and crust components, respectively (Zheng *et al.*, 1988; Takamatsu *et al.*, 1999; Kim *et al.*, 2006; McKenney *et al.*, 2010). They require SpoVM, SpoIVA and SpoVID for localization, and at least SafA interacts directly with SpoIVA and SpoVID (Driks *et al.*, 1994; Ozin *et al.*, 2000; Ozin *et al.*, 2001b; Costa *et al.*, 2006; Mullerova *et al.*, 2009; Wang *et al.*, 2009; Qiao *et al.*, 2012). Altogether, this indicates that protein-protein interactions play a major role in directing coat morphogenesis. It also suggests that assembly of the inner and the outer coat are largely independent processes, driven by different morphogenetic proteins (Fig 1.4).

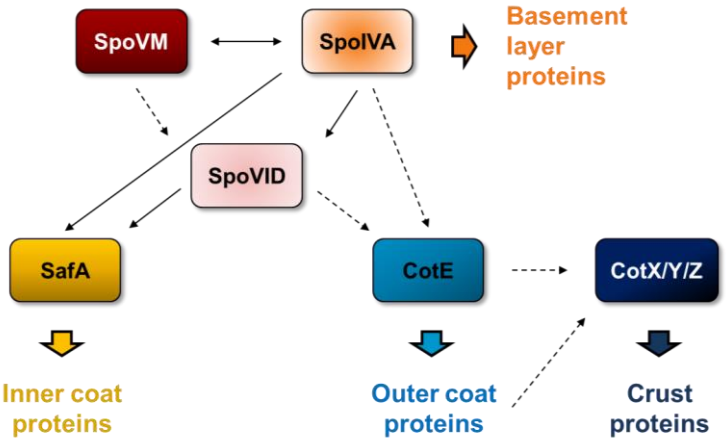

Figure 1.4 – Interactions and dependencies between the major morphogenetic proteins for assembly of the spore coat in *B. subtilis.* Filled arrows represent the dependencies and direct interactions already documented, while spotted arrows represent dependencies where a direct interaction was not reported to date.

According to this, coat proteins can be defined by its inability to localize at the spore surface in the absence of SpoIVA. If they also fail to localize in *safA* or *cotE* null mutants, they are catalogued as inner or outer coat/crust components, respectively. Using these criteria, more than 40 coat proteins fused to GFP were examined for their dependencies for assembly, revealing a network of genetic interactions. This network is organized in

three essentially independent modules: SafA-dependent proteins, CotE-dependent proteins, and proteins that are independent of SafA and CotE for localization, but are SpoIVA-dependent (Kim *et al.*, 2006; McKenney *et al.*, 2010). Moreover, it was demonstrated that these coat protein fusions localize at the spore surface in spatially distinct layers that correlate with their dependencies. SafA- and CotE-independent proteins assemble closest to the spore membrane, forming the basement layer. The next layer comprises SafA-dependent proteins that compose the inner coat. CotE-dependent proteins are the outermost ones, distributed in two significantly separated groups that correspond to the outer coat and the crust (Imamura *et al.*, 2010; McKenney *et al.*, 2010; McKenney and Eichenberger, 2012) (Fig 1.4).

It is likely that SafA and CotE interact with and recruit most coat proteins that constitute the inner coat and the outer coat and crust, respectively. Thus, SafA and CotE are presumably hub proteins, which bind a large number of partners. Hub proteins typically play essential roles in interactomes and the effect of their deletions is drastic. Also, they tend to be highly conserved across species comparing to other proteins in the same network, as happens with SafA and CotE in *Bacillus* (Henriques and Moran, 2007; McKenney *et al.*, 2013).

Two steps in coat assembly: targeting and encasement

In the absence of SpoIVA, the deposition of most of the 40 coat proteins-GFP fusions at the surface of the developing spore is compromised. In cells missing SpoVM or SpoVID, these fusions typically anchor to the spore surface, but then they fail to encircle it. This shows that there are two successive steps in coat assembly: localization, or targeting, and spore encasement. In the targeting step, governed by SpoIVA, coat proteins are recruited to the MCP pole of the developing spore. Then, during encasement, controlled by SpoVM and SpoVID, they encircle the spore in successive waves (Wang *et al.*, 2009; McKenney *et al.*, 2013). SpoIVA and the hubs SafA and

CotE are the core of the molecular machine responsible for recruitment of coat proteins to the spore surface, whereas SpoVM and SpoVID are involved in their transition to a symmetric distribution around it (Driks *et al.*, 1994; Wang *et al.*, 2009; McKenney and Eichenberger, 2012; McKenney *et al.*, 2013).

SpoVM is essential for encasement by all the coat protein fusions examined so far, while SpoVID is required for most of them. Moreover, the N-terminal domain of SpoVID plays a determinant role in the mechanism, specifically through a region between residues 86 and 136 (Wang *et al.*, 2009; McKenney *et al.*, 2013) (see Chapters 2 and 3 for details). The driving force that pulls encasement around the spore is unknown. Since at least some morphogenetic proteins form oligomers, including SpoVID (Little and Driks, 2001; Ozin *et al.*, 2001b; Ramamurthi and Losick, 2008; Krajcikova *et al.*, 2009; Mullerova *et al.*, 2009; Castaing *et al.*, 2013), it is possible that protein polymerization facilitates the process (McKenney *et al.*, 2013).

Successive waves of encasement during coat morphogenesis

The localization patterns of coat proteins over the course of sporulation were analysed in detail using the library of 40 fluorescent fusions mentioned before. This lead to the classification of coat components in six kinetics classes, three of them composed by earlier-localizing proteins (I, II and III) and the other three by the late-localizing ones (IV, V and VI) (McKenney and Eichenberger, 2012; McKenney *et al.*, 2013) (Fig. 1.5 and Table A1 of Appendices).

Earlier-localizing proteins are encoded by σ^E-dependent genes and include morphogenetic proteins required for assembly of all the coat sublayers. They start localizing simultaneously at the MCP pole once the asymmetric septum begins to curve, forming an organized, multilayered scaffold. Then, proteins that compose each class encase the spore at a different rate, according to their transcriptional dependencies. As a result,

the spore is encased in successive waves (Driks *et al.*, 1994; McKenney and Eichenberger, 2012). The first wave of encasement consists of proteins from the kinetic class I, which track along with the mother cell engulfing membrane. Among them are morphogenetic proteins required for assembly of the basement layer (SpoIVA) and presumably the inner coat (SafA), as well as the ones that guide encasement (SpoVM and SpoVID). Expression of class I protein genes is either exclusively regulated by σ^E, such as *spoVID*, or it is also repressed by SpoIIID, as *spoIVA*. After engulfment completion, the second wave of encasement takes place, composed by class II proteins. First, they localize at the MCP pole as a dot that turns into a cap. After MCD pole establishment, a second cap appears at the opposite pole and then the two caps expand and surround the spore. Class II protein genes are presumably transcribed under positive regulation of σ^E and SpoIIID, and include *cotE*. The last wave of encasement among the earlier-localizing proteins is composed by class III proteins, which localize identically as those from class II, yet encasement only begins after the forespores became phase-dark. These proteins are encoded by genes expressed under control of combinations of σ^E, σ^K and GerE, and include CotZ, required for crust assembly (McKenney and Eichenberger, 2012; McKenney *et al.*, 2013) (Fig. 1.5). According to this, the basement layer and the inner coat are the first layers encasing the spore, followed by the outer coat and finally the crust. The temporal differences in the encasement by coat layers reflect the timing of expression of their components, in particular of their morphogenetic proteins. Thus, pulses of gene expression have a determinant role in regulation of spore encasement, and consequently in coat formation (McKenney and Eichenberger, 2012; McKenney *et al.*, 2013) (Fig. 1.5).

Late-localizing proteins (classes IV, V and VI) are synthesized at later stages and are progressively added to the different layers of the developing coat. At that time, the MCD pole is already established, and therefore these proteins accumulate simultaneously at both poles. Class IV proteins start

localizing immediately after engulfment completion. Proteins from class V initiate assembling in phase-dark spores, and finally those from class VI only localize in phase-bright spores. All four coat layers contain components from late-localizing classes, indicating that coat formation does not occur by the ordered addition of each layer at a time, but rather there are proteins of all layers assembling simultaneously. This implicates that the coat remains permeable along morphogenesis, even to large proteins (McKenney and Eichenberger, 2012).

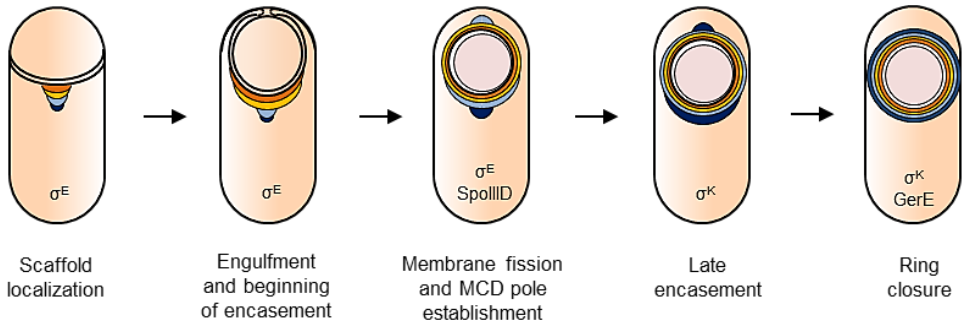

Figure 1.5 – Model for spore coat morphogenesis in *B. subtilis*. As soon as the asymmetric septum begins to curve, the major morphogenetic proteins involved in coat assembly, as well as other coat proteins, localize at the MCP pole of the prespore. An organized, multilayered scaffold is formed, comprising proteins whose genes are under σ^E regulation. These proteins encase the spore in successive waves, starting from the basement layer and inner coat components, followed by outer coat proteins and later by crust proteins. Among the earlier-localizing proteins, those from the basement layer and the inner coat are encoded by genes exclusively regulated by σ^E, or by σ^E and SpoIIID. Transcription of the outer coat protein genes requires combinations of σ^E, σ^K and SpoIIID, while transcription of those from the crust proteins depend on combinations of σ^E, σ^K and GerE. The basement layer is represented in orange, the inner coat in yellow, the outer coat in light blue and the crust in dark blue. Adapted from McKenney *et al.*, 2012 and McKenney *et al.*, 2013.

AIMS OF THIS WORK

With this work, we sought to elucidate the mechanisms governing coat assembly. The current model predicts that SpoVID promotes spore encasement by coat components via direct interactions with other

morphogenetic proteins. Direct interactions of SpoVID with SpoIVA and SafA, the hub for inner coat proteins, were previously demonstrated. However, the interaction between SpoVID and CotE, the hub for the outer coat/crust proteins has remained a missing link in the model. Thus, we wanted to investigate how SpoVID guides encasement by the outer coat components (Chapter 2). Also, we aim at understanding how a small region at the end of the N-terminal domain of SpoVID directs encasement by all coat layers (Chapters 2 and 3). Finally, we sought to explore the role of the LysM domain in the subcellular localization of SpoVID and SafA and in spore coat assembly (Chapter 4).

REFERENCES

Abanes-De Mello, A., Sun, Y.L., Aung, S., Pogliano, K., 2002. A cytoskeleton-like role for the bacterial cell wall during engulfment of the Bacillus subtilis forespore. Genes & Development 16, 3253-3264.

Abecasis, A.B., Serrano, M., Alves, R., Quintais, L., Pereira-Leal, J.B., Henriques, A.O., 2013. A genomic signature and the identification of new sporulation genes. Journal of Bacteriology 195, 2101-2115.

Abhyankar, W., Hossain, A.H., Djajasaputra, A., Permpoonpattana, P., Ter Beek, A., Dekker, H.L., Cutting, S.M., Brul, S., de Koning, L.J., de Koster, C.G., 2013. In pursuit of protein targets: proteomic characterization of bacterial spore outer layers. Journal of Proteome Research 12, 4507-4521.

Arigoni, F., Duncan, L., Alper, S., Losick, R., Stragier, P., 1996. SpoIIE governs the phosphorylation state of a protein regulating transcription factor sigma F during sporulation in Bacillus subtilis. Proceedings of the National Academy of Sciences of the United States of America 93, 3238-3242.

Aronson, A.I., 2012. The structure and composition of the outer layers of the bacterial spore. In: Abel-Santos, E. (Ed.), Bacterial spores: current research and applications. Caister Academic Press, Norfolk, UK, pp. 57-71.

Aronson, A.I., Ekanayake, L., Fitz-James, P.C., 1992. Protein filaments may initiate the assembly of the Bacillus subtilis spore coat. Biochimie 74, 661-667.

Aronson, A.I., Fitz-James, P.C., 1971. Reconstitution of bacterial spore coat layers in vitro. Journal of Bacteriology 108, 571-578.

Barbosa, T.M., Serra, C.R., Henriques, A.O., 2004. Gut sporeformers. In: Ricca, E., Henriques, A.O., Cutting, S. (Eds.), Bacterial sporeformers: probiotic and emerging applications. Horizon Bioscience, London, Uniten Kingdom, pp. 183-192.

Bauer, T., Little, S., Stover, A.G., Driks, A., 1999. Functional regions of the Bacillus subtilis spore coat morphogenetic protein CotE. Journal of Bacteriology 181, 7043-7051.

Beall, B., Driks, A., Losick, R., Moran, C.P., Jr., 1993. Cloning and characterization of a gene required for assembly of the Bacillus subtilis spore coat. Journal of Bacteriology 175, 1705-1716.

Blaylock, B., Jiang, X., Rubio, A., Moran, C.P., Jr., Pogliano, K., 2004. Zipper-like interaction between proteins in adjacent daughter cells mediates protein localization. Genes & Development 18, 2916-2928.

Bongiorni, C., Stoessel, R., Perego, M., 2007. Negative regulation of Bacillus anthracis sporulation by the Spo0E family of phosphatases. Journal of Bacteriology 189, 2637-2645.

Britton, R.A., Eichenberger, P., Gonzalez-Pastor, J.E., Fawcett, P., Monson, R., Losick, R., Grossman, A.D., 2002. Genome-wide analysis of the stationary-phase sigma factor (sigma-H) regulon of Bacillus subtilis. Journal of Bacteriology 184, 4881-4890.

Buist, G., Steen, A., Kok, J., Kuipers, O.P., 2008. LysM, a widely distributed protein motif for binding to (peptido)glycans. Molecular Microbiology 68, 838-847.

Burbulys, D., Trach, K.A., Hoch, J.A., 1991. Initiation of sporulation in B. subtilis is controlled by a multicomponent phosphorelay. Cell 64, 545-552.

Caldeira, J.C., Peabody, D.S., 2007. Stability and assembly in vitro of bacteriophage PP7 virus-like particles. Journal of Nanobiotechnology 5, 10.

Cartman, S.T., La Ragione, R.M., 2004. Spore probiotics as animal feed suplements. In: Ricca, E., Henriques, A.O., Cutting, S. (Eds.), Bacterial spore formers: probiotics and emerging applications. Horizon Bioscience, London, United Kingdom, pp. 155-162.

Castaing, J.P., Nagy, A., Anantharaman, V., Aravind, L., Ramamurthi, K.S., 2013. ATP hydrolysis by a domain related to translation factor GTPases drives

polymerization of a static bacterial morphogenetic protein. Proceedings of the National Academy of Sciences of the United States of America 110, E151-160.

Chastanet, A., Vitkup, D., Yuan, G.C., Norman, T.M., Liu, J.S., Losick, R.M., 2010. Broadly heterogeneous activation of the master regulator for sporulation in Bacillus subtilis. Proceedings of the National Academy of Sciences of the United States of America 107, 8486-8491.

Cortezzo, D.E., Koziol-Dube, K., Setlow, B., Setlow, P., 2004. Treatment with oxidizing agents damages the inner membrane of spores of Bacillus subtilis and sensitizes spores to subsequent stress. Journal of Applied Microbiology 97, 838-852.

Costa, T., Isidro, A.L., Moran, C.P., Jr., Henriques, A.O., 2006. Interaction between coat morphogenetic proteins SafA and SpoVID. Journal of Bacteriology 188, 7731-7741.

Costa, T., Serrano, M., Steil, L., Volker, U., Moran, C.P., Jr., Henriques, A.O., 2007. The timing of cotE expression affects Bacillus subtilis spore coat morphology but not lysozyme resistance. Journal of Bacteriology 189, 2401-2410.

Crawshaw, A.D., Serrano, M., Stanley, W.A., Henriques, A.O., Salgado, P.S., 2014. A mother cell-to-forespore channel: current understanding and future challenges. FEMS Microbiology Letters 358, 129-136.

de Hoon, M.J., Eichenberger, P., Vitkup, D., 2010. Hierarchical evolution of the bacterial sporulation network. Current biology 20, R735-745.

Decatur, A.L., Losick, R., 1996. Three sites of contact between the Bacillus subtilis transcription factor sigmaF and its antisigma factor SpoIIAB. Genes & Development 10, 2348-2358.

Dokland, T., McKenna, R., Ilag, L.L., Bowman, B.R., Incardona, N.L., Fane, B.A., Rossmann, M.G., 1997. Structure of a viral procapsid with molecular scaffolding. Nature 389, 308-313.

Dong, T.C., Cutting, S.M., 2003. SpoIVB-mediated cleavage of SpoIVFA could provide the intercellular signal to activate processing of Pro-sigmaK in Bacillus subtilis. Molecular Microbiology 49, 1425-1434.

Driks, A., 1999. Bacillus subtilis spore coat. Microbiology and Molecular Biology Reviews 63, 1-20.

Driks, A., Roels, S., Beall, B., Moran, C.P., Jr., Losick, R., 1994. Subcellular

localization of proteins involved in the assembly of the spore coat of Bacillus subtilis. Genes & Development 8, 234-244.

Duncan, L., Alper, S., Losick, R., 1996. SpoIIAA governs the release of the cell-type specific transcription factor sigma F from its anti-sigma factor SpoIIAB. Journal of Molecular Biology 260, 147-164.

Ebmeier, S.E., Tan, I.S., Clapham, K.R., Ramamurthi, K.S., 2012. Small proteins link coat and cortex assembly during sporulation in Bacillus subtilis. Molecular Microbiology 84, 682-696.

Eichenberger, P., Fujita, M., Jensen, S.T., Conlon, E.M., Rudner, D.Z., Wang, S.T., Ferguson, C., Haga, K., Sato, T., Liu, J.S., Losick, R., 2004. The program of gene transcription for a single differentiating cell type during sporulation in Bacillus subtilis. PLOS Biology 2, e328.

Eichenberger, P., Jensen, S.T., Conlon, E.M., van Ooij, C., Silvaggi, J., Gonzalez-Pastor, J.E., Fujita, M., Ben-Yehuda, S., Stragier, P., Liu, J.S., Losick, R., 2003. The sigmaE regulon and the identification of additional sporulation genes in Bacillus subtilis. Journal of Molecular Biology 327, 945-972.

Errington, J., 2003. Regulation of endospore formation in Bacillus subtilis. Nature Reviews Microbiology 1, 117-126.

Fawcett, P., Eichenberger, P., Losick, R., Youngman, P., 2000. The transcriptional profile of early to middle sporulation in Bacillus subtilis. Proceedings of the National Academy of Sciences of the United States of America 97, 8063-8068.

Ferreira, L.C., Schumann, W., 2012. Expression of recombinant proteins using *Bacillus subtilis* spores. In: Abel-Santos, E. (Ed.), Bacterial spores: current research and applications. Caister Academic Press, Norfolk, United Kingdom, pp. 263-272.

Fujita, M., Gonzalez-Pastor, J.E., Losick, R., 2005. High- and low-threshold genes in the Spo0A regulon of Bacillus subtilis. Journal of Bacteriology 187, 1357-1368.

Fujita, M., Losick, R., 2005. Evidence that entry into sporulation in Bacillus subtilis is governed by a gradual increase in the level and activity of the master regulator Spo0A. Genes & Development 19, 2236-2244.

Galperin, M.Y., Mekhedov, S.L., Puigbo, P., Smirnov, S., Wolf, Y.I., Rigden, D.J., 2012. Genomic determinants of sporulation in Bacilli and Clostridia: towards the minimal set of sporulation-specific genes. Environmental Microbiology 14, 2870-2890.

Gerhardt, P., Marquis, R.E., 1989. Spore thermoresistance mechanisms. In: Smith, I., Slepecky, R.A., Setlow, P. (Eds.), Regulation of Procariotic Development. American Society of Microbiology, Washington, D. C., United States of America, pp. 43-63.

Goehring, N.W., Beckwith, J., 2005. Diverse paths to midcell: assembly of the bacterial cell division machinery. Current Biology 15, R514-526.

Guinand, M., Michel, G., Tipper, D.J., 1974. Appearance of gamma-D-glutamyl-(L) meso-diaminopimealate peptidoglycan hydrolase during sporulation in Bacillus sphaericus. Journal of Bacteriology 120, 173-184.

Henriques, A.O., Melsen, L.R., Moran, C.P., Jr., 1998. Involvement of superoxide dismutase in spore coat assembly in Bacillus subtilis. Journal of Bacteriology 180, 2285-2291.

Henriques, A.O., Moran, C.P., Jr., 2000. Structure and assembly of the bacterial endospore coat. Methods 20, 95-110.

Henriques, A.O., Moran, C.P., Jr., 2007. Structure, assembly, and function of the spore surface layers. Annual Review of Microbiology 61, 555-588.

Higgins, D., Dworkin, J., 2012. Recent progress in Bacillus subtilis sporulation. FEMS Microbiology Reviews 36, 131-148.

Hilbert, D.W., Piggot, P.J., 2004. Compartmentalization of gene expression during Bacillus subtilis spore formation. Microbiology and Molecular Biology Reviews 68, 234-262.

Hoffmann, T., Troup, B., Szabo, A., Hungerer, C., Jahn, D., 1995. The anaerobic life of Bacillus subtilis: cloning of the genes encoding the respiratory nitrate reductase system. FEMS Microbiology Letters 131, 219-225.

Hofmeister, A., 1998. Activation of the proprotein transcription factor pro-sigmaE is associated with its progression through three patterns of subcellular localization during sporulation in Bacillus subtilis. Journal of Bacteriology 180, 2426-2433.

Hong, H.A., Khaneja, R., Tam, N.M., Cazzato, A., Tan, S., Urdaci, M., Brisson, A., Gasbarrini, A., Barnes, I., Cutting, S.M., 2009. Bacillus subtilis isolated from the human gastrointestinal tract. Research in Microbiology 160, 134-143.

Imamura, D., Kuwana, R., Takamatsu, H., Watabe, K., 2010. Localization of proteins to different layers and regions of Bacillus subtilis spore coats. Journal of Bacteriology 192, 518-524.

Imamura, D., Kuwana, R., Takamatsu, H., Watabe, K., 2011. Proteins involved in formation of the outermost layer of Bacillus subtilis spores. Journal of Bacteriology 193, 4075-4080.

Isticato, R., Cangiano, G., Tran, H.T., Ciabattini, A., Medaglini, D., Oggioni, M.R., De Felice, M., Pozzi, G., Ricca, E., 2001. Surface display of recombinant proteins on Bacillus subtilis spores. Journal of Bacteriology 183, 6294-6301.

Jiang, M., Shao, W., Perego, M., Hoch, J.A., 2000. Multiple histidine kinases regulate entry into stationary phase and sporulation in Bacillus subtilis. Molecular Microbiology 38, 535-542.

Jonas, R.M., Weaver, E.A., Kenney, T.J., Moran, C.P., Jr., Haldenwang, W.G., 1988. The Bacillus subtilis spoIIG operon encodes both sigma E and a gene necessary for sigma E activation. Journal of Bacteriology 170, 507-511.

Kaksonen, M., Toret, C.P., Drubin, D.G., 2005. A modular design for the clathrin- and actin-mediated endocytosis machinery. Cell 123, 305-320.

Karow, M.L., Glaser, P., Piggot, P.J., 1995. Identification of a gene, spoIIR, that links the activation of sigma E to the transcriptional activity of sigma F during sporulation in Bacillus subtilis. Proceedings of the National Academy of Sciences of the United States of America 92, 2012-2016.

Kim, H., Hahn, M., Grabowski, P., McPherson, D.C., Otte, M.M., Wang, R., Ferguson, C.C., Eichenberger, P., Driks, A., 2006. The Bacillus subtilis spore coat protein interaction network. Molecular Microbiology 59, 487-502.

Klobutcher, L.A., Ragkousi, K., Setlow, P., 2006. The Bacillus subtilis spore coat provides "eat resistance" during phagocytic predation by the protozoan Tetrahymena thermophila. Proceedings of the National Academy of Sciences of the United States of America 103, 165-170.

Krajcikova, D., Lukacova, M., Mullerova, D., Cutting, S.M., Barak, I., 2009. Searching for protein-protein interactions within the Bacillus subtilis spore coat. Journal of Bacteriology 191, 3212-3219.

Kunst, F., Ogasawara, N., Moszer, I., Albertini, A.M., Alloni, G., Azevedo, V., Bertero, M.G., Bessieres, P., Bolotin, A., Borchert, S., Borriss, R., Boursier, L., Brans, A., Braun, M., Brignell, S.C., Bron, S., Brouillet, S., Bruschi, C.V., Caldwell, B., Capuano, V., Carter, N.M., Choi, S.K., Cordani, J.J., Connerton, I.F., Cummings, N.J., Daniel, R.A., Denziot, F., Devine, K.M., Dusterhoft, A., Ehrlich, S.D., Emmerson, P.T., Entian, K.D., Errington, J., Fabret, C., Ferrari, E., Foulger, D., Fritz, C., Fujita, M., Fujita, Y., Fuma, S., Galizzi, A., Galleron, N., Ghim, S.Y., Glaser, P., Goffeau, A., Golightly, E.J., Grandi, G., Guiseppi, G., Guy, B.J., Haga, K., Haiech, J., Harwood, C.R., Henaut, A., Hilbert, H., Holsappel, S., Hosono, S.,

Hullo, M.F., Itaya, M., Jones, L., Joris, B., Karamata, D., Kasahara, Y., Klaerr-Blanchard, M., Klein, C., Kobayashi, Y., Koetter, P., Koningstein, G., Krogh, S., Kumano, M., Kurita, K., Lapidus, A., Lardinois, S., Lauber, J., Lazarevic, V., Lee, S.M., Levine, A., Liu, H., Masuda, S., Mauel, C., Medigue, C., Medina, N., Mellado, R.P., Mizuno, M., Moestl, D., Nakai, S., Noback, M., Noone, D., O'Reilly, M., Ogawa, K., Ogiwara, A., Oudega, B., Park, S.H., Parro, V., Pohl, T.M., Portelle, D., Porwollik, S., Prescott, A.M., Presecan, E., Pujic, P., Purnelle, B., Rapoport, G., Rey, M., Reynolds, S., Rieger, M., Rivolta, C., Rocha, E., Roche, B., Rose, M., Sadaie, Y., Sato, T., Scanlan, E., Schleich, S., Schroeter, R., Scoffone, F., Sekiguchi, J., Sekowska, A., Seror, S.J., Serror, P., Shin, B.S., Soldo, B., Sorokin, A., Tacconi, E., Takagi, T., Takahashi, H., Takemaru, K., Takeuchi, M., Tamakoshi, A., Tanaka, T., Terpstra, P., Togoni, A., Tosato, V., Uchiyama, S., Vandebol, M., Vannier, F., Vassarotti, A., Viari, A., Wambutt, R., Wedler, H., Weitzenegger, T., Winters, P., Wipat, A., Yamamoto, H., Yamane, K., Yasumoto, K., Yata, K., Yoshida, K., Yoshikawa, H.F., Zumstein, E., Yoshikawa, H., Danchin, A., 1997. The complete genome sequence of the gram-positive bacterium Bacillus subtilis. Nature 390, 249-256.

Le, A.T., Schumann, W., 2008. Regulation of the spoVM gene of Bacillus subtilis. Current Microbiology 57, 484-489.

Levin, P.A., Fan, N., Ricca, E., Driks, A., Losick, R., Cutting, S.M., 1993. An unusually small gene required for sporulation by Bacillus subtilis. Molecular Microbiology 9, 761-771.

Little, S., Driks, A., 2001. Functional analysis of the Bacillus subtilis morphogenetic spore coat protein CotE. Molecular Microbiology 42, 1107-1120.

Maughan, H., Van der Auwera, G., 2011. Bacillus taxonomy in the genomic era finds phenotypes to be essential though often misleading. Infection, Genetics and Evolution 11, 789-797.

McCarter, L.L., 2006. Regulation of flagella. Current Opinion in Microbiology 9, 180-186.

McKenney, P.T., Driks, A., Eichenberger, P., 2013. The Bacillus subtilis endospore: assembly and functions of the multilayered coat. Nature Reviews Microbiology 11, 33-44.

McKenney, P.T., Driks, A., Eskandarian, H.A., Grabowski, P., Guberman, J., Wang, K.H., Gitai, Z., Eichenberger, P., 2010. A distance-weighted interaction map reveals a previously uncharacterized layer of the Bacillus subtilis spore coat. Current Biology 20, 934-938.

McKenney, P.T., Eichenberger, P., 2012. Dynamics of spore coat morphogenesis in Bacillus subtilis. Molecular Microbiology 83, 245-260.

McPherson, D.C., Kim, H., Hahn, M., Wang, R., Grabowski, P., Eichenberger, P., Driks, A., 2005. Characterization of the Bacillus subtilis spore morphogenetic coat protein CotO. Journal of Bacteriology 187, 8278-8290.

Meisner, J., Wang, X., Serrano, M., Henriques, A.O., Moran, C.P., Jr., 2008. A channel connecting the mother cell and forespore during bacterial endospore formation. Proceedings of the National Academy of Sciences of the United States of America 105, 15100-15105.

Min, K.T., Hilditch, C.M., Diederich, B., Errington, J., Yudkin, M.D., 1993. Sigma F, the first compartment-specific transcription factor of B. subtilis, is regulated by an anti-sigma factor that is also a protein kinase. Cell 74, 735-742.

Molle, V., Fujita, M., Jensen, S.T., Eichenberger, P., Gonzalez-Pastor, J.E., Liu, J.S., Losick, R., 2003. The Spo0A regulon of Bacillus subtilis. Molecular Microbiology 50, 1683-1701.

Morlot, C., Uehara, T., Marquis, K.A., Bernhardt, T.G., Rudner, D.Z., 2010. A highly coordinated cell wall degradation machine governs spore morphogenesis in Bacillus subtilis. Genes & Development 24, 411-422.

Morrison, E.W., Rettger, L.F., 1930. Bacterial Spores II. A Study of Bacterial Spore Germination in Relation to Environment. Journal of Bacteriology 20, 313-342.

Mullerova, D., Krajcikova, D., Barak, I., 2009. Interactions between Bacillus subtilis early spore coat morphogenetic proteins. FEMS Microbiology Letters 299, 74-85.

Naclerio, G., Baccigalupi, L., Zilhao, R., De Felice, M., Ricca, E., 1996. Bacillus subtilis spore coat assembly requires cotH gene expression. Journal of Bacteriology 178, 4375-4380.

Nakano, M.M., Zuber, P., 1998. Anaerobic growth of a "strict aerobe" (Bacillus subtilis). Annual Review of Microbiology 52, 165-190.

Nazina, T.N., Lebedeva, E.V., Poltaraus, A.B., Tourova, T.P., Grigoryan, A.A., Sokolova, D., Lysenko, A.M., Osipov, G.A., 2004. Geobacillus gargensis sp. nov., a novel thermophile from a hot spring, and the reclassification of Bacillus vulcani as Geobacillus vulcani comb. nov. International Journal of Systematic and Evolutionary Microbiology 54, 2019-2024.

Nicholson, W.L., 2002. Roles of Bacillus endospores in the environment. Cellular and Molecular Life Sciences 59, 410-416.

Nicholson, W.L., Fajardo-Cavazos, P., Rebeil, R., Slieman, T.A., Riesenman, P.J., Law, J.F., Xue, Y., 2002. Bacterial endospores and their significance in stress resistance. Antonie van Leeuwenhoek 81, 27-32.

Nicholson, W.L., Munakata, N., Horneck, G., Melosh, H.J., Setlow, P., 2000. Resistance of Bacillus endospores to extreme terrestrial and extraterrestrial environments. Microbiology and Molecular Biology Reviews 64, 548-572.

Ozin, A.J., Costa, T., Henriques, A.O., Moran, C.P., Jr., 2001a. Alternative translation initiation produces a short form of a spore coat protein in Bacillus subtilis. Journal of Bacteriology 183, 2032-2040.

Ozin, A.J., Henriques, A.O., Yi, H., Moran, C.P., Jr., 2000. Morphogenetic proteins SpoVID and SafA form a complex during assembly of the Bacillus subtilis spore coat. Journal of Bacteriology 182, 1828-1833.

Ozin, A.J., Samford, C.S., Henriques, A.O., Moran, C.P., Jr., 2001b. SpoVID guides SafA to the spore coat in Bacillus subtilis. Journal of Bacteriology 183, 3041-3049.

Perego, M., Glaser, P., Hoch, J.A., 1996. Aspartyl-phosphate phosphatases deactivate the response regulator components of the sporulation signal transduction system in Bacillus subtilis. Molecular Microbiology 19, 1151-1157.

Permpoonpattana, P., Tolls, E.H., Nadem, R., Tan, S., Brisson, A., Cutting, S.M., 2011. Surface layers of Clostridium difficile endospores. Journal of Bacteriology 193, 6461-6470.

Piggot, P.J., Coote, J.G., 1976. Genetic aspects of bacterial endospore formation. Bacteriological Reviews 40, 908-962.

Piggot, P.J., Hilbert, D.W., 2004. Sporulation of Bacillus subtilis. Current Opinion in Microbiology 7, 579-586.

Piggot, P.J., Losick, R., 2002. Sporulation genes and intercompartmental regulation. In: Sonenshein, A.L. (Ed.), Bacillus subtilis and its closest relatives: from genes to cells. American Society of Microbiology, Washington, pp. 483-518.

Plomp, M., Carroll, A.M., Setlow, P., Malkin, A.J., 2014. Architecture and assembly of the Bacillus subtilis spore coat. PlOS One 9, e108560.

Popham, D.L., 2002. Specialized peptidoglycan of the bacterial endospore: the inner wall of the lockbox. Cellular and Molecular Life Sciences 59, 426-433.

Prajapati, R.S., Ogura, T., Cutting, S.M., 2000. Structural and functional studies on an FtsH inhibitor from Bacillus subtilis. Biochimica et Biophysica Acta 1475, 353-359.

Price, K.D., Losick, R., 1999. A four-dimensional view of assembly of a morphogenetic protein during sporulation in Bacillus subtilis. Journal of Bacteriology 181, 781-790.

Putnam, E.E., Nock, A.M., Lawley, T.D., Shen, A., 2013. SpoIVA and SipL are Clostridium difficile spore morphogenetic proteins. Journal of Bacteriology 195, 1214-1225.

Qiao, H., Krajcikova, D., Liu, C., Li, Y., Wang, H., Barak, I., Tang, J., 2012. The interactions of spore-coat morphogenetic proteins studied by single-molecule recognition force spectroscopy. Chemistry - An Asian Journal 7, 725-731.

Ragkousi, K., Eichenberger, P., van Ooij, C., Setlow, P., 2003. Identification of a new gene essential for germination of Bacillus subtilis spores with Ca2+-dipicolinate. Journal of Bacteriology 185, 2315-2329.

Ramamurthi, K.S., Clapham, K.R., Losick, R., 2006. Peptide anchoring spore coat assembly to the outer forespore membrane in Bacillus subtilis. Molecular Microbiology 62, 1547-1557.

Ramamurthi, K.S., Lecuyer, S., Stone, H.A., Losick, R., 2009. Geometric cue for protein localization in a bacterium. Science 323, 1354-1357.

Ramamurthi, K.S., Losick, R., 2008. ATP-driven self-assembly of a morphogenetic protein in Bacillus subtilis. Molecular Cell 31, 406-414.

Rasmussen, S., Nielsen, H.B., Jarmer, H., 2009. The transcriptionally active regions in the genome of Bacillus subtilis. Molecular Microbiology 73, 1043-1057.

Riesenman, P.J., Nicholson, W.L., 2000. Role of the spore coat layers in Bacillus subtilis spore resistance to hydrogen peroxide, artificial UV-C, UV-B, and solar UV radiation. Applied and Environmental Microbiology 66, 620-626.

Robleto, E.A., Martin, H.A., Pepper, A.M., Pedraza-Reyes, M., 2012. Gene regulation of sporulation in *Bacillus subtilis*. In: Abel-Santos, E. (Ed.), Bacterial spores: current research and applications. Caister Academic Press,

Norfolk, United Kingdom, pp. 9-17.

Roels, S., Driks, A., Losick, R., 1992. Characterization of spoIVA, a sporulation gene involved in coat morphogenesis in Bacillus subtilis. Journal of Bacteriology 174, 575-585.

Ryter, A., 1965. Etude morphologique de la sporulation de Bacillus subtilis. Annales de l'Institut Pasteur 108, 40-60.

Sato, T., Samori, Y., Kobayashi, Y., 1990. The cisA cistron of Bacillus subtilis sporulation gene spoIVC encodes a protein homologous to a site-specific recombinase. Journal of Bacteriology 172, 1092-1098.

Serrano, M., Real, G., Santos, J., Carneiro, J., Moran, C.P., Jr., Henriques, A.O., 2011. A negative feedback loop that limits the ectopic activation of a cell type-specific sporulation sigma factor of Bacillus subtilis. PLOS Genetics 7, e1002220.

Setlow, P., 2006. Spores of Bacillus subtilis: their resistance to and killing by radiation, heat and chemicals. Journal of applied microbiology 101, 514-525.

Smits, W.K., Bongiorni, C., Veening, J.W., Hamoen, L.W., Kuipers, O.P., Perego, M., 2007. Temporal separation of distinct differentiation pathways by a dual specificity Rap-Phr system in Bacillus subtilis. Molecular Microbiology 65, 103-120.

Sonenshein, A.L., 2000. Control of sporulation initiation in Bacillus subtilis. Current Opinion in Microbiology 3, 561-566.

Steil, L., Serrano, M., Henriques, A.O., Volker, U., 2005. Genome-wide analysis of temporally regulated and compartment-specific gene expression in sporulating cells of Bacillus subtilis. Microbiology 151, 399-420.

Stevens, C.M., Daniel, R., Illing, N., Errington, J., 1992. Characterization of a sporulation gene, spoIVA, involved in spore coat morphogenesis in Bacillus subtilis. Journal of Bacteriology 174, 586-594.

Stragier, P., Kunkel, B., Kroos, L., Losick, R., 1989. Chromosomal rearrangement generating a composite gene for a developmental transcription factor. Science 243, 507-512.

Sun, D.X., Stragier, P., Setlow, P., 1989. Identification of a new sigma-factor involved in compartmentalized gene expression during sporulation of Bacillus subtilis. Genes & Development 3, 141-149.

Takamatsu, H., Imamura, A., Kodama, T., Asai, K., Ogasawara, N., Watabe, K.,

2000a. The yabG gene of Bacillus subtilis encodes a sporulation specific protease which is involved in the processing of several spore coat proteins. FEMS Microbiology Letters 192, 33-38.

Takamatsu, H., Kodama, T., Imamura, A., Asai, K., Kobayashi, K., Nakayama, T., Ogasawara, N., Watabe, K., 2000b. The Bacillus subtilis yabG gene is transcribed by SigK RNA polymerase during sporulation, and yabG mutant spores have altered coat protein composition. Journal of Bacteriology 182, 1883-1888.

Takamatsu, H., Kodama, T., Nakayama, T., Watabe, K., 1999. Characterization of the yrbA gene of Bacillus subtilis, involved in resistance and germination of spores. Journal of Bacteriology 181, 4986-4994.

Tam, N.K., Uyen, N.Q., Hong, H.A., Duc le, H., Hoa, T.T., Serra, C.R., Henriques, A.O., Cutting, S.M., 2006. The intestinal life cycle of Bacillus subtilis and close relatives. Journal of Bacteriology 188, 2692-2700.

Tars, K., Fridborg, K., Bundule, M., Liljas, L., 2000. The three-dimensional structure of bacteriophage PP7 from Pseudomonas aeruginosa at 3.7-A resolution. Virology 272, 331-337.

Torred, M., Benjelloun, E., Dibala, E., Abel-Santos, E., Ross, C., 2012. Historical notes and introduction to bacterial spores. In: Abel-Santos, E. (Ed.), Bacterial spores: current research and applications. Caister Academic Press, Norfolk, United Kingdom, pp. 1-7.

van Ooij, C., Eichenberger, P., Losick, R., 2004. Dynamic patterns of subcellular protein localization during spore coat morphogenesis in Bacillus subtilis. Journal of Bacteriology 186, 4441-4448.

van Ooij, C., Losick, R., 2003. Subcellular localization of a small sporulation protein in Bacillus subtilis. Journal of Bacteriology 185, 1391-1398.

Vreeland, R.H., Rosenzweig, W.D., Powers, D.W., 2000. Isolation of a 250 million-year-old halotolerant bacterium from a primary salt crystal. Nature 407, 897-900.

Waller, L.N., Fox, N., Fox, K.F., Fox, A., Price, R.L., 2004. Ruthenium red staining for ultrastructural visualization of a glycoprotein layer surrounding the spore of Bacillus anthracis and Bacillus subtilis. Journal of Microbiological Methods 58, 23-30.

Wang, K.H., Isidro, A.L., Domingues, L., Eskandarian, H.A., McKenney, P.T., Drew, K., Grabowski, P., Chua, M.H., Barry, S.N., Guan, M., Bonneau, R., Henriques, A.O., Eichenberger, P., 2009. The coat morphogenetic protein

SpoVID is necessary for spore encasement in Bacillus subtilis. Molecular Microbiology 74, 634-649.

Westphal, A.J., Price, P.B., Leighton, T.J., Wheeler, K.E., 2003. Kinetics of size changes of individual Bacillus thuringiensis spores in response to changes in relative humidity. Proceedings of the National Academy of Sciences of the United States of America 100, 3461-3466.

Wu, L.J., Errington, J., 1997. Septal localization of the SpoIIIE chromosome partitioning protein in Bacillus subtilis. The EMBO Journal 16, 2161-2169.

Yukimura, K., Nakai, R., Kohshima, S., Uetake, J., Kanda, H., Naganuma, T., 2009. Spore-forming halophilic bacteria isolated from Arctic terrains: implications for long-range transportation of microorganisms. Polar Science 3, 163-169.

Zhang, J., Ichikawa, H., Halberg, R., Kroos, L., Aronson, A.I., 1994. Regulation of the transcription of a cluster of Bacillus subtilis spore coat genes. Journal of Molecular Biology 240, 405-415.

Zheng, L.B., Donovan, W.P., Fitz-James, P.C., Losick, R., 1988. Gene encoding a morphogenic protein required in the assembly of the outer coat of the Bacillus subtilis endospore. Genes & Development 2, 1047-1054.

Zilhao, R., Isticato, R., Martins, L.O., Steil, L., Volker, U., Ricca, E., Moran, C.P., Jr., Henriques, A.O., 2005. Assembly and function of a spore coat-associated transglutaminase of Bacillus subtilis. Journal of Bacteriology 187, 7753-7764.

Zilhao, R., Naclerio, G., Henriques, A.O., Baccigalupi, L., Moran, C.P., Jr., Ricca, E., 1999. Assembly requirements and role of CotH during spore coat formation in Bacillus subtilis. Journal of Bacteriology 181, 2631-2633.

Chapter 2

Interaction between SpoVID and CotE is necessary for spore encasement

This chapter contains data published in: de Francesco, M., Jacobs, J. Z., Nunes, F., Serrano, M., McKenney, P. T., Chua, M. H., Henriques, A. O. and Eichenberger, P. (2012) **Physical interaction between coat morphogenetic proteins SpoVID and CotE is necessary for spore encasement in *Bacillus subtilis***. *Journal of Bacteriology*, 194(18), pp. 4941-50.

The author of this dissertation participated directly in mapping of the interaction between SpoVID and SafA, in oligomerization assays and in SpoVID controlled digestion.

SUMMARY

During sporulation in *Bacillus subtilis*, a protective, multilayered, proteinaceous coat composed of at least 80 different proteins is assembled around the spore. Spore coat formation is divided in two distinct stages. The first is the recruitment of proteins to the spore surface, dependent on the morphogenetic protein SpoIVA. The second step, known as encasement, involves the migration of the coat proteins around the circumference of the spore in successive waves. This step is dependent on the morphogenetic protein SpoVID and the transcriptional regulation of individual coat genes.

In this study, we provide genetic and biochemical evidence supporting that SpoVID promotes encasement of the spore by establishing direct protein-protein interactions with other coat morphogenetic proteins. It was previously demonstrated that SpoVID directly interacts with SpoIVA and with the inner coat morphogenetic protein, SafA. Here, we show by yeast two-hybrid and pulldown assays that SpoVID also interacts directly with the outer coat morphogenetic protein, CotE. Mutational analysis revealed a specific residue in the N-terminal domain of SpoVID that is essential for the interaction with CotE but dispensable to bind SafA. We discuss the structural features of the N-terminal domain of SpoVID and we provide evidence for oligomerization of this domain. Finally, we propose an updated model of coat assembly and spore encasement that incorporates several physical interactions between the major coat morphogenetic proteins.

INTRODUCTION

The *Bacillus subtilis* spore coat is a macromolecular structure whose assembly involves the coordinated association of over 80 proteins (Driks, 1999; Kuwana *et al.*, 2002; Lai *et al.*, 2003; Henriques and Moran, 2007; McKenney and Eichenberger, 2012). These proteins are organized in four distinct structural layers: a basement layer, a lamellar inner coat, a thick outer coat, and an outermost layer, or crust (Henriques and Moran, 2007; McKenney *et al.*, 2010) (see *"Structure of the coat"*, in Chapter 1). Coat morphogenesis consists of two coordinated but genetically separable phenomena: protein localization and spore encasement (Wang *et al.*, 2009). As the coat genes are expressed at the mother cell compartment, the proteins assemble into a scaffold cap on the mother cell-proximal (MCP) pole of the forespore shortly after the beginning of engulfment (Driks *et al.*, 1994; McKenney and Eichenberger, 2012). Then, in three successive waves, coordinated sets of coat proteins encase the spore to establish shells of each coat layer. Throughout the course of sporulation, coat proteins are synthesized, localized to the spore surface, and added to the underlying spore coat scaffold (McKenney and Eichenberger, 2012) (for a detailed description, see sections "*Two steps in coat assembly: targeting and encasement"* and *"Successive waves of encasement during coat morphogenesis"*, in Chapter 1). During this process, protein-protein interactions between coat components, including homo-oligomerization, are thought to play a determinant role (Ozin *et al.*, 2000; Costa *et al.*, 2006; Ramamurthi *et al.*, 2006; Mullerova *et al.*, 2009).

The localization of the coat components is governed by morphogenetic proteins (Piggot and Coote, 1976; Zheng *et al.*, 1988; Roels *et al.*, 1992; Driks, 1999; Henriques and Moran, 2007). Among those, SpoIVA, SafA and CotE are primarily involved in localization of coat proteins to the spore surface. SpoIVA is required for attachment of the entire spore coat,

whereas SafA is specifically involved in assembly of the inner coat and CotE is responsible for assembly of the outer coat and the crust (Piggot and Coote, 1976; Zheng *et al.*, 1988; Roels *et al.*, 1992; Driks *et al.*, 1994; Takamatsu *et al.*, 1999; Ozin *et al.*, 2000; McKenney *et al.*, 2010; Imamura *et al.*, 2011). In contrast, SpoVM is necessary for spore encasement of all known coat proteins, and SpoVID is required for encasement of most of them (Driks *et al.*, 1994; Wang *et al.*, 2009). Domain analysis of SpoVID based on defined deletion mutations led to the identification of a region essential for encasement at the end of its N-terminal domain (residues 86 – 136). Regarding encasement by CotE, this region was restricted to only 12 amino acid residues, between L125 and L136 (Wang *et al.*, 2009) (Fig. 2.1).

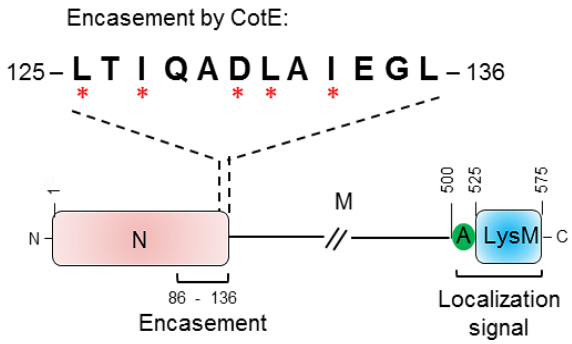

Figure 2.1 – The region between residues 86 and 136 at the N-terminal domain of SpoVID (N) is essential for encasement (Wang *et al.*, 2009). Within this region, encasement by CotE requires residues L125 – L136. Red asterisks point the residues whose roles were tested in this study.

The mechanism that promotes migration of the coat proteins around the spore during encasement is poorly understood. Since SpoVID forms oligomers *in vitro* (Ozin *et al.*, 2000; Mullerova *et al.*, 2009), it is possible that it multimerizes at the spore surface while establishing protein-protein interactions with other coat components. In this manner, coat proteins would be dragged by SpoVID around the spore circumference, eventually surrounding it.

In this study, we identified specific residues in the N-terminal domain of SpoVID that are necessary for encasement by the outer coat

morphogenetic protein CotE. We also discovered a direct interaction between SpoVID and CotE. Some of the same residues that are essential for the encasement function of SpoVID are also necessary for the physical interaction between SpoVID and CotE. This links the mechanism of spore encasement by the CotE and the outer coat proteins to a specific protein-protein interaction. Moreover, we investigated the function of the two cysteines of the N-terminal domain of SpoVID in oligomerization, and we show that this domain is likely to be structured. We propose a model for encasement that integrates the interactions of SpoVID with SafA (Ozin *et al.*, 2001b; Costa *et al.*, 2006) and CotE, as well as the oligomerization of SpoVID.

MATERIALS AND METHODS

Bacterial strains, media and general methods

All bacterial strains used in this study are listed in Table 2.1. DNA manipulation and other molecular methods were performed according to standard protocols. *Escherichia coli* DH5α (Invitrogen) was used for cloning, while *E. coli* BL21(DE3), *E. coli* BL21(DE3)/pLysS and *E.coli* CC118(DE3)/ pLysS were used for protein expression. All *B. subtilis* strains are congenic derivatives of the wild type strain PY79 (Youngman *et al.*, 1984). Cells were routinely grown in Luria-Bertani (LB) broth or in LB agar, supplemented with the appropriate antibiotics when needed. *B. subtilis* competent cells were prepared as described previously (Nicholson and Setlow, 1990), and sporulation was achieved by using a resuspension protocol (Sterlini and Mandelstam, 1969).

Plasmids and strains construction

Plasmids and oligonucleotides used in this study are listed in Tables A2 and A3 of the Appendices, respectively. For His-tag pulldown assays,

Table 2.1: Bacterial and yeast strains used in this study

Strains	Relevant properties	Source
B. subtilis		
PY79	Prototrophic derivative of *B. subtilis* 168	Youngman *et al*., 1984
RL1070	*spoVID*::*kan*	Driks *et al*., 1994
HS176	*cotZ*ΩpHS2 (*cotZ-gfp spc*)	Kim *et al*., 2006
KW363	*spoVID*::*kan amyE*::*spoVID-cfp cat cotE*ΩpPM19 (*cotE-yfp spc*)	Wang *et al*., 2009
PE793	*yaaH*ΩpKW10 (*yaaH-gfp spc*)	This study
PE1496	*cotO*ΩpPM4 (*cotO-yfp spc*)	"
PE1547	*spoIVA*Ω*spoIVA-yfp spc*	"
PE2091	*spoVID*::*kan amyE*::*spoVID*$_{\Delta 125\text{-}136}$*-cfp cat*	"
PE2094	*spoVID*::*kan amyE*::*spoVID*$_{\Delta 125\text{-}136}$*-cfp cat cotE*Ω*cotE-yfp spc*	"
PE2269	*spoVID*::*kan amyE*::*spoVID*$_{L131A}$*-cfp cat*	"
PE2273	*spoVID*::*kan amyE*::*spoVID*$_{L125A}$*-cfp cat cotE*Ω*cotE-yfp spc*	"
PE2274	*spoVID*::*kan amyE*::*spoVID*$_{I127A}$*-cfp cat cotE*Ω*cotE-yfp spc*	"
PE2275	*spoVID*::*kan amyE*::*spoVID*$_{D130A}$*-cfp cat cotE*Ω*cotE-yfp spc*	"
PE2276	*spoVID*::*kan amyE*::*spoVID*$_{L131A}$*-cfp* cat *cotE*Ω*cotE-yfp spc*	"
PE2277	*spoVID*::*kan amyE*::*spoVID*$_{I133A}$*-cfp cat cotE*Ω*cotE-yfp spc*	"
PE2283	*spoVID*::*kan amyE*::*spoVID*$_{L131A}$*-cfp cat spoIVA*Ω*spoIVA-yfp spc*	"
PE2608	*spoVID*::*kan amyE*::*spoVID*$_{\Delta 125\text{-}136}$*-cfp cat cotO*Ω*cotO-yfp spc*	"
PE2611	*spoVID*::*kan amyE*::*spoVID*$_{\Delta 125\text{-}136}$*-cfp cat cotZ*Ω*cotZ-gfp spc*	"
PE2612	*spoVID*::*kan amyE*::*spoVID*$_{\Delta 125\text{-}136}$*-cfp cat yaaH*Ω*yaaH-gfp spc*	"
PE2621	*spoVID*::*kan amyE*::*spoVID*$_{\Delta 125\text{-}136}$*-cfp cat spoIVA*Ω*spoIVA-yfp spc*	"
PE2616	*spoVID*::*kan amyE*::s*poVID*$_{L131A}$*-cfp cat cotO*Ω*cotO-yfp spc*	"
PE2619	*spoVID*::*kan amyE*::*spoVID*$_{L131A}$*-cfp cat cotZ*Ω*cotZ-gfp spc*	"
PE2620	*spoVID*::*kan amyE*::*spoVID*$_{L131A}$*-cfp cat yaaH*Ω*yaaH-gfp spc*	"
E. coli		
DH5α	F$^-$ Φ80*lac*ZΔM15 Δ(*lac*ZYA-*ara*F) U169 *rec*A1 *end*A1 *hsd*R17 (rK$^-$, mK$^+$) *pho*A *sup*E44 λ$^-$ *thi*-1 *gyr*A96 *rel*A1	Invitrogen
BL21	F$^-$ dcm ompT hsdS(rB$^-$ mB$^-$) gal λ(DE3)	Promega
BL21	F$^-$ dcm ompT hsdS(rB$^-$ mB$^-$) gal λ(DE3) pLysS (Cm^r)	Novagen
CC118	Δ(ara-leu) araD ΔlacX74 galE galK phoA20 thi-1 rpsE rpoB argE(Am) recAl λ(DE3) pLysS (Cm^r)	Colin Manoil
PE2622	DH5α */spoVID-his* in pET21b	This study
PE2623	BL21(DE3)/*spoVID-his* in pET21b	"
PE2624	BL21(DE3)/*cotE-STOP* in pET21b	"
PE2625	BL21(DE3)/*spoVIDL125A-his* in pET21b	"

Table 2.1: Bacterial and yeast strains used in this study (cont.)

Strains	Relevant properties	Source
PE2626	BL21(DE3)/*spoVIDI127A-his* in pET21b	This study
PE2627	BL21(DE3)/*spoVIDD130A-his* in pET21b	"
PE2628	BL21(DE3)/*spoVIDL131A-his* in pET21b	"
PE2629	BL21(DE3)/*spoVID125-136-his* in pET21b	"
PE2630	BL21(DE3)/*spoVIDI133A-his* in pET21b	"
AH1455	BL21(DE3)/pLysS/*his-S-spoVID* in pET30	Lab. stock
AH1982	BL21(DE3)/pLysS/pTC37 (*his-spoVID* in pET16b)	This study
AH5140	BL21(DE3)/pFN30 (*his-spoVID*$_{C16A}$ in pET16b)	"
AH5141	BL21(DE3)/pFN31 (*his-spoVID*$_{C90A}$ in pET16b)	"
AH5142	BL21(DE3)/pFN32 (*his-spoVID*$_{C16A,C90A}$ in pET16b)	"
AH5312	BL21(DE3)/pFN97 (*his-spoVID*$_{N160}$ in pET16b)	"
AH5348	BL21(DE3)/pFN98 (*his-spoVID*$_{N160, C16A}$ in pET16b)	"
AH5349	BL21(DE3)/pFN99 (*his-spoVID*$_{N160, C90A}$ in pET16b)	"
AH5350	BL21(DE3)/pFN100 (*his-spoVID*$_{N160, C16A,C90A}$ in pET16b)	"
AH2687	CC118(DE3)/pLysS/*gst* in pGEX-4T-3	Costa *et al*., 2006
AH2937	CC118(DE3)/pLysS/*gst-safA*$_{162}$ in pGEX-4T-3	"
Yeast		
Y8800	*MATa leu2-3,112 trp1-901 his3Δ200 ura3-52 gal4Δ gal80Δ cyh2R GAL2*::*ADE2*, *GAL1*::*HIS3-@LYS2*, *GAL7*::*lacZ@met2*	Boxem *et al*., 2008
Y8930	*MAT leu2-3,112 trp1-901 his3Δ200 ura3-52 gal4Δ gal80Δ cyh2R GAL2*::*ADE2*, *GAL1*::*HIS3-@LYS2*, *GAL7*::*lacZ@met2*	"
YPE324	Y8930 + p*cotE(1-158)-AD*	This study
YPE343	Y8800 + p*spoVID(1-144)-BD*	"
YPE511	Y8800 + p*spoVID(1-144 L131A)-BD*	"
YPE513	Y8800 + p*spoVID(1-144 I133A)-BD*	"
YPE518	Y8930 + pDEST-AD	"
YPE519	Y8800 + pDEST-BD	"
YPE600	Y8800/Y8930 + p*fos-AD* + p*jun-BD*	Walhout *et al.*, 2000a

the coding sequences of *spoVID* and *cotE* were cloned into pET21b vector (EMD4Biosciences), resulting in plasmids pET21b-*spoVID-his* and pET21b-*cotE-STOP*. *spoVID* was amplified and inserted into the NdeI and XhoI of the vector, creating when expressed, an in-frame His-tag fusion to the C terminus of SpoVID. *cotE* was also inserted into the same sites of pET21b, with the

exception that tandem stop codons were built into the primers, such that CotE, when expressed, would not harbor the C-terminal His-tag.

Plasmids pKW50, containing *spoVID-cfp* as well as sequences required for integration at the nonessential *amyE* locus (Wang *et al.*, 2009), and pET21b-*spoVID-his* were used as templates to insert single amino acid substitutions in SpoVID-CFP and SpoVID-His constructs. As reported previously (Wang *et al.*, 2009), the SpoVID-CFP fusion is functional in spore germination assays, which provide an indirect measurement of spore coat integrity. PCR mutagenesis was carried out using the QuikChange mutagenesis kit (Stratagene), and introduction of the mutations was confirmed by sequence analysis. The mutated plasmids with the *spoVID-his* and *spoVID-cfp* constructs were then transformed into the recipient strains *B. subtilis spoVID*::*kan* RL1070 (Driks *et al.*, 1994) and *E. coli* BL21(DE3), respectively. Integration into the *amyE* locus was selected for based on acquisition of chloramphenicol resistance and loss of spectinomycin resistance.

For oligomerization assays, *spoVID* was amplified and cloned into pET16b vector (Novagen), generating the plasmid pTC37, for His-SpoVID expression. This vector was used as a template to introduce two stop codons at the positions 161 and 162 of SpoVID by site-directed mutagenesis, creating, when expressed, a truncated version of His-SpoVID comprising only the first 160 amino acid residues (His-SpoVID$_{N160}$). The resulting plasmid was pFN97. By the same technique, the single alanine substitutions C16A or C90A were inserted in both His-SpoVID and His-SpoVID$_{N160}$ constructs, using pTC37 and pFN97 as templates. This generates plasmids pFN30 (*his-spoVID*$_{C16A}$), pFN31 (*his-spoVID*$_{C90A}$), pFN98 (*his-spoVID*$_{N160,\ C16A}$) and pFN99 (*his-spoVID*$_{N160,\ C90A}$). Finally, C90A was also introduced in pFN30 and pFN98, resulting in plasmids pFN32 (*his-spoVID*$_{C16A,C90A}$) and pFN100 (*his-spoVID*$_{N160,\ C16A,C90A}$). The eight vectors created were then transformed into the recipient strains *E. coli* BL21(DE3) or BL21(DE3)/pLysS, for proteins expression.

Fluorescence microscopy and MCD cap quantification

Fluorescence microscopy was performed as previously described (Kim *et al.*, 2006; McKenney and Eichenberger, 2012). All measurements were calculated using ImageJ. Background fluorescence was quantified by averaging the fluorescence intensity of 10 random cell-free regions of equal area by using the "measure" function. An ROI (region of interest) threshold ("threshold" function) was chosen empirically so that maximum separation of MCP and mother cell distal (MCD) caps in wild type cells expressing a CotE-GFP at hour 3 was observed. ROIs were drawn using the "analyze particles" function. Cells were then examined and scored individually as single cap (a sporangium that contains only a single ROI of the MCP cap) or 2 caps (a sporangium that contains an MCP and MCD cap). Sporangia containing 2 caps were subdivided into "unconnected" (2 separated ROIs of the MCP and MCD cap) and "connected" (a single continuous ROI that contains a protrusion of above-threshold pixels toward the MCD pole). The area of the MCD caps in pixels was recorded for each sporangium containing unconnected CotE-GFP caps.

Yeast two-hybrid assays

We followed the procedure described by Boxem *et al.* (Boxem *et al.*, 2008). Specifically, fusions of the N-terminal domain of SpoVID (residues 1 to 144) to the Gal4p DNA-binding domain (BD) and of a truncated version of CotE (residues 1 – 158) to the activation domain (AD) were created using the Gateway cloning system (Invitrogen). Genomic DNA from *B. subtilis* was PCR amplified with specific primers for *cotE* or *spoVID* and *attB* overhangs (CotE F1/R1 and SpoVID F1/R1 primers, respectively). PCR products were cloned into the pDONR221 entry vector with the BP Clonase II enzyme kit (Invitrogen) and subcloned into the pDEST-AD and pDEST-BD vectors (Walhout *et al.*, 2000b) using the LR Clonase II enzyme mix (Invitrogen). pDEST-AD and -BD vectors generated from the Gateway system were

checked for proper insertion by PCR and transformed into haploid strains Y8930 and Y8800 (gifts from Mike Boxem, Harvard Medical School), respectively, by using the lithium acetate transformation protocol (Walhout and Vidal, 2001). The genotypes of the *Saccharomyces cerevisiae* strains used in this study are listed in Table 2.1.

Self-activator constructs were discarded after plating all haploid yeast on medium lacking histidine. Strains to be tested for interaction were plated on yeast extract-peptone-dextrose (YEPD) and grown for 3 days at 30°C. Equal amounts of transformed haploid Y8800 and Y8930 strains (James *et al.*, 1996) were then mixed and plated on YEPD for 20 h at 30°C to encourage mating. Diploid yeast cells were selected on SC medium lacking leucine and tryptophan. After 3 days of growth at 30°C, diploid cells were diluted 1:1 000 and plated on SC medium lacking leucine and tryptophan (to maintain selection for both AD and BD vectors) and with histidine in the presence or absence of 5 mM 3-amino-1,2-4-triazole (3AT; Sigma). Growth was assayed after 3 days of incubation at 30°C. As a positive control, we included on every plate a yeast strain expressing Jun-AD and Fos-BD fragments (Walhout *et al.*, 2000a). As a negative control, we mated the *MATα* strain containing an empty pDEST-AD vector to a *MAT*a strain containing an empty pDEST-BD vector. The vectors still express Gal4AD and Gal4BD fragments, but the fragments themselves are unable to interact and induce *HIS3* expression.

His-tag pulldown assays

Twenty-milliliter cultures of *E. coli* BL21(DE3) cells harboring the various variants of pET21b-*spoVID-his* or pET21b-*cotE-STOP* were grown to mid-exponential phase. Protein expression was induced with 1 mM isopropyl β-D-1-thiogalactopyranoside (IPTG) for 3 hours, at 30°C. Cells were then harvested by spinning (4°C, 10 min at 5 500 × *g*), the pellets were resuspended in 10 mL cold lysis buffer (50 mM Na_2HPO_4, 300 mM NaCl, 10

mM imidazole; pH 8.0), and sonication was performed under optimal conditions for cell breakage (amplitude of 50 for 30 s, repeated 4 times; model CL5; QSonica, Misonix). The presence of protein was confirmed by Bradford assay (Bio-Rad). Protein lysates were harvested by centrifugation (4°C, 30 min at 18 000 × *g*) and the soluble fractions were mixed with 500 µL of Ni^{2+} resin (Qiagen) equilibrated in lysis buffer in a 50-mL conical tube (10 mL for the SpoVID lysate, 5 mL for the CotE lysate). The mixtures were incubated on a rotary shaker for 1 h at room temperature to facilitate binding. An a negative control, the CotE bead mixture was then applied to the column. For SpoVID-His samples (either wild type or mutated versions), the remainder of the CotE lysate (5 mL) was mixed in and incubated on a rotary shaker for an additional hour at room temperature. The protein-bead mixtures were poured into a column (Bio-Rad), allowed to flow through, and washed stringently with various wash buffers (40 mL of 50 mM Na_2HPO_4, 300 mM NaCl, 40 mM imidazole [pH 8.0]; 30 mL of 50 mM Na_2HPO_4, 300 mM NaCl, 100 mM imidazole [pH 8.0]; 6 mL of 50 mM Na_2HPO_4, 300 mM NaCl, 250 mM imidazole [pH 8.0]). The proteins were eluted in two stages in pulldown buffer with 500 mM and 1 M imidazole. Samples from each step of the pulldown assay were taken and prepared for SDS-PAGE 12% tris-glycine. Proteins samples were resolved and transferred to nitrocellulose membranes, which were them immunobloted with anti-CotE antibodies.

GST pulldown assays

For the overproduction of native glutathione *S*-transferase (GST) and GST-$SafA_{162}$, the derivatives of *E. coli* CC118(DE3)/pLysS (Costa *et al.*, 2006) were used. Cultures of 10 mL (for GST) or 100 mL (for GST-$SafA_{162}$) were grown to an optical density at 600 nm of 0.6 and protein expression was induced with 1 mM IPTG for 3 hours. SpoVID-His, either wild type or with the substitution L131A, were produced as described previously. Cells were harvested by centrifugation (4°C, 10 min at 7 500 × *g*), resuspended in 1 mL

cold VPEX-100 buffer (100 mM NaCl, 10 mM Tris-HCl [pH 8.0], 1 mM EDTA [pH 8.0], 0.1% Triton X-100, 10% glycerol) (Ozin *et al.*, 2001b) supplemented with 1 mM phenylmethylsulfonyl fluoride (PMSF) and Complete Mini EDTA-free protease inhibitor cocktail (Roche), and lysed in a French pressure cell (18 000 lb/in^2). The lysates were cleared by centrifugation (at 10 000 × *g* for 20 min, 4°C) and diluted in VPEX-100 to adjust concentrations (1:2 for GST-SafA$_{162}$, 1:4 for SpoVID-His variants, and 1:10 for GST). GST pulldown assays were performed as previously described (Ozin *et al.*, 2001b), excepting that the final washes were repeated six times in 0.5 mL of phosphate-buffered saline (PBS) containing 0.1% Tween 20 and 10% glycerol. Bead fractions were prepared and resolved in SDS-PAGE 12.5%. Gels were transferred to nitrocellulose membranes and immunoblotting was performed with anti-SpoVID antibodies.

Oligomerization assays

The His-SpoVID and His-SpoVID$_{N160}$ variants were overproduced using *E. coli* BL21(DE3) derivative strains. Cultures were induced with 1 mM IPTG for 3h, after which cells were harvested by centrifugation (4°C, 10 min at 7 500 × *g*), resuspended in 3 mL of VID buffer (20 mM Tris-HCl [pH 7.5], 150 mM NaCl, 20 mM imidazole, 20% glycerol) supplemented with 1 mM PMSF and Complete Mini EDTA-free protease inhibitor cocktail (Roche), and lysed in a French pressure cell (18 000 lb/in^2). The lysates were cleared by centrifugation (at 4°C, 10 000 × *g* for 20 min) and applied to a 1 mL column filled with Ni-nitriolotriacetic acid (NTA) agarose (Qiagen), previously equilibrated with VID buffer. Column were washed with 10 mL of VID buffer with 1M NaCl, followed by VID buffer with increasing concentrations of imidazole (40 mM, 60 mM, 100 mM). After washings, recombinant proteins were eluted in VID buffer with 200 mM imidazole, quantified by Bradford assay (Biorad), and resolved by SDS-PAGE to confirm purity.

For oligomerization assays, 2 µg of each recombinant protein were

diluted in VID buffer for a final volume of 30 µL, with or without 100 mM DTT. SDS-PAGE loading buffer without β-mercaptoethanol was added and samples were boiled for 5 min and resolved by SDS-PAGE. The acrylamide gels were stained with Coomassie R-blue, or transferred to nitrocellulose membranes for Western blot with anti-SpoVID antibodies.

SpoVID limited trypsinolysis

A derivative strain of the *E. coli* BL21(DE3)/pLysS was used for His-S-SpoVID overproduction. Protein expression and purification was performed as previously described for His-SpoVID variants, using a 1 mL HiTrap Chelating HP column (GE Healthcare). For controlled trypsinolysis, 250 µg of purified His-S-SpoVID were digested with trypsin (1:1 000) for 24h, at 37°C. The reaction was performed in a final volume of 200 µL, in the presence and in the absence of 100 mM DTT. Along the time, 20 µL samples were taken and prepared for SDS-PAGE 10%. Proteins within samples were resolved, and proteolysis-resistant bands were extracted from the gel for identification by MALDI-TOF/TOF MS/MS (Mass Spectrometry Laboratory, Analytical Services Unit, ITQB–AX, Universidade Nova de Lisboa). Each band was submitted to in-gel tryptic digestion and the resulting peptides were extracted, desalted, concentrated and applied into the MALDI plate. Mass spectra of peptides were acquired in a 4800plus MALDI TOF/TOF analyzer, with exclusion list for trypsin autolysis peaks. The collected MS and MS/MS spectra were analyzed using the Mascot search engine with 50 ppm peptide mass tolerance and no taxonomy restrictions. Only peptides with a confidence interval above 95% were considered.

An SDS-PAGE gel with the resolved samples of digested His-S-SpoVID was also transferred to a PVDF membrane. Proteolysis-resistant bands were extracted and analyzed by Edman degradation N-terminal sequencing (PO 101LA; Analytical Services Unit, ITQB–AX, Universidade Nova de Lisboa).

Western blot analysis

Transferred proteins to nitrocellulose membranes were detected using rabbit anti-CotE (a gift from Adam Driks, Loyola University, Chicago, IL) or anti-SpoVID (Costa *et al.*, 2006) polyclonal antibodies at a 1:1 000 dilution, followed by secondary anti-rabbit antibodies conjugated to horseradish peroxidase (1:10 000, Zymed or 1:1 000, Sigma). Secondary antibodies were detected using enhanced chemiluminescence (ECL, Amersham).

RESULTS

Specific residues in the N-terminal domain of SpoVID are essential for spore encasement

In order to further investigate our previous finding that a region of the N-terminal domain of SpoVID (between amino acids 125 and 136) is necessary for directing spore encasement by CotE (Wang *et al.*, 2009), we focused on individual residues in this region to determine if they were involved in this process. Based on sequence comparison to other spore-forming species (Wang *et al.*, 2009), highly conserved residues L125, I127, D130, L131, and I133 were selected as possible candidates. We performed site-directed mutagenesis on these residues, creating alanine substitution mutants for each, and investigated the consequences on encasement by fluorescence microscopy. Each *spoVID* construct was fused at the 3' end to the coding sequence of CFP. The fusion constructs were introduced at the nonessential *amyE* locus into a strain in which the endogenous *spoVID* gene has been knocked out. The ability to encase was determined by analysis of the subcellular localization of CotE-YFP in cells that express *cotE* fused at the 3' end to the coding sequence of yellow fluorescent protein (YFP).

In cells expressing wild-type *spoVID* fused to *cfp* during sporulation,

the localization of CotE-YFP, from hour 3 to 6 after resuspension in Sterlini-Mandelstam medium, followed a previously reported pattern (Wang *et al.*, 2009; McKenney and Eichenberger, 2012). CotE-YFP localized first as a single dot, then as a cap on the MCP pole of the engulfing forespore, expanding into 2 unconnected caps on both sides of the forespore and finally into a complete ring (a spherical shell in three dimensions) surrounding the entire forespore (Fig. 2.2 A). In cells expressing *spoVID*$_{\Delta 125-136}$*-cfp*, as previously reported by Wang *et al*., 2009, spore encasement was strongly impaired (Fig. 2.2 B). A majority of cells exhibiting CotE-YFP fluorescence showed a single cap of fluorescence on the MCP pole, even 6 h after resuspension. We found that the replacement of L131 by alanine is sufficient to cause a severe encasement block (Fig. 2.2 C), similar to that observed when the entire region between residues 125 and 136 is removed.

To obtain a more quantitative measurement of the encasement defect and to compare the severity of the phenotypes, we measured for every mutant the number of cells with a single cap or two caps, and in the latter

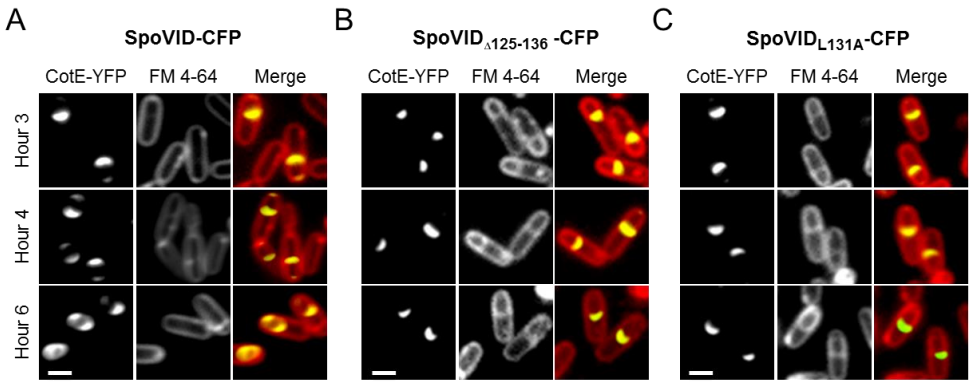

Figure 2.2 - Leucine 131 in the N-terminal domain of SpoVID is required for encasement by CotE. Cells harboring CotE-YFP and SpoVID-CFP variants were grown in sporulation media. Membranes were stained with FM 4-64 and cells were analyzed by fluorescence microscopy. A few cells are shown to represent the localization pattern of CotE-YFP fusion in strains carrying SpoVID-CFP **A)** wild type, **B)** with the deletion Δ125 - 136 or **C)** with the substitution L131A. First column: CotE-YFP signal; second column: fluorescence of stained membranes; third column: the overlay of YFP (yellow) and membranes (red) fluorescence signals. Scale bar: 1µm.

case distinguishing between connected and unconnected caps (Table 2.2). At hour 3 after resuspension, the strain expressing wild-type *spoVID-cfp* had CotE-YFP localized as two unconnected caps in 96% of cells exhibiting YFP fluorescence. In our negative control, containing *spoVID*$_{\Delta 125-136}$*-cfp*, CotE-YFP was localized only as a single cap in 84% of cells exhibiting YFP fluorescence. In two of our point mutants, *spoVID*$_{D130A}$*-cfp* and *spoVID*$_{I133A}$*-cfp*, CotE-YFP localization was unaffected, suggesting that the side chains of residues 130 and 133 are not critical for encasement. Two other point mutants, however, *spoVID*$_{L125A}$*-cfp* and *spoVID*$_{I127A}$*-cfp*, shared the same phenotype as *spoVID*$_{\Delta 125-136}$*-cfp* and *spoVID*$_{L131A}$*-cfp*, while CotE-YFP was unable to expand beyond a single cap, indicating that at least three conserved residues (L125, I127, and L131) are required for the encasement function of SpoVID.

Table 2.2: Quantification of encasement by CotE-YFP in various *spoVID-cfp* mutant strains

		Sporangia with 2 caps				
Genotype	**% single cap**	**Total % 2 caps**	**% unconnected**	**% connected**	**Mean (±SEM) MCD cap area (pixels)**	**n[a]**
spoVID-cfp	0	100	96	4	36 ± 20	140
spoVID$_{\Delta 125-136}$*-cfp*	84	16	16	0	13 ± 7	286
spoVID$_{L125A}$*-cfp*	95	5	5	0	8 ± 5	175
spoVID$_{I127A}$*-cfp*	87	13	13	0	14 ± 10	302
spoVID$_{D130A}$*-cfp*	0	100	99	1	51 ± 36	110
spoVID$_{L131A}$*-cfp*	94	6	6	0	19 ± 12	281
spoVID$_{I133A}$*-cfp*	1	99	94	5	38 ± 22	139

[a] The number of postengulfment sporangia with YFP fluorescence; SEM: standard error of the mean

We noted that even in the case of the *spoVID*$_{\Delta 125-136}$*-cfp* mutant, a second dot or a cap on the MCD pole was observed in some cells (16% of cells exhibiting YFP fluorescence). We quantified the extent to which this phenotype was observed in all strains and measured the area of the MCD cap of fluorescence (in pixels; Table 2.2). First, we observed that, similar to the *spoVID*$_{\Delta 125-136}$*-cfp* expressing strain, the three point mutants in which CotE-YFP did not encase the spore exhibited an MCD cap in only a small

percentage of cells (L125A, 5%; I127A, 13%; L131A, 6%). Second, that this second cap had a comparable size to that observed for the *spoVID*$_{\Delta 125–136}$-*cfp* mutant (Δ125–136, 13±7 pixels [mean ± standard error of the mean]; L125A, 8±5 pixels; I127A, 14±10 pixels; L131A, 19±12 pixels). This is significantly smaller than the area measured for the wild type and the unaffected mutants (wild type, 36±20 pixels; D130A, 51±36 pixels; I133A, 38±22 pixels). In total, we conclude that the L125A, I127A, and L131A point mutations inhibit the ability of SpoVID to direct encasement by CotE.

We decided to further investigate the phenotype of the *spoVID*$_{\Delta 125-136}$-*cfp* mutant by determining if it had an effect on the localization of additional coat proteins. We used YFP and GFP fusions to SpoIVA, the morphogenetic protein responsible for anchoring the coat to the spore surface (Piggot and Coote, 1976; Roels *et al.*, 1992; Wang *et al.*, 2009), YaaH, a SafA-dependent protein (McKenney *et al.*, 2010), CotO, a CotE-dependent protein (Eichenberger *et al.*, 2003), and CotZ, a protein required for the assembly of the newly identified spore crust (McKenney *et al.*, 2010; Imamura *et al.*, 2011). We assayed the localization of each fusion in the presence of SpoVID$_{\Delta 125-136}$-CFP, at hour 3 after resuspension for the early-localizing fusions (McKenney and Eichenberger, 2012) and at hour 6 for the late localizing protein, CotZ-GFP (Fig. 2.3). We found that all fusion proteins were arrested at the single-cap stage in the *spoVID*$_{\Delta 125-136}$-*cfp* deletion mutant. These data indicates that residues between L125 and L136 are essential for the function of SpoVID in directing spore encasement by all four layers of the coat. Thus, we name this region as region E, that codes for “encasement”. These data, however, do not imply that a direct interaction between SpoVID and CotE is a prerequisite for encasement by coat proteins that are not CotE dependent, such as SpoIVA or YaaH. It is more likely that SpoIVA interacts directly with the N terminus of SpoVID (in addition to the already-established interaction between SpoIVA and the C terminus of SpoVID) and that YaaH is dependent on SpoVID via its interaction with SafA.

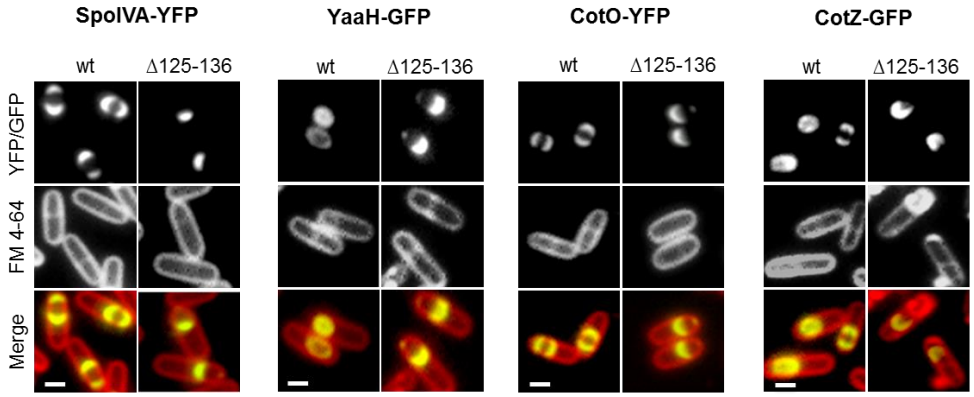

Figure 2.3 – Residues 125-136 are required for encasement by proteins of all four layers of the coat. The images show the subcellular localization of representative coat proteins fused to fluorescent proteins (SpoIVA-YFP, YaaH-GFP, CotO-YFP and CotZ-GFP) in *spoVID*$_{\Delta 125\text{-}136}$*-cfp* mutant strains. Cells were grown in sporulation media, stained with FM 4-64 and analysed by fluorescence microscopy. First column: GFP or YFP fluorescence; second column: fluorescence of membranes; third column: overlay of coat protein fusion (yellow) and membranes (red) fluorescence. Scale bar: 1μm.

SpoVID interacts with CotE in yeast two-hybrid assays

It had been previously observed that SpoVID interacts directly with SpoIVA (Mullerova *et al.*, 2009; Wang *et al.*, 2009), the morphogenetic protein required for recruiting all the spore coat proteins to the forespore surface, and SafA, the morphogenetic protein of the inner coat (Ozin *et al.*, 2000; Ozin *et al.*, 2001b; Costa *et al.*, 2006). In order to more fully understand the molecular mechanism of SpoVID-mediated encasement, we wanted to know whether SpoVID interacts directly with any other coat proteins, specifically, with other morphogenetic proteins. We focused our attention on CotE, the morphogenetic protein responsible for recruiting of the outer coat proteins. To determine whether there might be a direct interaction between SpoVID and CotE, we used a yeast Gal4-based two-hybrid assay as an initial test. We fused the N-terminal domain of SpoVID to Gal4BD and the C-terminally truncated CotE to Gal4AD. A protein-protein interaction between these fusion proteins will reconstitute a functional transcription factor that will drive the expression of the *HIS3* gene, required for survival on medium

lacking histidine. As shown in Fig. 2.4, we detected a positive interaction between SpoVID$_{\Delta 145\text{-}575}$-BD and CotE$_{\Delta 160\text{-}181}$-AD that persisted in the presence of 3-AT, a competitive inhibitor of the HIS3 enzyme (Hilton *et al.*, 1965). Growth on 3-AT suggests that the interaction between SpoVID and CotE is robust (Crump *et al.*, 1998). For reasons unknown, no interaction was detected when the protein fragments were fused to reciprocal Gal4 fragments. Nevertheless, as expected, the combination of either protein fragment with unfused Gal4AD or Gal4BD fragments produced no growth.

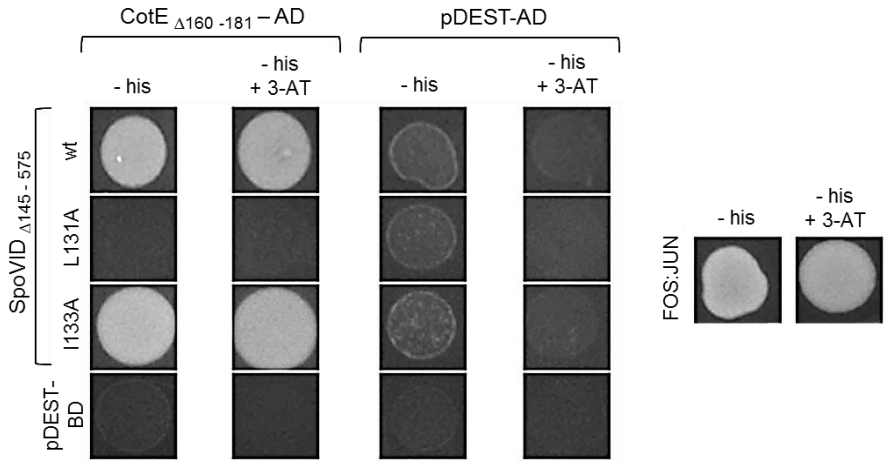

Figure 2.4 - CotE interaction with the N-terminal domain of SpoVID in yeast two-hybrid assays. *S. cerevisiae* strains producing SpoVID$_{\Delta 145\text{-}575}$-BD (first three rows) or the unfused Gal4BD (fourth row) and either CotE$_{\Delta 160\text{-}181}$-AD (first two columns) or unfused Gal4AD (third and fourth columns) were plated on selection plates (-his) with or without 3-AT. The first, second, and third rows contain strains expressing the SpoVID$_{\Delta 145\text{-}575}$-BD fragment in its wild-type, L131A, and I133A mutated forms, respectively. A positive control strain, containing AD and BD fusions to the known binding partners, Fos and Jun, respectively, was able to grow on selection medium (right panels).

Next, we wanted to determine whether SpoVID residues critical for encasement were also required for interaction with CotE. We constructed a SpoVID$_{\Delta 145\text{-}575}$-BD fusion with the substitution L131A and tested it for its ability to activate *HIS3* expression when mated with a strain producing CotE$_{\Delta 160\text{-}181}$-AD (Fig. 2.4). No growth was observed on selection plates,

indicating that the L131 residue was necessary for the interaction with CotE. We were unable to test interactions with the other two point mutants that were defective in encasement (L125A and L127A), because the constructs could drive *HIS3* reporter gene expression on their own (data not shown). As a negative control, we used a strain containing the I133A substitution, which had exhibited no encasement phenotype in our microscopy experiments. As expected, the I133A mutant was still able to interact with $CotE_{\Delta 160\text{-}181}$-AD, even in the presence of the 3-AT inhibitor. Taken as a whole, the yeast two-hybrid experiments suggested that the morphogenetic proteins SpoVID and CotE interact directly and that residue L131 of SpoVID is essential for this interaction.

SpoVID and CotE physically interact *in vitro*

To support the data from our yeast two-hybrid experiments, we decided to test this interaction biochemically with an *in vitro* His-tag pulldown assay. The assay was designed such that a C-terminally His-tagged version of SpoVID (*spoVID-his*) and an untagged copy of CotE (*cotE-STOP*) were overexpressed in separate *E. coli* strains. The SpoVID-His lysate was mixed with Ni-NTA beads and incubated for an hour. After incubation, CotE lysate was added to the mixture and incubated for an additional hour. The protein-bead mixture was then applied to a column and allowed to flow through it. For the negative control, CotE (from the same CotE lysate as above, split in half by volume) was incubated with Ni-NTA beads for an hour prior to application to the column. Three wash steps were performed with increasing imidazole concentrations. Elution was performed with two concentrations of imidazole, and samples from each step of the pulldown process were resolved by SDS-PAGE and analyzed by Western blot using anti-CotE antibodies (Fig. 2.5 A). As shown in Fig. 2.5 A, untagged CotE was pulled down only when SpoVID-His was present (first row), and on its own, it was unable to bind to the Ni-NTA beads (second row). These results

demonstrate that the morphogenetic proteins SpoVID and CotE physically interact *in vitro*, the first such demonstration of this interaction. This interaction may contribute significantly to the mechanism of SpoVID-mediated encasement.

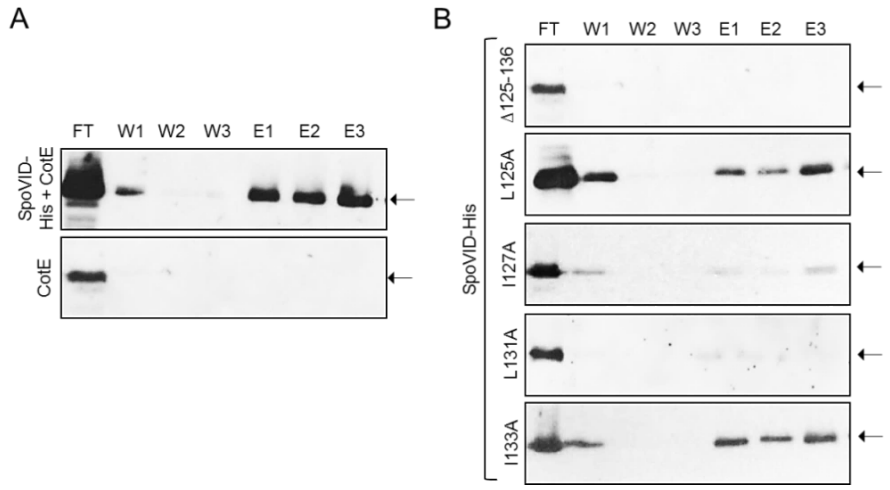

Figure 2.5 – Specific residues within region E of SpoVID are required for interaction with CotE *in vitro*. **A)** His-tag pulldown assay demonstrating that SpoVID-His physically interacts with CotE *in vitro*. Cell lysates containing untagged CotE were incubated with a mixture of Ni-NTA beads and *E. coli* lysates harboring SpoVID-His (top panel), or only with the beads (bottom panel). The mixtures were applied to a gravity column and allowed to flow through (FT). After washing (W1, W2 and W3), elution fractions were collected (E1, E2, and E3) and tested for retention of CotE. **B)** His-tag pulldown assays were performed as described, but using *E. coli* lysates containing SpoVID-His variants Δ125–136 (row 1), L125A (row 2), I127A (row 3), L131A (row 4), or I133A (row 5). Arrows point to CotE signal.

Specific residues in region E of SpoVID are required for binding to CotE

To complement our fluorescence microscopy and yeast two-hybrid data sets with biochemical evidence, we used the His-tag pulldown assay to identify residues within region E of SpoVID that might be involved in a direct interaction with CotE. The deletion allele missing region E, *spoVID*$_{\Delta 125-136}$*-his*, was generated and transformed in the *E. coli* expression system. We found that SpoVID$_{\Delta 125-136}$-His was not able to pull down CotE (Fig. 2.5 B, row 1). In order to further characterize the CotE-binding region, we generated the same

series of alanine substitution mutants in SpoVID-His used in our fluorescence microscopy experiments, and we assayed each construct for the ability to pull down CotE. As expected, I133A, the mutant that did not affect CotE-YFP localization and remained able to interact with CotE in the yeast two-hybrid assay, was able to pull down CotE. Surprisingly, we found that the L125A mutant, even though it was unable to localize CotE-YFP properly in fluorescence microscopy experiments, was still able to bind CotE. We did, however, find that both the I127A and L131A mutants did not efficiently pull down CotE in our assay. These results indicate that there are at least two specific residues in SpoVID (I127A and L131A) that are important both for binding to CotE and to promote spore encasement by CotE-YFP. Importantly, residue L131 has now been implicated in these activities by three distinct assays (epifluorescence microscopy, yeast two-hybrid experiment, and His-tag pulldown assays).

Residue L131 of SpoVID is dispensable for binding to SafA

Considering that the N-terminal domain of SpoVID was previously reported to interact directly with SafA (Costa *et al.*, 2006), we wondered if the same residue(s) required for interaction with CotE also played a role in the interaction with SafA. To test this, we performed GST-pulldown assays using a fusion of GST with the first 162 residues of SafA (GST-SafA$_{162}$), sufficient for interaction with SpoVID (Costa *et al.*, 2006), as a bait, and SpoVID-His (either wild type or with the substitution L131A) as prey. SpoVID-His variants were incubated with mixtures of glutathione beads and *E. coli* lysates harboring GST-SafA$_{162}$ or only GST, as a negative control for the retention of SpoVID-His. After several washings, fractions bond to the beads were resolved by SDS-PAGE and immunobloted for detection of SpoVID (Fig. 2.6). As expected, we were able to pull down the wild-type SpoVID-His construct with our GST-SafA$_{162}$. Moreover, we observed that the efficiency of the pulldown was not affected by the L131A substitution. Therefore, it

appears that the interaction with SafA relies on a different amino acid side chains than those that mediate the interaction with CotE.

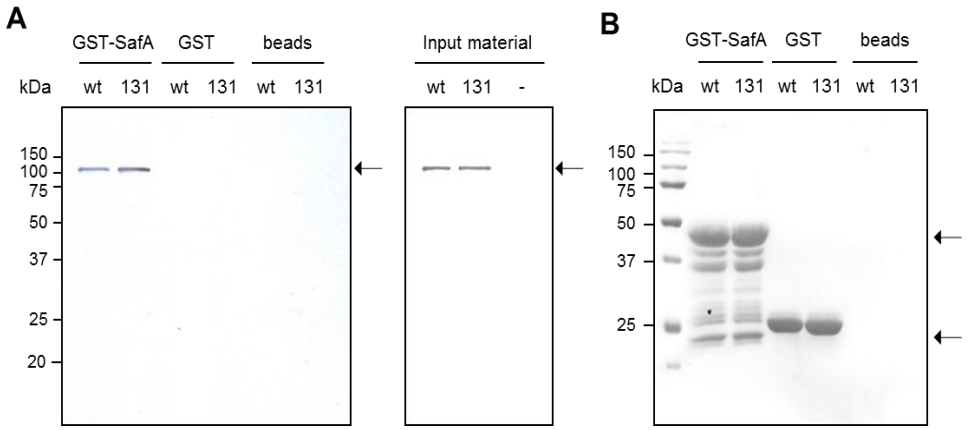

Figure 2.6 - Residue L131 is dispensable for direct interaction with SafA. **A)** A fusion of the first 162 residues of SafA to GST (GST-SafA$_{162}$) was bound to glutathione-Sepharose beads and incubated with extracts of *E. coli* producing wild type SpoVID-His or a version of SpoVID-His carrying the L131A substitution (left panel, first two columns). Immobilized GST and beads alone were also incubated with the two forms of SpoVID-His as negative controls (left panel, columns 3-6). Pulled down proteins were eluted, resolved by SDS-PAGE and immunobloted with anti-SpoVID antibodies. The amounts of SpoVID-His or SpoVID$_{L131A}$-His present in the extracts are shown in the right panel. Arrows indicate SpoVID signal. **B)** The nitrocellulose membrane used for immunoblotting was stained with Ponceau Red as a control for the amount of GST-SafA or GST bound to the glutathione beads. Arrows indicate stained GST-SafA$_{162}$ or GST.

Probing the function of cysteine residues within the N-terminal domain of SpoVID

Our data indicates that the N-terminal domain of SpoVID mediates spore encasement by establishing direct interactions with SafA and CotE, the morphogenetic proteins for the assembly of the inner and the outer coat/crust. As encasement may be facilitated by SpoVID multimerization around the spore surface, we further investigated the role of the cysteine residues within the N-terminal domain of SpoVID (C16 and C90). First, we fused a His-tag to the N-terminus of the full-length SpoVID (His-SpoVID) or to its isolated N-terminal domain (residues 1-160, His-SpoVID$_{N160}$), either wild

type or with single or double alanine substitutions in C16 and C90. Recombinant proteins were purified, incubated in the presence or absence of the reducing agent DTT, and resolved by SDS-PAGE.

As shown in Fig. 2.7 (top panel), the various forms of His-SpoVID$_{N160}$ migrate as a predominant species with approximately 22 kDa. This form corresponds to the monomer, as it is the only band detected under reducing conditions and in the variant missing both cysteines. The wild type His-SpoVID$_{N160}$ exhibits other DTT-sensitive forms above 45 kDa that are not visualized if cysteine residues were replaced by alanines. This suggests that the isolated N-terminal domain of SpoVID oligomerizes and that disulfide bonds may promote formation of these oligomers or otherwise their stability. A species migrating at approximately 20 kDa may be a monomeric form containing an intra-molecular disulfide bond (C16 to C90). When one of the cysteines is substituted by an alanine, only the monomer and one higher molecular weight, DTT-sensitive form were detected for each of the variants. These higher molecular weight forms exhibit different migration rates for His-SpoVID$_{N160\text{-}C16A}$ and SpoVID$_{N160\text{-}C90A}$. Most likely they are dimers formed

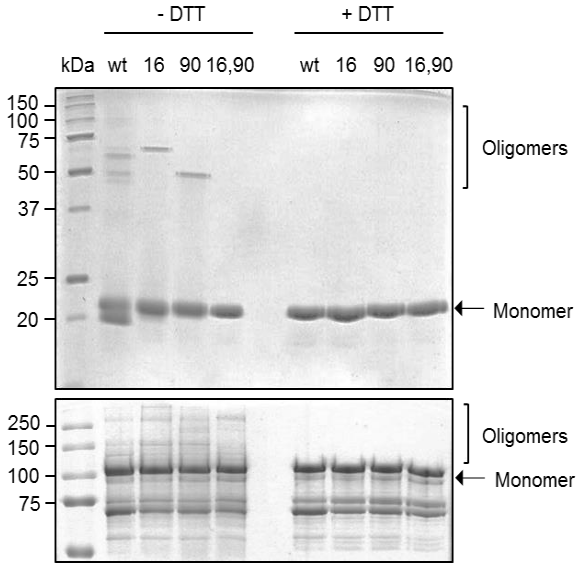

Figure 2.7 – Cysteine residues within the N-terminal domain of SpoVID are involved in domain oligomerization and stabilization of the SpoVID oligomeric complexes *in vitro.* His-tag fusions of the full-length protein and of a truncated version comprising its first 160 residues, either wild type or with single or double alanine substitutions of C16 and C90, were purified, incubated in the presence or absence of DTT, and resolved by SDS-PAGE. Monomeric and oligomeric forms of His-SpoVID$_{N160}$ (top panel) and His-SpoVID full-length (bottom panel), are indicated.

by two different types of disulfide bonds: C90 to C90, or C16 to C16. Thus, cysteine residues of the N-terminal domain of SpoVID are able to establish disulfide bonds of three types: C16 to C16, C90 to C90 and C16 to C90. This non-specific pattern of bond formation suggests that the N-terminal domain, at least when isolated from the remaining of the SpoVID protein, has a flexible structure.

For the full-length His-SpoVID variants, we observed a predominant DTT-resistant form with approximately 100 kDa that might correspond to a monomer (Fig. 2.7, bottom panel). Several DTT-resistant forms are also detected with faster migration, which we assume are SpoVID degradation products. Forms with apparent molecular weight higher than that of the presumed monomer are seen exclusively under non-reducing conditions, consistent with the idea that His-SpoVID oligomers contain disulfide bonds. Some of these oligomeric forms are still detected when one or both cysteines of the N-terminal domain are substituted by alanines, and therefore cysteine residues in other parts of the full-length SpoVID protein are involved in disulfide bond formation. However, as the pattern of oligomeric bands exhibited by the wild type His-SpoVID does not totally match those seen for the mutant forms, it is possible that C16 and C90 have a role in stabilization of SpoVID oligomers *in vitro*.

Single alanine substitutions of the SpoVID cysteine residues (C16, C90, C355, C525 and C537) did not affect encasement by SpoVID itself or by the SpoVID-dependent proteins SafA and CotE (as monitored by using fluorescent protein fusions; data not shown).

The N-terminal domain of SpoVID is structured

The oligomerization assays with the His-tagged N-terminal region of SpoVID suggested that this may be a flexible, unstructured region. This can be an advantage for proteins that bind different targets, as is possibly the case of SpoVID, since it allows them to acquire several inter-converting

conformations (Wright and Dyson, 1999; Xue *et al.*, 2010). Therefore, we aimed at determining whether the N-terminal domain of SpoVID is intrinsically disordered. We started by analyzing the amino acid sequence of SpoVID using the meta-predictor of intrinsically disordered regions PONDR-FIT (www.disprot. org/pondr-fit). This algorithm generates scores from 0 to 1 for all protein regions and represents them in a chart. Values above 0.5 indicate that the region is predicted to be intrinsically disordered (Xue *et al.*, 2010). According to PONDR-FIT, the N- and C-terminal regions of SpoVID are structured, while the middle region, approximately between residues 140 – 500, is intrinsically disordered (Fig. 2.8 A). This is in agreement with previous structure predictions for SpoVID, which suggested that its N-terminal domain has a similar conformation as the phage-capsid protein PP7, and the C-terminal region folds into a LysM motif (Costa *et al.*, 2006; Wang *et al.*, 2009). As shown in Fig. 2.8 A, the region E of SpoVID, between residues 125 and 136, locates closer to an order/disorder boundary. Since the

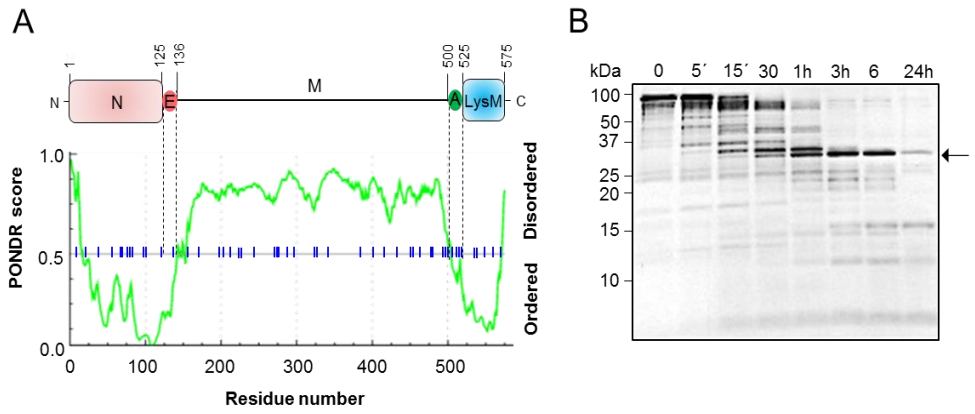

Figure 2.8 – The N-terminal domain of SpoVID (N) is structured **A)** Chart representing the PONDR-FIT score for SpoVID. A score above 0.5 indicates that the region is predicted to be disordered. A diagram of SpoVID is represented above the chart, showing that the regions predicted to be structured by PONDR-FIT match with the previous model. The dark blue lines in the chart axis represent trypsin cleavage sites along the SpoVID sequence. **B)** His-S-SpoVID controlled trypsinolysis. The purified recombinant protein was digested with trypsin for 24h. Samples were taken along the time and resolved by SDS-PAGE. The arrow indicates the 30 kDa proteolysis-resistant band that was identified as the N-terminal domain of SpoVID by MALDI-TOF/TOF MS/MS and N-terminal sequencing.

accuracy of the predictor decreases in these type of regions (Xue *et al.*, 2010), we cannot infer if region E is likely to be structured or not.

In an attempt to validate the structural predictions, we submitted SpoVID fused to a His-tag and a S-tag at the N terminus to limited proteolysis with trypsin. As proteases typically do not cut within structured regions, but mostly in interdomain linkers and disordered regions, identification of the proteolysis-resistant fragments helps determining the domain organization of proteins (Blatter *et al.*, 1994; Fontana *et al.*, 2004). We chose trypsin, as this enzyme has a higher frequency of potential cleavage sites in SpoVID (see Fig. 2.8 A, where the trypsin cleavage sites are represented in the chart axis by dark blue lines). Purified His-S-SpoVID was digested for 24h, and samples were taken along the time and resolved by SDS-PAGE (Fig. 2.8 B). Three hours after adding trypsin, we observed a strong digestion-resistant band with approximately 30 kDa that persisted even after 24 hours. At that time, we also detected three other protease-resistant bands with approximately 15 kDa, 12 kDa and 5 kDa.

Except for the 12 kDa band, whose level was not sufficient for analysis, these bands were extracted and subject to tandem mass spectrometry and N-terminal sequencing. Both techniques indicated that the 30 kDa band corresponds to the N-terminal domain of SpoVID. Through N-terminal sequencing, we identified the residues QHMDSP for this band, corresponding to part of the S-tag sequence fused to the N terminus of SpoVID. Tandem mass spectrometry identified fragments between residues L7 and R123 (Table 2.3), covering 72% of the N-terminal domain. Therefore, controlled proteolysis supported the PONDR-FIT predictions that the SpoVID N-terminal domain is folded. Since oligomerization assays indicated that this domain may be unstructured, we infer that it exhibits a different behavior when isolated from the context of the full-length protein, and that it presumably requires other SpoVID regions to acquire its fold.

The results were not so clear for the bands with 15 and 5 kDa. N-

terminal sequencing was not conclusive, and tandem mass spectrometry identified regions from different SpoVID domains in both bands (Table 2.3), showing that they are composed of a mixture of fragments. These data indicates that there are proteolysis-resistant regions along all the SpoVID sequence. Interestingly, region E was identified in fragments that compose the 15 kDa band (Table 2.3, in bold), and not in those of the band that corresponds to the N-terminal domain (30 kDa). Trypsin was able to cut at position R123, showing that this residue, immediately adjacent to region E, is exposed to digestion and may not be included in the structured N-terminal domain of SpoVID. However, the next cleavage site in the sequence (K143), was not cut by trypsin. Further studies are necessary to clarify the structural features of region E.

Table 2.3: Regions of SpoVID identified by MS/MS in bands resulting from trypsinolysis

Digestion band	Regions of SpoVID identified by MS/MS	Residue number	SpoVID domain
30 kDa	LQFSVEESICFQKGQEVSELLSISLDPDIRVQEVND YVSIIGSLELTGEYNIDQNK	L7-K62	N
	KREDGSAELTHCFPVDITIPK	K79-K99	N
	VSHLQDVFVFIDAFDYQLTDSR	V102-R123	N
15 kDa	GQEVSELLSISLDPDIR	G20-R36	N
	I**LTIQADLAIEGL**LDDTQDKEPEIPLYEAPAAFR*	I124-R157	N and M
	EKEETTVSPNHEYALR	E321-R336	M
	ETASAVYMENDNADLHFHFNQK	E380-K401	M
5 kDa	VSHLQDVFVFIDAFDYQLTDSR	V102-R123	N
	TFLPEQEEEDSFYSAPKLLEEEEQEEESFEIEVR	T419-R452	M
	YEITSQQLIR	Y540-R549	LysM
	AGQILYIPQYK	A561-K571	LysM

* Residues in bold correspond to region E

Finally, we tested whether the cysteine residues of the N-terminal domain of SpoVID could affect the pattern of controlled proteolysis. We perform similar controlled trypsinolysis experiments, but in the presence of

DTT, and we obtained the same patterns of proteolysis-resistant bands (data not shown). This suggests that putative intramolecular disulfide bonds, if formed, are not strictly necessary for the fold of the N-terminal domain of SpoVID.

DISCUSSION

Formation of the *B. subtilis* spore coat illustrates the challenges associated with the assembly of complex macromolecular structures at specific sub-cellular addresses, an issue that all cells face. We began this work with the goal of investigating the mechanism behind spore encasement by coat proteins, which requires SpoVM and SpoVID. Previously, it was found that the N-terminal domain of SpoVID was essential for encasement, while its C terminus was necessary for localization to the spore surface, most likely via interaction with SpoIVA (Mullerova *et al.*, 2009; Wang *et al.*, 2009). It was also reported that the N-terminal domain of SpoVID binds directly to SafA (Costa *et al.*, 2006), the morphogenetic protein of the inner coat layer (Takamatsu *et al.*, 1999; Ozin *et al.*, 2000; McKenney *et al.*, 2010). Additionally, evidence suggests that SpoVID oligomerizes *in vitro*, and that the oligomers contain disulfide bridges (Domingues, L., Isidro A. L. and Henriques, A. O., unpublished results; this work). Taken together, these data suggest a mechanism for encasement by the basement and inner coat layers mediated by interactions between SpoIVA or SafA with SpoVID and multimerization of the later. Information on the mechanism of encasement by the outer coat and crust was missing.

By comparative sequence analysis of SpoVID orthologues, we identified a conserved stretch of amino acids (L125 to L136). We generated alanine substitution mutants for five highly conserved residues within this region (L125, I127, D130, L131, and I133) and found that three of them

(L125, I127, and L131) were essential for spore encasement by a fusion of CotE, the morphogenetic protein for the outer coat and the crust, to YFP. We were also able to show that the encasement phenotype associated with the absence of residues 125-136 was not exclusive to CotE-YFP, since encasement by YFP and GFP fusions to representative proteins of each layer of the spore coat was also impaired. Considering the role of this stretch of amino acid residues in encasement, we named it region E.

We then focused our attention on the putative interaction between SpoVID and CotE, since it appeared to be a missing link in a general model of coat assembly. We used an existing yeast two-hybrid library (J. Jacobs, H. Eskandarian, P. Grabowski, and P. Eichenberger, unpublished results) to assess the potential for a direct interaction between the two proteins. For reasons unknown, we were unable to detect an interaction between full-length SpoVID and CotE, a result consistent with prior efforts. However, we observed an interaction when we tested a C-terminally truncated mutant of CotE ($CotE_{\Delta 160\text{-}181}$) for binding with $SpoVID_{\Delta 145\text{-}575}$. It is not unusual in yeast two-hybrid assays that the sensitivity of the technique is improved when smaller fragments are used (Boxem *et al.*, 2008). We also managed to detect this interaction using an *in vitro* system: SpoVID-His was able to pull down untagged CotE after application to a nickel column. This was the first time a physical connection was revealed between SpoVID and an outer coat protein. This result, combined with previous data showing that SpoVID can directly interact with SpoIVA (Mullerova *et al.*, 2009; Wang *et al.*, 2009) and SafA (Costa *et al.*, 2006), strongly suggests that the molecular mechanism behind encasement is rooted in direct protein-protein interactions between morphogenetic proteins.

We used our point mutants to further investigate the nature of the interaction between SpoVID and CotE. By both yeast two-hybrid and His-tag pulldown, we singled out L131 as an essential residue for the binding of CotE to SpoVID. I127 was also identified as essential for the interaction based in

His-tag pull down, but due to self-activation of the corresponding SpoVID$_{\Delta 145\text{-}575,L127A}$-BD construct, we were unable to confirm this interaction in the yeast two-hybrid assay. Unexpectedly, the L125A mutant that was unable to localize CotE-YFP in our fluorescence microscopy assay was still able to bind CotE in the pulldown assay, suggesting that this mutant of SpoVID must be dysfunctional for a reason other than abrogated binding to CotE. Taken together, our results tie the mechanism of spore encasement by the outer coat layer directly to the ability of SpoVID to bind CotE through region E. Nevertheless, after the completion of this work, Qiao *et al.* showed by pulldown assays that the first 200 residues of SpoVID are dispensable for this interaction (Qiao *et al.*, 2013). This result may reflect the sensitivity of the different techniques; in any event, it suggests the existence of a second surface in SpoVID that interacts with CotE (see Chapter 3).

To better understand the mechanisms governing spore encasement, we studied to role of the two cysteine residues within the morphogenetic, N-terminal domain of SpoVID in oligomerization. While these cysteine residues can form disulfide bonds at least in the context of the isolated domain, they do not seem to be required for oligomerization or for the function of the protein *in vivo*. It is possible that other cysteines within the middle region or the LysM domain might make more significant contributions to the function of SpoVID. Although single alanine substitutions of the cysteine residues did not impair encasement, we cannot exclude that more than one substitution is required to detect an effect on encasement.

Our data suggests that the N-terminal region of SpoVID is structured, and that it presumably requires the context of the full-length protein to acquire its fold. Due to technical limitations, we were unable to determine if region E is structured or disordered. We know that the mechanism by which this region directs encasement by the outer coat implies binding to CotE. If this region also interacts directly with other morphogenetic proteins, SafA and SpoIVA being likely candidates (see Chapter 3), disorder may be an

advantage (Wright and Dyson, 1999; Xue *et al.*, 2010).

Protein-protein interactions, including homo-oligomer formation, *e.g*. by SpoVID, are responsible for encasement of all layers of the spore coat. We propose that SpoVID is anchored to the spore surface by the interaction between its C-terminal domain and SpoIVA (Fig. 2.9 A). Then, SpoVID multimerizes around the spore, encircling it. It is conceivable that, due to its ability to bind SpoIVA, SpoVID is polymerized along with SpoIVA, which is known to self-assemble into filamentous structures in the presence of ATP (Ramamurthi and Losick, 2008). However, SpoVM also plays a critical role during encasement and is located upstream of SpoVID in the genetic hierarchy controlling coat morphogenesis (Wang *et al.*, 2009). Similarly, SpoIVA is dependent on *spoVID* for encasement (Wang *et al.*, 2009); in particular, we showed here that encasement by SpoIVA also requires region E in SpoVID. Therefore, it appears likely that a second interaction has to be established between SpoIVA and SpoVID, this time involving the N terminus of SpoVID, which is required for encasement, in order to promote encasement by the basement layer of the coat, whose components are dependent on SpoIVA for localization. Biochemical evidence for this second interaction is currently lacking, as is a more detailed characterization of the mechanism by which SpoVM promotes encasement. SpoVM might enable this second interaction by triggering a conformational change, or it could promote the multimerization of SpoIVA and SpoVID. Perhaps simultaneously or otherwise shortly thereafter, the N-terminal region of SpoVID interacts with SafA (Costa *et al.*, 2006) (Fig. 2.7 A and B), allowing encasement by SafA and the short form $SafA_{C30}$ (Ozin *et al.*, 2001a), and in turn, by several SafA-dependent proteins of the inner coat (such as YaaH) during the first wave of encasement (McKenney and Eichenberger, 2012). The same domain of SpoVID would also bind directly to CotE (Fig. 2.7 B and C), facilitating encasement by the outer coat and crust in successive waves (but see also Chapter 3).

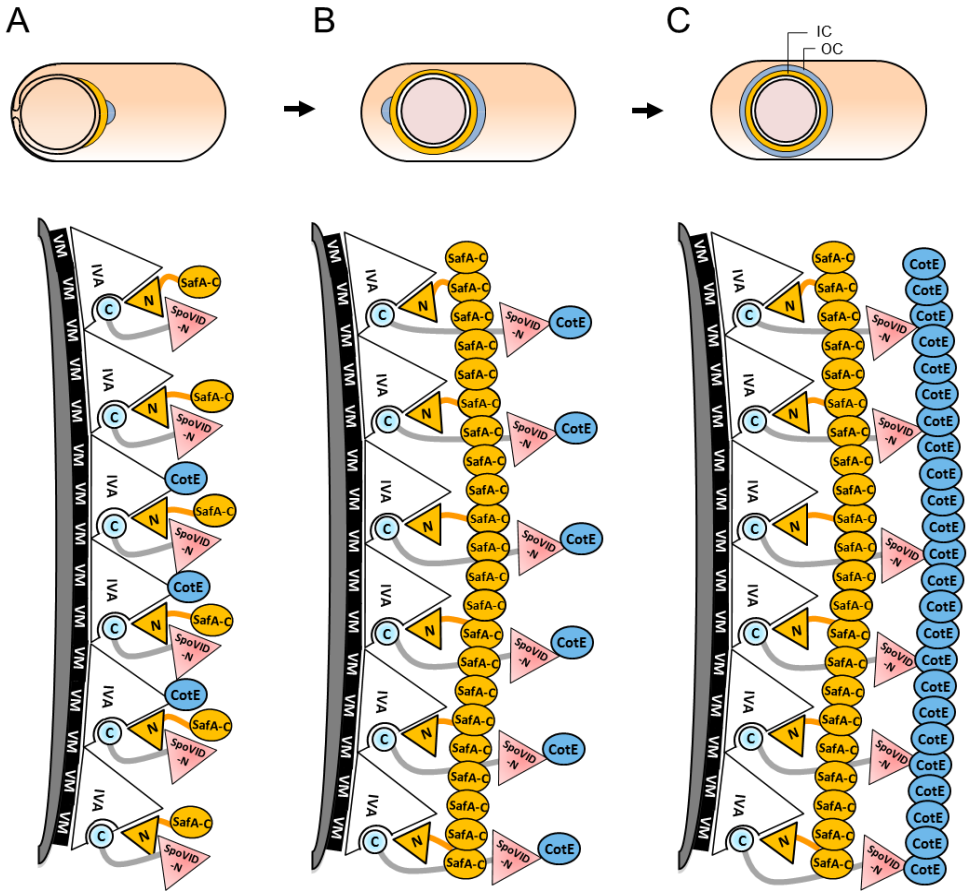

Figure 2.9 - A model for spore encasement mediated by SpoVID. **A)** Proteins of the basement layer of the coat localize to the surface of the spore coat. SpoVM (black) binds to curved membranes (Ramamurthi *et al.*, 2009) and interacts directly with SpoIVA (white triangles) (Ramamurthi *et al.*, 2006). SpoIVA multimerizes (Ramamurthi and Losick, 2008) at the spore surface, restricts SpoVM to the forespore (Ramamurthi *et al.*, 2006), and interacts with the C-terminal domain of SpoVID (light blue circles) (Mullerova *et al.*, 2009; Wang *et al.*, 2009) and with SafA (Mullerova *et al.*, 2009; Qiao *et al.*, 2012). SpoVID also oligomerizes (Mullerova *et al.*, 2009), and its N-terminal region (pink triangles) interacts with the N-terminal domain of SafA (yellow triangles) (Costa *et al.*, 2006; Mullerova *et al.*, 2009). Initial localization of CotE (blue ovals) is also dependent on SpoIVA (Webb *et al.*, 1995). **B)** Encasement is favored by the N-terminal domain of SpoVID and its interactions with SafA and CotE. The SafA full-length interacts with $SafA_{C30}$ form (yellow ovals) (Ozin *et al.*, 2001a). **C)** Completion of encasement, with multimerization of CotE (Little and Driks, 2001; Costa *et al.*, 2007) around the spore. IC: inner coat; OC: outer coat.

Our data suggest that the interaction with SafA and CotE does not require the same residues on the N-terminal domain of SpoVID. We currently do not know if SafA and CotE can bind simultaneously to this domain. Future

experiments would be necessary to determine if SafA and CotE compete for binding to SpoVID and, if so, whether competition between the two proteins impacts the regulation of the encasement process (see Chapter 3). Also, the identification of the second region of interaction with CotE in SpoVID, suggested by the experiments of Qiao *et al*, 2013 (Qiao *et al.*, 2013), might contribute for a better understanding of this mechanism. As previously noted (Wang *et al.*, 2009), our model does not currently incorporate an explanation for the formation of a focus of CotE-YFP fluorescence on the mother cell distal side of the forespore. This is another part of the mechanism that will necessitate further investigation.

In conclusion, we have shown that a specific region in the N-terminal domain of SpoVID is responsible for encasement of the spore by proteins that make up the different layers of the coat, from the basement layer to the spore crust. We have demonstrated, for the first time, a direct physical link between SpoVID and the outer coat, via a protein-protein interaction with CotE, the outer coat morphogenetic protein. At least in the case of CotE, the inability of the L131A mutant to direct encasement is related to its inability to bind to CotE. Moreover, the N-terminal domain of SpoVID, that directs encasement, is structured, and its cysteines may contribute to stabilize multimeric forms of SpoVID *in vivo*, under conditions not detected by our assays. Along with previous work, our results make a case for protein-protein interactions between morphogenetic proteins being the paramount mechanism for spore encasement.

ACKNOWLEDGMENTS

We thank Kumaran Ramamurthi for critical reading of the manuscript. We are grateful to Adam Driks for providing the CotE antibody, Mike Boxem and Anita Fernandez for yeast strains, Ezio Ricca for advice on

the pulldown assays, Katherine Honghua Wang for advice on the site-directed mutagenesis, Paul Grabowski and Haig Alexander Eskandarian for initiating the yeast two-hybrid experiments, and Elizabeth Glicksman and Rati Krishna for technical help. This work was supported by grant GM081571 from the National Institutes of Health to P.E. Work in the A.O.H. laboratory was supported by Fundação para a Ciência e a Tecnologia through grants RA-PTG/SAU/ 0002/2008 and PEst-OE/EQB/LA0004/2011. F.N. and M.S. were the recipients of doctoral (SFRH/BD/64470/2009) and postdoctoral fellowships (SFRH/BPD/36328/2007), respectively, from the FCT.

REFERENCES

Blatter, E.E., Ross, W., Tang, H., Gourse, R.L., Ebright, R.H., 1994. Domain organization of RNA polymerase alpha subunit: C-terminal 85 amino acids constitute a domain capable of dimerization and DNA binding. Cell 78, 889-896.

Boxem, M., Maliga, Z., Klitgord, N., Li, N., Lemmens, I., Mana, M., de Lichtervelde, L., Mul, J.D., van de Peut, D., Devos, M., Simonis, N., Yildirim, M.A., Cokol, M., Kao, H.L., de Smet, A.S., Wang, H., Schlaitz, A.L., Hao, T., Milstein, S., Fan, C., Tipsword, M., Drew, K., Galli, M., Rhrissorrakrai, K., Drechsel, D., Koller, D., Roth, F.P., Iakoucheva, L.M., Dunker, A.K., Bonneau, R., Gunsalus, K.C., Hill, D.E., Piano, F., Tavernier, J., van den Heuvel, S., Hyman, A.A., Vidal, M., 2008. A protein domain-based interactome network for C. elegans early embryogenesis. Cell 134, 534-545.

Costa, T., Isidro, A.L., Moran, C.P., Jr., Henriques, A.O., 2006. Interaction between coat morphogenetic proteins SafA and SpoVID. Journal of Bacteriology 188, 7731-7741.

Costa, T., Serrano, M., Steil, L., Volker, U., Moran, C.P., Jr., Henriques, A.O., 2007. The timing of cotE expression affects Bacillus subtilis spore coat morphology but not lysozyme resistance. Journal of Bacteriology 189, 2401-2410.

Crump, C.M., Williams, J.L., Stephens, D.J., Banting, G., 1998. Inhibition of the interaction between tyrosine-based motifs and the medium chain subunit of the AP-2 adaptor complex by specific tyrphostins. The Journal of Biological

chemistry 273, 28073-28077.

Driks, A., 1999. Bacillus subtilis spore coat. Microbiology and Molecular Biology Reviews 63, 1-20.

Driks, A., Roels, S., Beall, B., Moran, C.P., Jr., Losick, R., 1994. Subcellular localization of proteins involved in the assembly of the spore coat of Bacillus subtilis. Genes & Development 8, 234-244.

Eichenberger, P., Jensen, S.T., Conlon, E.M., van Ooij, C., Silvaggi, J., Gonzalez-Pastor, J.E., Fujita, M., Ben-Yehuda, S., Stragier, P., Liu, J.S., Losick, R., 2003. The sigmaE regulon and the identification of additional sporulation genes in Bacillus subtilis. Journal of Molecular Biology 327, 945-972.

Fontana, A., de Laureto, P.P., Spolaore, B., Frare, E., Picotti, P., Zambonin, M., 2004. Probing protein structure by limited proteolysis. Acta Biochimica Polonica 51, 299-321.

Henriques, A.O., Moran, C.P., Jr., 2007. Structure, assembly, and function of the spore surface layers. Annual Review of Microbiology 61, 555-588.

Hilton, J.L., Kearney, P.C., Ames, B.N., 1965. Mode of action of the herbicide, 3-amino-1,2,4-triazole(amitrole): inhibition of an enzyme of histidine biosynthesis. Archives of Biochemistry and Biophysics 112, 544-547.

Imamura, D., Kuwana, R., Takamatsu, H., Watabe, K., 2011. Proteins involved in formation of the outermost layer of Bacillus subtilis spores. Journal of Bacteriology 193, 4075-4080.

James, P., Halladay, J., Craig, E.A., 1996. Genomic libraries and a host strain designed for highly efficient two-hybrid selection in yeast. Genetics 144, 1425-1436.

Kim, H., Hahn, M., Grabowski, P., McPherson, D.C., Otte, M.M., Wang, R., Ferguson, C.C., Eichenberger, P., Driks, A., 2006. The Bacillus subtilis spore coat protein interaction network. Molecular Microbiology 59, 487-502.

Kuwana, R., Kasahara, Y., Fujibayashi, M., Takamatsu, H., Ogasawara, N., Watabe, K., 2002. Proteomics characterization of novel spore proteins of Bacillus subtilis. Microbiology 148, 3971-3982.

Lai, E.M., Phadke, N.D., Kachman, M.T., Giorno, R., Vazquez, S., Vazquez, J.A., Maddock, J.R., Driks, A., 2003. Proteomic analysis of the spore coats of Bacillus subtilis and Bacillus anthracis. Journal of Bacteriology 185, 1443-1454.

Little, S., Driks, A., 2001. Functional analysis of the Bacillus subtilis morphogenetic spore coat protein CotE. Molecular Microbiology 42, 1107-1120.

McKenney, P.T., Driks, A., Eskandarian, H.A., Grabowski, P., Guberman, J., Wang, K.H., Gitai, Z., Eichenberger, P., 2010. A distance-weighted interaction map reveals a previously uncharacterized layer of the Bacillus subtilis spore coat. Current Biology 20, 934-938.

McKenney, P.T., Eichenberger, P., 2012. Dynamics of spore coat morphogenesis in Bacillus subtilis. Molecular Microbiology 83, 245-260.

Mullerova, D., Krajcikova, D., Barak, I., 2009. Interactions between Bacillus subtilis early spore coat morphogenetic proteins. FEMS Microbiology Letters 299, 74-85.

Nicholson, W.L., Setlow, P., 1990. Sporulation, germination and outgrowth. In: Harwood, C.R., Cutting, S.M. (Eds.), Molecular biological methods for Bacillus. John Wiley & Sons, Chichester, United Kingdom, pp. 391-450.

Ozin, A.J., Costa, T., Henriques, A.O., Moran, C.P., Jr., 2001a. Alternative translation initiation produces a short form of a spore coat protein in Bacillus subtilis. Journal of Bacteriology 183, 2032-2040.

Ozin, A.J., Henriques, A.O., Yi, H., Moran, C.P., Jr., 2000. Morphogenetic proteins SpoVID and SafA form a complex during assembly of the Bacillus subtilis spore coat. Journal of Bacteriology 182, 1828-1833.

Ozin, A.J., Samford, C.S., Henriques, A.O., Moran, C.P., Jr., 2001b. SpoVID guides SafA to the spore coat in Bacillus subtilis. Journal of Bacteriology 183, 3041-3049.

Piggot, P.J., Coote, J.G., 1976. Genetic aspects of bacterial endospore formation. Bacteriological Reviews 40, 908-962.

Qiao, H., Krajcikova, D., Liu, C., Li, Y., Wang, H., Barak, I., Tang, J., 2012. The interactions of spore-coat morphogenetic proteins studied by single-molecule recognition force spectroscopy. Chemistry - an Asian Journal 7, 725-731.

Qiao, H., Krajcikova, D., Xing, C., Lu, B., Hao, J., Ke, X., Wang, H., Barak, I., Tang, J., 2013. Study of the interactions between the key spore coat morphogenetic proteins CotE and SpoVID. Journal of Structural Biology 181, 128-135.

Ramamurthi, K.S., Clapham, K.R., Losick, R., 2006. Peptide anchoring spore coat assembly to the outer forespore membrane in Bacillus subtilis.

Molecular Microbiology 62, 1547-1557.

Ramamurthi, K.S., Lecuyer, S., Stone, H.A., Losick, R., 2009. Geometric cue for protein localization in a bacterium. Science 323, 1354-1357.

Ramamurthi, K.S., Losick, R., 2008. ATP-driven self-assembly of a morphogenetic protein in Bacillus subtilis. Molecular Cell 31, 406-414.

Roels, S., Driks, A., Losick, R., 1992. Characterization of spoIVA, a sporulation gene involved in coat morphogenesis in Bacillus subtilis. Journal of Bacteriology 174, 575-585.

Sterlini, J.M., Mandelstam, J., 1969. Commitment to sporulation in Bacillus subtilis and its relationship to development of actinomycin resistance. Biochemical Journal 113, 29-37.

Takamatsu, H., Kodama, T., Nakayama, T., Watabe, K., 1999. Characterization of the yrbA gene of Bacillus subtilis, involved in resistance and germination of spores. Journal of Bacteriology 181, 4986-4994.

Walhout, A.J., Sordella, R., Lu, X., Hartley, J.L., Temple, G.F., Brasch, M.A., Thierry-Mieg, N., Vidal, M., 2000a. Protein interaction mapping in C. elegans using proteins involved in vulval development. Science 287, 116-122.

Walhout, A.J., Temple, G.F., Brasch, M.A., Hartley, J.L., Lorson, M.A., van den Heuvel, S., Vidal, M., 2000b. GATEWAY recombinational cloning: application to the cloning of large numbers of open reading frames or ORFeomes. Methods in Enzymology 328, 575-592.

Walhout, A.J., Vidal, M., 2001. High-throughput yeast two-hybrid assays for large-scale protein interaction mapping. Methods 24, 297-306.

Wang, K.H., Isidro, A.L., Domingues, L., Eskandarian, H.A., McKenney, P.T., Drew, K., Grabowski, P., Chua, M.H., Barry, S.N., Guan, M., Bonneau, R., Henriques, A.O., Eichenberger, P., 2009. The coat morphogenetic protein SpoVID is necessary for spore encasement in Bacillus subtilis. Molecular Microbiology 74, 634-649.

Webb, C.D., Decatur, A., Teleman, A., Losick, R., 1995. Use of green fluorescent protein for visualization of cell-specific gene expression and subcellular protein localization during sporulation in Bacillus subtilis. Journal of Bacteriology 177, 5906-5911.

Wright, P.E., Dyson, H.J., 1999. Intrinsically unstructured proteins: re-assessing the protein structure-function paradigm. Journal of Molecular Biology 293, 321-331.

Xue, B., Dunbrack, R.L., Williams, R.W., Dunker, A.K., Uversky, V.N., 2010. PONDR-FIT: a meta-predictor of intrinsically disordered amino acids. Biochimica et Biophysica Acta 1804, 996-1010.

Youngman, P., Perkins, J.B., Losick, R., 1984. Construction of a cloning site near one end of Tn917 into which foreign DNA may be inserted without affecting transposition in Bacillus subtilis or expression of the transposon-borne erm gene. Plasmid 12, 1-9.

Zheng, L.B., Donovan, W.P., Fitz-James, P.C., Losick, R., 1988. Gene encoding a morphogenic protein required in the assembly of the outer coat of the Bacillus subtilis endospore. Genes & Development 2, 1047-1054.

Chapter 3

Binding of SafA to region E of SpoVID

This chapter contains data to be published in: Nunes, F., Fernandes, C., Freitas, C., Sousa, A., Tranfield, E., Serrano, M., Eichenberger, P. and Henriques, A. O. (2015) **Binding of the inner spore coat hub SafA to region E of the encasement protein SpoVID of *Bacillus subtilis***.

All the experiments in this chapter were performed by the author of this dissertation, except for transmission electron microscopy and the construction of plasmids pCF149 and pET21b-cotE-STOP, and of strains AH2687, AH2692 and PE655.

SUMMARY

During sporulation in *Bacillus subtilis*, a group of mother cell-specific morphogenetic proteins guides the assembly of four main layers of the spore coat: the basement layer, the inner and outer coat and the crust. Among those proteins, SafA and CotE behave as interaction hubs, governing assembly of the inner and the outer coat substructures. Targeting of SafA and CotE to the spore surface is followed by spore encasement by the inner and the outer coat components, a process that requires the N-terminal domain of SpoVID. In Chapter 2, we demonstrated that a small region at the end of this domain, named region E, is required for encasement by the four layers of the coat and for a direct interaction with CotE. Now, we show that region E is also important for the interaction with SafA, linking the process of encasement by both the inner and outer coat modules to specific protein interactions involving the same region of SpoVID. We found single amino acid substitutions in region E that cause mislocalization of SafA and prevent its binding to SpoVID. Moreover, high concentrations of peptides with the sequence of region E promote binding of SafA and CotE to SpoVID *in vitro* and bypass the need of region E for interaction with SafA. This suggests that region E functions by shuttling or otherwise promoting binding of SafA and CotE to a second surface in SpoVID.

We also show that the two residues within region E required for encasement by both SafA and CotE are important for coat integrity. Our data indicates that mislocalized SafA and/or its dependent proteins acts as an attractor for CotE. Thus, although the SafA and CotE modules are largely independent, our study reveals a tight connection between the inner and outer coat substructures.

INTRODUCTION

Morphogenesis of the spore coat in *B. subtilis* has been extensively studied, contributing to our understanding of how supramolecular structures are assembled during cell differentiation at a specific subcellular localization. The coat is an organelle that encloses the spore, protecting it and arbitrating many of its environmental interactions. It comprises more than 80 different proteins, organized in four sublayers: the basement layer, the inner coat, the outer coat and the crust (Henriques and Moran, 2000; Kim *et al.*, 2006; Henriques and Moran, 2007; McKenney and Eichenberger, 2012; McKenney *et al.*, 2013). The coat proteins are synthesized in the mother cell compartment, and after asymmetric division the earlier-localizing ones assemble at the mother cell proximal (MCP) pole of the developing spore, forming a scaffold (Fig. 3.1 A). Then, these proteins encircle the spore in successive waves of encasement, establishing the four layers of the coat (Fig. 3.1 B and C). Coat morphogenesis continues along spore development, with proteins being synthesized and added to each layer (Driks *et al.*, 1994; Wang *et al.*, 2009; McKenney and Eichenberger, 2012; McKenney *et al.*, 2013) (see *"Two step of coat assembly: targeting and encasement"* and *"Successive waves of encasement during coat morphogenesis"*, in Chapter 1).

Assembly of the coat components is guided by morphogenetic proteins (Driks *et al.*, 1994; Henriques and Moran, 2000; Errington, 2003; Henriques and Moran, 2007; McKenney *et al.*, 2010; McKenney and Eichenberger, 2012; McKenney *et al.*, 2013). Among those, SpoIVA is important for the localization of all spore coat proteins at the surface of the developing spore, while SpoVM and SpoVID drive spore encasement (Wang *et al.*, 2009) (see *"Two step of coat assembly: targeting and encasement"*, in Chapter 1). These three proteins localize earlier at the MCP pole and encase the spore in the first wave of encasement; they are referred to as class I proteins. The absence of SpoIVA, SpoVM or SpoVID results in spores without

a coat (Roels *et al.*, 1992; Beall *et al.*, 1993; Levin *et al.*, 1993).

Morphogenetic proteins SafA and CotE are specifically required for formation of the inner coat and of the outer coat and the crust, respectively (Driks *et al.*, 1994; Takamatsu *et al.*, 1999). SafA and CotE appear to act as hubs for assembly of the inner and outer coat, while CotE additionally recruits CotZ, responsible for assembly of the crust. These proteins may

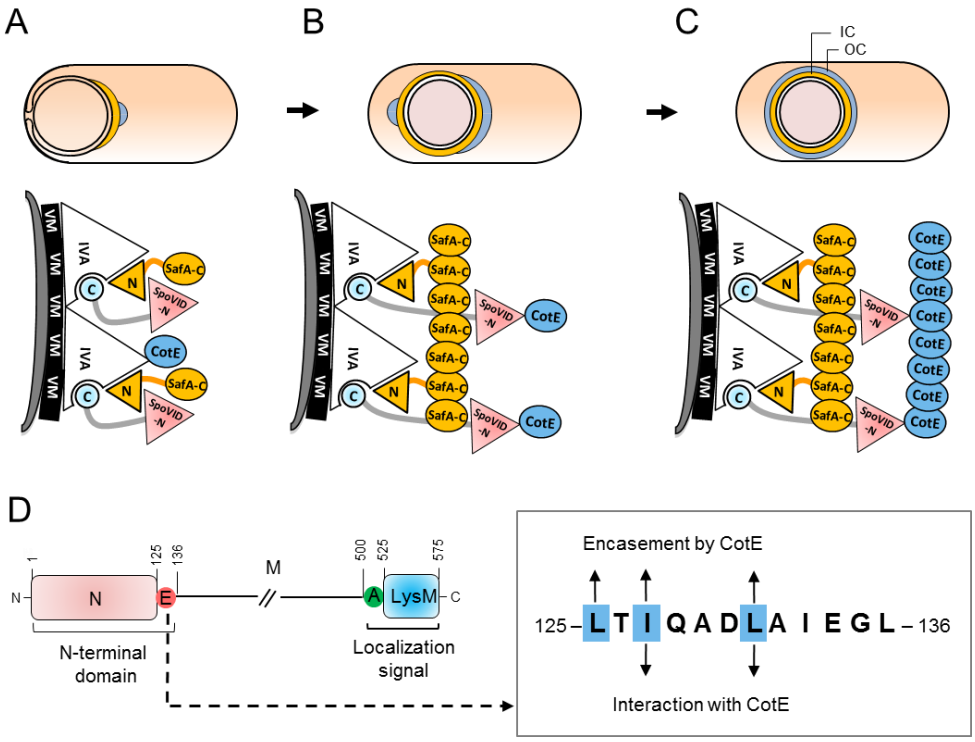

Figure 3.1 – Schematic view of spore encasement mediated by the region E of SpoVID. **A)** Proteins of the basement layer localize to the surface of the developing spore. SpoVM (black) recognizes and binds to the spore membrane and recruits SpoIVA (white triangles). SpoIVA multimerizes around the spore and interacts with the C-terminal domain of SpoVID (light blue circles), which oligomerizes as well. SpoIVA also interacts with SafA (yellow), and possibly with CotE (blue circles), recruiting them. Encasement is favored by the N-terminal domain of SpoVID (pink triangles), as it interacts with SafA **B)** and CotE. The full-length form of SafA is required for the localization of $SafA_{C30}$ (yellow ovals), which may function as the hub for inner coat proteins. **C)** Completion of encasement. CotE multimerizes, forming a basal layer for assembly of the outer coat. IC: inner coat; OC: outer coat. **D)** Diagram of SpoVID (left panel), with region E in evidence (right panel). Region E comprises residues 125 – 136, among which L125, I127 and L131 are involved in encasement by CotE. L127A and L131A substitutions reduce the interaction between SpoVID and CotE.

function by interacting with several proteins that compose a particular layer and recruiting them to the spore surface. Regarding SafA, the hub function may be performed by its C-terminal region. Thus, accumulation of the $SafA_{C30}$ form, resulting from the internal translation of the *safA* mRNA (Takamatsu *et al.*, 2000a; Ozin *et al.*, 2001a), could be a strategy to increase the surface area available for the interaction of the inner coat components. Both SafA and CotE localize earlier at the surface of the prespore; however, whereas SafA is presumed to encircle the spore in the first wave of encasement (since at least some SafA-dependent proteins belong to the kinetic class I), CotE encases the spore in the second wave, belonging to the kinetic class II (McKenney and Eichenberger, 2012). Both hubs require SpoIVA and SpoVID for localization, interact directly with SpoVID, and at least SafA also binds SpoIVA (Driks *et al.*, 1994; Ozin *et al.*, 2000; Ozin *et al.*, 2001b; Costa *et al.*, 2006; Mullerova *et al.*, 2009; Wang *et al.*, 2009; de Francesco *et al.*, 2012; Qiao *et al.*, 2012; Qiao *et al.*, 2013). This suggests that the mechanisms of targeting and encasement by the coat components are linked to specific protein-proteins interactions between the major morphogenetic proteins. Moreover, the N terminus of SpoVID is sufficient for a direct interaction with SafA *in vitro* (Costa *et al.*, 2006).

In Chapter 2, we showed that a small stretch of residues within the end of the N-terminal domain of SpoVID, termed region E (residues L125 – L136; Fig. 3.1 D), is essential for encasement by all coat layers. Also, we linked the mechanism of encasement by CotE and its interactors to a direct interaction between CotE and SpoVID that requires region E (de Francesco *et al.*, 2012). Now, we extended the analysis of region E, focusing on the mechanism by which it governs encasement by SafA and its interactors. We identified specific residues within this region that are involved in a direct interaction with and encasement by SafA. Also, experiments using peptides with the sequence of region E suggest that this region facilitates binding of SafA and CotE to a second surface in SpoVID. We show that two residues

required for encasement by SafA are also involved in encasement by CotE and have a major role in coat integrity. Finally, we provide data supporting the idea that mislocalized SafA and/or its partners act as an attractor for CotE, revealing a tight connection between the SafA- and CotE-dependent assembly modules.

MATERIALS AND METHODS

Bacterial strains, media and general methods

DNA manipulation and other molecular methods were performed according to standard protocols, using *E. coli* DH5α for cloning. All *B. subtilis* strains are congenic derivatives of the wild type PY79 (Youngman *et al.*, 1984). Bacterial strains used in this study are listed in Table 3.1, and plasmids and oligonucleotide primers required for their construction are described in Tables A4 and A5 of the Appendices. Routine growth of *E. coli* and *B. subtilis* was done at 37 °C in Luria-Bertani (LB) medium, supplemented with appropriate antibiotics. For sporulation induction, strains were resuspended in Sterlini-Mandelstam sporulation (SM) medium and incubated at 37 °C (Sterlini and Mandelstam, 1969). Lysozyme and heat resistance tests were performed on samples from cultures grown in SM at 37°C for 48 hours, as previously described (Nicholson and Setlow, 1990).

Table 3.1: Bacterial strains used in this study

Strains	Relevant properties	Source
B. subtilis		
PY79	Prototrophic derivative of *B. subtilis* 168	Youngman *et al.*, 1984
PE655	*ΔsafA::safA-gfp* Spec^r	Wang *et al.*, 2009
AH5367	*ΔsafA*	This study

Table 3.1: Bacterial strains used in this study (cont.)

Strains	Relevant properties	Source
AH5370	*ΔsafA, amyE'::safA-yfp::'amyE* Neo^r	This study
AH5371	*ΔsafA, amyE'::safA-yfp::'amyE, ΔspoVID* Neo^r	"
AH5383	*ΔsafA, amyE'::safA-yfp::'amyE, spoVID$_{\Delta E}$* Neo^r	"
AH5384	*ΔsafA, amyE'::safA-yfp::'amyE, spoVID$_{L125A}$* Neo^r	"
AH5385	*ΔsafA, amyE'::safA-yfp::'amyE, spoVID$_{T126A}$* Neo^r	"
AH5386	*ΔsafA, amyE'::safA-yfp::'amyE, spoVID$_{I127A}$* Neo^r	"
AH5387	*ΔsafA, amyE'::safA-yfp::'amyE, spoVID$_{Q128A}$* Neo^r	"
AH5388	*ΔsafA, amyE'::safA-yfp::'amyE, spoVID$_{D130A}$* Neo^r	"
AH5389	*ΔsafA, amyE'::safA-yfp::'amyE, spoVID$_{L131A}$* Neo^r	"
AH5390	*ΔsafA, amyE'::safA-yfp::'amyE, spoVID$_{I133A}$* Neo^r	"
AH5391	*ΔsafA, amyE'::safA-yfp::'amyE, spoVID$_{E134A}$* Neo^r	"
AH5392	*ΔsafA, amyE'::safA-yfp::'amyE, spoVID$_{G135A}$* Neo^r	"
AH5393	*ΔsafA, amyE'::safA-yfp::'amyE, spoVID$_{L136A}$* Neo^r	"
AH5246	*ΔspoVID*	"
AH5354	*ΔspoVID, amyE'::spoVID::'amyE* Neo^r	"
AH5355	*ΔspoVID, amyE'::spoVID$_{\Delta E}$::'amyE* Neo^r	"
AH5356	*ΔspoVID, amyE'::spoVID$_{L125A}$::'amyE* Neo^r	"
AH5359	*ΔspoVID, amyE'::spoVID$_{T126A}$::'amyE* Neo^r	"
AH5357	*ΔspoVID, amyE'::spoVID$_{I127A}$::'amyE* Neo^r	"
AH5358	*ΔspoVID, amyE'::spoVID$_{L131A}$::'amyE* Neo^r	"
AH5362	*ΔspoVID, amyE'::spoVID$_{I133A}$::'amyE* Neo^r	"
AH5363	*ΔspoVID, amyE'::spoVID$_{E134A}$::'amyE* Neo^r	"
AH5404	*ΔcotE::cat*	"
AH5413	*ΔspoVID, yaaHΩyaaH-gfp* Spc^r	"
AH5414	*ΔspoVID, amyE'::spoVID::'amyE, yaaHΩyaaH-gfp* Neo^r Spc^r	"
AH5415	*ΔspoVID, amyE'::spoVID$_{\Delta E}$::'amyE, yaaHΩyaaH-gfp* Neo^r Spc^r	"
AH5416	*ΔspoVID, amyE'::spoVID$_{L125A}$::'amyE, yaaHΩyaaH-gfp* Neo^r Spc^r	"
AH5417	*ΔspoVID, amyE'::spoVID$_{I127A}$::'amyE, yaaHΩyaaH-gfp* Neo^r Spc^r	"
AH5418	*ΔspoVID, amyE'::spoVID$_{L131A}$::'amyE, yaaHΩyaaH-gfp* Neo^r Spc^r	"
AH5419	*ΔspoVID, amyE'::spoVID$_{I133A}$::'amyE, yaaHΩyaaH-gfp* Neo^r Spc^r	"
AH5421	*ΔspoVID, cotMΩcotM-gfp* Spc^r	"
AH5422	*ΔspoVID, amyE'::spoVID::'amyE, cotMΩcotM-gfp* Neo^r Spc^r	"
AH5423	*ΔspoVID, amyE'::spoVID$_{\Delta E}$::'amyE, cotMΩcotM-gfp* Neo^r Spc^r	"
AH5424	*ΔspoVID, amyE'::spoVID$_{L125A}$::'amyE, cotMΩcotM-gfp* Neo^r Spc^r	"

Table 3.1: Bacterial strains used in this study (cont.)

Strains	Relevant properties	Source
AH5425	*ΔspoVID*, *amyE'::spoVID$_{I127A}$::'amyE*, *cotMΩcotM-gfp* Neo^r Spc^r	This study
AH5426	*ΔspoVID*, *amyE'::spoVID$_{L131A}$::'amyE*, *cotMΩcotM-gfp* Neo^r Spc^r	"
AH5427	*ΔspoVID*, *amyE'::spoVID$_{I133A}$::'amyE*, *cotMΩcotM-gfp* Neo^r Spc^r	"
AH5464	*ΔsafA*, *amyE'::safA-yfp::'amyE*, *cotEΩcotE-cfp* Neo^r Spc^r	"
AH5465	*ΔsafA*, *amyE'::safA-yfp::'amyE*, *ΔspoVID, cotEΩcotE-cfp* Neo^r Spc^r	"
AH5463	*ΔsafA*, *cotEΩcotE-cfp*, Spc^r	"
AH5420	*ΔsafA*, *amyE'::safA-yfp::'amyE*, *cotE::cat* Neo^r Cm^r	"
AH5466	*ΔsafA*, *amyE'::safA-yfp::'amyE*, *spoVID$_{ΔE}$, cotEΩcotE-cfp* Neo^r Spc^r	"
AH5467	*ΔsafA*, *amyE'::safA-yfp::'amyE*, *spoVID$_{L125A}$, cotEΩcotE-cfp* Neo^r Spc^r	"
AH5468	*ΔsafA*, *amyE'::safA-yfp::'amyE*, *spoVID$_{I127A}$, cotEΩcotE-cfp* Neo^r Spc^r	"
AH5469	*ΔsafA*, *amyE'::safA-yfp::'amyE*, *spoVID$_{L131A}$, cotEΩcotE-cfp* Neo^r Spc^r	"
AH5470	*ΔsafA*, *amyE'::safA-yfp::'amyE*, *spoVID$_{I133A}$, cotEΩcotE-cfp* Neo^r Spc^r	"
E. coli		
DH5α	F$^-$ Φ80*lac*ZΔM15 Δ(*lac*ZYA-*ara*F) U169 *rec*A1 *end*A1 *hsd*R17 (rK$^-$, mK$^+$) *pho*A *sup*E44 λ$^-$ *thi*-1 *gyr*A96 *rel*A1	Invitrogen
BL21	F$^-$ dcm ompT hsdS(rB$^-$ mB$^-$) gal λ(DE3)	Promega
BL21	F$^-$ dcm ompT hsdS(rB$^-$ mB$^-$) gal λ(DE3) pLysS (Cm^r)	Novagen
CC118	Δ(ara-leu) araD ΔlacX74 galE galK phoA20 thi-1 rpsE rpoB argE(Am) recAl λ(DE3) pLysS (Cm^r)	Colin Manoil
AH2687	CC118(DE3)/pLysS/pTC55 Amp^r Cm^r	Costa *et al*., 2006
AH2692	CC118(DE3)/pLysS/pOZ169 Amp^r Cm^r	"
AH5291	CC118(DE3)/pLysS/pFN86 Amp^r Cm^r	This study
AH5301	CC118(DE3)/pLysS/pFN88 Amp^r Cm^r	"
AH5302	CC118(DE3)/pLysS/pFN89 Amp^r Cm^r	"
AH5303	CC118(DE3)/pLysS/pFN90 Amp^r Cm^r	"
AH5304	CC118(DE3)/pLysS/pFN91 Amp^r Cm^r	"
AH5305	CC118(DE3)/pLysS/pFN92 Amp^r Cm^r	"
AH5290	CC118(DE3)/pLysS/pFN85 Amp^r Cm^r	"
AH5306	CC118(DE3)/pLysS/pFN93 Amp^r Cm^r	"
AH5307	CC118(DE3)/pLysS/pFN94 Amp^r Cm^r	"
AH5308	CC118(DE3)/pLysS/pFN95 Amp^r Cm^r	"
AH5309	CC118(DE3)/pLysS/pFN96 Amp^r Cm^r	"
AH5236	BL21(DE3)/pFN76 Cm^r	"
AH5240	BL21(DE3)/ pET21b-*cotE-STOP* Amp^r	"

In-frame deletions of *spoVID* and *safA*, and a *ΔcotE::cat* null mutant

SOE-PCR was used to generate an amplicon composed by the *spoVID* coding sequence with an in-frame deletion that eliminates residues 39-548, as well as the upstream and downstream regions of the gene. This DNA fragment was cloned into the vector pJET1.2/blunt (ThermoFisher Scientific), digested with BglII, and subcloned in the plasmid pMAD (Arnaud *et al.*, 2004) to create pFN87. SOE-PCR was also used to obtain a DNA fragment containing the *safA* coding sequence with an in-frame deletion that eliminates residues 46 – 249 (required for production of $SafA_{C30}$ and $SafA_{N20}$ and for SafA localization) and *safA* flanking regions. The fragment was digested with EcoRI and SalI and inserted into pMAD (Arnaud *et al.*, 2004), generating pFN115. pFN87 and pFN115 were then transformed into PY79 cells, as previously described (Arnaud *et al.*, 2004), creating strains AH5246 and AH5367. Integration of the in-frame deletions in *spoVID* or in *safA* was confirmed by PCR. Heat and lysozyme resistance assays and germination tests by overlay (Nicholson and Setlow, 1990) were used to address the phenotypes of these null mutants.

The *cotE* null mutant was obtained by transformation of PY79 cells with the chromosomal DNA of AH2835 (Costa *et al.*, 2007), followed by selection for chloramphenicol resistance.

Integration of *spoVID* alleles at the *amyE* locus

The coding sequence of *spoVID* and its flanking regions were PCR amplified with primers SpoVID-24D and SpoVID-1952R. These primers, in combination with each of those pairs listed in Table A5 of the Appendices, were used to amplify *spoVID* versions with modifications within region E or with the deletion of this region, through site-directed mutagenesis. PCR products were digested with XbaI and BamHI and cloned into the vector pMLK83 (Karow and Piggot, 1995) to create pFN101–105, pFN107 and pFN110–111. These vectors were then transformed into the *spoVID* null

mutant strain AH5246, resulting in strains AH5354–5359, AH5362 and AH5363, expressing the various *spoVID* alleles from the *amyE* locus.

Construction of a functional SafA-YFP fusion

The vector pCF75 (Fernandes, C. and Henriques, A. O., not published) was constructed by insertion of the *safA* coding sequence and its flanking regions into pMLK83 (Karow and Piggot, 1995). A DNA fragment composed by the 3' region of *safA*, a sequence coding for the flexible linker FL3 (residues LGGGGSGGGGSGGGGSAAA, Arai *et al.*, 2001) and the 5' region of *yfp* was amplified without template using oligonucleotides safA-fl3D and fl3-yfpR. This fragment was fused to *yfp* by SOE-PCR with primers fl3-yfpD and yfp-TsafAR, and the resulting amplicon was used as a megaprimer to insert *fl3* and *yfp* into pCF75, generating pCF149. The *safA* null mutant AH5367 was then transformed with this vector, resulting in a strain expressing *safA-fl3-yfp* (herein *safA-yfp*) from the *amyE* locus (AH5370). The functionality of the fluorescent fusion was addressed by heat and lysozyme resistance assays and by the profile of extractable coat proteins resolved in SDS-PAGE, in comparison with a strain expressing the pre-existing *safA-gfp* fusion.

***B. subtilis* strains expressing fluorescent fusions**

For expression of SafA-YFP from the *amyE* locus, strain AH5370 was constructed as described above. To obtain cells producing this fusion in the absence of SpoVID, *spoVID* null mutant cells (AH5246) were transformed with pFN115 for insertion of the *safA* in-frame deletion (Arnaud *et al.*, 2004), and with pCF149 to insert *safA-yfp* into the *amyE* locus, creating the strain AH5371. To express SafA-YFP in a *cotE* null mutant background, the strain AH5370 was transformed with the chromosomal DNA of AH2835 cells (Costa *et al.*, 2007), followed by selection for chloramphenicol resistance. The maintenance of the *safA* in-frame deletion in the resulting strain, AH5240, was confirmed by PCR. For expression of SafA-YFP in the presence of SpoVID

variants without region E or with alanine substitutions within this region, new pMAD (Arnaud *et al.*, 2004) derivative vectors were designed. The various *spoVID* alleles were amplified by SOE-PCR (primers listed in Table A5 of Appendices), digested with BglII and BamHI, and inserted into pMAD to generate plasmids pFN116-126. Then, strain AH5370 was transformed with these plasmids, replacing the wild type *spoVID* for *spoVID* versions through double crossing-over (Arnaud *et al.*, 2004). The presence of each mutation in the new strains, AH5383–5393, was finally confirmed by sequencing.

To obtain cells expressing YaaH-GFP or CotM-GFP, strains AH5354–5358 and AH5362, expressing the various *spoVID* alleles form the locus *amyE*, as well as the *spoVID* null mutant strain AH5246, were transformed with the chromosomal DNA of PE793 or PE787 (Wang *et al.*, 2009), harboring *yaaH-gfp* and *cotM-gfp* fusions, respectively. Cells were then selected for spectinomycin resistance, resulting in strains AH5413–5419 and AH5421–5427.

For expression of SafA-YFP and CotE-CFP within the same cell, strains AH5367, AH5370–5371, AH5383–5384, AH5386 and AH5389–5390, harboring *safA-yfp*, were transformed with the chromosomal DNA of PE1945 (McKenney and Eichenberger, unpublished), containing *cotE-cfp*, and selected for spectinomycin resistance. The maintenance of *safA* and *spoVID* in-frame deletions in the new strains (AH5463–5470) was confirmed by PCR.

Strains for overproduction of GST-SpoVID variants

DNA fragments corresponding to the various *spoVID* alleles were generated by site-directed mutagenesis using pairs of oligonucleotides described in Table A5 of the Appendices. These fragments were digested with BamHI and XhoI and inserted into pGEX-4T-2 to create vectors pFN85–86 and pFN88–96, harboring *gst* fused to *spoVID* variants. *E. coli* CC118(DE3)/pLysS cells were transformed with these expression vectors, resulting in strains AH5290–5291 and AH5301–5309. For overproduction of

untagged SafA, the *safA* coding sequence was amplified with primers safA-364D and SafA1364R, digested with NcoI and BamHI and inserted in the same cloning sites of pACYCDuet-1 (Merck Millipore). The vector was introduced in *E. coli* BL21(DE3) cells, creating strain AH5236. Overproduction of untagged CotE was achieved using an *E. coli* BL21(DE3) derivative harboring pET21b-*cotE-STOP* vector (de Francesco *et al.*, 2012), AH5240.

Fluorescence microscopy and image analysis

One-milliliter samples were collected from SM cultures of *B. subtilis* strains. Cells were harvested by centrifugation (4000 × *g*, 10 min, at 4°C) and resuspended in 0.1 mL of PBS supplemented with 1 μL of a 2 mg/mL solution of the membrane dye FM 4-64 (Molecular Probes, Invitrogen). Fluorescence microscopy was conducted in Leica DM6000B or in Nikon 90i microscopes, as previously described (Serrano *et al.*, 2011; McKenney and Eichenberger, 2012). The Leica microscope was coupled with a phase contrast objective Uplan F1 100x, and images were acquired with a CCD camera Andor Ixon^{EM} (Andor Technologies) using the software Metamorph v5.8 (Molecular Devices). The Nikon microscope was equipped with an objective Plan Fluor 1.3NA 100x (Nikon), a Roper 1K digital camera and the software NIS Elements AR 3.0 (Nikon). Metamorph v5.8, NIS Elements AR 3.0 and ImageJ (http://rsbweb. nih.gov/ij/) were used for image analysis. For quantification of the subcellular localization patterns of fluorescent fusions, at least 100 sporulating cells were randomly examined and scored for each strain. The 3D graphics of the fluorescent intensity patterns in sporulating cells were obtained using the ImageJ plugin *Interactive 3D Surface Plot* v2.33.

Accumulation of SpoVID variants during sporulation

Ten-milliliter samples were collected from SM cultures of the strains PY79, AH5246, AH5354–5359 and AH5362–5363. Cells were harvested by

centrifugation (7500 × *g*, 10 min, at 4°C), resuspended in French press buffer (10 mM Tris pH 8.0, 10 mM $MgCI_2$, 0.5 mM EDTA, 0.2 M NaCI, 10% glycerol, 0.1 mM DTT, 1 mM PMSF), and lysed in a French pressure cell (18,000 lb/in^2). Cell extracts were quantified using the Bio-Rad mini protein system according to manufacturer's instructions. 10 µg of each sample were prepared for SDS-PAGE 10%, and proteins were resolved, transferred to nitrocellulose membranes and immunobloted using purified anti-SpoVID antibodies. As a control for the amount of cell extracts loaded in the gel, membranes were stripped with stripping buffer (50 mM Tris, pH 6.8, 2% SDS, 100 mM β-mercaptoethanol) and reprobed with anti-σ^{70} antibody (Abcam), that recognizes σ^A.

GST pulldown assays

For overproduction of glutathione *S*-transferase (GST) fused to SpoVID variants and of native GST, the derivatives of *E. coli* CC118 (DE3)/pLysS listed in Table 3.1 were used. SafA expression was performed with the *E. coli* BL21(DE3) derivative AH5236. Cultures of 10 mL (for GST and SafA) or 50 mL (for GST-SpoVID variants) were grown to an optical density at 600 nm of 0.6 and induced with 1 mM IPTG for 3 h (for GST and GST-SpoVID variants) or for 30 min (for SafA). Cells were harvested by centrifugation (at 4°C for 10 min, at 7500 × *g*) and resuspended in 1 mL of cold buffer. GST-SpoVID variants and GST producing cells were resuspended in VPEX-100 buffer with β-mercaptoethanol (Ozin *et al.*, 2001b; de Francesco *et al.*, 2012), while SafA producing cells were resuspended in buffer I (PBS- 0,1% Tween 20 + 10% glycerol), both supplemented with 1 mM PMSF and Complete Mini EDTA-free protease inhibitor cocktail (Roche). Cell lysis was performed in a French pressure cell (18,000 lb/in^2) or in a sonicator QSonica CL5 (Misonix) under optimal conditions for cell breakage (amplitude of 50 for 30s, repeated 4 times with 10s intervals). The lysates were cleared by centrifugation (at 4°C for 20 min, at 10 000 × *g*) and diluted

to adjust concentrations (1:1 to 1:5 for GST-SpoVID variants, 1:20 for GST and 1:500 for SafA). Pulldown assays were performed as previously described (de Francesco *et al.*, 2012), except that GST and GST-SpoVID variants were used as baits and SafA was used as prey. As a negative control, a BL21(DE3) cleared lysate was incubated with GST-SpoVID immobilized in glutathione beads. Proteins retained by the beads were resuspended in protein loading buffer, boiled for 5 min, and resolved in SDS-PAGE 12.5%. Gels were transferred to nitrocellulose membranes for immunoblot analysis with anti-SafA antibodies. Membranes were finally stained with Ponceau Red, as a control for the retention of GST-SpoVID variants and GST.

Spore purification, coat proteins extraction, and spore fractionation

Spores were purified from SM cultures with 24 hours by a two-step gradient of gastrografin (Bayer Schering Pharma), as previously described (Seyler *et al.*, 1997; Henriques and Moran, 2000). Extraction of coat proteins was achieved by boiling the purified spores (equivalent to an OD_{580nm} of 2) for 8 min in extraction buffer (10% glycerol, 4% SDS, 250 mM Tris pH 6.8, 10% β-mercaptoethanol, 1 mM DTT, 0.05% bromophenol blue), followed by centrifugation (2 min, 16200 × *g*). Coat proteins within the supernatant were then resolved by SDS-PAGE 15% (Seyler *et al.*, 1997; Henriques and Moran, 2000), and gels were stained with Coomassie brilliant blue R-250 for protein visualization.

For spore fractionation, spores corresponding to an OD_{580nm} of 2 were boiled for 5 min in extraction buffer without bromophenol blue and centrifuged (2 min at 16200 × *g*). The supernatant, consisting of the soluble coat fraction, was removed and stored in a new tube, where bromophenol blue was added for final concentration of 0.05% before analysis in SDS-PAGE 15%. The sediment, containing the decoated spores, was washed twice with Tris-buffered saline with Tween 20 (TBS-T: 50 mM Tris, 150 mM NaCl, pH 8.0, 0.1% Tween 20) and divided into two equal volume samples. These

samples were incubated at 37° C for 2 hours in 50 mM Tris buffer (pH 8.0), with or without lysozyme (2 mg/mL). Then, they were boiled for 5 min in protein loading buffer, and proteins were resolved in SDS-PAGE 15%, along with half of the volume of the coat fractions (above). Gels were transferred to nitrocellulose membranes for immunoblot analysis using anti-SafA, anti-CotE and anti-SpoVID antibodies. As a control for the decoating, membranes were stripped as described above and reprobed with anti-CotA antibodies.

Peptide-binding assays

Three types of N-terminal biotinylated peptides were used in these experiments: one with the wild type sequence of region E plus 3 residues upstream and one downstream (SRILTIQADLAIE GLLD), and two variants of this peptide with alanine substitutions in residues corresponding to L125 and L131 in SpoVID (SRIATIQADLAIEGLLD and SRILTIQADAAIEGLLD). Peptides were synthesized by ThermoFisher Scientific (with purities of >73,121% for wild type, >92,361% for L125A and >83,514% for L131A variants) and diluted in PBS – 0,1% Tween 20.

Overproduction of GST-SpoVID variants, GST and SafA, as well as preparation of the cell lysates, was performed as described for GST pulldown assays. For CotE overproduction, 10 mL cultures of AH5240 were grown to an OD_{600nm} of 0.6 and induced with 1 mM IPTG for 3 h. Cells were harvested by centrifugation (at 4°C for 10 min, at 7500 × *g*), resuspended in 1 mL of cold buffer I supplemented with 1 mM PMSF and protease inhibitor cocktail, and lysed. The lysate was cleared by centrifugation and the soluble fraction was diluted 1:10. Pulldown assays were performed as described above, except that CotE was also used as prey. Also, peptides were added to the diluted lysates containing SafA, CotE or GST-SpoVID variants, depending on the binding assay, for the final concentrations of 1, 10 or 100 μM, and incubated for 1 hour (at 4ºC with agitation) before addition to the beads fractions. For CotE detection, anti-CotE antibodies were used.

Transmission electron microscopy

Cells from SM cultures with 8 hours were collected by centrifugation, fixed and processed for thin sectioning electron microscopy, as previously described (Ozin *et al.*, 2000).

Immunoblot analysis

Immunoblot analysis was conducted using the SuperSignal West Pico Chemiluminiscent Substrate (ThermoFisher Scientific) according to the manufacturer´s instructions. 5% low fat powder milk in PBS- 0,1% Tween 20 (0.001%) was used as the blocking agent. Antibodies were used at the following dilutions: anti-SafA (a gift from Charles P. Moran Jr.) 1:15 000, and anti-CotA, anti-CotE, anti-SpoVID and anti-σ^{70} (laboratory stocks) at 1:1 000. Secondary horseradish peroxidase-conjugated antibody (Sigma) was used at a dilution of 1:5 000.

RESULTS

Specific residues in region E are essential for encasement by SafA

Our previous findings (see Chapter 2) showed that region E, at the end of the N-terminal domain of SpoVID, is essential for spore encasement by proteins residing in each of the four coat sublayers. The SafA-dependent, inner coat protein YaaH is one of these proteins, suggesting that SafA also requires region E for encasement. Moreover, SafA interacts directly with the N terminus of SpoVID (Costa *et al.*, 2006). Residue L131, within region E, is essential for a direct interaction with and encasement by CotE, but dispensable for a direct interaction with SafA (Chapter 2,(de Francesco *et al.*, 2012). Therefore, we aimed at determining if region E is involved in encasement by SafA, and if so, which residues within this region have a major role.

We started by performing alanine scanning mutagenesis of region E, in order to analyze the contribution of the side chains of residues in this region to the subcellular localization of SafA. To do this, we first constructed a strain with an in-frame deletion of *safA* and expressing *safA* fused to *yfp* (*safA-yfp*, Fig. 3.2 A) from the non-essential locus *amyE*. The in-frame deletion of *safA* reduces the polar effects on downstream genes of the operon. Spores produced by this deletion mutant are sensitive to lysozyme treatment (Fig. 3.2 B) and have an altered profile of extractable coat proteins in SDS-PAGE (Fig. 3.2 C), in line with the phenotype of *safA* insertional mutants previously constructed (Takamatsu *et al.*, 1999; Ozin *et al.*, 2000). Regarding the *safA-yfp* fusion, it comprises the flexible linker *fl3* (Arai *et al.*, 2001) connecting *safA* and *yfp* (Fig. 3.2 A). Cells expressing this fusion exhibit a profile of coat proteins closer to the wild type, in comparison with cells harboring pre- existing fluorescent protein fusions to SafA (Fig. 3.2 C). Also, spores produced by this strain are resistant to heat and lysozyme treatments (Fig. 3.2 B), suggesting integrity of the cortex and coat. We then generated

A

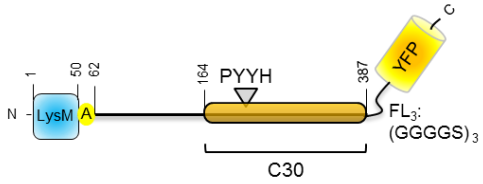

B

	Titer of spores (CFU/mL)		
	Viable	Heat	Lysozyme
wt	$1.8\pm0.4\times10^{8}$	$1.8\pm0.4\times10^{8}$	$1.7\pm0.3\times10^{8}$
safA-yfp	$2.3\pm0.9\times10^{8}$	$1.6\pm0.3\times10^{8}$	$1.7\pm0.3\times10^{8}$
safA-gfp	$2.4\pm0.1\times10^{8}$	$2.4\pm0.1\times10^{8}$	$1.6\pm0.7\times10^{8}$
Δ*safA*	$1.6\pm0.5\times10^{8}$	$1.7\pm0.4\times10^{8}$	$7.4\pm2.5\times10^{7}$

C

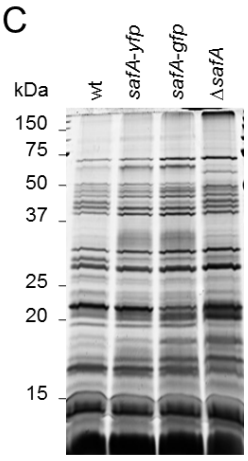

Figure 3.2 – **A)** Schematic view of the SafA-YFP construction, in which YFP was inserted at the C terminus of SafA, separated by the flexible linker FL3. **B)** Heat and lysozyme resistant spore counts in wild type cells (wt), in cells with the in-frame deletion of *safA* (Δ*safA*) and in cells expressing either *safA-yfp* or *safA-gfp* fusions. **C)** SDS-PAGE profiles of the extractable coat proteins from spores produced by those strains.

spoVID alleles with alanine substitutions for all residues within region E other than alanines, and the entire region was also deleted. These alleles were transferred to the *spoVID* locus of the strain expressing *safA-yfp*. As a control, an in-frame s*poVID* deletion mutation was also transferred to the *safA-yfp* background.

Mutant strains with the various *spoVID* alleles or with the in-frame deletion of *spoVID* and expressing *safA-yfp* were resuspended in SM medium and imaged by fluorescence microscopy along sporulation (Figs. 3.3; Fig S1 of Appendices; Table 3.2). In cells expressing the wild type *spoVID*, SafA-YFP starts localizing at the asymmetrical septum as soon it begins to curve, forming a dot that expands into a cap (visible in 91% of the sporulating cells at hour 2). Then, after engulfment completion but before the spore became phase-dark, a second cap appears at the opposite pole (in 47%, at hour 4), and finally SafA-YFP completely encircles the spore (in 83%, at hour 6). This progression, particularly evident on three-dimensional representations of the YFP signal in sporulating cells (Fig 3.3, 3rd rows), is consistent with the localization pattern of coat proteins belonging to kinetic class II, according to the classification of McKenney and Eichenberger, 2012. Similar patterns of SafA-YFP localization were observed for strains with substitutions T126A, Q128A, D130A, L131A, E134A, G135A or L136A in SpoVID (Fig. S1; Table 3.2), indicating that the side chains of these residues are not critical for SafA localization. Therefore, it appears that residue L131 has a specific role in encasement by CotE and its partners.

In cells with the deletion of region E, as well as in sporangia bearing a deletion of *spoVID*, SafA-YFP localizes as a dot at the MCP pole in the first targeting step, but then the encasement is impaired. Six hours after resuspension, SafA-YFP remains accumulated as a dot or as a single cap in some sporulating cells, while in others the YFP signal spreads into the mother cell cytoplasm (Fig. 3.3, 2nd column; Fig. S1; Table 3.2). This confirms that region E of SpoVID is required for encasement by SafA, as suggested by

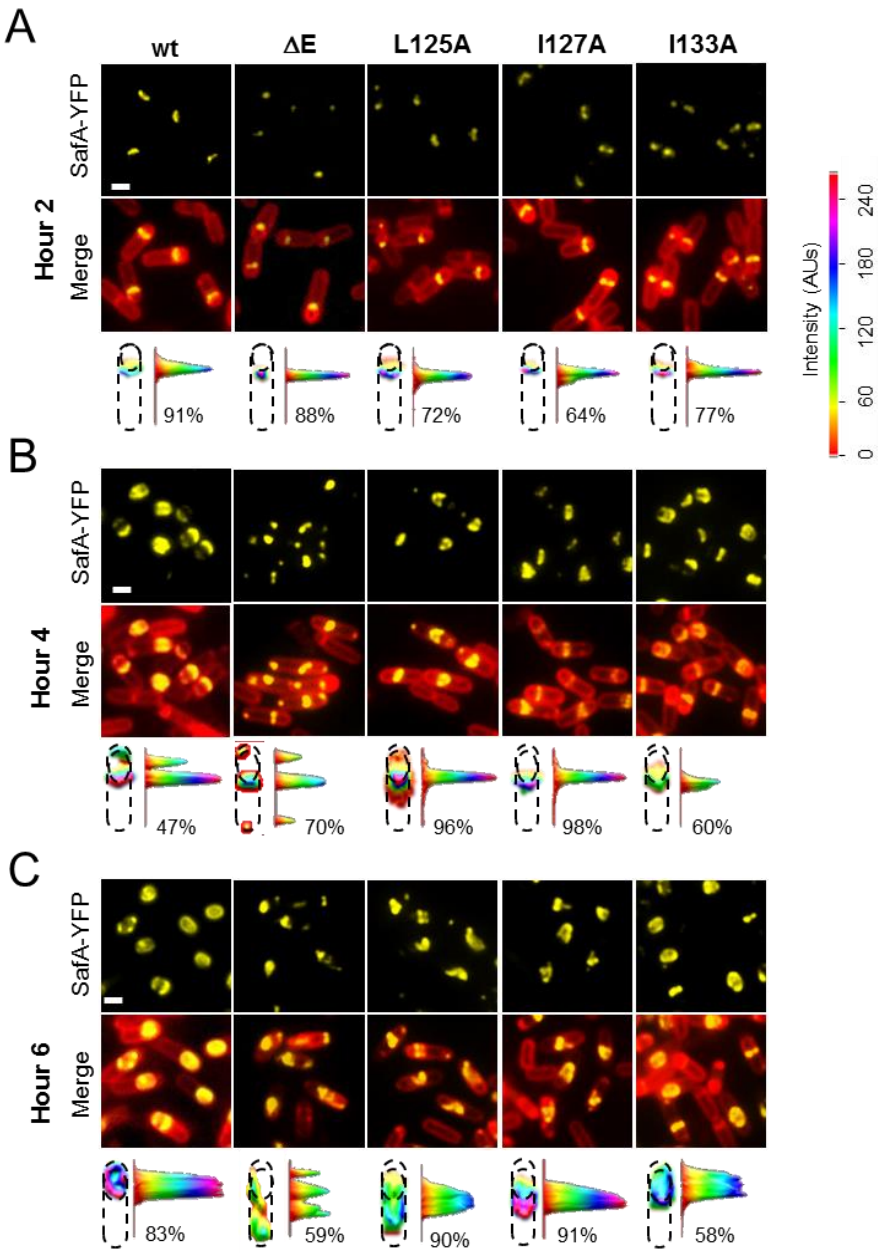

Figure 3.3 – Specific residues within region E are required for encasement by SafA-YFP. Strains expressing SafA-YFP and the various SpoVID forms were colected at **A)** 2, **B)** 4 and **C)** 6 hours after the onset of sporulation, stained with the membrane dye FM 4-64 and analysed by fluorescence microscopy. A few representative cells are shown for mutant strains that revealed a different subcellular localization pattern of SafA-YFP comparing to wild type cells. 1st rows: SafA-YFP signal; 2nd rows: merge between the signals of SafA-YFP and stained membranes; 3rd rows: 3D distribution of the YFP signal for one representative cell of each strain, with the percentage of cells that exhibit that pattern indicated bellow each graph. Scale bar: 1µm.

our previous results (Chapter 2). However, the deletion of region E does not totally resemble the phenotype of the *spoVID* null mutant. In cells expressing *spoVID*$_{\Delta E}$, SafA-YFP commonly mislocalizes in the mother cell cytoplasm (59%) or accumulates as a foci at the MCP pole of the spore (24%) at later stages (hour 6), whereas *spoVID* null mutant cells typically exhibit a single YFP cap (59%). Yet, the YFP signal also spreads in the mother cell cytoplasm in 35% of the null mutant cells.

Table 3.2: Quantification of the encasement by SafA-YFP in strains expressing the various *spoVID* alleles [a]

	Hour 2			Hour 4				Hour 6				
												
wt	3	**91**	6	0	21	**47**	**32**	0	10	7	**83**	0
Δ*spoVID*	**84**	16	0	**34**	**66**	0	0	6	**59**	0	0	**35**
ΔE	**88**	12	0	**30**	**70**	0	0	24	17	0	0	**59**
L125A	**28**	**72**	0	3	**96**	1	0	0	**90**	0	0	10
T126A	5	**93**	2	0	19	**58**	**23**	0	11	13	**76**	0
I127A	**36**	**64**	0	0	**98**	0	2	3	**91**	1	2	3
Q128A	4	**89**	7	0	12	**42**	**46**	0	11	7	**80**	2
D130A	0	**100**	0	0	28	**33**	**39**	0	10	14	**76**	0
L131A	1	**95**	4	0	15	**47**	**38**	0	13	16	**71**	0
I133A	**23**	**77**	0	0	**60**	16	**28**	0	**35**	3	**58**	4
E134A	6	**94**	0	0	25	**47**	**28**	0	17	13	**70**	0
G135A	2	**94**	4	0	28	**27**	**45**	0	13	15	**70**	2
L136A	3	**96**	1	0	26	**33**	**41**	0	15	11	**74**	0

[a] The numbers correspond to the percentages of sporulating cells with each of the SafA-YFP localization patterns represented, at 2, 4 and 6 hour after the onset of sporulation.

We found that substitutions L125A and I127A, within region E, are sufficient to block encasement by SafA-YFP. In strains expressing *spoVID*$_{L125A}$ or *spoVID*$_{I127A}$, approximately 90% of the sporulating cells exhibit a single fluorescent cap at the MCP pole of the spore at later stages (hour 6). Although a small fluorescent dot can be visible in the mother cell distal (MCD) pole in a few cells, a second cap or a complete ring is rarely formed (Fig. 3.3; Fig S1;

Table 3.2). Interestingly, L125 and I127 are also required for encasement by CotE (de Francesco *et al.*, 2012). Substitution I133A also causes a defect in encasement by SafA-YFP. In strains with this substitution, SafA-YFP is able to encircle the spore, yet the proportion of sporulating cells exhibiting a single fluorescent cap after 4 and 6 hours of sporulation is higher than in the wild type (60% and 35% in the I133A variant *vs* 21% and 10% in the wild type). This suggests that encasement by SafA-YFP is delayed in these cells (Fig. 3.3; Fig S1; Table 3.3).

We then investigated whether the SpoVID variants that caused mislocalization of SafA-YFP accumulate in sporulating cells. We constructed new strains with the in-frame deletion of *spoVID* and expressing the various *spoVID* alleles from the locus *amyE*. Cells were collected at 2, 4 and 6 hours after the onset of sporulation and lysed. Then, we carried out immunoblot assays on cell extracts using anti-SpoVID antibodies (Fig. 3.4, 1st row) and, as a loading control, with antibodies that recognize σ^A (Fig. 3.4, 2nd row). Bands of the expected molecular mass were detected for all mutant strains, showing that the various SpoVID forms accumulate in these cultures. This is in line with previous experiments that showed that these variants, when fused to CFP, localize in sporulating cells in identical patterns as the wild type SpoVID-CFP (de Francesco *et al.*, 2012).

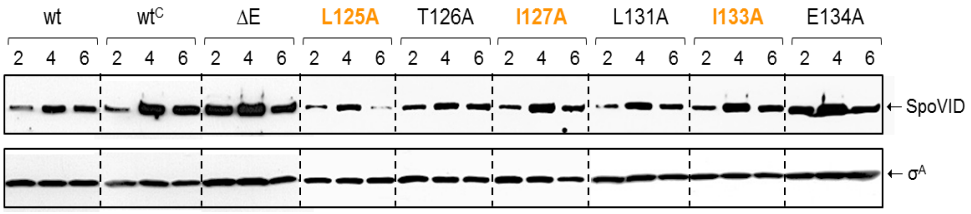

Figure 3.4 – SpoVID variants that led to mislocalization of SafA-YFP accumulate in sporulating cells along the time. Samples of SM media cultures were collected at 2, 4 and 6 hours after resuspension, and cells were lysed. Identical quantities of cell extracts were resolved in SDS-PAGE and immunobloted with anti-SpoVID antibodies (1st panel). Anti-σ^{70} antibodies, that recognize σ^A, were used as a loading control (2nd panel). wt: PY79 wild type cells; wtC: *amyE'::spoVID::'amyE*.

Residues involved in encasement by SafA are important for a direct interaction between SafA and SpoVID

In order to determine whether region E residues that are important for encasement by SafA are also required for a direct interaction between SafA and SpoVID, we conducted *in vitro* GST pulldown assays. We immobilized each N-terminally GST-tagged variant of SpoVID, as well as GST alone, in glutathione beads and incubated the beads with extracts prepared from *E. coli* producing SafA (Fig. 3.5 A). After several washings, proteins retained by the beads were resolved by SDS-PAGE and immunoblotted with anti-SafA antibodies (Fig. 3.5 B, 1st row). As an antibody specificity control, lysates of *E. coli* producing or not SafA were directly applied in the gel (Fig. 3.5 B, *input material*). Also, the membranes were stained with Ponceau Red

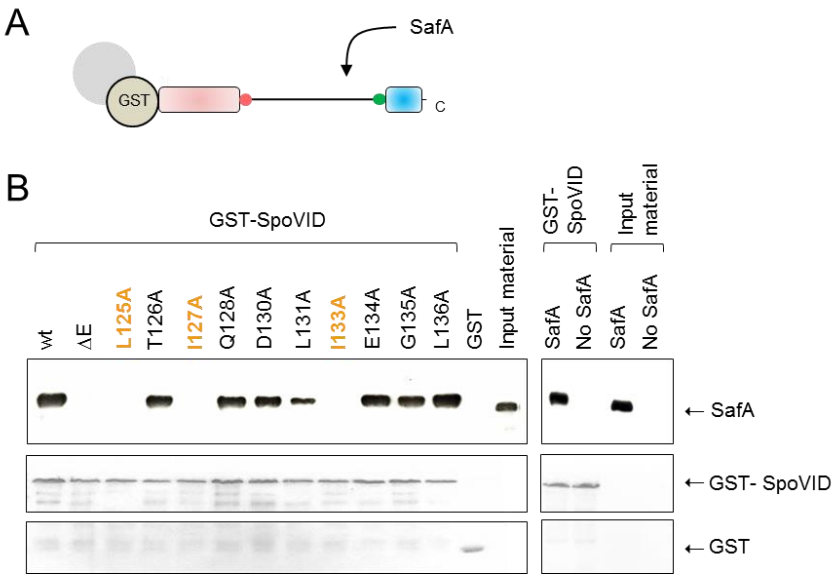

Figure 3.5 – L125, I127 and I133 are required for a direct interaction with SafA *in vitro.* **A)** Scheme of the GST pulldown assay. GST-SpoVID variants bound to glutathione beads were used as baits and were incubated with extracts of *E. coli* producing SafA. **B)** Proteins within beads fractions were resolved and immunobloted with anti-SafA antibodies (1st row). The membranes were stained with Ponceau Red as a control for the amount of GST-SpoVID variants or GST bond to glutathione beads (2nd and 3rd rows). As an antibody specificity control, we incubated *E. coli* extracts with or without SafA with the wild type GST-SpoVID (right pannel, 1st and 2nd lanes), and we also aplied directly the two cell extracts in the gel (last lane of the left panel, 3rd and 4th lanes of the right panel).

as a control for the amounts of GST-SpoVID variants or GST bond to the beads (Fig. 3.5 B, 2nd and 3rd rows). As expected (Ozin *et al.*, 2000; Ozin *et al.*, 2001b; Costa *et al.*, 2006), the wild type SpoVID fused to GST, but not GST alone, was able to pull-down SafA from the extracts. Of all the GST-SpoVID variants, only the ones missing region E or with the substitutions L125A, I127A or I133A did not pull-down SafA. This shows that the three residues of SpoVID required for encasement by SafA are involved in the direct interaction with this protein. The L131A substitution, which impairs binding of SpoVID to CotE, also reduces the ability of GST-SpoVID to pull-down SafA from the extracts. Therefore, this residue has a role in binding to SafA as well, but it is not as important as for binding to CotE. Together with the data from Chapter 2, we conclude that there are three residues within region E (L125, I127 and I133) that are important for the interaction of SpoVID with SafA and have a role in encasement by this protein. Of those, two are also required for encasement by CotE (L125 and I127), yet only one of them (I127) is required for a direct interaction with SpoVID.

Residues in region E required for interaction with SafA have a role in anchoring SafA to the spore surface

We then investigated the distribution of SafA across the different layers of the spore in strains harboring SpoVID variants for which binding to SafA was affected *in vitro*. We purified spores produced by cells expressing different *spoVID* alleles from the *amyE* locus, as well as wild type spores and spores missing *safA* or *cotE* as controls. Then, the coat proteins were extracted (coat fraction), and the decoated spores were submitted to a lysozyme treatment that digests the exposed cortex and is thought to release cortex-associated proteins (cortex fraction). Proteins within these spore fractions, along with those retained in decoated spores not-digested with lysozyme, were resolved by SDS-PAGE and immunobloted for the detection of SafA (Fig. 3.6 A, 1st row).

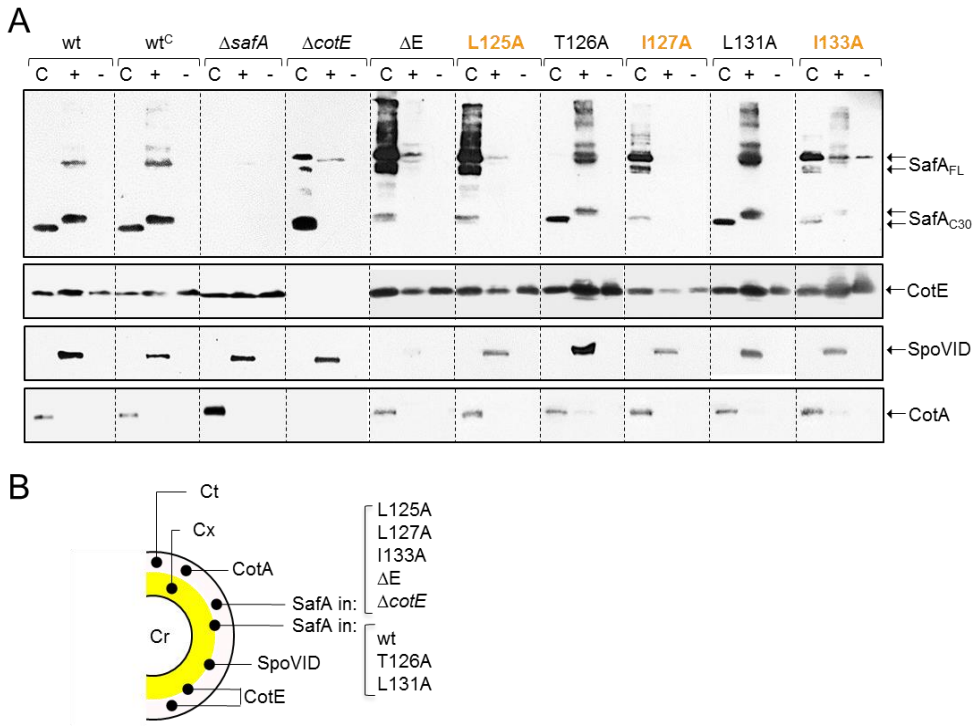

Figure 3.6 – Substitutions L125A, I127A and I133A increase the extractability of SafA. **A)** Spores produced by cells expressing the various *spoVID* variants, as well as by wild type and *safA* or *cotE* null mutant cells, were purified and decoated. The exposed cortex was then digested with lysozyme, and proteins within the different spore fractions were resolved by SDS-PAGE and immunobloted with anti-SafA (1st panel), anti-CotE (2nd panel), anti-SpoVID (3rd panel) and anti-CotA antibodies (4th panel). wtC: Δ*spoVID, amyE'::spoVID::'amyE*; C: coat fraction; +: cortex fraction submitted to lysozyme treatment; -: cortex frsction not digested with lysozyme. **B)** Model for the localization of SpoVID, SafA and CotE within the spore layers. Cr: core; Cx: cortex; Ct: coat.

In spores with the wild type *spoVID*, either expressed from the native locus or from *amyE* (Fig. 3.6, wt and wtC), the full-length form of SafA was detected exclusively in the cortex fraction. The higher molecular weight forms visualized may correspond to SafA oligomers or to highly cross-linked coat material. Regarding $SafA_{C30}$, it was present in the coat and in the cortex fractions in identical amounts. This form migrates slightly faster in the coat fraction, which may be due to processing by the YabG protease (Takamatsu *et al.*, 2000a; Takamatsu *et al.*, 2000b) in the coat, but not in the cortex. The presence of both forms of SafA in the cortex fraction indicates that they are

associated with this layer in mature spores. The $SafA_{N21}$ form was not detected in our assays, suggesting that it is not abundant (or extractable) at later stages of spore development. As an indication of the decoating efficiency, the bona fide coat protein CotA (Martins *et al.*, 2002) was present mainly in the coat fraction (Fig. 3.6 A, 4th row) and no proteins were immunologically detected in the decoated spores not digested with lysozyme. We were not able to use a specific marker for the cortex, since no presently known protein serves this propose.

In spores with the deletion of region E or with the substitutions L125A, I127A or I133A, but not with the substitutions T126A or L131A, SafA and $SafA_{C30}$ are mainly present in the coat fraction (Fig. 3.6 A, 1st row). The form of SafA that migrates slightly faster than the full-length in these mutant spores may correspond to the full-length form processed by YabG in the coat, as happens with $SafA_{C30}$. Also, in mutant spores where the SafA distribution is altered, especially in those expressing $spoVID_{\Delta E}$ or $spoVID_{L125A}$, the total amount of the extracted full-length form of SafA was higher than in wild type spores. We conclude that alanine substitutions within region E that affect the interaction between SafA and SpoVID also increase the extractability of SafA. This suggests that residues L125, I127 and I133 in SpoVID are important to anchor SafA to the spore surface, presumably via SpoVID, or that the later has a key role in allowing proper localization of SafA. In contrast, the $SafA_{C30}$ form was detected in lower amounts in the mutant spores, in line with the idea that it requires binding to the full-length form for localization. Additionally, in spores with the substitution I133A, we also detected SafA in the decoated spores not digested with lysozyme. This reinforces that the effect of this substitution in mislocalization of SafA is distinct from the effect of L125A and I127A.

In *cotE* null mutant spores, both forms of SafA were detected mainly in the coat fraction, suggesting that CotE and/or the outer coat are important for localization of SafA. However, the substitution L131A, that led to the

mislocalization of CotE, did not alter the distribution of SafA. We infer that the presence of CotE in this mutant, even if not assembled properly, is sufficient for SafA localization. We did not detect CotA in *cotE* null mutant spores, as this protein is CotE-dependent for localization (Fig. 3.6 A, 4th row).

We further investigated whether alanine substitutions within region E also affect the distribution of CotE or SpoVID in the spore layers. The incubation of the membranes from the spore fractionation assays with anti-CotE antibodies revealed that CotE is distributed across all the spore fractions (Fig. 3.6 A, 2nd row). Also, deletion of region E or substitutions within this region, including L131A, did not interfere with the distribution of this protein. Thus, despite the importance of region E in encasement by CotE, the effect of its deletion in CotE localization is not as pronounced as for the localization of SafA. The absence of SafA did not interfere with the distribution of CotE, supporting that CotE and the outer coat do not require SafA for localization.

SpoVID was detected exclusively in the cortex fraction (Fig. 3.6 A, 3rd row), suggesting that it is associated with the cortex layer in mature spores. Single alanine substitution within region E did not interfere with the distribution of SpoVID. We were not able to detect $SpoVID_{\Delta E}$ in these assays, yet it accumulates in sporulating cells (Fig. 3.4). Moreover, $SpoVID_{\Delta E}$-CFP localizes at the spore surface at least until 6 hours after the onset of sporulation (see chapter 2). Possibly, this form of SpoVID is able to localize at the surface of the spore, but it is not retained there at later stages.

Region E facilitates binding of SafA and CotE hubs to a second surface in SpoVID

GST pull-down assays showed that region E is required for the interactions of SpoVID with SafA and CotE *in vitro*. Next, we wanted to investigate whether this region is sufficient to bind directly both proteins. We started by using biotinylated peptides with the sequence of region E to

test whether they would compete with GST-SpoVID for binding to SafA or to CotE in pulldown assays. Versions of these peptides with substitutions corresponding to L125A or L131A in SpoVID, which impair the interaction with SafA and CotE, respectively, were used as well. The peptides, at the final concentrations of 1, 10 or 100 μM, were incubated with extracts of *E. coli* producing SafA or CotE. Then, the mixtures were added to GST-SpoVID or GST alone (as a control for the retention of SafA and CotE) immobilized in glutathione beads. After several washings, proteins retained by the beads were released, resolved SDS-PAGE and immunobloted for the detection of SafA or CotE.

We observed that the ability of GST-SpoVID to pull down SafA from the extracts decreases in the presence of 10 μM peptides with the wild type sequence of region E in comparison with a peptide concentration ten times lower (Fig. 3.7 A). In some assays, the reduction in the amount of pulled down SafA is also visible if comparing the absence of the peptide with the presence of 1 μM wild type peptide (as shown in Fig. 3.7 A), yet this is not consistent. This indicates that wild type peptides compete with GST-SpoVID to bind SafA, and therefore, region E is sufficient for the interaction with SafA. However, raising the concentration of the wild type peptides to 100 μM resulted in increased binding of SafA to GST-SpoVID, suggesting that higher concentrations of these peptides promote the interaction between the two proteins *in vitro*. Peptides with the substitution L125A also reduced the amount of SafA pulled down by GST-SpoVID. Thus, they are still able to interact with SafA, even with a substitution that reduces binding in the context of the full-length protein. Yet, this version of the peptide did not promote the interaction between SafA and SpoVID above a certain concentration, in line with importance of residue L125 for binding.

The presence of peptides with the sequence of region E, either wild type or with the substitution L131A, did not reduce the amount of CotE pulled down from the extracts by GST-SpoVID (Fig. 3.7 B). This suggests that

the peptides do not compete with GST-SpoVID for binding to CotE at least under our experimental conditions. However, as is the case for SafA, there is an increment in the amount of CotE that binds GST-SpoVID in the presence of 100 µM peptides. The same effect was observed for peptides with the substitution L131A, indicating that this residue is not essential to promote

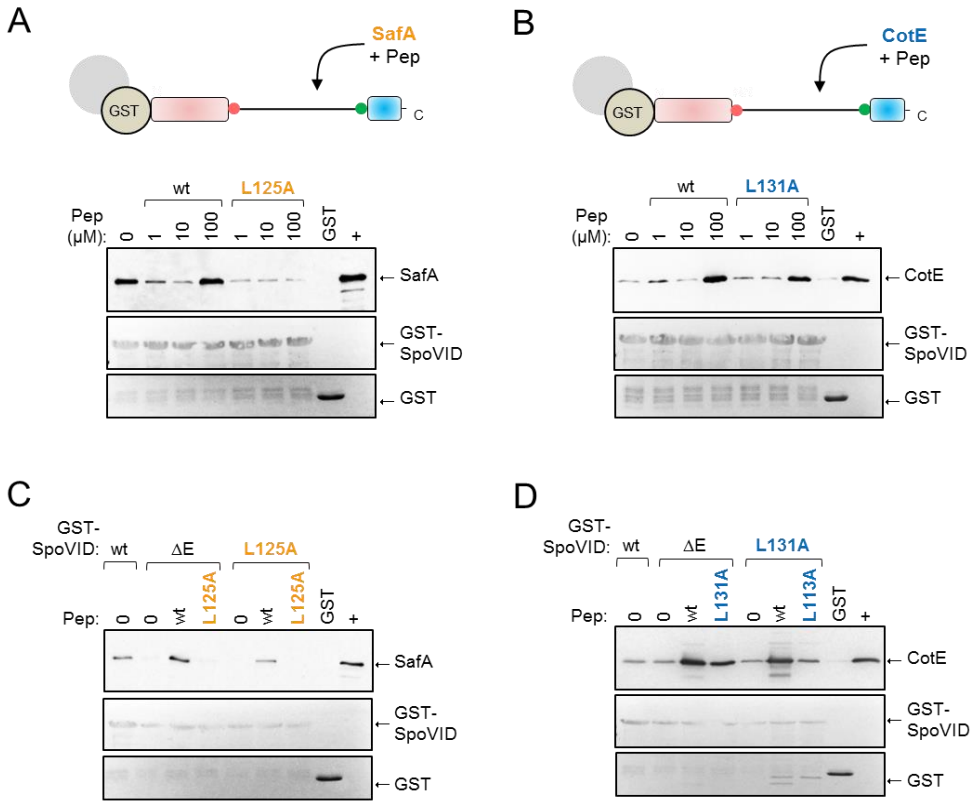

Figure 3.7 – Region E is sufficient for interaction with SafA and CotE and appears to facilitate their binding to a second surface in SpoVID. Peptides with the sequence of region E, with or without substitutions corresponding to L125A or L131A in SpoVID, were incubated with *E. coli* extracts producing **A)** SafA or **B)** CotE, in the final concentrations of 1, 10 or 100 µM. The mixtures were incubated with GST-SpoVID or GST immobilized in glutathione beads. Proteins within beads fractions were resolved by SDS-PAGE and immunobloted with anti-SafA (A) or anti-CotE (B) antibodies (top panels). The membranes were stained with Ponceau Red as a loading control for the amounts of GST-SpoVID and GST bond to the beads (bottom panels). Mixtures of the peptides (at a final concentration of 100 µM) and *E. coli* extract producing **C)** SafA or **D)** CotE were also added to wild type GST-SpoVID or to its variants ΔE, L125A or L131A bond to glutathione beads. Again, proteins within beads fractions were resolved by SDS-PAGE and immunobloted with anti-SafA (C) or anti-CotE (D) antibodies (top panels), and Ponceau Red was used for loading control (bottom panels). Pep: peptides with the sequence of region E.

binding. Altogether, we conclude that region E is sufficient to interact with both SafA and CotE, and presumably, that it facilitates binding of either protein to SpoVID at high concentrations.

We also conducted similar GST pulldown assays after incubating the peptides with *E. coli* producing GST-SpoVID extracts instead of with the extracts containing SafA or CotE. As we did not observe any difference in the amount of SafA or CotE pulled down by GST-SpoVID in these conditions (data not shown), we conclude that region E peptides interact directly with SafA and CotE, and not with GST-SpoVID.

Since binding of the peptides to SafA and CotE increases their interaction with SpoVID, it is possible that region E somehow promotes binding of either hub proteins to a second surface in SpoVID. If so, the presence of the region E peptides must bypass the effect of the deletion of region E or the L125A/L131A substitutions in impairing SafA and CotE binding *in vitro*. To test this, we incubated cell extracts containing SafA or CotE with 100 μM of region E peptides. The mixtures were added to immobilized GST-SpoVID versions, either wild type, with the deletion of region E or with substitutions L125A or L131A. When SafA was incubated with wild type peptides, the protein was not only pulled down by GST-SpoVID wild type, but also by GST-SpoVID variants that impair binding to SafA (Fig. 3.7 C). In the absence of the peptide, or using the peptide with the substitution L125A, SafA was not pulled down by the altered versions of GST-SpoVID. This lends strong support to the interpretation that the wild type peptide bypasses the effect of deleting region E or substituting L125 by an alanine for the interaction with SafA. In these conditions, GST-SpoVID versions missing region E or with the substitution L131A were able to pull-down CotE from the extracts in the absence of peptides (Fig. 3.7 D), not allowing us to test the bypass of the substitution L131A. In any event, this reinforces the view that deletion of region E has a more severe effect on the interaction with SafA than with CotE.

Residues required for encasement by both SafA and CotE are important for coat integrity

We further investigated the effect of substitutions that affect encasement by SafA or CotE on the subcellular localization of other inner and outer coat proteins. We constructed strains with the in-frame deletion of *spoVID* or with the various *spoVID* alleles and expressing *yaaH-gfp* or *cotM-gfp*. YaaH is an inner coat, SafA-dependent protein whose pattern of localization matches the kinetic class I, whereas CotM is a CotE-dependent protein from the outer coat, classified as a kinetic class II protein (McKenney and Eichenberger, 2012). Strains were grown in sporulation medium, and we followed the localization patterns of the fusions. Similarly to SafA-YFP and CotE-YFP, YaaH-GFP and CotM-GFP are able to localize in the first targeting step in all strains, but encasement was impaired in the *spoVID* null mutant and in $spoVID_{\Delta E}$, $spoVID_{L125A}$ and $spoVID_{I127A}$ mutant strains (Fig. 3.8; Tables 3.3 and 3.4). Encasement by CotM-GFP was also blocked by the substitution

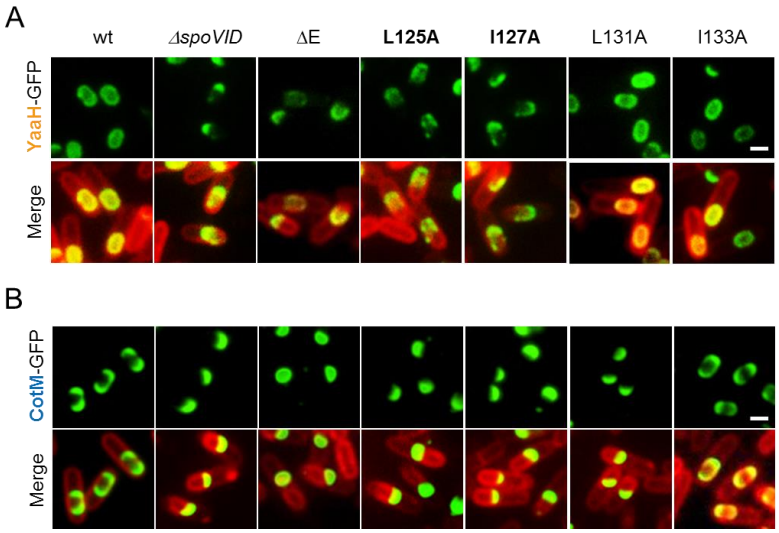

Figure 3.8 – L125 and I127 are required for encasement by **A)** SafA-dependent inner coat and **B)** CotE-dependent outer coat proteins. Sporulating cells with the various SpoVID versions and expressing YaaH-GFP (A) or CotM-GFP (B) were stained with FM 4-64 and imaged. A few representative cells are shown for each strain at hour 6. 1st rows: GFP signal; 2nd rows: merge between GFP and membranes signals. Scale bar: 1µm.

Table 3.3: Quantification of the encasement by YaaH-GFP in strains expressing the various *spoVID* alleles [a]

	Hour 2			Hour 4				Hour 6			
											
wt	0	**82**	18	0	17	**47**	**36**	6	19	**75**	0
Δ*spoVID*	7	**93**	0	0	**100**	0	0	**83**	4	5	8
ΔE	**32**	68	0	8	**89**	0	3	**73**	5	5	17
L125A	**13**	87	0	0	**100**	0	0	**85**	3	2	12
I127A	**19**	81	0	0	**100**	0	0	**84**	5	4	7
L131A	0	**82**	18	0	24	**29**	**47**	11	26	**63**	0
I133A	0	**100**	0	0	**48**	5	**47**	**37**	2	**61**	0

[a] The numbers correspond to the percentages of sporulating cells with each of the localization patterns of YaaH-GFP represented, at 2, 4 and 6 hour after the onset of sporulation.

L131A, likewise CotE-YFP, and I133A causes a delay in encasement by YaaH-GFP, as also happens with SafA-YFP (Fig. 3.8; Tables 3.3 and 3.4). We conclude that alanine substitutions that affect encasement by SafA or CotE also affect encasement by at least some of their dependent proteins.

Table 3.4: Quantification of the encasement by CotM-GFP in strains expressing the various *spoVID* alleles [a]

	Hour 2			Hour 4			Hour 6		
									
wt	55	41	4	8	18	**74**	0	10	**90**
Δ*spoVID*	44	56	0	7	**93**	0	0	**100**	0
ΔE	61	39	0	7	**93**	0	4	**96**	0
L125A	55	45	0	5	**95**	0	0	**100**	0
I127A	50	50	0	6	**93**	1	0	**100**	0
L131A	69	31	0	15	**83**	2	0	**100**	0
I133A	48	46	4	2	20	**78**	0	17	**83**

[a] The numbers correspond to the percentages of sporulating cells with each localization pattern of CotM-GFP represented, at 2, 4 and 6 hour after the onset of sporulation.

According to this, substitutions that impair encasement by SafA and CotE, and consequently by SafA- and CotE-dependent proteins, are likely to cause drastic effects in the coat. Therefore, as an indirect measurement of the

cortex and coat integrity, we used heat and lysozyme resistance assays in strains with alanine substitutions in region E or with the deletion of this region. As controls, we used the wild type strain, a complemented strain expressing the wild type *spoVID* from the *amyE* locus (wt^{C}), and *spoVID*, *safA* and *cotE* null mutant strains. We observed that spores produced by the *spoVID* in-frame deletion mutant are susceptible to heat and lysozyme treatments, with approximately 10^{7} resistant spores/mL, compared with 10^{8} spores/mL for the wild type strain (Table 3.5). The *spoVID* mutant spores previously described were also sensitive to both treatments, although they exhibited higher susceptibility to lysozyme (10^{5} resistant spores/mL) (Beall *et al.*, 1993). This suggests that pre-existing *spoVID* null mutants display polar effects on genes downstream *spoVID*. Spores produced by *safA* and *cotE* null mutants are also sensitive to lysozyme (about 10^{7} resistant spores/mL; Table 3.5), in line with previous studies (Costa *et al.*, 2006; Costa *et al.*, 2007). However, in strains with substitutions L131A or I133A, that specifically affect the encasement by SafA or CotE, respectively, no susceptibility to heat or lysozyme was observed. We conclude that the effect of these substitutions in the inner and outer coat substructures is not as drastic as the absence of SafA or CotE. In contrast, strains missing region E or with substitutions

Table 3.5: Heat and lysozyme resistant spore counts in mutant strains

	Titer of spores (CFU/mL)		
	Viable	**Heat**	**Lysozyme**
wt	$1.8\pm0.4\times10^{8}$	$1.7\pm0.2\times10^{8}$	$1.7\pm0.3\times10^{8}$
wt^{C}	$2.2\pm0.3\times10^{8}$	$1.9\pm0.4\times10^{8}$	$2.0\pm0.2\times10^{8}$
Δ*spoVID*	$8.0\pm1.6\times10^{7}$	**$3.7\pm1.5\times10^{7}$**	**$3.6\pm1.0\times10^{7}$**
Δ*safA*	$1.6\pm0.5\times10^{8}$	$1.7\pm0.4\times10^{8}$	**$7.4\pm2.5\times10^{7}$**
Δ*cotE*	$1.3\pm0.2\times10^{8}$	$9.9\pm2.9\times10^{7}$	**$4.5\pm1.9\times10^{7}$**
ΔE	**$6.2\pm0.7\times10^{7}$**	**$3.4\pm0.5\times10^{7}$**	**$1.8\pm0.7\times10^{6}$**
L125A	**$5.2\pm0.8\times10^{7}$**	**$5.4\pm5.1\times10^{7}$**	**$3.2\pm1.8\times10^{6}$**
I127A	**$6.6\pm1.3\times10^{7}$**	**$6.3\pm4.4\times10^{7}$**	**$1.0\pm0.7\times10^{7}$**
L131A	$2.2\pm0.3\times10^{8}$	$1.9\pm0.2\times10^{8}$	$1.9\pm0.3\times10^{8}$
I133A	$1.9\pm0.2\times10^{8}$	$1.8\pm0.3\times10^{8}$	$1.6\pm0.2\times10^{8}$

wt^{C}: *amyE'::spoVID::'amyE*

L125A or I127A, which impair encasement by SafA, CotE and their inner and outer coat partners, produce less viable spores (approximately 6×10^7/mL; Table 3.5). Also, the spores produced by these strains are susceptible to lysozyme treatment (10^6 resistant spores/mL), suggesting that L125A and I127A drastically compromise the assembly of the coat.

We then purified and decoated the spores produced by these strains, with the exception for the *spoVID* null mutant, as we did not obtained sufficient spores for the assay. The extracted coat proteins were then resolved by SDS-PAGE and the gels were stained. As shown in Fig. 3.9 A, the profiles of extractable coat proteins from spores expressing $spoVID_{\Delta E}$, $spoVID_{L125A}$ or $spoVID_{I127A}$ are identical and differ from the profile of wild type spores. Interestingly, they are also distinct from the profile of extractable coat proteins obtained from *safA* and *cotE* null mutants. This reinforces the view that the coat is significantly altered, but still present, in mutant spores missing region E or with substitutions L125A or I127A. However, the phenotypes did not match the ones exhibited by *safA* or *cotE* null mutants.

As we were able to extract coat proteins from mutant spores where encasement is impaired, we aimed at investigated the subcellular localization of SafA-YFP and CotE-CFP fusions in these mutants at later stages of sporulation. We constructed strains missing *spoVID* or with *spoVID* variants that affect encasement, and expressing simultaneously *safA-yfp* and *cotE-cfp*. Cells were grown in sporulation media for 18 hours and imaged (Fig. 3.9 B). In strains with the deletion of region E or with substitutions L125A or I127A, but not in those with L131A or I133A, there was an accumulation of phase-dark material in the mother cell cytoplasm, similarly to the phenotype of the *spoVID* null mutant. In these cells, the YFP and CFP signals were commonly dispersed into the mother cell cytoplasm, although we found some cells in which the fluorescent signals were solely at the MCP pole of the spore. It is possible that the phase-dark material observed, presumably corresponding to misassembled coat proteins, could be purified with the mutant spores,

resulting in the profiles of coat proteins showed below (Fig. 3.9A). We also observed that in *spoVID*$_{L131A}$ mutant cells, SafA-YFP encircles the spore as previously described, but the polar caps and rings are often asymmetrical

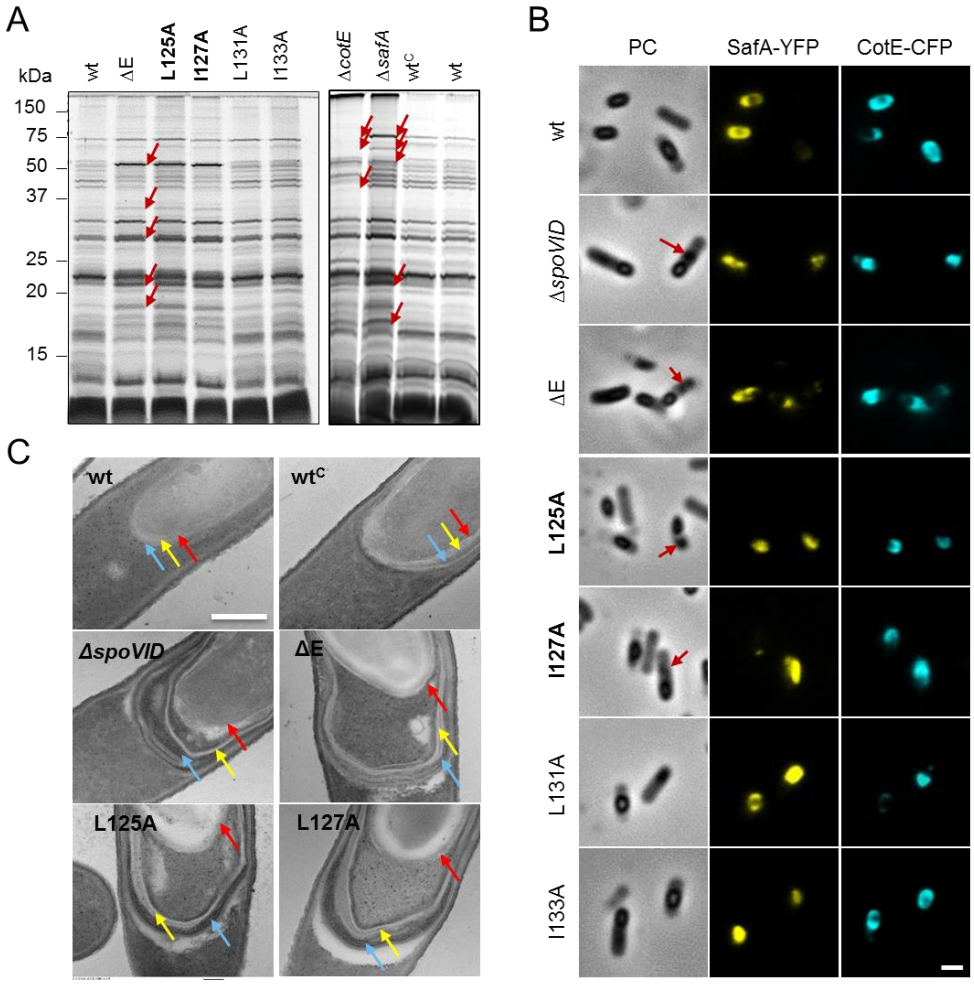

Figure 3.9 – The phenotypes of L125A and L127A mutant cells resemble the *spoVID* null mutant. **A)** Spores produced by strains with the various *spoVID* alleles, as well as *safA* and *cotE* null mutant spores, were decoated and proteins within coat fractions were resolved by SDS-PAGE. Red arrows indicate some of the protein bands that are different in comparison to wild type spores. wt^{C}: Δ*spoVID, amyE'::spoVID::'amyE*. **B)** Cells expressing *spoVID* variants and both SafA-YFP and CotE-CFP fusions were grown in SM medium and imaged 18 hours after the onset of sporulation. A few representative cells are shown for each strain. Red arrows point at the accumulation of phase-dark material in the mother cell. 1st column: phase contrast; 2nd column: SafA-YFP; 3rd column: CotE-CFP. Scale bar: 1µm. **C)** Transmission electron microscopy images of wild type (wt) and *spoVID* mutant sporangia. Red arrows point at the spore surface, and yellow and blue arrows point the inner and the outer coat. Scale bar: 0.5 µm.

and diffuse comparing to those from wild type spores. This is consistent with the pull-down assays that showed that L131A reduces the interaction between SafA and SpoVID *in vitro*. The effect of this substitution in encasement by CotE was also detected, as CotE-CFP localizes mainly as one cap on the MCP pole of the spore and one dot or a small, diffuse cap at the opposite pole. In cells expressing $spoVID_{I133A}$, CotE-CFP encircles the spore, in line with previous data (Chapter 2), yet SafA-YFP does not. The more severe effect of I133A in encasement by SafA-YFP in this background may be due to a synergistic effect with a functionally impaired CotE-CFP fusion.

Altogether, these results suggest that the phenotypes of L125A and I127A mutant cells resemble the *spoVID* null mutant. As a final test to this idea, we analysed these mutant strains by transmission electron microscopy (Fig. 3.9 C). Indeed, in $spoVID_{\Delta E}$, $spoVID_{L125A}$ and $spoVID_{I127A}$ mutants, the inner and the outer coat are detached from the spore surface, as in the *spoVID* null mutant. Thus, the L125A or I127A substitutions phenocopy a *spoVID* deletion mutation.

A mislocalized inner coat acts as an attractor for the outer coat

We have shown that residues L125 and I127 of SpoVID are required for encasement by both SafA and CotE. Substituting L127 for an alanine, binding of SafA and CotE to SpoVID were reduced; however, the substitution L125A only affects the interaction with SafA. This suggests that encasement by CotE may require proper assembly of SafA. In contrast, residue L131 is important for a direct interaction with CotE and encasement by this protein, and its substitution for an alanine does not interfere with encasement by SafA, indicating that SafA does not need CotE to localize. To test this, we analyzed the deposition of SafA-YFP and CotE-CFP in *cotE* and *safA* null mutants, respectively, along sporulation (Fig. S2 of Appendices; Table 3.6). Until 6 hours after resuspension, the localization of these fusions in null mutant strains resembles the wild type, showing that SafA and CotE do not

depend on each other for targeting or encasement. However, at later stages, the percentage of sporulating cells in which SafA-YFP forms a complete ring around the spore is lower in the *cotE* null mutant (43%, comparing to 66% for the wild type, at hour 8), and those rings are diffuse and asymmetric. This suggests that CotE and/or the outer coat are important to restrict SafA and the inner coat around the spore at later stages of sporulation.

Table 3.6: Quantification of the encasement by SafA-YFP and CotE-CFP [b]

		Hour 2	Hour 4			Hour 6		Hour 8	
									
SafA-YFP	**wt**	96	25	61	13	38	57	16	**66**
	Δ*cotE*	92	26	51	21	45	43	23	**43**
CotE-CFP	**wt**	72	25	74	0	95	0	89	0
	Δ*safA*	81	22	75	0	88	0	95	0

[b] The numbers correspond to the percentages of sporulating cells in which SafA-YFP or CotE-CFP localize as each represented pattern, at 2, 4, 6 and 8 hours after the onset of sporulation.

Similar assays were then conducted with strains missing *spoVID* or with the various *spoVID* alleles, and expressing both *safA-yfp* and *cotE-cfp* (Fig. 3.10; Fig. S2 of Appendices). The localization patterns of SafA-YFP and CotE-CFP were imaged and compared in individual cells along sporulation, as shown in Table 3.7. To facilitate data analysis, we grouped the localization patterns in three major classes for each fusion: fluorescent signal exclusively in the MCP pole (1P), in both poles (2P), or dispersed in the mother cytoplasm (D). The subcellular localization of SafA-YFP and CotE-CFP in wild type and mutant cells was consistent with our previous results (Fig. 3.3 and Fig. S1 of Appendices; Chapter 2), with the exception that, in this background, encasement by SafA-YFP is blocked in the $spoVID_{I133A}$ mutant, as discussed above (Fig. 3.9 C). The dynamics of deposition of SafA-YFP and CotE-CFP are very similar, supporting that both fusions exhibit class II kinetics. At later stages of sporulation (hours 6 and 8), some of the cells expressing $spoVID_{\Delta E}$,

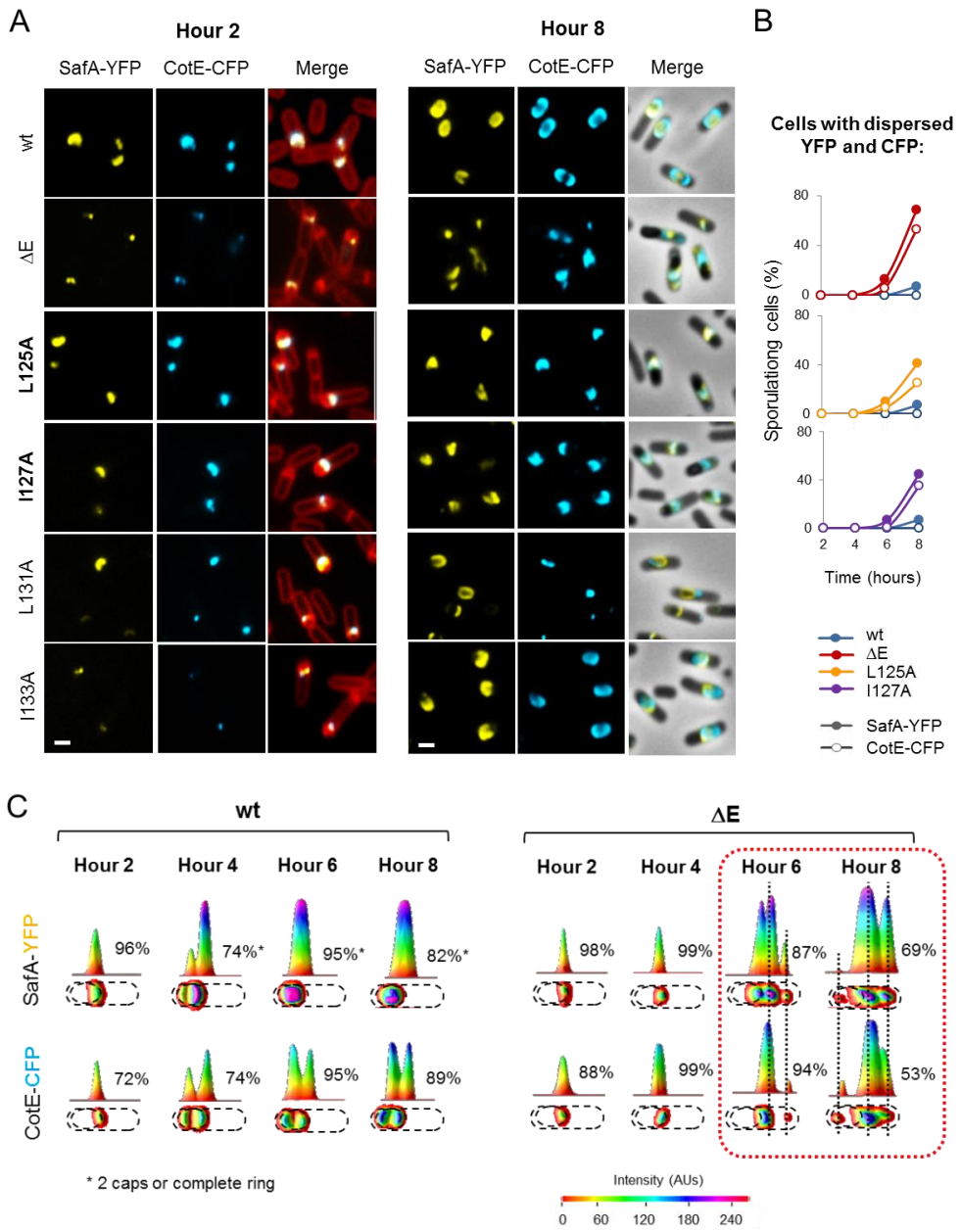

Figure 3.10 – Subcellular localization of SafA-YFP and CotE-CFP along sporulation in strains expressing the various *spoVID* alleles. **A)** Cells were grown in SM medium, stained with FM 4-64 and imaged along the time. 1st and 2nd panels show a few representative cells 2 and 8 hours after resuspension. 1st columns: SafA-YFP; 2nd columns: CotE-CFP; 3rd columns: merge between YFP, CFP and membranes/phase-contrast signals. Scale bar: 1 µm. **B)** Charts representing the percentage of sporulating cells with dispersed SafA-YFP (filled circles) or CotE-CFP (empty circles) signals along sporulation. **C)** 3D intensity graphs of the distribution of SafA-YFP (1st row) and CotE-CFP (2nd row) signals, for representative wild type (left panel) and *spoVID*$_{\Delta E}$ (right panel) cells, along sporulation.

spoVID$_{L125A}$ or *spoVID*$_{I127A}$ exhibited fluorescence signals dispersed in the mother cell cytoplasm (Fig. 3.10 A; Table 3.7). The simultaneous analysis of YFP and CFP signals showed that CotE-CFP was exclusively dispersed in cells in which SafA-YFP was also dispersed (at hour 8, 53% for *spoVID*$_{\Delta E}$, 25% for *spoVID*$_{L125A}$ and 35% for *spoVID*$_{I127A}$ mutants). In contrast, there were cells in which only SafA-YFP was dispersed in the mother cell cytoplasm, while CotE-CFP remained localized as a cap at the MCP pole (Fig. 3.10 B; Table 3.7). This suggests that SafA disperses in the mother cell cytoplasm of these mutants earlier that CotE. Therefore, it is possible that CotE may be dragged by the mislocalized SafA and/or the inner coat components, which would explain the mislocalization of CotE in cells expressing *spoVID*$_{L125A}$.

Table 3.7: Quantification of encasement by SafA-YFP and CotE-CFP in strains expressing the various *spoVID* alleles [c]

	Hour 2		Hour 4				Hour 6						Hour 8							
SafA-YFP	1P		1P		2P		1P		2P		D		1P		2P			D		
CotE-CFP	No	1P	1P	2P	1P	2P	1P	2P	1P	2P	1P	D	1P	2P	1P	2P	D	1P	2P	D
wt	24	72	25	0	0	**74**	5	0	0	**95**	0	0	0	0	0	**82**	0	0	7	0
Δ*spoVID*	13	83	**98**	0	0	0	**59**	0	0	0	7	31	**79**	0	0	0	0	10	0	7
ΔE	10	88	**99**	0	0	0	**87**	0	0	0	7	6	27	0	0	0	0	16	0	**53**
L125A	4	91	**100**	0	0	0	**90**	0	0	0	5	5	**55**	0	0	0	0	16	0	**25**
I127A	6	92	**100**	0	0	0	**88**	0	0	0	6	1	**49**	0	0	0	0	10	0	**35**
L131A	14	79	32	0	**58**	0	3	0	**92**	0	0	2	0	0	**78**	0	9	0	0	10
I133A	3	94	28	**70**	0	0	9	**79**	0	3	0	0	0	**65**	0	17	0	0	3	2

[c] The numbers represent the percentages of sporulating cells in which SafA-YFP or CotE-CFP localize exclusively at the MCP pole (1P), at both poles of the spore (2 caps or complete ring – 2P), or dispersed in the mother cell cytoplasm (D), at 2, 4, 6 and 8 hours after the onset of sporulation. No: absence of fluorescent signal.

We represented three-dimensionally the distribution of YFP and CFP signals in several sporulating cells and compare the patterns of (mis)localization along sporulation. As exemplified by the intensity graphs for representative wild type and *spoVID*$_{\Delta E}$ mutant cells (Fig. 3.10 C), when both SafA-YFP and CotE-CFP are dispersed in the mother cell, the patterns of

YFP and CFP signals commonly overlap. This is in agreement with the hypothesis that mislocalized SafA and/or inner coat proteins act as an attractor for CotE. Thus, even knowing that assembly of the inner and the outer coat are largely independent, there is a tight connection between the two structures. SafA and the inner coat may facilitate the localization of CotE and the outer coat, and when mislocalized can act as an attractor, while CotE and the outer coat help restricting SafA and the inner coat to the surface of the developing spore at later stages.

DISCUSSION

In this study, we aimed at understanding the mechanism by which the N-terminal domain of SpoVID governs spore encasement. In Chapter 2, we showed that region E, within this domain, is required for encasement by all the spore coat layers. We focused our studies on the hub protein for the outer coat assembly, CotE, and demonstrated that region E is important for its binding to SpoVID, which is a critical interaction for encasement by CotE and its partners. We further identified three residues within region E that are essential for encasement by CotE (L125, I127 and L131), and showed that two of them (I127 and I131) are required for the interaction between CotE and SpoVID (de Francesco *et al.*, 2012) (Fig. 3.11). Since the hub protein for the inner coat assembly, SafA, binds to the N-terminal region of SpoVID, we aimed at investigating if this interaction also involves region E.

We started by constructing a new strain expressing *safA-yfp* in order to overcome the functionality problems associated with previous fluorescent fusions of SafA. This allowed us to show that SafA-YFP has a pattern of deposition at the spore surface consistent with the coat proteins from kinetic class II, which is supported by the similarities with the localization pattern of CotE-CFP. It was previously suggested that SafA may be a class I protein, as it

directly interacts with the class I protein SpoVID and at least two SafA-dependent proteins, YaaH and YuzC, belong to class I (McKenney and Eichenberger, 2012). However, CotE is a class II protein and also binds SpoVID. Our data supports that at least the localization of YaaH-GFP matches kinetic class I, which could be explained by the existence of localization determinants other than SafA for this protein. In fact, YaaH has two LysM motifs (that typically bind glycans) at the N-terminus that are sufficient for localization of a β-lactamase at the spores (Kodama *et al.*, 2000) and one possibility is that these domains, together, contribute to the initial localization of YaaH. LysM domains are often repeated (Buist *et al.*, 2008), increasing the affinity for the peptidoglycan. In contrast to YaaH, SafA only has one LysM domain. Further work is required to test the role of the LysM domains of both YaaH and SafA in the kinetics of assembly.

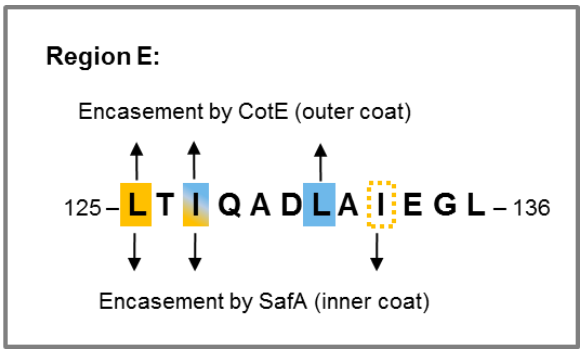

Figure 3.11 – Specific residues within region E are important for encasement by SafA and CotE hubs. Encasement by CotE and outer coat proteins requires L125, I127 and L131, and of those, I127 and L131 (in blue) are involved in a direct interaction with CotE. L125, I127 and I133 (in yellow) are important for binding to SafA. Substitutions L125A and I127A impair encasement by SafA and inner coat proteins, while I133A only delays it.

Using the new SafA-YFP fusion, we were able to show that region E is a prerequisite for encasement by SafA. Among the 12 residues that compose this region, we found two (L125 and I127) that are essential for encasement by SafA and SafA-dependent inner coat proteins. Interestingly, these two residues are also important for encasement by CotE and the outer coat. Residue I133 has a role in encasement by SafA as well, but its substitution

does not completely block the mechanism (Fig. 3.11). GST pulldown assays showed that the three residues that are involved in encasement by SafA are also required for its binding to SpoVID, linking the encasement by the inner coat to a specific protein-protein interaction. Together with the results from Chapter 2, we are able to state that encasement by both inner and outer coat substructures relies on interactions of their hubs (SafA and CotE) to the encasement protein SpoVID, and that these interactions require the same region in SpoVID. Moreover, spore fractionation assays showed that binding of SafA to SpoVID involving region E residues is not only important for the encasement by SafA, but also for its retention at the spore surface.

Experiments with peptides revealed that region E binds directly SafA and CotE and is sufficient for the interactions. In lower concentrations, the peptides with the sequence of region E compete with GST-SpoVID to bind SafA *in vitro*. As we did not detect competition between the peptides and GST-SpoVID for CotE binding, we infer that SpoVID has a second region of interaction with CotE. This is supported by the work of Qiao *et al.* (Qiao *et al.*, 2013), as they showed that the N terminus of SpoVID is dispensable to bind CotE *in vitro*. Additionally, high concentrations of the region E peptides led to an increment in the amount of SafA and CotE retained by GST-SpoVID. Therefore, it is likely that region E facilitates binding of SafA and CotE to a second surface in SpoVID *in vitro*. In fact, we showed that the wild type peptides bypass the need of region E for SafA interaction with SpoVID. Since putative bindings of SafA and CotE to the second surface in SpoVID only occurs at high concentrations of region E peptides, we propose a model for the interaction of SpoVID with the hubs for inner and outer coat *in vivo* in which region E interacts with two different surfaces in SafA and in CotE (Fig. 3.12). Initially, region E binds preferentially one of these surfaces, possibly owing to a higher affinity. This first interaction may have a role in recruitment (together with SpoIVA) or proper positioning of SafA and CotE at the surface of the developing spore. Then, the region E of an adjacent SpoVID

protein binds to the second region of interaction in SafA or CotE, allowing their shuttling to another surface in SpoVID. This would lead to the migration of SafA and CotE around the spore in the second wave of encasement. It is possible that the second interaction with region E induces conformational changes in SafA and CotE that are required for the interaction with the second region in SpoVID. However, in the case of CotE, it remains to be verified if it requires a second interaction with region E for binding to another SpoVID surface, as we did not observe a reduction in the interaction of CotE with GST-SpoVID in the presence of region E peptides. Also, we cannot exclude the possibility that the isolation of region E from the context of the full-length protein, as well as the high peptide concentrations used in the assay, may result in a different behavior of this region *in vitro*.

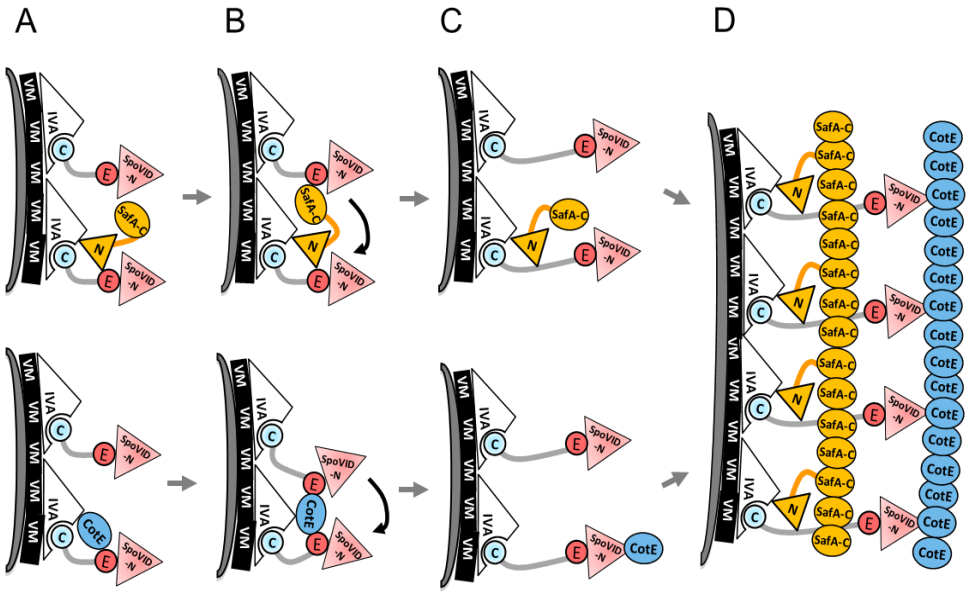

Figure 3.12 – Model for the interaction between SpoVID and the hubs for inner and outer coat, SafA (yellow, top panel) and CotE (blue, botton panel). **A)** Targetting of SafA and CotE to the spore surface requires SpoIVA (white).Then, SafA and CotE interact with SpoVID via region E (pink circles). **B)** A second interaction with the region E from an adjacent SpoVID molecule triggers a conformational change that **C)** promotes binding of SafA and CotE to another region of SpoVID. This allows spore encasement by SafA and CotE. **D)** SafA recruits $SafA_{C30}$ to the spore surface, which presumably functions as the hub for the inner coat components. SafA, $SafA_{C30}$ and CotE encircle the spore, and along the process they drive encasement by the inner and the outer coat components.

According to this model, SafA and CotE interact with region E in a transient manner and then they bind a second region in SpoVID. This may be the reason why we did not detect evidences of competition between the two hubs to bind SpoVID *in vitro* or *in vivo* (data not shown), even though the region E residues involved in their binding are in close proximity, and at least one (I127) is important for interaction with both proteins. Moreover, the existence of a region other than E in SpoVID that binds SafA and CotE may explain why the subcellular localization of SafA-YFP differs in *spoVID* null mutant cells and in cells with the deletion of region E.

Another important finding was that alanine substitutions that impair encasement by both SafA and CotE (L125A or I127A), and consequently by the inner and the outer coat, drastically affect coat integrity. In sporulating cells with these substitutions or with the deletion of region E, the inner and the outer coat are detached from the spore surface, similarly to the phenotype exhibited by the *spoVID* null mutant. Consequently, mutant spores have an altered coat composition and are susceptible to lysozyme. Moreover, the percentage of viable spores produced by these mutants is smaller comparing to the wild type. We infer that the presence of this non-fully functional forms of SpoVID, although localizing as the wild type, result in a more severe effect in the viability of the spores than the absence of SpoVID. This is supported by the lower number of cells with mislocalized SafA-YFP in the *spoVID* null mutant comparing to cells with the deletion of region E.

We also found that in the absence of CotE there is a deficiency in the retention of SafA-YFP at the spore surface at later stages. Indeed, spore fractionation showed that SafA distribution across the spore layers is affected by the absence of CotE. CotE-CFP localizes properly in the absence of SafA, but alanine substitutions that impair encasement by SafA (L125A and I127A) also blocked encasement by CotE, even if they do not interfere with the interaction between CotE and SpoVID (L125A). In mutant cells where SafA and CotE are dispersed in the mother cell cytoplasm, the patterns of

SafA and CotE mislocalization commonly match. Thus, we infer that the presence of SafA is not required for CotE and outer coat assembly, but a mislocalized SafA and/or inner coat functions as an attractor for CotE. Altogether, these results suggest that, even though the inner and the outer coat assembly modules are essentially independent, the two structures are tightly associated.

This work contributes to the general model of coat assembly suggested in Chapter 2. We provide additional evidence that inner and outer coat encasement is driven by protein-protein interactions. Also, we revealed a role for specific region E residues in encasement and in the overall integrity of the coat, and in doing so, we provide evidence for a tight interconnection between the inner and the outer coat sublayers.

ACKNOWLEDGMENTS

This work was supported by grants ERA-PTG/SAU/0002/2008 (ERA-NET PathoGenoMics) and Pest-C/EQB/LA0006/2011 from the "Fundação para a Ciência e a Tecnologia" (FCT) to A.O.H.. F.N. (SFRH/BD/64470/2009) and C.F. (SFRH/BD/45459/08) were the recipients of doctoral fellowships from the FCT. F.N. was also the recipient of a short-term fellowship (2014/CON3/CAN34) from the "Fundação Luso-Americana Para o Desenvolvimento" (FLAD). M.S. is an iFCT investigator.

REFERENCES

Arai, R., Ueda, H., Kitayama, A., Kamiya, N., Nagamune, T., 2001. Design of the linkers which effectively separate domains of a bifunctional fusion protein. Protein Engineering 14, 529-532.

Arnaud, M., Chastanet, A., Debarbouille, M., 2004. New vector for efficient

allelic replacement in naturally nontransformable, low-GC-content, gram-positive bacteria. Applied and Environmental Microbiology 70, 6887-6891.

Beall, B., Driks, A., Losick, R., Moran, C.P., Jr., 1993. Cloning and characterization of a gene required for assembly of the Bacillus subtilis spore coat. Journal of Bacteriology 175, 1705-1716.

Buist, G., Steen, A., Kok, J., Kuipers, O.P., 2008. LysM, a widely distributed protein motif for binding to (peptido)glycans. Molecular Microbiology 68, 838-847.

Costa, T., Isidro, A.L., Moran, C.P., Jr., Henriques, A.O., 2006. Interaction between coat morphogenetic proteins SafA and SpoVID. Journal of Bacteriology 188, 7731-7741.

Costa, T., Serrano, M., Steil, L., Volker, U., Moran, C.P., Jr., Henriques, A.O., 2007. The timing of cotE expression affects Bacillus subtilis spore coat morphology but not lysozyme resistance. Journal of Bacteriology 189, 2401-2410.

de Francesco, M., Jacobs, J., Nunes, F., Serrano, M., McKenney, P.T., Chua, M.H., Henriques, A.O., Eichenberger, P., 2012. Physical interaction between coat morphogenetic proteins SpoVID and CotE is necessary for spore encasement in Bacillus subtilis. Journal of Bacteriology 194, 4941-4950.

Driks, A., Roels, S., Beall, B., Moran, C.P., Jr., Losick, R., 1994. Subcellular localization of proteins involved in the assembly of the spore coat of Bacillus subtilis. Genes & Development 8, 234-244.

Errington, J., 2003. Regulation of endospore formation in Bacillus subtilis. Nature Reviews Microbiology 1, 117-126.

Henriques, A.O., Moran, C.P., Jr., 2000. Structure and assembly of the bacterial endospore coat. Methods 20, 95-110.

Henriques, A.O., Moran, C.P., Jr., 2007. Structure, assembly, and function of the spore surface layers. Annual Review of Microbiology 61, 555-588.

Karow, M.L., Piggot, P.J., 1995. Construction of gusA transcriptional fusion vectors for Bacillus subtilis and their utilization for studies of spore formation. Gene 163, 69-74.

Kim, H., Hahn, M., Grabowski, P., McPherson, D.C., Otte, M.M., Wang, R., Ferguson, C.C., Eichenberger, P., Driks, A., 2006. The Bacillus subtilis spore coat protein interaction network. Molecular Microbiology 59, 487-502.

Kodama, T., Takamatsu, H., Asai, K., Ogasawara, N., Sadaie, Y., Watabe, K., 2000. Synthesis and characterization of the spore proteins of Bacillus subtilis YdhD, YkuD, and YkvP, which carry a motif conserved among cell wall binding proteins. Journal of Biochemistry 128, 655-663.

Levin, P.A., Fan, N., Ricca, E., Driks, A., Losick, R., Cutting, S.M., 1993. An unusually small gene required for sporulation by Bacillus subtilis. Molecular Microbiology 9, 761-771.

Martins, L.O., Soares, C.M., Pereira, M.M., Teixeira, M., Costa, T., Jones, G.H., Henriques, A.O., 2002. Molecular and biochemical characterization of a highly stable bacterial laccase that occurs as a structural component of the Bacillus subtilis endospore coat. Journal of Biological Chemistry 277, 18849-18859.

McKenney, P.T., Driks, A., Eichenberger, P., 2013. The Bacillus subtilis endospore: assembly and functions of the multilayered coat. Nature Reviews Microbiology 11, 33-44.

McKenney, P.T., Driks, A., Eskandarian, H.A., Grabowski, P., Guberman, J., Wang, K.H., Gitai, Z., Eichenberger, P., 2010. A distance-weighted interaction map reveals a previously uncharacterized layer of the Bacillus subtilis spore coat. Current Biology 20, 934-938.

McKenney, P.T., Eichenberger, P., 2012. Dynamics of spore coat morphogenesis in Bacillus subtilis. Molecular Microbiology 83, 245-260.

Mullerova, D., Krajcikova, D., Barak, I., 2009. Interactions between Bacillus subtilis early spore coat morphogenetic proteins. FEMS Microbiology Letters 299, 74-85.

Nicholson, W.L., Setlow, P., 1990. Sporulation, germination and outgrowth. In: Cutting, C.R.H.a.S.M. (Ed.), Molecular biology methods for *Bacillus*. John Wiley & Sons, Ltd., Chichester, pp. 391-450.

Ozin, A.J., Costa, T., Henriques, A.O., Moran, C.P., Jr., 2001a. Alternative translation initiation produces a short form of a spore coat protein in Bacillus subtilis. Journal of Bacteriology 183, 2032-2040.

Ozin, A.J., Henriques, A.O., Yi, H., Moran, C.P., Jr., 2000. Morphogenetic proteins SpoVID and SafA form a complex during assembly of the Bacillus subtilis spore coat. Journal of Bacteriology 182, 1828-1833.

Ozin, A.J., Samford, C.S., Henriques, A.O., Moran, C.P., Jr., 2001b. SpoVID guides SafA to the spore coat in Bacillus subtilis. Journal of Bacteriology 183, 3041-3049.

Qiao, H., Krajcikova, D., Liu, C., Li, Y., Wang, H., Barak, I., Tang, J., 2012. The interactions of spore-coat morphogenetic proteins studied by single-molecule recognition force spectroscopy. Chemistry - An Asian Journal 7, 725-731.

Qiao, H., Krajcikova, D., Xing, C., Lu, B., Hao, J., Ke, X., Wang, H., Barak, I., Tang, J., 2013. Study of the interactions between the key spore coat morphogenetic proteins CotE and SpoVID. Journal of Structural Biology 181, 128-135.

Roels, S., Driks, A., Losick, R., 1992. Characterization of spoIVA, a sporulation gene involved in coat morphogenesis in Bacillus subtilis. Journal of Bacteriology 174, 575-585.

Serrano, M., Real, G., Santos, J., Carneiro, J., Moran, C.P., Jr., Henriques, A.O., 2011. A negative feedback loop that limits the ectopic activation of a cell type-specific sporulation sigma factor of Bacillus subtilis. PLOS Genetics 7, e1002220.

Seyler, R.W., Jr., Henriques, A.O., Ozin, A.J., Moran, C.P., Jr., 1997. Assembly and interactions of cotJ-encoded proteins, constituents of the inner layers of the Bacillus subtilis spore coat. Molecular Microbiology 25, 955-966.

Sterlini, J.M., Mandelstam, J., 1969. Commitment to sporulation in Bacillus subtilis and its relationship to development of actinomycin resistance. Biochemical Journal 113, 29-37.

Takamatsu, H., Imamura, A., Kodama, T., Asai, K., Ogasawara, N., Watabe, K., 2000a. The yabG gene of Bacillus subtilis encodes a sporulation specific protease which is involved in the processing of several spore coat proteins. FEMS Microbiology Letters 192, 33-38.

Takamatsu, H., Kodama, T., Imamura, A., Asai, K., Kobayashi, K., Nakayama, T., Ogasawara, N., Watabe, K., 2000b. The Bacillus subtilis yabG gene is transcribed by SigK RNA polymerase during sporulation, and yabG mutant spores have altered coat protein composition. Journal of Bacteriology 182, 1883-1888.

Takamatsu, H., Kodama, T., Nakayama, T., Watabe, K., 1999. Characterization of the yrbA gene of Bacillus subtilis, involved in resistance and germination of spores. Journal of Bacteriology 181, 4986-4994.

Wang, K.H., Isidro, A.L., Domingues, L., Eskandarian, H.A., McKenney, P.T., Drew, K., Grabowski, P., Chua, M.H., Barry, S.N., Guan, M., Bonneau, R., Henriques, A.O., Eichenberger, P., 2009. The coat morphogenetic protein SpoVID is necessary for spore encasement in Bacillus subtilis. Molecular Microbiology 74, 634-649.

Youngman, P., Perkins, J.B., Losick, R., 1984. Construction of a cloning site near one end of Tn917 into which foreign DNA may be inserted without affecting transposition in Bacillus subtilis or expression of the transposon-borne erm gene. Plasmid 12, 1-9.

Chapter 4

The LysM module of SafA in spore morphogenesis

This chapter contains data to be published in: Pereira, F. C., Nunes, F., Fernandes, C., Isidro, A. L., Soares, C. M., Serrano, M. and Henriques, A. O. (2015) **A LysM domain determines the subcellular localization of coat morphogenetic protein SafA in *Bacillus subtilis.***

The author of this dissertation participated directly in fluorescence microscopy experiments in cells expressing SafA-YFP variants, spore fractioning assays, and peptidoglycan and chitin binding assays with the LysM domain of SpoVID.

SUMMARY

Bacterial spores are encased by two protective layers: the innermost cortex, composed of peptidoglycan, and the proteinaceous coat, subdivided into the basement layer, the inner coat, the outer coat and the crust. SafA is the morphogenetic protein that governs recruitment and assembly of the inner coat components, and localizes at the cortex/coat interface. Here, we analyzed the role of the peptidoglycan-binding LysM domain in the localization and function of SafA during spore morphogenesis. We found that alanine substitutions in conserved, surface-exposed residues of this domain affect its ability to bind purified peptidoglycan *in vitro* and cause mislocalization of SafA-YFP. Two of these substitutions affect the deposition of SafA-YFP at earlier stages of encasement, increase SafA extractability, and cause mislocalization of at least one SafA-dependent inner coat protein. The other three substitutions affect the localization SafA at later stages of spore development. Moreover, the late localization of SafA requires the cortex, suggesting a link in the assembly of the cortex and the coat. We propose a model in which both the interactions with SpoIVA and SpoVID (via region A), as well as peptidoglycan recognition (via LysM domain), are required for the subcellular localization and function of SafA. Finally, our results suggest that the LysM domain of SpoVID, a morphogenetic protein required for spore encasement by coat proteins, does not recognize peptidoglycan in the same conditions of the LysM domain of SafA. This bears implications for the function of this domain in SpoVID localization.

INTRODUCTION

In response to adverse conditions, *B. subtilis* cells are able to undergo a differentiation process that culminates with the formation of a spore. Spores can persist under a variety of stresses, including heat, noxious chemicals, radiation and predators (Nicholson *et al.*, 2000; Nicholson, 2002; Nicholson *et al.*, 2002; Klobutcher *et al.*, 2006; Setlow, 2006). The resilience of these structures is in part related to the physical and chemical properties of the two main protective layers that encase them: the outermost proteinaceous coat, and the underlying cortex, composed of peptidoglycan (Driks, 1999; de Hoon *et al.*, 2010).

Spore formation begins with an asymmetric cell division that yields a smaller forespore, which develops into a mature spore, and a larger mother cell (Errington, 2003). Soon after polar division, the mother cell engulfs the forespore in a mechanism that requires controlled synthesis and hydrolysis of peptidoglycan by sporulation-specific enzymes (Abanes-De Mello *et al.*, 2002; Chastanet and Losick, 2007; Gutierrez *et al.*, 2010; Meyer *et al.*, 2010; Morlot *et al.*, 2010). First, the peptidoglycan within the division septum is thinned, starting from the center of the septal plate (Holt *et al.*, 1975; Chastanet and Losick, 2007). Then, as the engulfing membranes move forward, new peptidoglycan is synthesized at the leading edges of the membranes, while the old cross-links to the mother cell wall are hydrolyzed on the back side (Abanes-De Mello *et al.*, 2002; Meyer *et al.*, 2010; Tocheva *et al.*, 2013). Engulfment is concluded through membrane fusion near the mother cell distal pole, releasing the forespore, surrounded by two membranes, into the mother cell cytoplasm (Errington, 2003).

The space between the forespore membranes is the site of assembly of two peptidoglycan layers. The innermost one, and the first being synthesized (Meador-Parton and Popham, 2000; Vasudevan *et al.*, 2007), is the primordial germ cell wall. This layer has structural similarities with the

vegetative cell wall, consisting of glycan strands of alternating N-acetylglucosamine (GlcNAc) and N-acetylmuramic acid (MurNAc) residues, cross-linked by short peptide side chains attached to MurNAc (Tipper and Linnett, 1976). Indeed, it serves as the initial cell wall of the outgrowing cells after germination (Santo and Doi, 1974; Atrih *et al.*, 1998). The primordial germ cell wall is encased by the cortex, synthesized from mother cell precursors after engulfment completion (Vasudevan *et al.*, 2007). It is composed of a modified form of peptidoglycan with approximately half of the MurNAc residues substituted by muramic δ-lactam, a reduced peptide side chains content, and no teichoic acids (Warth and Strominger, 1969, 1972; Popham, 2002).

The coat is synthesized at the surface of the outer forespore membrane and comprises up to 80 different proteins arranged into 4 sublayers: the basement layer, the inner coat, the outer coat and the crust. Coat assembly begins as soon as the asymmetric septum starts to curve and proceeds for several hours through the expression of several temporal classes of mother cell-specific genes (Henriques and Moran, 2007). Initially, coat proteins deposit into a scaffold cap, and then they encase the spore in successive waves (McKenney *et al.*, 2010; McKenney and Eichenberger, 2012; McKenney *et al.*, 2013) (see *"Successive waves of encasement during coat morphogenesis"*, in Chapter 1). A group of so-called morphogenetic proteins play a key role in these two processes. Among those, SpoIVA is essential for the initial targeting of coat proteins, while SpoVM and SpoVID are required for spore encasement (Wang *et al.*, 2009). Also, SafA and CotE are involved in inner and outer coat proteins assembly, respectively (Zheng *et al.*, 1988; Takamatsu *et al.*, 1999; Kim *et al.*, 2006) (see *"Two step of coat assembly: targeting and encasement"*, in Chapter 1).

Morphogenesis of the cortex and the coat are considered essentially independent processes. This idea stems primarily from electron microscopy characterization of mutants lacking either the cortex or the coat. For

example, in *spoVID* null mutant spores, the coat fails to assemble, yet the cortex is formed (Beall *et al.*, 1993). In contrast, *spoVE* mutants produce spores with an apparently normal coat, but fail to form the cortex (Piggot and Coote, 1976; Henriques *et al.*, 1992; Vasudevan *et al.*, 2007). However, the work of Ebmeier *et al.*, 2012 revealed that formation of the cortex requires initiation of coat assembly.

Morphogenetic coat proteins SpoVID and SafA carry LysM motifs, which typically bind peptidoglycan and related compounds. This, together with the localization of these proteins at the cortex/coat interface in matures spores (Driks *et al.*, 1994; Ozin *et al.*, 2000), as well as their association with the spore cortex (see Chapter 3), prompted speculations that they could provide anchor points to the underlying cortex (Ozin *et al.*, 2000; Ozin *et al.*, 2001a; Ozin *et al.*, 2001b). Supporting this hypothesis, the LysM module of another coat protein, YaaH, is sufficient to direct a β-lactamase to the spore surface (Kodama *et al.*, 2000). In SpoVID, the LysM domain (henceforth $LysM^{SpoVID}$) is located at the C terminus and is part of a localization signal that also includes the SpoIVA-binding region A (Wang *et al.*, 2009). Both components are essential for SpoVID localization, although region A appears to play a more significant role (Wang *et al.*, 2009). The LysM domain of SafA (herein $LysM^{SafA}$) is located at the N terminus and is followed by a region, also named A, that interacts with SpoVID and is required for localization (Ozin *et al.*, 2000; Costa *et al.*, 2006). Therefore, in an analogy with SpoVID, it is possible that the LysM domain of SafA would be part of a localization signal together with region A, perhaps acting as a peptidoglycan recognition module.

LysM motifs are found singly or repeatedly in eukaryotic, prokaryotic and viral proteins. They consist of 44 to 65 amino acid residues (Buist *et al.*, 2008) that generally adopt a βααβ fold, with the two α-helices packed against one side of a two-stranded antiparallel β-sheet (Bateman and Bycroft, 2000; Bielnicki *et al.*, 2006). Several studies shown that they recognize

peptidoglycan and/or chitin (Andre *et al.*, 2008; Ohnuma *et al.*, 2008; Yamamoto *et al.*, 2008; Iizasa *et al.*, 2010; Willmann *et al.*, 2011; Liu *et al.*, 2012; Sanchez-Vallet *et al.*, 2013; Mesnage *et al.*, 2014; Leo *et al.*, 2015), or even nodulation (Nod) factors produced by nitrogen fixing bacteria (Mulder *et al.*, 2006; Broghammer *et al.*, 2012). At least some LysMs recognize the common GlcNAc sugar present in these compounds (Ohnuma *et al.*, 2008; Mesnage *et al.*, 2014), but binding appears to be modulated by other cell wall components that serve as specific discriminants between different types of peptidoglycan, chitin and Nod factors (Steen *et al.*, 2003; Andre *et al.*, 2008; Yamamoto *et al.*, 2008; Mesnage *et al.*, 2014; Leo *et al.*, 2015). Also, the number of GlcNAc units within glycan strands influences the recognition by LysM (Ohnuma *et al.*, 2008; Iizasa *et al.*, 2010; Liu *et al.*, 2012; Mesnage *et al.*, 2014).

In this study, we addressed the role of the LysM domain in localization and function of SafA. We identified conserved, surface-exposed LysM residues required for SafA-YFP subcellular localization and for peptidoglycan recognition *in vitro.* Also, we provide evidence that late localization of SafA requires the cortex, suggesting a link in the assembly of the cortex and the coat. We propose a model for SafA localization that includes interactions with SpoIVA and SpoVID (via region A), as well as peptidoglycan recognition (via LysM domain). Finally, we found that the LysM domain of SpoVID does not recognize peptidoglycan in the same conditions as the $LysM^{SafA}$, which has implications in the overall model of coat assembly.

MATERIALS AND METHODS

Bacterial strains, media and general methods

DNA manipulation and other molecular methods were performed

using standard protocols. *B. subtilis* strains used in this study are congenic derivatives of the wild-type strain MB24 (*trp2 metC3*). *Escherichia coli* DH5α was used for molecular cloning and for overproduction of StrepTagII fusion proteins, except for LysM^{SpoVID}-StrepTagII, that was expressed in *E. coli* BL21(DE3). Maintenance and growth of *E. coli* and *B. subtilis* was performed in Luria-Bertani medium (LB) with antibiotic selection when needed. Sporulation was induced by growth and nutrient exhaustion in Difco sporulation medium (DSM), except for microscopy experiments, where it was performed resuspension in Sterlini-Mandelstam sporulation medium (SM) (Sterlini and Mandelstam, 1969). All strains used in this study are listed in Table 4.1, and plasmids and oligonucleotide primers required for their construction can be found in Tables A6 and A7 of the Appendices, respectively.

Table 4.1: Bacterial strains used in this study

Strains	Relevant properties	Source
B. subtilis		
MB24	*trp2 metC3*, Spo$^+$	Lab. stock
AH4745	*trp2 metC3 ΔsafA::safA*, Sp^r Nm^r	This study
AH4746	*trp2 metC3 ΔsafA::safA$_{D10A}$*, Sp^r Nm^r	"
AH4747	*trp2 metC3 ΔsafA::safA$_{S11A}$*, Sp^r Nm^r	"
AH4748	*trp2 metC3 ΔsafA::safA$_{L12A}$*, Sp^r Nm^r	"
AH4749	*trp2 metC3 ΔsafA::safA$_{N30A}$*, Sp^r Nm^r	"
AH4750	*trp2 metC3 ΔsafA::safA$_{I39A}$*, Sp^r Nm^r	"
AH10297	*trp2 metC3 ΔsafA ΔamyE::cm*	"
AH10302	*trp2 metC3 ΔsafA, amyE'::safA::'amyE* Neo^r	"
AH10555	*trp2 metC3 ΔsafA, amyE'::safA$_{D10A}$::'amyE* Neo^r	"
AH10556	*trp2 metC3 ΔsafA, amyE'::safA$_{S11A}$::'amyE* Neo^r	"
AH10557	*trp2 metC3 ΔsafA, amyE'::safA$_{L12A}$::'amyE* Neo^r	"
AH10558	*trp2 metC3 ΔsafA, amyE'::safA$_{N30A}$::'amyE* Neo^r	"
AH10561	*trp2 metC3 ΔsafA, amyE'::safA$_{I39A}$::'amyE* Neo^r	"
AH10487	*trp2 metC3 ΔsafA, amyE'::safA-yfp::'amyE* Neo^r	"

Table 4.1: Bacterial strains used in this study (cont.)

Strains	Relevant properties	Source
AH10562	*trp2 metC3 ΔsafA, amyE'::safA$_{D10A}$-yfp::'amyE* Neo^r	This study
AH10563	*trp2 metC3 ΔsafA, amyE'::safA$_{S11A}$-yfp::'amyE* Neo^r	"
AH10564	*trp2 metC3 ΔsafA, amyE'::safA$_{L12A}$-yfp::'amyE* Neo^r	"
AH10565	*trp2 metC3 ΔsafA, amyE'::safA$_{I39A}$-yfp::'amyE* Neo^r	"
AH10566	*trp2 metC3 ΔsafA, amyE'::safA$_{N30A}$-yfp::'amyE* Neo^r	"
AH5429	*trp2 metC3 ΔsafA, amyE'::safA-yfp::'amyE, ΔspoVE::tet* Neo^r	"
AH5430	*trp2 metC3 ΔsafA, amyE'::safA$_{D10A}$-yfp::'amyE , ΔspoVE::tet* Neo^r	"
AH5431	*trp2 metC3 ΔsafA, amyE'::safA$_{S11A}$-yfp::'amyE , ΔspoVE::tet* Neo^r	"
AH5432	*trp2 metC3 ΔsafA, amyE'::safA$_{L12A}$-yfp::'amyE , ΔspoVE::tet* Neo^r	"
AH5433	*trp2 metC3 ΔsafA, amyE'::safA$_{N30A}$-yfp::'amyE , ΔspoVE::tet* Neo^r	"
AH5434	*trp2 metC3 ΔsafA, amyE'::safA$_{I39A}$-yfp::'amyE , ΔspoVE::tet* Neo^r	"
AH4835	*trp2 metC3 ΔsafA::sp ΔcotD::cotD-gfp* Sp^r Cm^r	"
AH4836	*trp2 metC3 ΔsafA::safA ΔcotD::cotD-gfp* Sp^r Nm^r Cm^r	"
AH4837	*trp2 metC3 ΔsafA::safA$_{D10A}$ ΔcotD::cotD-gfp* Sp^r Nm^r Cm^r	"
AH4838	*trp2 metC3 ΔsafA::safA$_{S11A}$ ΔcotD::cotD-gfp* Sp^r Nm^r Cm^r	"
AH4839	*trp2 metC3 ΔsafA::safA$_{L12A}$ ΔcotD::cotD-gfp* Sp^r Nm^r Cm^r	"
AH4840	*trp2 metC3 ΔsafA::safA$_{N30A}$ ΔcotD::cotD-gfp* Sp^r Nm^r Cm^r	"
AH4841	*trp2 metC3 ΔsafA::safA$_{I39A}$ ΔcotD::cotD-gfp* Sp^r Nm^r Cm^r	"
AH4856	*trp2 metC3 yycR*::P$_{sspE}$*-cfp*	"
AH4857	*trp2 metC3 ΔspoVE::tet yycR*::P$_{sspE}$*-cfp*	"
E. coli		
DH5α	F$^-$ Φ80*lac*ZΔM15 Δ(*lac*ZYA-*arg*F) U169 *rec*A1 *end*A1 *hsd*R17 (rK$^-$, mK$^+$) *pho*A *sup*E44 λ$^-$ *thi*-1 *gyr*A96 *rel*A1	Invitrogen
BL21	F$^-$ dcm ompT hsdS(rB$^-$ mB$^-$) gal λ(DE3)	Promega
AH4504	DH5α /pTC182 Amp^r	This study
AH4505	DH5α /pAI1 Amp^r	"
AH4506	DH5α /pAI2 Amp^r	"
AH4507	DH5α /pAI3 Amp^r	"
AH4508	DH5α /pAI4 Amp^r	"
AH4509	DH5α /pAI5 Amp^r	"
AH4520	DH5α /pTC178 Amp^r	"
AH4522	DH5α /pAI12 Amp^r	"
AH5104	BL21(DE3)/ pFN45 Amp^r	"

B. subtilis strains expressing *safA* alleles

We constructed strains expressing the various *safA* alleles from the native locus. First, an amplicon with the 3' terminus of *safA* and the coding sequence of *gfpmut2* (amplified from pEA18, a gift from Alan Grossman) was generated by SOE-PCR. The amplicon was digested with SmaI and NotI, and cloned into the same sites of pBEST501 (Itaya *et al.*, 1989), yielding pTC207. This vector was then used as a template to insert the alanine substitutions D10A, S11A, L12A, N30A or I39A in *safA-gfp* through QuickChange site-directed mutagenesis, with the pairs of primers listed in Table A7. *gfp* was removed from the resulting plasmids, as well as from pTC207, by digestion with pfIMI and EcoRI, and substituted by the 3' terminus of *safA*, generating pFP2-pFP7. Finally, AOB68 *safA* null mutant cells (Ozin *et al.*, 2000) were transformed with each of this vectors, creating strains AH4745-AH4750.

We also constructed strains with the in-frame deletion of *safA* and expressing *safA* alleles from the non-essential locus *amyE*. By SOE-PCR, we obtained a DNA fragment containing the *safA* coding sequence with an in-frame deletion that eliminates residues 46 – 249, as well as *safA* flanking regions (see detailed description in Chapter 3). The fragment was digested with SalI and EcoRI and cloned into the same sites of pUC18 (New England Biolabs), yielding pCF72. Then, *B. subtilis* cells were co-transformed with pDG364 (Cutting and Vander Horn, 1990) and pCF72 to create a *safA* null mutant strain bearing the chloramphenicol resistance *cat* gene at *amyE* (AH10297). The presence of the in-frame deletion in *safA* was confirmed by PCR and supported by the lysozyme sensitivity of the cells (Nicholson and Setlow, 1990). Then, the vector pCF75, a derivative of pMLK83 (Karow and Piggot, 1995) with the *safA* coding sequence and its flanking regions bordered by 5' and 3' regions of *amyE*, was used as template for insertion of single alanine substitutions in the LysM domain of SafA by site-directed mutagenesis, using the pairs of primers listed in Table A7 of the Appendices. The resulting vectors, (pCF181–185) as well as pCF75, were transferred to

the *safA* null mutant AH10297, creating strains AH10302, AH10555–10558 and AH10561.

B. subtilis strains expressing fluorescent fusions

To obtain strains expressing the various *safA-yfp* alleles, we digested the vector pCF149, containing *safA-fl3-yfp* fusion (see detailed description in Chapter 3), with HindIII and BamHI. A DNA fragment with the terminus of *safA* followed by the linker *fl3* and *yfp* was released and inserted in the same cloning sites of pCF181–185, yielding vectors pCF186–190. These vectors, as well as pCF149, were then used to substitute the *cat* gene for the *safA-fl3-yfp* construction at the *amyE* locus of AH10297, originating strains AH10487 and AH10562–10566. Also, strain AH10297 was transformed with the chromosomal DNA of JDB1752 (Real *et al.*, 2008), in order to knock-out *spoVE*. These cells were then transformed with pCF149 and pCF186–190, generating strains expressing *safA-yfp* variants in the absence of *spoVE* (AH5429–5434).

For cells expressing *cotD-gfp* in the presence of the various *safA* alleles, we started by constructing a vector to change the spectinomycin resistance for chloramphenicol resistance in *B. subtilis*. pAH250 (Henriques *et al.*, 1997) was digested with BamHI and SnaBI, and the *cat* gene was inserted within the base pairs 384 and 465 of the *spec* cassette, resulting in pFP8. Then, we transformed PE659 (Wang *et al.*, 2009), with *cotD-GFP* fusion, with this vector and used the chromosomal DNA of the resulting strain to transform AOB64 and AH4745–4750, generating the strains AH4835–AH4841.

For expression of *cfp* under control of a σ^G-responsive promotor, both wild type and *spoVE* null mutant strains (JDB1752, Real *et al*., 2008) were transformed with the chromosomal DNA of AH6566 (Serrano *et al.*, 2008), harboring P_{sspE}-*cfp*. Cells were selected for chloramphenicol resistance, resulting in strains AH4856 and AH4857.

Strains for overproduction of StrepTagII fusions

The coding sequence of the LysM domain of *safA* was PCR amplified, digested with XbaI and NcoI, and cloned into the same sites of the vector pASK-IBA3 (IBA GmBH) to create pTC178. Then, the *gfp* gene, amplified from pEA18, was inserted into the AatII site of pTC178, yielding pTC182, for expression of LysM^{SafA}-GFP-StrepTagII. This vector was used as template to introduce the alanine substitutions D10A, S11A, L12A, N30A or I39A at the LysM by site-directed mutagenesis, generating plasmids pAI4, pAI1, pAI2, pAI5 and pAI3, respectively. For GFP-StrepTagII overproduction, the *gfp* gene was digested with XbaI and Eco47III and cloned into the same sites of pASK-IBA3, creating pAI12. These vectors were transferred to in *E. coli* DH5α for protein overproduction, resulting in strains AH4504–4509, AH4520 and AH4522.

For overproduction of LysM^{SpoVID}-StrepTagII, the coding region of the LysM domain of SpoVID was amplified, digested with XbaI and NcoI and inserted into pASK-IBA3. The resulting vector was introduced in *E. coli* BL21(DE3), yielding strain AH5104.

Fluorescence microscopy and image analysis

One-millilitre samples were collected from SM cultures at different times. Cells were harvested by centrifugation and resuspended in 0.1 mL of PBS supplemented with 1 μL of a 2 mg/mL solution of the membrane dye FM 4-64 (Molecular Probes, Invitrogen). Fluorescence microscopy was performed as previously described (Serrano *et al.*, 2011), and images were analysed with Metamorph v7.7 (Molecular Devices) and ImageJ (http://rsbweb.nih.gov/ij/). For quantification of the subcellular localization of SafA-YFP in each strain, at least 100 sporulating cells were randomly examined and scored. The 3D graphics of the distribution of the fluorescent signal in sporulating cells were obtained using the ImageJ plugin *Interactive 3D Surface Plot* v2.33.

Accumulation of SafA variants during sporulation

In these assays, we used the strains expressing the various *safA* alleles from the native locus, as well as wild type cells. Cultures were grown in DSM at 37° C and samples were taken at 2, 4 and 6 hours after the onset of sporulation. Cells were harvested by centrifugation (7500 × *g*, 10 min, at 4° C), resuspended in French press buffer (10 mM Tris pH 8.0, 10 mM $MgCI_2$, 0.5 mM EDTA, 0.2 M NaCI, 10% glycerol, 0.1 mM DTT, 1 mM PMSF), and lysed in a French pressure cell (18,000 lb/in^2). The extracts were quantified using the Bio-Rad mini protein system according to manufacturer's instructions. 10 µg of protein from each sample were prepared for SDS-PAGE, and proteins were resolved, transferred to nitrocellulose membranes and immunobloted using anti-SafA antibodies.

Spore purification and fractionation

For spore fractionation, we used strains with the in-frame deletion of *safA* and expressing *safA* alleles from the non-essential locus *amyE* (AH10302, AH10555–10558 and AH10561), as well as wild type and *safA* null mutant cells. Cells were grown in DSM for 24h after the onset of sporulation, and the produced spores were purified by a two-step gradient of gastrografin (Bayer Schering Pharma) (Seyler *et al.*, 1997; Henriques and Moran, 2000). Spore fractioning was performed as described in Chapter 3. Proteins within each spore fraction were resolved by SDS-PAGE and transferred to nitrocellulose membranes for immunoblot analysis with anti-SafA and anti-Tgl antibodies. As a control for the decoating, membranes were stripped with stripping buffer (50 mM Tris, pH 6.8, 2% SDS, 100 mM β-mercaptoethanol) and reprobed with anti-CotA antibodies.

Peptidoglycan- and chitin-binding assays

Cultures of *E. coli* producing the various StrepTagII fusions were grown to mid-log phase, induced with 200 µg/ml of anhydrotetracycline, and

incubated for 3 to 5 h before harvesting the cells. The pellets corresponding to 50 mL of induced cultures were resuspended in 3 mL of buffer W (100 mM Tris pH 8.0, 1mM EDTA) supplemented with 100 mM NaCl, 1 mM PMSF and Complete Mini EDTA-free protease inhibitor cocktail (Roche). Cells were lysed in a French pressure cell (18,000 lb/in^2), and the lysates were cleared by centrifugation. The StrepTagII fusion proteins were purified from the lysates using StrepTactin Sepharose columns, according to manufacturer instructions (IBA, GmbH), and finally were quantified through the Bradford method.

For cortex purification, wild type *B. subtilis* cells were grown in DSM medium for 24 hours after the onset of sporulation. Spores were purified as described above (Seyler *et al.*, 1997; Henriques and Moran, 2000), and the cortex was extracted (Fein and Rogers, 1976; Kuroda and Sekiguchi, 1990), purified by removal of peptidoglycan-associated polymers and quantified (Yamamoto *et al.*, 2008).

Peptidoglycan an chitin binding assays were adapted from Yamamoto *et al.*, 2008. In short, 1 mg of purified cortex was incubated for 2 hours on ice in 40 µL of HEPES buffer, with or without lysozyme (40 µg/mL). Digested and non-digested cortex, or alternatively 25 µL of chitin beads (New England Biolabs), were washed and resuspended in 30 µL of phosphate-buffered saline with Tween 20 (PBS-T). Then, 1 µM of purified LysM-(GFP)-StrepTagII and of GFP-StrepTagII were added. After a 15 min incubation on ice, pellet and supernatant fractions were separated by centrifugation (2min, 5000 × *g*) and the pellets were washed with PBS-T. Proteins within each fraction were resolved by TSDS-PAGE and immunobloted with anti-StrepTagII antibodies (Abcam).

Western blot analysis

Proteins transferred to nitrocellulose membranes were immunobloted according to the instructions for the SuperSignal West Pico

Chemiluminescent Substrate (Thermo Scientific), using 5% low fat powder milk in PBS-0.1% Tween-20 (0,001%) as blocking agent. Antibodies were used at the following dilutions: anti-SafA (a gift from Charles P. Moran Jr.) 1:15 000, anti-Tgl (Zilhao *et al.*, 2005) 1:15 000, anti-CotA (laboratory stock) 1:1 000 and anti-StrepTagII (Abcam) 1:1 000. Secondary peroxidase-conjugated antibodies, anti-rabbit and anti-mouse, were used at the dilutions of 1:5 000 and 1:2 000, respectively.

RESULTS

Conserved features of the LysM domain of SafA

We started the study on the LysM domain of SafA ($LysM^{SafA}$) by performing a sequence comparison with other LysM motifs present in *B. subtilis* sporulation-specific proteins. We also used the sequences of the well-characterized LysMs from the *E. coli* murein transglycosylase D (MltD), which recognizes peptidoglycan (Bateman and Bycroft, 2000), and from the *Pteris ryukyuensis* chitinase-A (PrChiA), that recognizes chitin (Ohnuma *et al.*, 2008; Onaga and Taira, 2008). All sequences were available at the *National Center for Biotechnology Information* (NCBI) database (http://www.ncbi.nlm.nih.gov). Our analysis supports that the first 16 residues of the LysM motifs are particularly conserved, as previously reported (Buist *et al.*, 2008). Also, there is some conservation of the C-terminal region, whereas the central residues of the motif are poorly conserved, excepting for the positions 26 and 30, according to SafA numbering (Buist *et al.*, 2008) (Fig 4.1 A).

The residues that compose the two α-helices and the two β-sheets in the LysM of *E. coli* MltD (Bateman and Bycroft, 2000) are indicated in the sequence alignment, as well as the two binding sites for GlcNAc oligomers in the LysM of *P. ryukyuensis* PrChiA (Ohnuma *et al.*, 2008) (Fig 4.1 A). These binding sites, which form a groove by a cluster of hydrophobic residues, are

consistent with those from the LysM motifs of the *Enterococcus faecalis* AtlA (Mesnage *et al.*, 2014), the *Arabidopsis* AtCERK1 (Liu *et al.*, 2012), and the *Cladosporium fulvum* Ecp6 (Sanchez-Vallet *et al.*, 2013). Moreover, they overlap with the conserved residues G9, D10, S11, L12 (in binding site 1), N30 and I39 (in binding site 2) of SafA. In order to assess the position of these conserved residues within the folded domain, we produced a structural

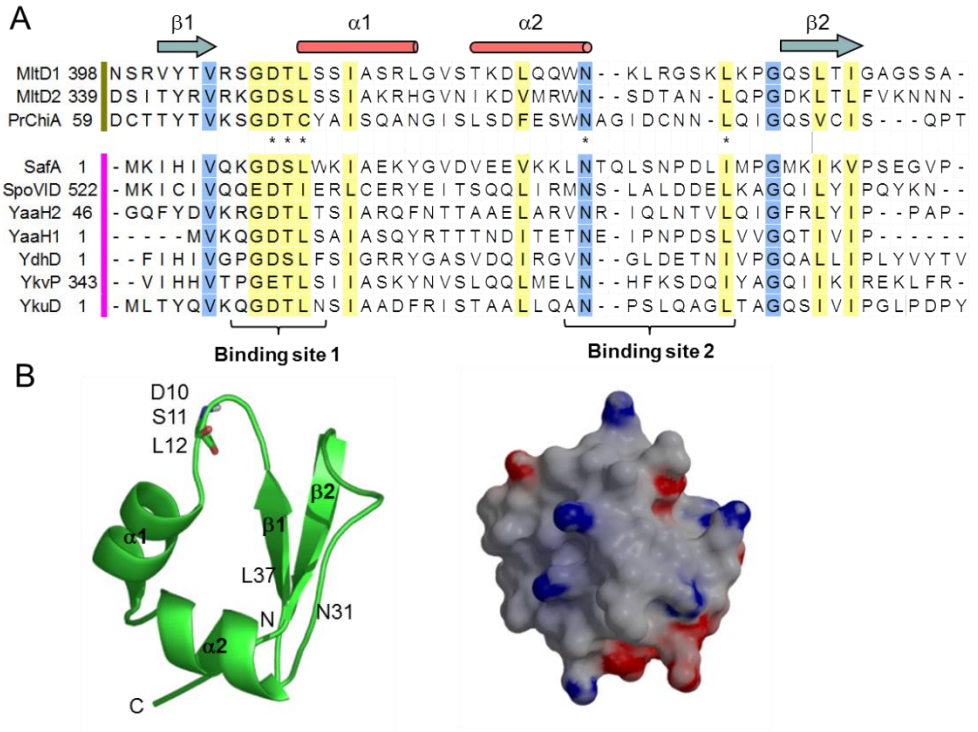

Figure 4.1 - LysM is a well-conserved domain. **A)** Sequence alignment of the LysM motifs from SafA, MltD (*E. coli*), PrChi-A (*P. ryukyuensis*) and five *B. subtilis* sporulation-specific proteins, including SpoVID. Identical residues are shaded in blue, while similar residues are shaded in yellow. The numbers on the left indicate the first residue of each LysM motif. Asterisks denote the five residues within LysM^{SafA} whose role was investigated in this study. On top, we indicate the residues that compose the α-helices and β-strands on the LysM domain of MltD (Bateman and Bycroft, 2000). On the bottom, we denote the two binding sites for GlcNAc oligomers on the LysM of PrChiA (Ohnuma *et al.*, 2008). **B)** Representation of the NMR structure of the LysM motif of *E. coli* MltD (Bateman and Bycroft, 2000). Left panel shows the position of the two α-helices and the two β-sheets. The conserved residues D10, S11, L12, N31 and L37 (the last two corresponding to N30 and I39 in SafA) are indicated. Right panel shows the surface charge model, with the acidic residues in red and the basic residues in blue.

model of the LysM^{SafA} based on the similarity to the LysM domain of MltD (Bateman and Bycroft, 2000) (Fig. 4.1 B). In this domain, as well as in other LysM modules whose structure was determined (Bielnicki *et al.*, 2006; Liu *et al.*, 2012; Mesnage *et al.*, 2014), the two α-helices are packed against the two antiparallel β-sheets. According to the model, the side chains of residues D10, S11 and N30 localize at the walls of the groove and are surface-exposed. The side chains of residues L12 and I39 form part of the basement of the groove and are also partially exposed (Fig. 4.1 B). Therefore, these five residues are good candidates for a role in peptidoglycan binding and/or protein localization.

The LysM domain is required for SafA subcellular localization

In SafA, the removal of the LysM domain results in an unstable protein that fails to accumulate in sporulating cells (Costa *et al.*, 2006). Therefore, in order to address the role of this domain in SafA localization, we performed loss-of-side-chain mutagenesis of LysM^{SafA} individual conserved residues predicted to be surface-exposed. We constructed strains with an in-frame deletion of *safA* and expressing *safA-yfp* variants with the substitutions D10A, S11A, L12A, N30A or I39A from the non-essential locus *amyE*. Mutant cells were grown in sporulation medium and imaged by fluorescence microscopy along the time (Fig. 4.2; Table 4.2).

As described in Chapter 3, SafA-YFP exhibits a kinetic of localization that matches coat protein fusions of class II. It starts localizing as a dot at the mother cell proximal (MCP) pole of the prespore as soon as the asymmetric septum begins to curve. The dot expands into a cap, and after engulfment completion a second cap appears at the opposite pole. Then, SafA-YFP completely encircles the spore, forming a fluorescent ring (Fig. 4.2, 1st column; Table 4.2). We found that SafA-YFP variants with D10A or N30A substitutions localize at the septum, but fail to encase the spore, accumulating as a dot or a cap at the MCP pole. SafA$_{D10A}$-YFP accumulates as a

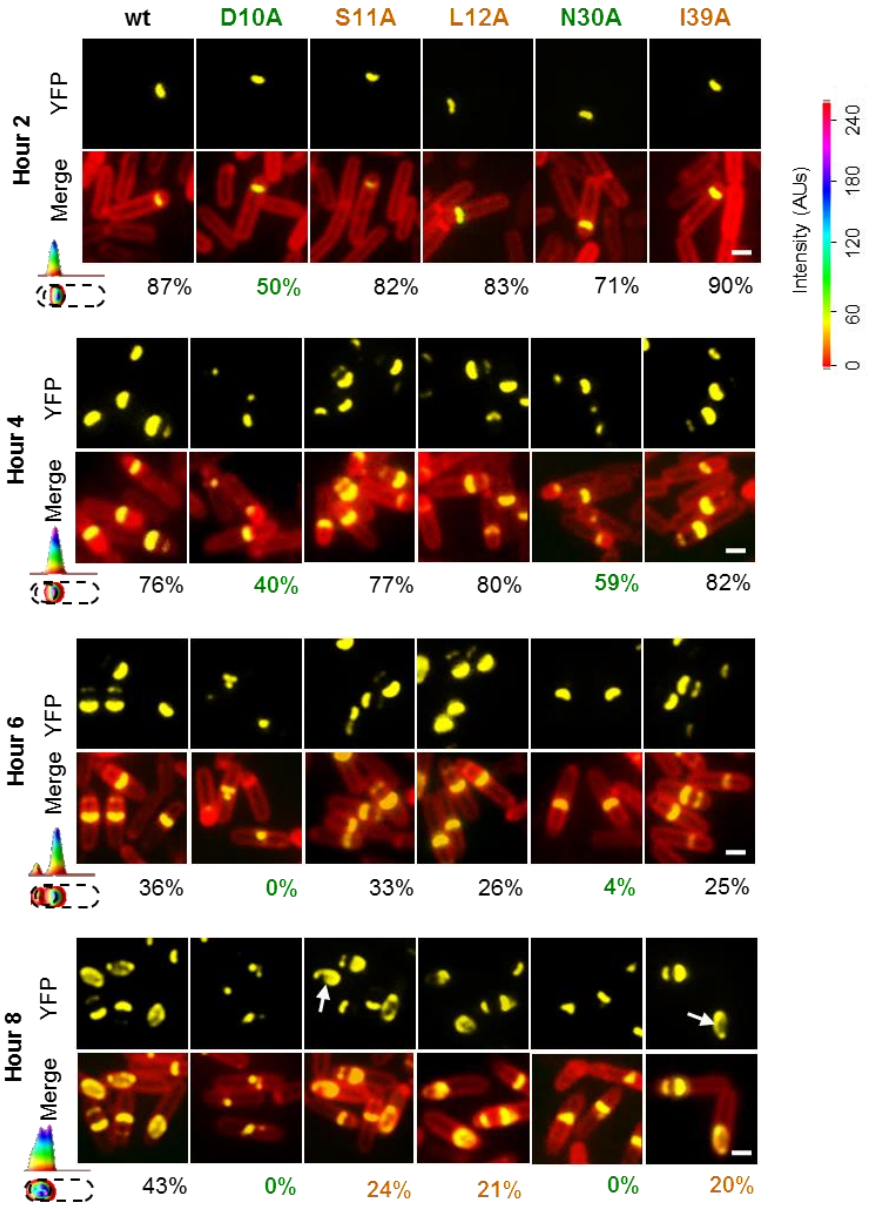

Figure 4.2 – Exposed, conserved residues within LysM^{SafA} are important for SafA-YFP localization. Cells expressing the various *safA-yfp* alleles were collected at 2, 4, 6 and 8 hours after the onset of sporulation, stained with FM 4-64 and imaged by fluorescence microscopy. For each sporulation time, the 1st row shows the YFP signal and the 2nd row shows the merge between the signals of the stained membranes (red) and SafA-YFP (yellow). White arrows at hour 8 point to the intermediate phenotype between 1 and 2 caps. The 3D graphs in the lower left corners represent the distribution of the YFP signal in a wild type cell with the predominant pattern of SafA-YFP localization. The percentages bellow each image correspond to the sporulating cells in each strain exhibiting that pattern. Scale bar, 1µm.

dot in a higher percentage of sporulating cells comparing to $SafA_{N30A}$-YFP, and the difference is accentuated along the time (Fig. 4.2; Table 4.2). In contrast, $SafA_{S11A}$-YFP, $SafA_{L12A}$-YFP and $SafA_{I39A}$-YFP variants localize as the wild type SafA-YFP at initial stages of sporulation. However, 8 hours after resuspension, the percentage of cells expressing these mutated variants that exhibit a complete fluorescent YFP ring is lower comparing to cells expressing the wild type SafA-YFP (24% for S11A, 21% for L12A and 20% for I39A, *versus* 43% for the wild type). In these mutant strains, the percentage of cells with two YFP caps is higher. Also, for those strains with substitutions L12A or I39A, there is an increment on the proportion of cells with an intermediate pattern of SafA-YFP localization between one and two caps, in which one side of the cap at the MCP pole spreads to reach the opposite pole (Fig. 4.2, white arrows at hour 8, Table 4.2). We conclude that residues D10 and N30 are important for initial stages of SafA-YFP localization, before engulfment completion and synthesis of the cortex, whereas S11, L12 and I39 have a role in localization at later stages.

We then investigated if SafA variants that mislocalize in sporulating cells are able to accumulate along the time. Cells expressing the different *safA* alleles, as well as wild type cells, were grown in sporulation medium, collected at different times, and lysed. Then, equal amounts of cell extracts were used to carry out immunoblot assays for the detection of the various SafA forms: the full-length, the $SafA_{C30}$ (that results from internal translation) and the $SafA_{N21}$ (which corresponds to the N terminus of SafA) (Ozin *et al.*, 2000; Takamatsu *et al.*, 2000a; Takamatsu *et al.*, 2000b; Ozin *et al.*, 2001a). In all strains, the full-length form accumulated to wild type levels, and the timing of appearance and levels of $SafA_{C30}$ was not grossly affected (Fig. 4.3). $SafA_{N21}$ accumulated in lower levels in all the strains constructed, including in the strain complemented with the wild type form of *safA* (wt^{C}). Therefore, alanine substitutions that resulted in SafA mislocalization did not significantly affect the accumulation of the protein *in vivo*.

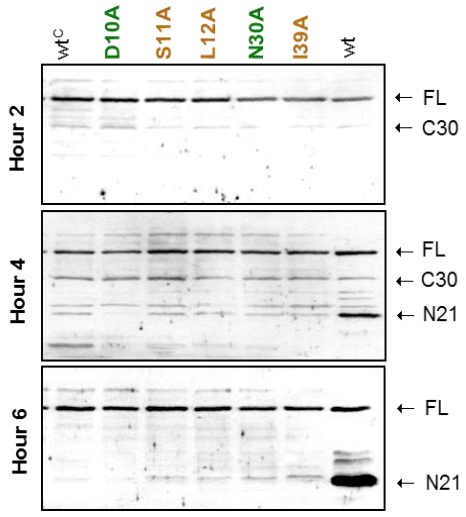

Figure 4.3 – Accumulation of the SafA variants that mislocalize in sporulating cells. Cells with the various *safA* alleles, as well as wild type cells (wt), were grown sporulation media. Samples were taken at 2, 4 and 6 hours after the onset of sporulation and cells were lysed. Proteins within equal amounts of cell extracts were resolved by SDS-PAGE and immunobloted with anti-SafA antibodies. The SafA full-length (FL), $SafA_{C30}$ (C30) and $SafA_{N21}$ (N21) forms are indicated. wt^{C}: Δ*safA::safA*.

We further tested if alanine substitutions within $LysM^{SafA}$ that led to mislocalization of SafA-YFP also affect the subcellular localization of SafA-dependent inner coat proteins, as CotD. To do this, we imaged sporulating cells missing *safA* or with the various *safA* alleles and expressing *cotD-gfp* (Fig. 4.4). In cells with the wild type form of SafA, as well as in those expressing versions with S11A, L12A or I39A substitutions, CotD-GFP completely encircles the spore. However, in cells with the substitutions D10A

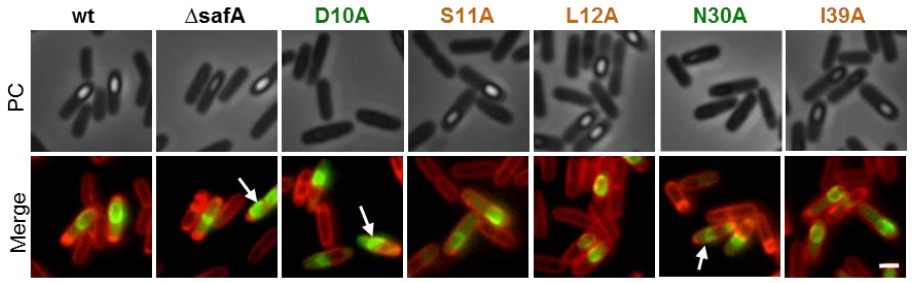

Figure 4.4 – Alanine substitutions D10A and N30A in SafA cause mislocalization of the SafA-dependent inner coat protein CotD. Cells missing *safA* or with the different *safA* alleles and expressing CotD-GFP were imaged 6 hours after the onset of sporulation. Samples were stained with FM 4-64. 1st row: phase contrast signal; 2nd row: merge between CotD-GFP (green) and stained membranes (red) signals. White arrows point to cells exhibiting mislocalization of CotD-GFP. Scale bar, 1μm.

or N30A or in the absence of *safA*, CotD-GFP do not encase the spore, and often a strong fluorescence signal was found in the mother cell cytoplasm. Thus, substitutions D10A and N30A not only impair encasement by SafA, but also by at least some inner coat, SafA-dependent proteins.

The LysM domain is required for SafA association with the cortex

SafA localizes at the interface between the cortex and the coat (Ozin *et al.*, 2000), and spore fractionation assays in Chapter 3 revealed that it associates with the cortex. Now, we aimed at determining if $LysM^{SafA}$ is required for cortex association. To test this, we fractionated spores produced by strains expressing the various *safA* alleles, as described in Chapter 3. In short, purified spores were decoated and incubated in the presence or absence of lysozyme. The lysozyme treatment digests the cortex peptidoglycan, releasing the cortex-associated proteins. As controls, we included wild type and *safA* null mutant spores in the assay. Proteins within each spore fraction were resolved, and the presence of SafA was assessed by immunoblot (Fig 4.5, 1st panel). The efficiency of spore fractionation was demonstrated by the detection of the bona fide coat protein CotA (Martins *et al.*, 2002) exclusively in the coat fraction (Fig 4.5, 3rd panel), as well as by the lack of detected proteins in the non-digested cortex fractions.

We observed that the full-length form of the wild type SafA, either expressed from the native locus (wt) or from *amyE* (wt^C), is equally distributed between the digested cortex and coat fractions, while $SafA_{C30}$ is detected mainly in the coat. This distribution pattern differs from those obtained in Chapter 3, which we attributed to strain-specific variations. As stated in Chapter 3, $SafA_{C30}$ migrates faster in the coat fraction, presumably due to processing by the protease YabG in this layer (Takamatsu *et al.*, 2000a; Takamatsu *et al.*, 2000b). Also, we did not detect $SafA_{N21}$, reinforcing that, as in PY79 derivatives, this form in not abundant at later stages of spore development. The higher molecular weight forms of SafA above the full-

length form may correspond to SafA oligomers or to cross-linked coat material. The band between the full-length and $SafA_{C30}$ in the coat fraction may be either cross-linked $SafA_{C30}$ or a degradation product. We found that in strains with substitutions D10A or N30A, most of the SafA was extracted in the coat fraction, suggesting that these forms of SafA interact less efficiently with the cortex. Also, in cells with the substitution I39A, the overall amount of full-length SafA is lower comparing to the wild type, perhaps because this protein is impaired in its localization to the spore surface.

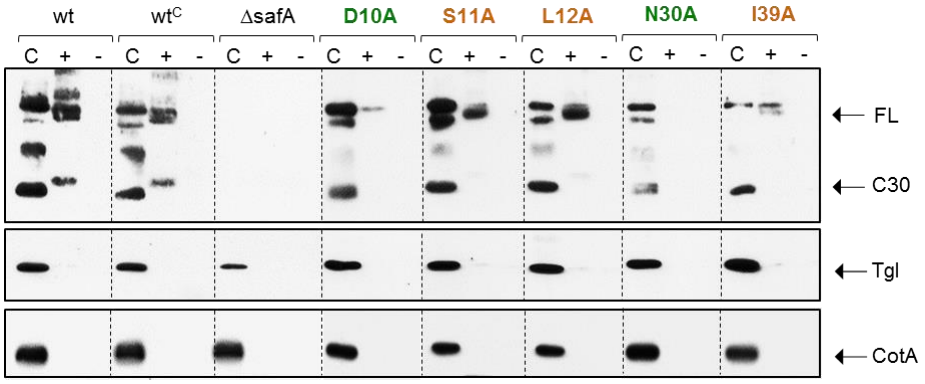

Figure 4.5 – Alanine substitutions D10A and N30A increase the extractability of SafA in the coat fraction, whereas I39A diminishes the SafA retention at the spore surface (1st row). However, these substitutions do not affect the distribution of Tgl across the spore layers (2nd row). Cells were collected 24 hours after entering in sporulation. Spores were purified, decoated and incubated in the presence or absence of lysozyme. Proteins within each spore fraction were resolved by SDS-PAGE and immunobloted with anti-SafA, anti-Tgl and anti-CotA antibodies. wt^C: Δ*safA, amyE'::safA::'amyE*; C: coat fraction; +: cortex fraction digested with lysozyme; -: cortex fraction non-digested with lysozyme; FL: $SafA_{FL}$; C30: $SafA_{C30}$.

Recently, it was found that SafA is required for the localization of Tgl, a transglutaminase that cross-links coat proteins at the surface of the spore (Fernandes, C. F. and Henriques, A. O., unpublished data). Knowing the importance of this enzyme in maturation of the spore coat, we further analysed the effect of alanine substitutions in $LysM^{SafA}$ in the distribution of Tgl across the spore layers. We stripped Western blot membranes from

spore fractionation assays and incubated them with anti-Tgl antibodies (Fig. 4.6, 2nd panel). As previously shown (Fernandes, C. F. and Henriques, A. O., unpublished data), Tgl is present mainly in the coat fraction, and the absence of SafA led to a reduction in the amount of the enzyme in the spore. The distribution and levels of Tgl were identical in all strains expressing the various *safA* alleles, indicating that alanine substitutions in LysM^{SafA} that result in SafA mislocalization do not interfere with the distribution of Tgl in the spore. This supports that Tgl requires SafA for localization, but does not exclusively depends on it.

The LysM domain of SafA binds to spore peptidoglycan *in vitro*

The results of the preceding sections showed that LysM^{SafA} is important for the subcellular localization of SafA and its attachment to the spore surface. Therefore, we wanted to test whether this domain would recognize spore peptidoglycan, and if substitutions that led to SafA mislocalization would interfere with binding. To address this, we incubated purified spore peptidoglycan with fusions of LysM^{SafA} variants to GFP and StrepTagII. The ability of these fusions to bind peptidoglycan was assessed through co-sedimentation following low speed centrifugation (Steen *et al.*, 2003; Shah *et al.*, 2008). As a control for the retention of the fusions in the pellet, GFP-StrepTagII was added together with the various LysM^{SafA}-GFP-StrepTagII, at the same concentration. Unbound supernatant and bound pellet fractions were then resolved and immunobloted (Fig. 4.6).

In no instance did we observe co-sedimentation of GFP-StrepTagII with the peptidoglycan. In contrast, about 71% of the wild type LysM^{SafA}-GFP-StrepTagII co-sedimented, showing that the LysM domain of SafA binds spore peptidoglycan *in vitro*. For all LysM^{SafA}-GFP-StrepTagII mutant variants tested, there was a reduction in co-sedimentation. This reduction was more accentuated for variants with substitutions I39A and L12A (3% and 10% of co-sedimentation, respectively), and not so pronounced for those with D10A,

S11A and N30A (31%, 32% and 58% of co-sedimentation). Importantly, the lower capacity of the variant with the substitution I39A to bind peptidoglycan is in line with spore fractioning data, which showed that this form of SafA is less retained at the spore surface. We also observed that a treatment of the peptidoglycan with lysozyme prior to incubation resulted in the enrichment of the LysM^{SafA}-GFP-StrepTagII fusions in the supernatant (Fig. 4.6, bottom panel), indicating that sedimentation was due to an interaction with the insoluble peptidoglycan.

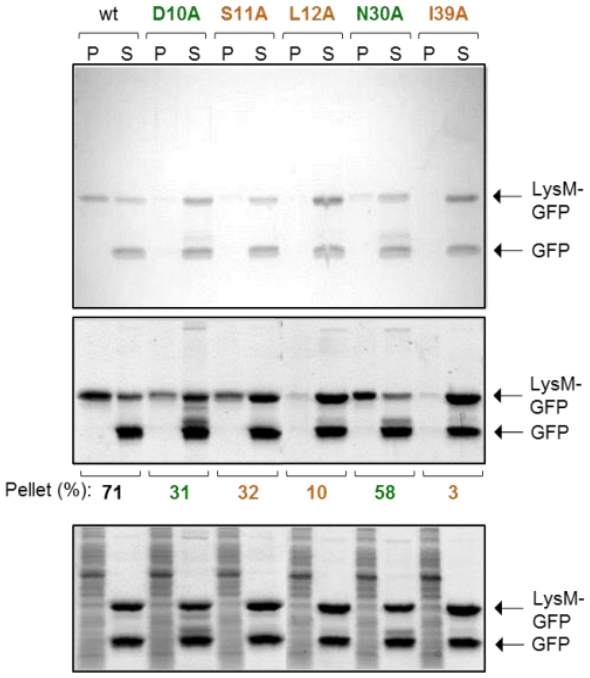

Figure 4.6 – *In vitro* peptidoglycan binding assays with LysM^{SafA}-GFP-StrepTagII fusions. Spore peptidoglycan was incubated with LysM^{SafA}-GFP-StrepTagII variants and GFP-StrepTagII. Pellet (P) and supernatant (S) fractions, with peptidoglycan-bound proteins and proteins that do not bind peptidoglycan, respectively, were resolved and stained with Coomassie blue (top panel) or immuno-bloted with anti-StrepTagII antibodies (2nd panel). Bands corresponding to LysM-GFP-StrepTagII were quantified and the percentage of each form in the peptidoglycan-bound fraction is indicated. The procedure was also performed using digested peptidoglycan (bottom panel).

The localization of SafA is dependent on cortex biogenesis

We further tested if the cortex is required for SafA localization by analysing the deposition of SafA-YFP variants along sporulation in strains missing *spoVE*. SpoVE localizes to the outer forespore membrane and, together with its physical partner SpoVD (a transpeptidase and penicillin-

binding protein), is required for cortex synthesis (Piggot and Coote, 1976; Henriques *et al.*, 1992; Daniel *et al.*, 1994; Real *et al.*, 2008; Fay *et al.*, 2010). We found that, at initial stages of sporulation (until hour 4 after resuspension), the localization of SafA-YFP does not differ significantly in the presence or in the absence of *spoVE* (Fig. S3 of Appendices; Table 4.2). However, at later stages, after engulfment completion and initiation of cortex synthesis in wild type strains, the percentage of cells in which SafA-YFP completely encircles the spore is lower in the absence of *spoVE* (2% and 9% at hours 6 and 8, comparing to 23% and 43% for wild type cells – Fig. 4.7; Fig. S3; Table 4.2). Similar results were obtained for SafA-YFP variants with substitutions S11A, L12A or I39A (Fig. S3; Table 4.2). These substitutions caused mislocalization of SafA at later stages by themselves, but the absence of *spoVE* emphasized the effect. Regarding substitutions D10A and N30, which affect the localization of SafA at earlier stages, the absence of *spoVE* did not have an impact in the phenotypes observed (Fig. S3; Table 4.2). Therefore, we conclude that the late localization of SafA or its maintenance at the spore surface requires the cortex.

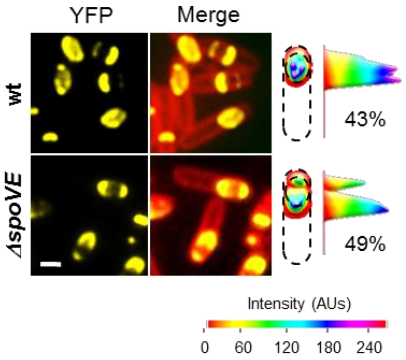

Figure 4.7 – The cortex is important for late subcellular localization of SafA. Sporulating cells expressing SafA-YFP, with or without *spoVE*, were stained with FM 4-64 and imaged at different times. A few representative cells are shown for 8 hours after resuspension. 1st column: SafA-YFP signal; 2nd column: overlap between the signals of SafA-YFP (yellow) and stained membranes (red); 3rd columns: 3D distribution of the YFP signal in one representative cell for each strain. Scale bar, 1µm.

Importantly, both SpoIVA and SpoVID, required for the early localization of SafA, showed normal deposition around the forespore in *spoVE* null mutant cells (data not shown). This reinforces that the late

Table 4.2: Quantification of the encasement by SafA-YFP variants in wild type and Δ*spoVE* background [a]

		Hour 2		Hour 4			Hour 6				Hour 8				
															
wt	wt	13	87	0	76	24	0	41	36	23	0	28	10	19	43
	D10A	**50**	50	**60**	40	0	**89**	11	0	0	**98**	2	0	0	0
	S11A	18	82	0	77	23	0	44	33	23	0	27	10	**39**	**24**
	L12A	17	83	0	80	20	0	55	26	19	0	30	21	**28**	**21**
	N30A	**29**	71	**41**	59	0	**46**	50	4	0	**47**	53	0	0	0
	I39A	10	90	0	82	18	0	59	25	16	0	25	18	**37**	**20**
Δ*spoVE*	wt	13	87	0	84	16	0	44	54	2	0	10	**32**	**49**	9
	D10A	58	42	86	14	0	92	8	0	0	95	5	0	0	0
	S11A	9	91	0	79	21	0	29	71	0	0	10	**39**	**34**	17
	L12A	12	88	4	75	21	0	26	72	2	0	20	**45**	**30**	5
	N30A	44	56	41	59	0	26	74	0	0	51	49	0	0	0
	I39A	4	96	0	65	35	0	57	42	1	0	17	**43**	**34**	6

[a] The numbers correspond to the percentages of sporulating cells exhibiting each of the SafA-YFP localization patterns represented, at 2, 4, 6 and 8 hours after the onset of sporulation.

mislocalization of SafA-YFP does not result from the absence of these proteins from the spore surface.

In these experiments, we observed that engulfment appears to be delayed in *spoVE* null mutant cells. To test this, we looked at the expression of a fusion of the σ^G-responsive promoter P_{sspE} to the *cfp* gene in a wild type strain and in a congenic *spoVE* mutant, during sporulation. As σ^G is activated after engulfment completion, CFP-positive cells must have passed this stage in sporulation. Four hours after resuspension, the percentage of *spoVE* null mutant cells expressing P_{sspE}-*cfp* is lower than in wild type cells (Fig. 4.8), confirming that the absence of SpoVE led to a delay in engulfment. This revealed a role of SpoVE at this stage of sporulation, in line with the reported contribution of the peptidoglycan synthesis for membrane migration around the forespore (Meyer *et al.*, 2010). Also, it is in agreement with the requirement of SpoVD, which forms a complex with SpoVE during cortex formation (Fay *et al.*, 2010), for peptidoglycan synthesis throughout

engulfment (Meyer *et al.*, 2010). Our results therefore suggest that SpoVD and SpoVE cooperate for peptidoglycan synthesis required at this point of sporulation. Importantly, 5 hours after the onset of sporulation, *spoVE* null mutant cells already recovered the lag in engulfment (Fig. 4.8). Therefore, we infer that this delay in *spoVE* null mutant cells does not influence the localization of SafA-YFP at later times.

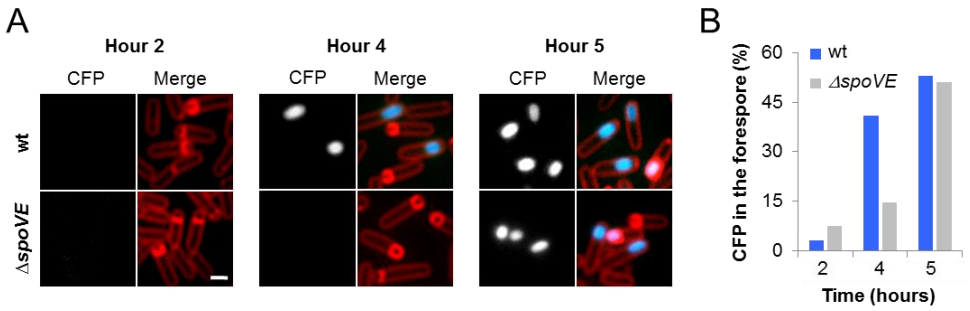

Figure 4.8 – Engulfment is delayed in *spoVE* null mutant cells. **A)** Cells expressing CFP under control of the σ^G-responsive promotor P_{sspE}, with or without *spoVE*, were grown in sporulation media, stained with FM 4-64, and imaged. 1st column: CFP signal; 2nd column: merge between signals of CFP and stained membranes. **B)** Quantification of sporulating cells exhibiting fluorescent signal in the forespore.

The LysM domain of SpoVID in peptidoglycan recognition *in vitro*

It was previously demonstrated that the LysM domain of SpoVID ($LysM^{SpoVID}$) is required for localization, suggesting a role in spore peptidoglycan recognition (Wang *et al.*, 2009). Supporting this, sequence comparison revealed that the five exposed residues in $LysM^{SafA}$ involved in peptidoglycan binding are identical or similar in $LysM^{SpoVID}$ (Fig. 4.1 A). However, SpoVID appears to be insensitive to the absence of *spoVE* for localization, raising questions about the potential function of its LysM domain as a peptidoglycan-binding module. To clarify this, we performed *in vitro* peptidoglycan binding assays as described previously, but using fusions of $LysM^{SpoVID}$ and $LysM^{SafA}$ to StrepTagII. Contrarily to $LysM^{SafA}$-StrepTagII, we

were not able to detect LysM^{SpoVID}-StrepTagII in the peptidoglycan-bond fraction (Fig. 4.9 A). This indicates that, at least in the conditions of our assay, the LysM module of SpoVID does not recognize spore peptidoglycan.

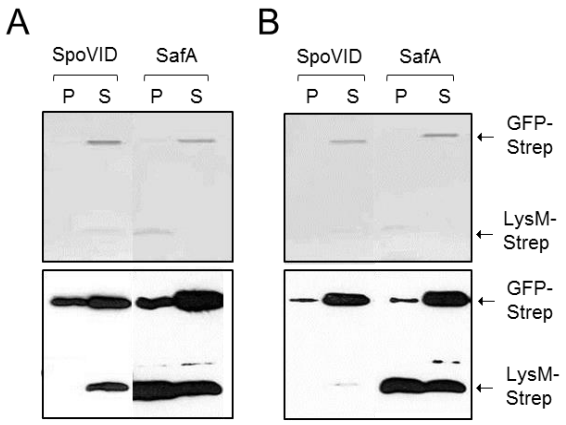

Figure 4.9 – LysM^{SpoVID} does not bind GlcNAc oligomers *in vitro* in the same condition as the LysM^{SafA}. Cortex **(A)** and chitin **(B)** binding assays using fusion of SpoVID and SafA LysM domains to StrepTagII were performed. Proteins within pellet (P) and supernatant (S) fractions were resolved and the gels were stained with Coomassie blue (top panels) or transferred and immunobloted with anti-StrepTagII antibodies (bottom panels).

We observed that, in *B. subtilis* and related species, the LysM domain of SpoVID comprises two cysteines (Fig. 4.10, in pink) that are not conserved among other LysM motifs (Fig 4.1 A). This suggests the formation of an intramolecular disulfide bond that may be the cause of peptidoglycan insensitivity. Disulfide bonds are common in eukaryotic LysM motifs, but not in prokaryotic ones (Bateman and Bycroft, 2000; Buist *et al.*, 2008), and it was proposed that multiple cysteine residues could determine binding specificity for chitin (Buist *et al.*, 2008). For this reason, we further tested the ability of the LysM^{SpoVID} to recognize this oligomer. We repeated the *in vitro* binding assays using chitin beads instead of spore peptidoglycan, and we found that LysM^{SafA}-StrepTagII co-sedimented with the beads, yet LysM^{SpoVID}-StrepTagII did not (Fig. 4.8 B). We conclude that, in the same conditions, the LysM^{SafA} recognizes the common GlcNAc residues present in both peptidoglycan and chitin oligomers, whereas LysM^{SpoVID} does not. This does not exclude, however, the possibility that LysM^{SpoVID} could bind peptidoglycan *in vivo* or under different experimental conditions.

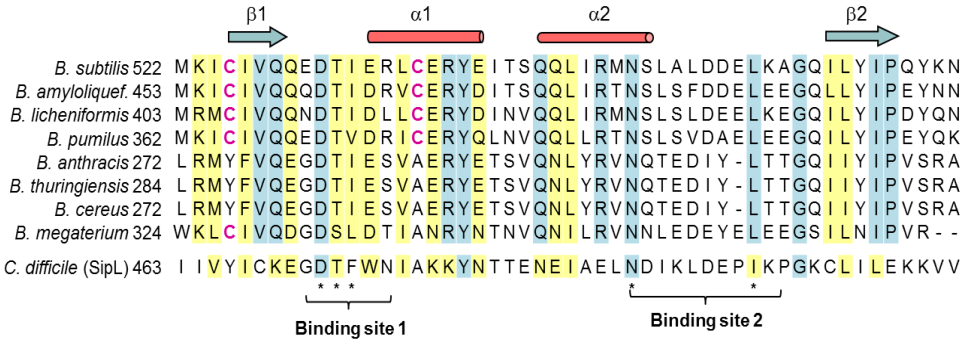

Figure 4.10 – Sequence alignment of the LysM domains of SpoVID from several *Bacillus* species, as well as the LysM domain of SipL, the *C. difficile* functional analogous of SpoVID. Identical residues are shaded in blue, while similar residues are shaded in yellow. Numbers on the left indicate the first residue of each LysM motif. Asterisks denote the residues analysed in this study (see Fig. 4.1 A). Cysteines in pink are conserved in *B. subtilis* and related species, but not in other LysM modules. The residues that compose α-helices and β-strands on the LysM domain of MltD (Bateman and Bycroft, 2000) are represented on top, and the $(GlcNAc)_n$ binding sites on the LysM domain of PrChiA (Ohnuma *et al.*, 2008) are indicated on the bottom.

DISCUSSION

The morphogenetic protein SafA is essential for assembly of the inner coat. Therefore, it is important to understand the mechanisms governing SafA localization at the spore surface. Previous work showed that SafA requires the morphogenetic proteins SpoIVA for initial targeting and SpoVID for spore encasement (Ozin *et al.*, 2001b; Wang *et al.*, 2009). The main contribution of the present study is the finding that the spore peptidoglycan is also important for SafA localization and function. We showed that five surface-exposed, conserved residues in the $LysM^{SafA}$ domain are involved in SafA subcellular localization and peptidoglycan recognition *in vitro*. Of those, two (D10 and N30) are required for SafA deposition before engulfment completion and initiation of cortex synthesis (Meador-Parton and Popham, 2000), while the other three (S11, L12 and I39) are important for localization at later stages.

In cells with substitutions D10A or N30A, SafA-YFP is retained at the MCP pole of the spore as a dot or a cap. It appears that D10A affects SafA localization earlier than N30A, as $SafA_{D10A}$-YFP accumulates as a dot in a higher percentage of sporulating cells comparing to $SafA_{N30A}$-YFP variant. Both substitutions increase the extractability of SafA in the coat fraction of purified spores, showing that these SafA variants are less attached to the spore cortex than the wild type. They also affect the localization of at least one inner coat, SafA-dependent protein (CotD), which indicates that D10 and N30 are required for the integrity of the inner coat. Moreover, the mislocalization of these SafA-YFP variants before assembly of the cortex suggests that the $LysM^{SafA}$ may somehow recognize other type of peptidoglycan located in the intermembrane space, or precursors accumulating during engulfment. In fact, Tocheva *et al.*, 2013 showed that peptidoglycan is always present around the prespore throughout engulfment (Tocheva *et al.*, 2013). Another possibility is that these two residues are indirectly important for interaction with other localization determinants, such as SpoIVA or SpoVID. For example, D10A and N30A may affect the capacity of region A, immediately adjacent to the LysM domain (Costa *et al.*, 2006), to access or recognize SpoVID.

Substitutions S11A, L12A or I39A affect the ability of SafA-YFP to form a complete, symmetric, circumference at the surface of the developing spore at later stages. A similar phenotype is observed in *spoVE* null mutant cells, where the cortex is almost absent, supporting that these residues may be key cortex binding determinants required for late localization of SafA. Furthermore, the substitution I39A, which is the one that most affects the peptidoglycan binding ability, led to a reduction in the amount of SafA extracted from purified spores. Thus, residue I39 is important for the maintenance of SafA at the spore surface, presumably via cortex binding.

Our data also indicates that the five conserved residues we tested are part of the $LysM^{SafA}$ glycan binding site. This is in line with the binding sites

identified in other prokaryotic and eukaryotic LysM motifs (Ohnuma *et al.*, 2008; Liu *et al.*, 2012; Sanchez-Vallet *et al.*, 2013; Mesnage *et al.*, 2014). For example, in the LysM domain of the *E. faecalis* AtlA, alanine substitutions in residues corresponding to S11, L12 or I39 in SafA also reduce the peptidoglycan binding ability (Mesnage *et al.*, 2014). Also, we showed that the binding site of $LysM^{SafA}$ recognizes both spore peptidoglycan and chitin oligomers *in vitro*, and as a precedent, the LysM domain of AtlA also binds these two types of glycans (Mesnage *et al.*, 2014). However, SafA is a component of the spore coat, which, at least at initial stages of development, is separated by the spore peptidoglycan by the outer forespore membrane. SafA has no recognizable secretion signals, and there is no evidence of a secretion machinery preferentially at the outer forespore membrane during sporulation. It was proposed that this membrane may not retain its integrity later in sporulation (Setlow, 2006), which would allow SafA to gain access to the cortex at that stage. Also, SafA may be transported through the membrane by a mechanism independent of a typical signal peptide, or the LysM domain may interact with peptidoglycan precursors accumulating at the mother cell-facing surface of the membrane (Ozin *et al.*, 2000).

Since the LysM domain is required for the subcellular localization of SafA, we conclude that, as in SpoVID, it forms a complex localization signal with the immediately adjacent region A, that is also involved in localization via interaction with SpoVID (Costa *et al.*, 2006; Wang *et al.*, 2009). Both regions are more conserved among SafA orthologues than the remaining of the protein, suggesting conservation of the mechanism of SafA localization.

To the best of our knowledge, this was the first time that was reported the mislocalization of a coat protein (SafA) in *spoVE* null mutant cells. Therefore, proper coat formation requires the synthesis of the cortex. SafA may act as a molecular staple, binding to the cortex in mature spores through its LysM domain and recruiting the inner coat proteins presumably via the C-terminal domain. As the cortex formation also requires initiation of

coat assembly (Ebmeier *et al.*, 2012), we can state that morphogenesis of the two main spore protective layers are mutually dependent processes.

Finally, we showed that the LysM domain of SpoVID did not recognize purified spore peptidoglycan under our experimental conditions. Indeed, the subcellular localization of SpoVID-GFP was not affected by the absence of *spoVE*. We cannot exclude, however, that $LysM^{SpoVID}$ may recognize GlcNAc oligomers *in vivo* or under different experimental conditions. Interestingly, the functional analogous of SpoVID in *Clostridium difficile*, SipL, also has a LysM motif at the C terminus. This motif preserves identical or similar residues in the positions corresponding to D10, S11, N30 and I39 in SafA (Fig. 4.10), but in contrast to SpoVID (Wang *et al.*, 2009), it interacts directly with SpoIVA (Putnam *et al.*, 2013).

Altogether, these data allow us to propose a model for SafA deposition at the spore surface that includes SpoIVA, SpoVID and the spore cortex as localization determinants (Fig. 4.11). As most of the coat proteins known to date, initial targeting of SafA to the septum depends on the interaction with SpoIVA (Mullerova *et al.*, 2009; Wang *et al.*, 2009; Qiao *et al.*, 2012). Then, SafA interacts with the region E of SpoVID (see Chapter 3), allowing spore encasement by SafA. Two regions of interaction with SpoVID were already reported in SafA: A and B, or PYYH. We favour that region A may be the one that binds region E, as it appears to contribute more significantly for the interaction with SpoVID. While SafA encases the spore, the C-terminal domain interacts with and recruits several proteins that compose the inner coat. At this stage, $SafA_{C30}$, that localizes through interaction with the full-length form of SafA, plays a major role by increasing the surface of interaction with inner coat proteins. After engulfment completion, the synthesis of the cortex initiates. The LysM domain of SafA recognizes it, which facilitates the distribution of the protein around the spore. Binding to the cortex may also be important for the maintenance of SafA at the spore surface at late stages in spore development.

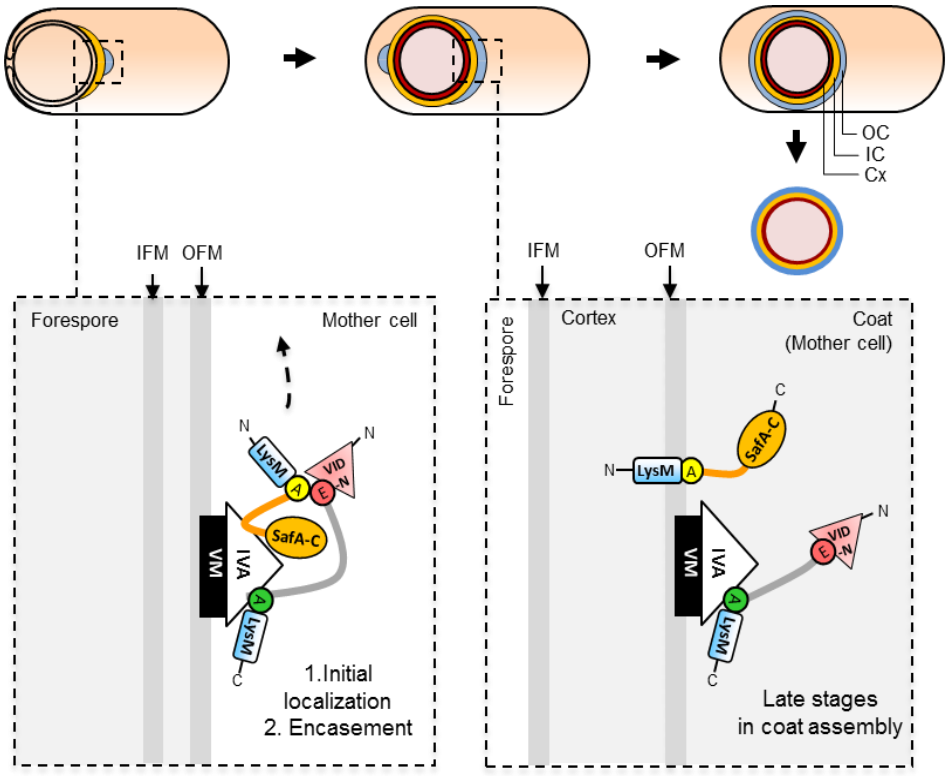

Figure 4.11 - Model for SafA subcellular localization. SpoIVA (white) binds to SpoVM (black) at the surface of the developing spore and recruits SafA (yellow). SpoIVA also interacts with region A of SpoVID (red), allowing targeting of SpoVID to the spore surface. Then, SpoVID and SafA interact, presumably via regions A in SafA and E in SpoVID, which allows encasement by SafA and inner coat proteins. After spore engulfment, the cortex begins to be synthesised, and the LysM domain of SafA gets access to it. Binding of this domain to the cortex peptidoglycan facilitates SafA localization or its retention at the spore surface. IFM: inner forespore membrane; OFM: outer forespore membrane; OC: outer coat; IC: inner coat; Cx: cortex.

ACKNOWLEDGMENTS

This work was supported by grants ERA-PTG/SAU/0002/2008 (ERA-NET PathoGenoMics), and Praxis XXI/PCNA/C/BIO/13201/98, PRAXIS/BIO/35109/99 and Pest-C/EQB/LA0006/2011 from the "Fundação para a Ciência e a Tecnologia" (FCT) to A.O.H.. F.N. (SFRH/BD/64470/2009),

F.P. (SFRH/BD/45459/08) and C.F. (SFRH/BD/45459/08), were the recipients of doctoral fellowships from the FCT. M.S. is an iFCT investigator.

REFERENCES

Abanes-De Mello, A., Sun, Y.L., Aung, S., Pogliano, K., 2002. A cytoskeleton-like role for the bacterial cell wall during engulfment of the Bacillus subtilis forespore. Genes & Development 16, 3253-3264.

Andre, G., Leenhouts, K., Hols, P., Dufrene, Y.F., 2008. Detection and localization of single LysM-peptidoglycan interactions. Journal of Bacteriology 190, 7079-7086.

Atrih, A., Zollner, P., Allmaier, G., Williamson, M.P., Foster, S.J., 1998. Peptidoglycan structural dynamics during germination of Bacillus subtilis 168 endospores. Journal of Bacteriology 180, 4603-4612.

Bateman, A., Bycroft, M., 2000. The structure of a LysM domain from E. coli membrane-bound lytic murein transglycosylase D (MltD). Journal of Molecular Biology 299, 1113-1119.

Beall, B., Driks, A., Losick, R., Moran, C.P., Jr., 1993. Cloning and characterization of a gene required for assembly of the Bacillus subtilis spore coat. Journal of Bacteriology 175, 1705-1716.

Bielnicki, J., Devedjiev, Y., Derewenda, U., Dauter, Z., Joachimiak, A., Derewenda, Z.S., 2006. B. subtilis ykuD protein at 2.0 A resolution: insights into the structure and function of a novel, ubiquitous family of bacterial enzymes. Proteins 62, 144-151.

Broghammer, A., Krusell, L., Blaise, M., Sauer, J., Sullivan, J.T., Maolanon, N., Vinther, M., Lorentzen, A., Madsen, E.B., Jensen, K.J., Roepstorff, P., Thirup, S., Ronson, C.W., Thygesen, M.B., Stougaard, J., 2012. Legume receptors perceive the rhizobial lipochitin oligosaccharide signal molecules by direct binding. Proceedings of the National Academy of Sciences of the United States of America 109, 13859-13864.

Buist, G., Steen, A., Kok, J., Kuipers, O.P., 2008. LysM, a widely distributed protein motif for binding to (peptido)glycans. Molecular Microbiology 68, 838-847.

Chastanet, A., Losick, R., 2007. Engulfment during sporulation in Bacillus

subtilis is governed by a multi-protein complex containing tandemly acting autolysins. Molecular Microbiology 64, 139-152.

Costa, T., Isidro, A.L., Moran, C.P., Jr., Henriques, A.O., 2006. Interaction between coat morphogenetic proteins SafA and SpoVID. Journal of Bacteriology 188, 7731-7741.

Cutting, S.M., Vander Horn, P.B., 1990. Genetic Analysis. In: Harwood, C.R., Cutting, S.M. (Eds.), Molecular Biological Methods for Bacillus. John Wiley & Sons, Chichester, pp. 27-74.

Daniel, R.A., Drake, S., Buchanan, C.E., Scholle, R., Errington, J., 1994. The Bacillus subtilis spoVD gene encodes a mother-cell-specific penicillin-binding protein required for spore morphogenesis. Journal of Molecular Biology 235, 209-220.

de Hoon, M.J., Eichenberger, P., Vitkup, D., 2010. Hierarchical evolution of the bacterial sporulation network. Current biology 20, R735-745.

Driks, A., 1999. Bacillus subtilis spore coat. Microbiology and Molecular Biology Reviews 63, 1-20.

Driks, A., Roels, S., Beall, B., Moran, C.P., Jr., Losick, R., 1994. Subcellular localization of proteins involved in the assembly of the spore coat of Bacillus subtilis. Genes & Development 8, 234-244.

Ebmeier, S.E., Tan, I.S., Clapham, K.R., Ramamurthi, K.S., 2012. Small proteins link coat and cortex assembly during sporulation in Bacillus subtilis. Molecular Microbiology 84, 682-696.

Errington, J., 2003. Regulation of endospore formation in Bacillus subtilis. Nature Reviews Microbiology 1, 117-126.

Fay, A., Meyer, P., Dworkin, J., 2010. Interactions between late-acting proteins required for peptidoglycan synthesis during sporulation. Journal of Molecular Biology 399, 547-561.

Fein, J.E., Rogers, H.J., 1976. Autolytic enzyme-deficient mutants of Bacillus subtilis 168. Journal of Bacteriology 127, 1427-1442.

Gutierrez, J., Smith, R., Pogliano, K., 2010. SpoIID-mediated peptidoglycan degradation is required throughout engulfment during Bacillus subtilis sporulation. Journal of Bacteriology 192, 3174-3186.

Henriques, A.O., Beall, B.W., Moran, C.P., Jr., 1997. CotM of Bacillus subtilis, a member of the alpha-crystallin family of stress proteins, is induced during

development and participates in spore outer coat formation. Journal of Bacteriology 179, 1887-1897.

Henriques, A.O., de Lencastre, H., Piggot, P.J., 1992. A Bacillus subtilis morphogene cluster that includes spoVE is homologous to the mra region of Escherichia coli. Biochimie 74, 735-748.

Henriques, A.O., Moran, C.P., Jr., 2000. Structure and assembly of the bacterial endospore coat. Methods 20, 95-110.

Henriques, A.O., Moran, C.P., Jr., 2007. Structure, assembly, and function of the spore surface layers. Annual Review of Microbiology 61, 555-588.

Holt, S.C., Gauther, J.J., Tipper, D.J., 1975. Ultrastructural studies of sporulation in Bacillus sphaericus. Journal of Bacteriology 122, 1322-1338.

Iizasa, E., Mitsutomi, M., Nagano, Y., 2010. Direct binding of a plant LysM receptor-like kinase, LysM RLK1/CERK1, to chitin in vitro. The Journal of Biological Chemistry 285, 2996-3004.

Itaya, M., Kondo, K., Tanaka, T., 1989. A neomycin resistance gene cassette selectable in a single copy state in the Bacillus subtilis chromosome. Nucleic Acids Research 17, 4410.

Karow, M.L., Piggot, P.J., 1995. Construction of gusA transcriptional fusion vectors for Bacillus subtilis and their utilization for studies of spore formation. Gene 163, 69-74.

Kim, H., Hahn, M., Grabowski, P., McPherson, D.C., Otte, M.M., Wang, R., Ferguson, C.C., Eichenberger, P., Driks, A., 2006. The Bacillus subtilis spore coat protein interaction network. Molecular Microbiology 59, 487-502.

Klobutcher, L.A., Ragkousi, K., Setlow, P., 2006. The Bacillus subtilis spore coat provides "eat resistance" during phagocytic predation by the protozoan Tetrahymena thermophila. Proceedings of the National Academy of Sciences of the United States of America 103, 165-170.

Kodama, T., Takamatsu, H., Asai, K., Ogasawara, N., Sadaie, Y., Watabe, K., 2000. Synthesis and characterization of the spore proteins of Bacillus subtilis YdhD, YkuD, and YkvP, which carry a motif conserved among cell wall binding proteins. Journal of Biochemistry 128, 655-663.

Kuroda, A., Sekiguchi, J., 1990. Cloning, sequencing and genetic mapping of a Bacillus subtilis cell wall hydrolase gene. Journal of General Microbiology 136, 2209-2216.

Leo, J.C., Oberhettinger, P., Chaubey, M., Schutz, M., Kuhner, D., Bertsche, U., Schwarz, H., Gotz, F., Autenrieth, I.B., Coles, M., Linke, D., 2015. The Intimin periplasmic domain mediates dimerisation and binding to peptidoglycan. Molecular Microbiology 95, 80-100.

Liu, T., Liu, Z., Song, C., Hu, Y., Han, Z., She, J., Fan, F., Wang, J., Jin, C., Chang, J., Zhou, J.M., Chai, J., 2012. Chitin-induced dimerization activates a plant immune receptor. Science 336, 1160-1164.

Martins, L.O., Soares, C.M., Pereira, M.M., Teixeira, M., Costa, T., Jones, G.H., Henriques, A.O., 2002. Molecular and biochemical characterization of a highly stable bacterial laccase that occurs as a structural component of the Bacillus subtilis endospore coat. Journal of Biological Chemistry 277, 18849-18859.

McKenney, P.T., Driks, A., Eichenberger, P., 2013. The Bacillus subtilis endospore: assembly and functions of the multilayered coat. Nature Reviews Microbiology 11, 33-44.

McKenney, P.T., Driks, A., Eskandarian, H.A., Grabowski, P., Guberman, J., Wang, K.H., Gitai, Z., Eichenberger, P., 2010. A distance-weighted interaction map reveals a previously uncharacterized layer of the Bacillus subtilis spore coat. Current Biology 20, 934-938.

McKenney, P.T., Eichenberger, P., 2012. Dynamics of spore coat morphogenesis in Bacillus subtilis. Molecular Microbiology 83, 245-260.

Meador-Parton, J., Popham, D.L., 2000. Structural analysis of Bacillus subtilis spore peptidoglycan during sporulation. Journal of Bacteriology 182, 4491-4499.

Mesnage, S., Dellarole, M., Baxter, N.J., Rouget, J.B., Dimitrov, J.D., Wang, N., Fujimoto, Y., Hounslow, A.M., Lacroix-Desmazes, S., Fukase, K., Foster, S.J., Williamson, M.P., 2014. Molecular basis for bacterial peptidoglycan recognition by LysM domains. Nature Communications 5, 4269.

Meyer, P., Gutierrez, J., Pogliano, K., Dworkin, J., 2010. Cell wall synthesis is necessary for membrane dynamics during sporulation of Bacillus subtilis. Molecular Microbiology 76, 956-970.

Morlot, C., Uehara, T., Marquis, K.A., Bernhardt, T.G., Rudner, D.Z., 2010. A highly coordinated cell wall degradation machine governs spore morphogenesis in Bacillus subtilis. Genes & Development 24, 411-422.

Mulder, L., Lefebvre, B., Cullimore, J., Imberty, A., 2006. LysM domains of Medicago truncatula NFP protein involved in Nod factor perception. Glycosylation state, molecular modeling and docking of chitooligosaccharides

and Nod factors. Glycobiology 16, 801-809.

Mullerova, D., Krajcikova, D., Barak, I., 2009. Interactions between Bacillus subtilis early spore coat morphogenetic proteins. FEMS Microbiology Letters 299, 74-85.

Nicholson, W.L., 2002. Roles of Bacillus endospores in the environment. Cellular and Molecular Life Sciences 59, 410-416.

Nicholson, W.L., Munakata, N., Horneck, G., Melosh, H.J., Setlow, P., 2000. Resistance of Bacillus endospores to extreme terrestrial and extraterrestrial environments. Microbiology and Molecular Biology Reviews 64, 548-572.

Nicholson, W.L., Setlow, B., Setlow, P., 2002. UV photochemistry of DNA in vitro and in Bacillus subtilis spores at earth-ambient and low atmospheric pressure: implications for spore survival on other planets or moons in the solar system. Astrobiology 2, 417-425.

Nicholson, W.L., Setlow, P., 1990. Sporulation, germination and outgrowth. In: Cutting, C.R.H.a.S.M. (Ed.), Molecular biology methods for *Bacillus*. John Wiley & Sons, Ltd., Chichester, pp. 391-450.

Ohnuma, T., Onaga, S., Murata, K., Taira, T., Katoh, E., 2008. LysM domains from Pteris ryukyuensis chitinase-A: a stability study and characterization of the chitin-binding site. Journal of Biological Chemistry 283, 5178-5187.

Onaga, S., Taira, T., 2008. A new type of plant chitinase containing LysM domains from a fern (Pteris ryukyuensis): roles of LysM domains in chitin binding and antifungal activity. Glycobiology 18, 414-423.

Ozin, A.J., Costa, T., Henriques, A.O., Moran, C.P., Jr., 2001a. Alternative translation initiation produces a short form of a spore coat protein in Bacillus subtilis. Journal of Bacteriology 183, 2032-2040.

Ozin, A.J., Henriques, A.O., Yi, H., Moran, C.P., Jr., 2000. Morphogenetic proteins SpoVID and SafA form a complex during assembly of the Bacillus subtilis spore coat. Journal of Bacteriology 182, 1828-1833.

Ozin, A.J., Samford, C.S., Henriques, A.O., Moran, C.P., Jr., 2001b. SpoVID guides SafA to the spore coat in Bacillus subtilis. Journal of Bacteriology 183, 3041-3049.

Piggot, P.J., Coote, J.G., 1976. Genetic aspects of bacterial endospore formation. Bacteriological Reviews 40, 908-962.

Popham, D.L., 2002. Specialized peptidoglycan of the bacterial endospore: the

inner wall of the lockbox. Cellular and Molecular Life Sciences 59, 426-433.

Putnam, E.E., Nock, A.M., Lawley, T.D., Shen, A., 2013. SpoIVA and SipL are Clostridium difficile spore morphogenetic proteins. Journal of Bacteriology 195, 1214-1225.

Qiao, H., Krajcikova, D., Liu, C., Li, Y., Wang, H., Barak, I., Tang, J., 2012. The interactions of spore-coat morphogenetic proteins studied by single-molecule recognition force spectroscopy. Chemistry - An Asian Journal 7, 725-731.

Real, G., Fay, A., Eldar, A., Pinto, S.M., Henriques, A.O., Dworkin, J., 2008. Determinants for the subcellular localization and function of a nonessential SEDS protein. Journal of Bacteriology 190, 363-376.

Sanchez-Vallet, A., Saleem-Batcha, R., Kombrink, A., Hansen, G., Valkenburg, D.J., Thomma, B.P., Mesters, J.R., 2013. Fungal effector Ecp6 outcompetes host immune receptor for chitin binding through intrachain LysM dimerization. eLife 2, e00790.

Santo, L.Y., Doi, R.H., 1974. Ultrastructural analysis during germination and outgrowth of Bacillus subtilis spores. Journal of Bacteriology 120, 475-481.

Serrano, M., Real, G., Santos, J., Carneiro, J., Moran, C.P., Jr., Henriques, A.O., 2011. A negative feedback loop that limits the ectopic activation of a cell type-specific sporulation sigma factor of Bacillus subtilis. PLOS Genetics 7, e1002220.

Serrano, M., Vieira, F., Moran, C.P., Jr., Henriques, A.O., 2008. Processing of a membrane protein required for cell-to-cell signaling during endospore formation in Bacillus subtilis. Journal of Bacteriology 190, 7786-7796.

Setlow, P., 2006. Spores of Bacillus subtilis: their resistance to and killing by radiation, heat and chemicals. Journal of Applied Microbiology 101, 514-525.

Seyler, R.W., Jr., Henriques, A.O., Ozin, A.J., Moran, C.P., Jr., 1997. Assembly and interactions of cotJ-encoded proteins, constituents of the inner layers of the Bacillus subtilis spore coat. Molecular Microbiology 25, 955-966.

Shah, I.M., Laaberki, M.H., Popham, D.L., Dworkin, J., 2008. A eukaryotic-like Ser/Thr kinase signals bacteria to exit dormancy in response to peptidoglycan fragments. Cell 135, 486-496.

Steen, A., Buist, G., Leenhouts, K.J., El Khattabi, M., Grijpstra, F., Zomer, A.L., Venema, G., Kuipers, O.P., Kok, J., 2003. Cell wall attachment of a widely distributed peptidoglycan binding domain is hindered by cell wall

constituents. The Journal of Biological Chemistry 278, 23874-23881.

Sterlini, J.M., Mandelstam, J., 1969. Commitment to sporulation in Bacillus subtilis and its relationship to development of actinomycin resistance. Biochemical Journal 113, 29-37.

Takamatsu, H., Imamura, A., Kodama, T., Asai, K., Ogasawara, N., Watabe, K., 2000a. The yabG gene of Bacillus subtilis encodes a sporulation specific protease which is involved in the processing of several spore coat proteins. FEMS Microbiology Letters 192, 33-38.

Takamatsu, H., Kodama, T., Imamura, A., Asai, K., Kobayashi, K., Nakayama, T., Ogasawara, N., Watabe, K., 2000b. The Bacillus subtilis yabG gene is transcribed by SigK RNA polymerase during sporulation, and yabG mutant spores have altered coat protein composition. Journal of Bacteriology 182, 1883-1888.

Takamatsu, H., Kodama, T., Nakayama, T., Watabe, K., 1999. Characterization of the yrbA gene of Bacillus subtilis, involved in resistance and germination of spores. Journal of Bacteriology 181, 4986-4994.

Tipper, D.J., Linnett, P.E., 1976. Distribution of peptidoglycan synthetase activities between sporangia and forespores in sporulating cells of Bacillus sphaericus. Journal of Bacteriology 126, 213-221.

Tocheva, E.I., Lopez-Garrido, J., Hughes, H.V., Fredlund, J., Kuru, E., Vannieuwenhze, M.S., Brun, Y.V., Pogliano, K., Jensen, G.J., 2013. Peptidoglycan transformations during Bacillus subtilis sporulation. Molecular Microbiology 88, 673-686.

Vasudevan, P., Weaver, A., Reichert, E.D., Linnstaedt, S.D., Popham, D.L., 2007. Spore cortex formation in Bacillus subtilis is regulated by accumulation of peptidoglycan precursors under the control of sigma K. Molecular Microbiology 65, 1582-1594.

Wang, K.H., Isidro, A.L., Domingues, L., Eskandarian, H.A., McKenney, P.T., Drew, K., Grabowski, P., Chua, M.H., Barry, S.N., Guan, M., Bonneau, R., Henriques, A.O., Eichenberger, P., 2009. The coat morphogenetic protein SpoVID is necessary for spore encasement in Bacillus subtilis. Molecular Microbiology 74, 634-649.

Warth, A.D., Strominger, J.L., 1969. Structure of the peptidoglycan of bacterial spores: occurrence of the lactam of muramic acid. Proceedings of the National Academy of Sciences of the United States of America 64, 528-535.

Warth, A.D., Strominger, J.L., 1972. Structure of the peptidoglycan from

spores of Bacillus subtilis. Biochemistry 11, 1389-1396.

Willmann, R., Lajunen, H.M., Erbs, G., Newman, M.A., Kolb, D., Tsuda, K., Katagiri, F., Fliegmann, J., Bono, J.J., Cullimore, J.V., Jehle, A.K., Gotz, F., Kulik, A., Molinaro, A., Lipka, V., Gust, A.A., Nurnberger, T., 2011. Arabidopsis lysin-motif proteins LYM1 LYM3 CERK1 mediate bacterial peptidoglycan sensing and immunity to bacterial infection. Proceedings of the National Academy of Sciences of the United States of America 108, 19824-19829.

Yamamoto, H., Miyake, Y., Hisaoka, M., Kurosawa, S., Sekiguchi, J., 2008. The major and minor wall teichoic acids prevent the sidewall localization of vegetative DL-endopeptidase LytF in Bacillus subtilis. Molecular Microbiology 70, 297-310.

Zheng, L.B., Donovan, W.P., Fitz-James, P.C., Losick, R., 1988. Gene encoding a morphogenic protein required in the assembly of the outer coat of the Bacillus subtilis endospore. Genes & Development 2, 1047-1054.

Zilhao, R., Isticato, R., Martins, L.O., Steil, L., Volker, U., Ricca, E., Moran, C.P., Jr., Henriques, A.O., 2005. Assembly and function of a spore coat-associated transglutaminase of Bacillus subtilis. Journal of Bacteriology 187, 7753-7764.

Chapter 5

General discussion

The work presented in this thesis contributed to a better understanding on the formation of the spore coat. Our studies focused on the morphogenetic proteins SpoVID, SafA and CotE, as they assume major roles in the assembly of this protective layer.

We started by showing that a small region at the N terminus of SpoVID, that we named region E, is required for spore encasement by all the four layers of the coat. Within this region, we identified specific residues important for binding and encasement by SafA and CotE, the hubs for the inner coat and for the outer coat and crust substructures, respectively (Chapters 2 and 3). Therefore, we linked the mechanism of spore encasement to specific protein-protein interactions involving the same region of SpoVID. Direct interactions of SafA and CotE to region E appear to promote their binding to a second surface in SpoVID (Chapter 3). Moreover, analysis of single alanine substitutions within this region provides evidences that residues required for encasement by both SafA and CotE are important for coat integrity, and that the inner coat functions as an attractor for the outer coat (Chapter 3). We also investigated the role of the two cysteines of the N-terminal domain of SpoVID in oligomerization, and showed that this domain is likely to be structured (Chapter 2). Finally, we found that, contrarily to SpoVID, proper localization of SafA requires recognition of the spore peptidoglycan via LysM domain (Chapter 4). Functional analysis of this domain also indicated that formation of the coat requires cortex synthesis (Chapter 4)

Altogether, our data highlighted the importance of protein-protein interactions in coat assembly. Also, they showed a tight association between assemblies of the main spore protective layers (Chapters 3 and 4). We were able to propose an updated model for coat formation that combines the

known interactions between the main coat morphogenetic proteins (Chapter 2), and we refined some specific steps of the model in Chapters 3 and 4.

The major role of the region E of SpoVID in spore encasement

One of the main goals of this work was to investigate the mechanisms directing spore encasement. Previously, Wang *et al*., 2009 identified a small region at the N-terminal domain of SpoVID (residues 125 – 136) required for encasement by CotE. We sought to determine if this region, that we named region E, is important for encasement by other coat components as well, and if so, how does it directs the movement of several proteins around the developing spore. Our results support that region E is required for encasement by all the four layers of the coat. All the coat protein fusions to GFP or YFP tested so far encase the spore in a region E-dependent manner: SpoIVA-YFP from the basement layer; SafA-YFP, YaaH-GFP and CotP-GFP from the inner coat; CotE-YFP, YtxO-YFP, CotM-GFP and CotO-YFP from the outer coat and CotZ-GFP from the crust (Wang *et al*., 2009; Chapters 2 and 3).

We found that the hubs for the inner coat and for the outer coat and crust components, SafA and CotE, interact directly with region E (Chapters 2 and 3), linking the encasement by inner and outer coat/crust modules to specific protein interactions of their hubs to the same region of SpoVID. As region E is conserved among SpoVID orthologues, the mechanism by which this morphogenetic protein directs spore encasement may be conserved in *Bacillus* species. We assume that SafA- and CotE-dependent proteins require region E for encasement in an indirect manner; however, it must be tested if they also interact directly with SpoVID. Also, our model predicts that SpoIVA would establish a second interaction with region E of SpoVID (in addition to the demonstrated interaction with the C terminus, required for SpoVID localization) that would allow encasement by SpoIVA and its interactors within the basement layer. Yet, this second interaction remains to be mapped.

We identified specific residues within region E that are important for binding and encasement by SafA and CotE. Specifically, SafA requires residues L125, I127 and I133 of region E to interact with SpoVID and encase the spore; whereas encasement by CotE involves L125, I127 and L131, but only the last two residues have a role in a direct interaction with SpoVID (Chapters 2 and 3). Of those, L125 and I127, required for encasement by both SafA and CotE, are important for coat integrity (Chapter 3). Interestingly, all these residues are leucines or isoleucines (L125, I127, L131 and I133), suggesting that SpoVID establishes hydrophobic interactions with SafA and CotE. We cannot exclude, however, a possible role of some of these residues to the proper folding of region E, facilitating in that way binding by SafA and CotE.

Our data suggested that SafA and CotE establish single or double interactions with region E that facilitate their shuttling to another surface in SpoVID (Chapter 3). According to this, the interactions with region E would be transient, resulting in permanently available regions E to bind SafA and CotE hubs at the spore surface. However, further studies will be required to support this hypothesis. It would be important to identify the other region(s) in SpoVID that interact with SafA and CotE, as well as to determine which regions within SafA and CotE bind each SpoVID surface. In SafA, two regions of contact with SpoVID (A and B, or PYYH motif) were already described, and one of them could interact with region E (Ozin *et al.*, 2000; Costa *et al.*, 2006). It would be interesting to use peptide arrays covering the full sequences of SpoVID, SafA and CotE to virtually map all the possible regions of interaction between these three morphogenetic proteins. The data obtained would require refinement through other techniques, such as pulldown assays using truncated versions of each protein, or even peptides. Label transfer or FeBABE interaction mapping techniques, for example, can be used as alternatives. After mapping the interactions, it would be important to test their specific roles in SafA and CotE subcellular localizations.

SpoVID oligomerization as the driving force for encasement

It is possible that spore encasement could be driven by multimerization of SpoVID around the spore circumference while interacting with other coat components. In fact, we confirmed that SpoVID forms oligomers *in vitro* (Chapter 2; Ozin *et al.*, 2000; Mullerova *et al.*, 2009), and we showed that they contain disulfide bonds. The two cysteine residues within the N-terminal domain of SpoVID (C16 and C90) are not strictly required for oligomerization, although they appear to have a role in stabilization of the SpoVID oligomers *in vitro* (Chapter 2). It would be interesting to determine if other cysteine residues within the middle region or the LysM domain of SpoVID have a major contribution for oligomerization. Preliminary results indicate that none of the five cysteines of SpoVID is essential for the encasement function of this protein or for coat integrity (data not shown), yet it is possible that multiple cysteine substitutions are required to obtain a detectable phenotype.

SpoVID interacts with SpoIVA, which self-assembles in an ATP-dependent manner. Together with disulfide bond formation, this interaction may facilitate SpoVID oligomerization along with SpoIVA around the surface of the developing spore.

SafA and CotE as hubs for inner and outer coat proteins

According to the current model, SafA and CotE behave as hubs for assembly of the inner coat and of the outer coat and crust substructures, respectively. This assumption stems on the dependency of the inner and the outer coat/crust components on SafA or CotE for deposition. It is likely that the hub function of SafA is conferred by its C terminus, which coincides with the $SafA_{C30}$ form. However, the ability of SafA, $SafA_{C30}$ and CotE to interact directly with several coat proteins was not demonstrated so far.

In terms of kinetics, there are two types of hub: party hubs, which interact with most of their partners simultaneously, and date hubs, that bind

different partners at different times. Hub proteins are also classified at a structural level as singlish interface hubs, if they exhibit only one or two binding sites, or as multiple interface hubs, if they have up to three binding sites (Jeong *et al.*, 2001; Han *et al.*, 2004; Kim *et al.*, 2006b). During coat assembly, SafA, $SafA_{C30}$ and CotE presumably interact with several coat proteins. Therefore, it is conceivable that they would be party, multiple interface hubs. Intrinsic disorder would be an advantage, allowing them to acquire different conformations. In fact, according to PONDR-FIT predictions, the extended middle region of SafA and most of its C terminus, as well as the C terminus of CotE (which has a role in recruitment of the outer coat proteins; Little and Driks, 2001), are predicted to be disordered (Fig. 5.1 A and B). Further experiments will be necessary to characterize structurally these two hubs and to understand the mechanisms by which they interact with several coat proteins.

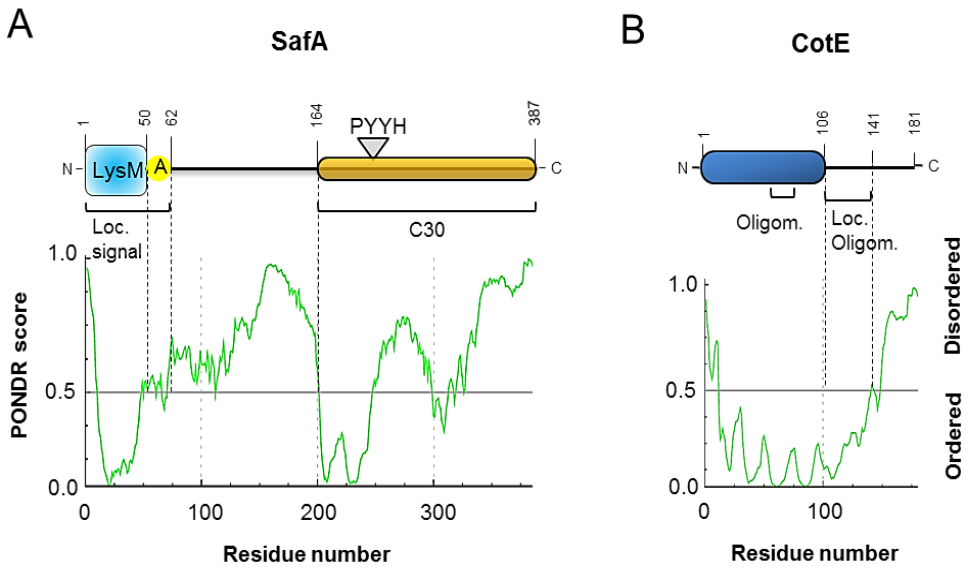

Figure 5.1 – Charts representing PONDR-FIT scores for **A)** SafA and **B)** CotE hub proteins. Scores above 0.5 indicate that the region is predicted to be disordered. The diagrams above the charts represent SafA and CotE, with the predicted domains and important regions in evidence.

SafA and CotE belong to the same kinetic class of coat proteins

The SafA-YFP fusion constructed allowed us to determine that SafA, similarly to CotE, fits in the kinetic class II of encasement (Chapter 3). As described for class II proteins, SafA-YFP and CotE-CFP start encasing the spore after engulfment completion, but before it became phase-dark, with the formation of a second cap at the mother cell distal (MCD) pole (Chapter 3; McKenney and Eichenberger, 2012). Moreover, in sporulating cells expressing simultaneously SafA-YFP and CotE-CFP, either the two signals are visible at the MCD pole or none of them is (Fig. 3.10 and Table 3.7 of Chapter 3; Fig. S2 of Appendices). This indicates that both fusions deposit at the MCD pole approximately at the same time, supporting that SafA and CotE belong to the same kinetic class.

According to the model suggested by McKenney and Eichenberger, 2012, the earlier-localizing proteins of the basement layer and the inner coat start encasing the spore in the first wave of encasement, followed by earlier-localizing proteins of the outer coat and the crust, in the second and third waves, respectively (McKenney and Eichenberger, 2012; McKenney *et al.*, 2013). However, the classification of SafA as a class II protein implies that the inner coat initiates encasement simultaneously with the outer coat, in the second wave, and not with the basement layer. Importantly, this does not reject the model of spore encasement by multiple co-ordinated waves.

McKenney and Eichenberger, 2012 classified two SafA-dependent, inner coat protein fusions, YaaH-GFP and YuzC-GFP, as belonging to the kinetic class I. Our data supports that localization of YaaH-GFP matches the class I, and we suggested that it is may be related with the presence of two LysM domains in this protein (that were shown to be sufficient to localize a β-lactamase at the spore;(Kodama *et al.*, 2000). It would be important to define if there are other SafA-dependent proteins that match the class I, including YuzC, and to investigate if they have other localization determinants in addition to SafA.

The LysM modules of SpoVID and SafA as localization determinants

Both SpoVID and SafA comprise a LysM motif linked to the remaining protein by a region essential for localization (Costa *et al.*, 2006; Wang *et al.*, 2009). Wang *et al*., 2009 showed that in SpoVID, the LysM domain is part of the localization signal. Now we found that, similarly to SpoVID, the deposition of SafA also requires LysM (Chapter 4). Thus, SafA has at least three localization determinants: SpoIVA (for initial targeting), SpoVID (for encasement), and spore peptidoglycan, recognized by the LysM domain.

We identified five conserved, surface-exposed residues in the LysM domain of SafA that are involved in SafA-YFP subcellular localization and spore peptidoglycan recognition *in vitro*, and we found that SafA-YFP requires the cortex to completely encircle the spore, or for maintenance at the spore surface, at later stages (Chapter 4). Two of the residues (D10 and N30) are required for localization of SafA before synthesis of the cortex (Meador-Parton and Popham, 2000). This raised two hypothesis: either D10 and N30 are required for recognition of peptidoglycan other than the cortex (or peptidoglycan precursors accumulating during engulfment) at initial stages of SafA deposition, or these two residues are indirectly important for interaction with the other localization determinants of SafA. The continuous presence of peptidoglycan around the prespore along engulfment (Tocheva *et al.*, 2013), together with the conservation of D10 and N30 in other LysM motifs, are in line with the first hypothesis. However, we favour the second possibility at least for N30, because the substitution of this residue for an alanine led to a minor reduction in the ability of $LysM^{SafA}$-GFP-StrepTagII to bind peptidoglycan *in vitro* (only 13%, Chapter 4). However, further experiments will be required to clarify this.

Residues S11, L12 and I39 are important for SafA-YFP localization at later stages, where the cortex is already present in the spore (Chapter 4). We assume that SafA binds to the cortex during sporulation in a S11, L12 and I39 dependent manner, but further studies will be needed to confirm it. It would

be important to determine if LysM^{SafA} also binds non-purified peptidoglycan, as it is displayed in the spore, and if it distinguishes between cortex and primordial germ-cell wall peptidoglycan. Also, it must be confirmed that the mislocalization of SafA in *spoVE* null mutant cells is due to the absence of the cortex. This could be attained by looking at the subcellular localization of SafA-YFP in other mutant backgrounds with defects in cortex assembly, such as in *ybaN* null mutant cells.

According to this, SafA has to reach the peptidoglycan layers of the spore for proper localization. However, at least at initial stages of spore development, these layers are enclosed by the outer forespore membrane that separates them from the coat. It is not known if this membrane retains its integrity at later stages of sporulation (Setlow, 2014). Since there is no evidence of a secretion signal in SafA, one possibility is that this protein would only reach the peptidoglycan layers of the spore at later stages, at a time where the outer forespore membrane would be absent. If so, the role of the LysM^{SafA} in localization at initial stages of spore development may rely on binding to peptidoglycan precursors that accumulate on the mother cell side of the outer forespore membrane, or in assisting on the interaction with other localization determinants of SafA, as previously discussed. Another possibility is that SafA may be transported across the membrane via non-classical secretion. This type of protein secretion independent of typical signal peptides is relatively common in bacteria (Tjalsma *et al.*, 2004; Bendtsen *et al.*, 2005). Several characteristics, such as disordered regions, have been associated to proteins that are translocated this way, leading to the development of the non-classical protein secretion predictor SecretomeP 2.0 (http://www.cbs.dtu.dk/services/SecretomeP/, Bendtsen *et al.*, 2005). According to this algorithm, that SafA harbours the characteristics to be secreted in a signal independent manner.

The LysM domain of SpoVID is required for localization (Wang *et al.*, 2009), yet it does not recognize spore peptidoglycan *in vitro* in the same

experimental conditions as the LysM^{SafA}. This is in line with the insensibility of SpoVID-GFP to the absence of *spoVE* for localization. Nevertheless, we do not exclude the possibility that the LysM domain of SpoVID recognizes spore peptidoglycan under other experimental conditions. For example, it may require the context of the full-length protein, higher order glycan polymers, peptidoglycan-associated molecules that were removed by purification, or stretched glycan strands in intact cells for an efficient binding. Also, the pH in the binding assay may influence the interaction, as at least some LysMs bind glycan strands in a pH-dependent manner (Buist *et al.*, 2008; Leo *et al.*, 2015). In fact, the LysM domain of SpoVID has an isoelectric point below the average (4.2, comparing to 5 – 10; Buist *et al.*, 2008), indicating that it may require a lower pH to bind glycan strands. If so, peptidoglycan recognition at lower pHs may be an adaptation to changing pHs in different environments (Buist *et al.*, 2008; Leo *et al.*, 2015).

Moreover, it is possible that the two cysteine residues within the LysM domain of SpoVID, which are present in *B. subtilis* and related species but are not conserved among other LysM domains (Figs. 4.1 A and 4.10), may establish a disulfide bond that compromises the ability to recognize glycans. However, preliminary results indicate that single or double alanine substitutions of these residues did not restore the capacity of the domain to bind peptidoglycan or chitin *in vitro* (data not shown). Another residue that could be responsible for the glycan insensibility of LysM^{SpoVID} is the glutamic acid E530, in the loop between the first β-strand and the first α-helix. Commonly, there is a glycine at this position (Fig. 4.1 A); therefore, the replacement for a glutamic acid may result in less flexibility, altering the typical LysM fold. To clarify this, it would be useful to solve the structure of this domain, in order to compare it with the available structures of other LysM motifs.

Also, it would be interesting to determine if the LysM domain of SipL, the functional analogue of SpoVID in *C. difficile*, recognizes peptidoglycan.

Four of the residues required for peptidoglycan binding in SafA are identical or similar in the LysM domain of SipL. Moreover, this domain appears to have a different behavior comparing to LysM^{SpoVID}, as it interacts with SpoIVA (Putnam *et al.*, 2013).

The interdependency on assembly of the spore protective layers

The cortex, the inner coat and the outer coat have been considered as largely independent modules for assembly (Piggot and Coote, 1976; Henriques and Moran, 2007). This is supported by electron microscopy images of several mutants that miss exclusively one of these layers (Piggot and Coote, 1976; Zheng *et al.*, 1988; Takamatsu *et al.*, 1999). Furthermore, the absence of the hub of the inner coat proteins, SafA, does not interfere with the deposition of the hub for the outer coat and crust proteins, CotE, and *vice-versa* (Chapter 3). However, the localization of some inner coat proteins is affected in *cotE* null mutants, as well as the localization of some outer coat components in cells missing *safA* (Zheng *et al.*, 1988; Ozin *et al.*, 2000; Kim *et al.*, 2006a; Henriques and Moran, 2007), suggesting an interdependency between these structures for assembly. Our results are in agreement with this, as we have seen that the inner coat functions as an attractor for CotE, presumably facilitating the assembly of the outer coat, and in turn, the outer coat helps restricting the inner coat proteins at the spore surface (Chapter 3).Also,(Ebmeier *et al.*, 2012)showed that the formation of the cortex only begins after initiation of coat assembly, and in Chapter 4 we showed that SafA localization, and consequently proper inner coat assembly, requires the presence of the cortex. Therefore, our work highlighted that, although the cortex, the inner coat and the outer coat modules are mainly independent, their morphogenesis is tightly connected.

An updated model for spore coat assembly

Our work reinforced that coat formation relies on protein-protein

interactions. In particular, we revealed that the region of SpoVID involved in encasement interacts directly with the morphogenetic proteins required for assembly of the inner coat, the outer coat and the crust sublayers (Chapters 2 and 3). This allowed us to propose a general model for coat assembly that integrates all the known interactions between the main morphogenetic proteins (Chapter 2). Then, we went further on some specific details of the model, specifically on the interactions of SafA and CotE with SpoVID (Chapter 3) and on the role of spore peptidoglycan in SafA localization (Chapter 4). In this model, evidences for direct interactions of SpoIVA with CotE and with the region E of SpoVID are currently missing. Also, as mentioned before, it remains to be identified the second surface of interaction with SafA and CotE in SpoVID.

According to the current model, SpoIVA is required for initial targeting of coat proteins at the spore surface (Wang *et al.*, 2009). However, in the absence of SpoIVA, some of the coat protein-GFP fusions analyzed so far are still able localize as a dot at the MCP pole of the spore. What guides coat proteins for that localization remains to be identified. We discarded a possible involvement of the spore peptidoglycan, as SafA variants with substitutions that decrease the ability to recognize it still accumulate as a dot at the spore surface.

Another aspect that required further investigation is the mechanism by which SpoVM promotes encasement along with SpoVID. SpoVM is required for encasement by all the coat protein fusions tested to date, and is located upstream of SpoVID in the hierarchy of genetic dependencies for coat assembly (Wang *et al*., 2009; Fig 1.4 of Chapter 1). However, a direct interaction between those proteins was not reported so far. It is possible that SpoVM may be required for triggering a conformational change in region E of SpoVID, or for favouring SpoIVA and/or SpoVID multimerization around the spore circumference.

Finally, our results supported that SafA and SpoVID localize at the

cortex/coat interface, but the distribution of CotE in the spore was not clear. Therefore, it would be interesting to determine the dynamics of CotE localization across the spore protective layers along sporulation.

In summary, we went deeper in the mechanisms governing spore coat assembly. Several important aspects were clarified, allowing us to propose a unifying model. However, many questions remain to be answered. We believed that the results we presented in this dissertation will have a significant impact not only in the study of spore development, but also in the comprehension of the assembly of supramolecular structures *in vivo*.

REFERENCES

Bendtsen, J.D., Kiemer, L., Fausboll, A., Brunak, S., 2005. Non-classical protein secretion in bacteria. BMC Microbiology 5, 58.

Buist, G., Steen, A., Kok, J., Kuipers, O.P., 2008. LysM, a widely distributed protein motif for binding to (peptido)glycans. Molecular Microbiology 68, 838-847.

Costa, T., Isidro, A.L., Moran, C.P., Jr., Henriques, A.O., 2006. Interaction between coat morphogenetic proteins SafA and SpoVID. Journal of Bacteriology 188, 7731-7741.

Ebmeier, S.E., Tan, I.S., Clapham, K.R., Ramamurthi, K.S., 2012. Small proteins link coat and cortex assembly during sporulation in Bacillus subtilis. Molecular Microbiology 84, 682-696.

Han, J.D., Bertin, N., Hao, T., Goldberg, D.S., Berriz, G.F., Zhang, L.V., Dupuy, D., Walhout, A.J., Cusick, M.E., Roth, F.P., Vidal, M., 2004. Evidence for dynamically organized modularity in the yeast protein-protein interaction network. Nature 430, 88-93.

Henriques, A.O., Moran, C.P., Jr., 2007. Structure, assembly, and function of the spore surface layers. Annual Review of Microbiology 61, 555-588.

Jeong, H., Mason, S.P., Barabasi, A.L., Oltvai, Z.N., 2001. Lethality and centrality in protein networks. Nature 411, 41-42.

Kim, H., Hahn, M., Grabowski, P., McPherson, D.C., Otte, M.M., Wang, R., Ferguson, C.C., Eichenberger, P., Driks, A., 2006a. The Bacillus subtilis spore coat protein interaction network. Molecular Microbiology 59, 487-502.

Kim, P.M., Lu, L.J., Xia, Y., Gerstein, M.B., 2006b. Relating three-dimensional structures to protein networks provides evolutionary insights. Science 314, 1938-1941.

Kodama, T., Takamatsu, H., Asai, K., Ogasawara, N., Sadaie, Y., Watabe, K., 2000. Synthesis and characterization of the spore proteins of Bacillus subtilis YdhD, YkuD, and YkvP, which carry a motif conserved among cell wall binding proteins. Journal of Biochemistry 128, 655-663.

Leo, J.C., Oberhettinger, P., Chaubey, M., Schutz, M., Kuhner, D., Bertsche, U., Schwarz, H., Gotz, F., Autenrieth, I.B., Coles, M., Linke, D., 2015. The Intimin periplasmic domain mediates dimerisation and binding to peptidoglycan. Molecular Microbiology 95, 80-100.

Little, S., Driks, A., 2001. Functional analysis of the Bacillus subtilis morphogenetic spore coat protein CotE. Molecular Microbiology 42, 1107-1120.

McKenney, P.T., Driks, A., Eichenberger, P., 2013. The Bacillus subtilis endospore: assembly and functions of the multilayered coat. Nature Reviews Microbiology 11, 33-44.

McKenney, P.T., Eichenberger, P., 2012. Dynamics of spore coat morphogenesis in Bacillus subtilis. Molecular Microbiology 83, 245-260.

Meador-Parton, J., Popham, D.L., 2000. Structural analysis of Bacillus subtilis spore peptidoglycan during sporulation. Journal of Bacteriology 182, 4491-4499.

Mullerova, D., Krajcikova, D., Barak, I., 2009. Interactions between Bacillus subtilis early spore coat morphogenetic proteins. FEMS Microbiology Letters 299, 74-85.

Ozin, A.J., Henriques, A.O., Yi, H., Moran, C.P., Jr., 2000. Morphogenetic proteins SpoVID and SafA form a complex during assembly of the Bacillus subtilis spore coat. Journal of Bacteriology 182, 1828-1833.

Piggot, P.J., Coote, J.G., 1976. Genetic aspects of bacterial endospore formation. Bacteriological Reviews 40, 908-962.

Putnam, E.E., Nock, A.M., Lawley, T.D., Shen, A., 2013. SpoIVA and SipL are Clostridium difficile spore morphogenetic proteins. Journal of Bacteriology 195, 1214-1225.

Setlow, P., 2014. Germination of spores of Bacillus species: what we know and do not know. Journal of Bacteriology 196, 1297-1305.

Takamatsu, H., Kodama, T., Nakayama, T., Watabe, K., 1999. Characterization of the yrbA gene of Bacillus subtilis, involved in resistance and germination of spores. Journal of Bacteriology 181, 4986-4994.

Tjalsma, H., Antelmann, H., Jongbloed, J.D., Braun, P.G., Darmon, E., Dorenbos, R., Dubois, J.Y., Westers, H., Zanen, G., Quax, W.J., Kuipers, O.P., Bron, S., Hecker, M., van Dijl, J.M., 2004. Proteomics of protein secretion by Bacillus subtilis: separating the "secrets" of the secretome. Microbiology and Molecular Biology Reviews 68, 207-233.

Tocheva, E.I., Lopez-Garrido, J., Hughes, H.V., Fredlund, J., Kuru, E., Vannieuwenhze, M.S., Brun, Y.V., Pogliano, K., Jensen, G.J., 2013. Peptidoglycan transformations during Bacillus subtilis sporulation. Molecular Microbiology 88, 673-686.

Wang, K.H., Isidro, A.L., Domingues, L., Eskandarian, H.A., McKenney, P.T., Drew, K., Grabowski, P., Chua, M.H., Barry, S.N., Guan, M., Bonneau, R., Henriques, A.O., Eichenberger, P., 2009. The coat morphogenetic protein SpoVID is necessary for spore encasement in Bacillus subtilis. Molecular Microbiology 74, 634-649.

Zheng, L.B., Donovan, W.P., Fitz-James, P.C., Losick, R., 1988. Gene encoding a morphogenic protein required in the assembly of the outer coat of the Bacillus subtilis endospore. Genes & Development 2, 1047-1054.

Appendices

Table A1 lists the *B. subtilis* spore coat proteins identified so far, grouped by coat sublayer. Also, their relevant characteristics (molecular weight, transcriptional regulation, kinetic class, phenotype of the null mutant, assembly requirements and conservation among sporeformers) are indicated.

Tables A2 – A7 list the vectors and oligonucleotides used during the course of the work presented in this dissertation.

Figures S1 and S2 support Chapter 3, whereas Figure S3 supports Chapter 4. Figure S1 shows the subcellular localization of SafA-YFP in strains missing *spoVID* or expressing the various *spoVID* alleles with alanine substitutions in region E residues. Figure S2 illustrates the subcellular localization of SafA-YFP and CotE-CFP in mutant strains expressing both fusions. Figure S3 shows the localization of SafA-YFP variants with alanines substitutions in residues within the LysM domain, both in wild type and in *spoVE* null mutant backgrounds.

Table A1: list of known spore coat proteins in *B. subtilis*

	MW (kDa)	Transcriptional regulation	Class	Null mutant relevant phenotype	Assembly requirements	Relevant features	Conservation	Refs.
Basement layer proteins								
SpoVM	3	σ^E,	I	- Absence of cortex; - Altered coat.	SpoIVA, SpoVID	- Morphogenetic protein essential for coat and cortex formation; - amphipathic α-helix; - Required for localization of all coat protein fusions tested.	Some Bacillaceae	Henriques and Moran, 2007; Levin *et al.*, 1993; McKenney and Eichenberger, 2012; McKenney *et al.*, 2010; Ramamurthi *et al.*, 2009; Steil *et al.*, 2005; Wang *et al.*, 2009
SpoIVA	55	σ^E, SpoIIID(-)	I	- Absence of cortex; - Misassembled coat; - Heat and lysozyme sensitivity.	SpoVM, SpoVID	- Morphogenetic protein essential for coat and cortex formation; - ATPase; - Required for localization of all coat protein fusions tested.	All endospore formers	Eichenberger *et al.*, 2004; Henriques and Moran, 2007; McKenney and Eichenberger, 2012; McKenney *et al.*, 2010; Roels *et al.*, 1992; Steil *et al.*, 2005; Wang *et al.*, 2009
SpoVID	64	σ^E	I	- Misassembled coat; - Heat and lysozyme sensitivity.	SpoIVA	- Morphogenetic protein; - Required for localization of all coat protein fusions tested; - Contains a LysM domain.	Most Bacillaceae	Beall *et al.*, 1993; Henriques and Moran, 2007; McKenney and Eichenberger, 2012; McKenney *et al.*, 2010; Steil *et al.*, 2005; Wang *et al.*, 2009
YhaX	32	σ^E, SpoIIID(-)	I	–	SpoIVA	- Haloacid dehydrogenase family.	All Bacillaceae and most *Clostridium* species	Eichenberger *et al.*, 2004; Henriques and Moran, 2007; McKenney *et al.*, 2013; McKenney and Eichenberger, 2012; McKenney *et al.*, 2010; Steil *et al.*, 2005
YheD	51	σ^E, SpoIIID	II	–	SpoIVA	–	Some Bacillaceae	Henriques and Moran, 2007; McKenney *et al.*, 2013; McKenney and Eichenberger, 2012; Steil *et al.*, 2005
YcsK/ LipC	23	σ^K, GerE	V	–	SpoIVA	- Phospholipase; - Essential for germination.	Most Bacillaceae and *Clostridium* species	Henriques and Moran, 2007; Masayama *et al.*, 2007; McKenney and Eichenberger, 2012; Steil *et al.*, 2005
YjzB	8	σ^K, GerE	V	–	SpoIVA	–	Some Bacillaceae	Eichenberger *et al.*, 2004; McKenney and Eichenberger, 2012

Table A1: list of known spore coat proteins in *B. subtilis* (cont.)

	MW (kDa)	Transcriptional regulation	Class	Null mutant relevant phenotype	Assembly requirements	Relevant features	Conservation	Refs.
YppG	14	σ^K, GerE(-)	V	–	SpoIVA	–	Most Bacillaceae	Eichenberger *et al.*, 2004; Henriques and Moran, 2007; McKenney and Eichenberger, 2012
CotJC	21	σ^E, SpoIIID	–	–	CotJA	- Putative manganese-dependent catalase.	All endospore formers	Henriques *et al.*, 1995; Henriques and Moran, 2007; Seyler *et al.*, 1997
Inner coat proteins								
SafA/ YrbA	43	σ^E	–	- Absence of IC and reduced OC; - Lysozyme sensitivity; - Deficient germination.	SpoVID	- Morphogenetic protein essential for IC assembly; - Contains a LysM domain; - In the cortex/coat interface.	Most Bacillaceae	Costa *et al.*, 2006; Henriques and Moran, 2007; Takamatsu *et al.*, 1999
YaaH/ SleL	48	σ^E, SpoIIID(-)	I	- Deficient germination.	SafA, CotE	- N-acetylglucosaminidase; - Contains 2 LysM domains; - Involved in spore resistance and germination.	All Bacillaceae and most *Clostridium* species	Buist *et al.*, 2008; Eichenberger *et al.*, 2004; Henriques and Moran, 2007; Little and Driks, 2001; McKenney and Eichenberger, 2012; McKenney *et al.*, 2010
YuzC	14	σ^E	I	–	SafA	–	Some Bacillaceae	Henriques and Moran, 2007; McKenney and Eichenberger, 2012; McKenney *et al.*, 2010; Steil *et al.*, 2005
YhjR	17	σ^E, σ^K, GerE(-)	II	–	SafA	–	Most Bacillaceae	Eichenberger *et al.*, 2004; Henriques and Moran, 2007; McKenney and Eichenberger, 2012
YisY	30	σ^E, σ^G, σ^K, GerE(-)	III	–	SafA	- Hydrolase.	Most Bacillaceae	Eichenberger *et al.*, 2004; Henriques and Moran, 2007; McKenney and Eichenberger, 2012
YsxE	40	σ^E	III	–	SafA	- Gene downstream *spoVID*, in the same operon.	Most Bacillaceae and some *Clostridium* species	Beall *et al.*, 1993; Henriques and Moran, 2007; McKenney and Eichenberger, 2012; Steil *et al.*, 2005

Table A1: list of known spore coat proteins in *B. subtilis* (cont.)

	MW (kDa)	Transcriptional regulation	Class	Null mutant relevant phenotype	Assembly requirements	Relevant features	Conservation	Refs.
YutH	40	σ^E, SpoIIID(-)	III	–	SafA	–	All Bacillaceae and most *Clostridium* species	Eichenberger *et al.*, 2004; Henriques and Moran, 2007; McKenney and Eichenberger, 2012
CwlJ	16	σ^E, SpoIIID, σ^K	III	- Deficient germination.	SafA, CotE, GerQ	- Cell wall hydrolase.	All endospore formers	Henriques and Moran, 2007; McKenney and Eichenberger, 2012; Ragkousi *et al.*, 2003; Steil *et al.*, 2005
Tgl	28	σ^E, σ^K, GerE(-)	III	–	SafA, CotE	- Transglutaminase, cross-linking coat components.	Most Bacillaceae	Henriques and Moran, 2007; McKenney and Eichenberger, 2012; Steil *et al.*, 2005; Zilhao *et al.*, 2005
CotD	8	σ^K, GerE, SpoIIID(-)	VI	–	SafA	–	Most Bacillaceae	Henriques and Moran, 2007; McKenney and Eichenberger, 2012; McKenney *et al.*, 2010; Steil *et al.*, 2005
CotT	12	σ^E, SpoIIID, σ^K, GerE(-)	IV	- Altered IC; - Deficient germination.	SafA	–	Only *B. subtilis*	Bourne *et al.*, 1991; Henriques and Moran, 2007; McKenney and Eichenberger, 2012; McKenney *et al.*, 2010; Steil *et al.*, 2005
YsnD	11	σ^E, σ^K, GerE(-)	IV	–	SafA	–	Only *B. subtilis*	Henriques and Moran, 2007; McKenney and Eichenberger, 2012; Steil *et al.*, 2005
YybI	29	σ^E	IV	–	SafA	–	Some Bacillaceae and *Clostridium* species	Henriques and Moran, 2007; McKenney and Eichenberger, 2012; Steil *et al.*, 2005
CotP	16	σ^K, GerE(-)	V	–	SafA	–	Some Bacillaceae	Henriques and Moran, 2007; McKenney and Eichenberger, 2012; Steil *et al.*, 2005
CotS	40	σ^K, GerE	V	–	CotE, CotH	- Controls assembly of CotSA.	Most Bacillaceae and *Clostridium* species	Henriques and Moran, 2007; McKenney and Eichenberger, 2012; McKenney *et al.*, 2010; Steil *et al.*, 2005; Takamatsu *et al.*, 1998
OxdD/ YoaN	43	σ^K, GerE(-)	V	–	SafA, CotE	- Oxalate decarboxylase involved in resistance against noxious chemicals.	Some Bacillaceae	Costa *et al.*, 2004; Henriques and Moran, 2007; McKenney and Eichenberger, 2012

Table A1: list of known spore coat proteins in *B. subtilis* (cont.)

	MW (kDa)	Transcriptional regulation	Class	Null mutant relevant phenotype	Assembly requirements	Relevant features	Conservation	Refs.
YeeK	15	σ^K, GerE	V	–	SafA, CotE	–	Only *B. subtilis*	Henriques and Moran, 2007; Imamura *et al.*, 2010; McKenney and Eichenberger, 2012; Takamatsu *et al.*, 2009
YmaG	13	σ^K, GerE	V	–	SafA	–	Only *B. subtilis*	Henriques and Moran, 2007; Imamura *et al.*, 2010; McKenney and Eichenberger, 2012; Steil *et al.*, 2005
YqjC	15	σ^K, GerE(-)	V	–	SafA	- Putative lyase.	Some Bacillaceae and *Clostridium* species	Eichenberger *et al.*, 2004; McKenney and Eichenberger, 2012
YxeE	14	σ^K, GerE	V	–	SafA	–	Some Bacillaceae	Henriques and Moran, 2007; Kuwana *et al.*, 2007; McKenney and Eichenberger, 2012; Steil *et al.*, 2005
CotF	18	σ^K, SpoIIID	–	–	–	–	Most Bacillaceae and some *Clostridium* species	Henriques and Moran, 2007; Imamura *et al.*, 2010; Steil *et al.*, 2005
CotH	42	σ^K, GerE(-)	–	- Altered coat.	CotE, GerE	- Morphogenetic protein required for IC and OC assembly; - In the interface between IC and OC.	Some Bacillaceae	Henriques and Moran, 2007; Steil *et al.*, 2005; Zilhao *et al.*, 1999
CotJA	9	σ^E, SpoIIID	–	–	CotJC	- May either be a component of the basement layer.	Some Bacillaceae	Henriques *et al.*, 1995; Henriques and Moran, 2007; Seyler *et al.*, 1997
CotJB	11	σ^E, SpoIIID	–	–	–	- May either be a component of the basement layer.	Some Bacillaceae and *Clostridium* species	Henriques *et al.*, 1995; Henriques and Moran, 2007
GerQ	20	σ^E	–	- Deficient germination.	CotE, Tgl, SpoIVA	- Controls assembly of CwlD; - Essential for germination by $Ca2^+$.	Most Bacillaceae	Henriques and Moran, 2007; Imamura *et al.*, 2010; Ragkousi *et al.*, 2003; Steil *et al.*, 2005

Table A1: list of known spore coat proteins in *B. subtilis* (cont.)

	MW (kDa)	Transcriptional regulation	Class	Null mutant relevant phenotype	Assembly requirements	Relevant features	Conservation	Refs.
Outer coat proteins								
CotE	20	σ^E, SpoIIID, σ^K, GerE(-)	II	- Misassembled OC; - Lysozyme sensitivity; - Deficient germination.	SpoIVA, SpoVID, CotH	- Morphogenetic protein essential for OC and crust assembly; - In the interface between the IC and the OC.	Most Bacillaceae	Costa *et al.*, 2007; Henriques and Moran, 2007; McKenney and Eichenberger, 2012; Qiao *et al.*, 2013; Zheng *et al.*, 1988
CotM	15	σ^E, σ^K, GerE(-)	II	- Altered OC; - Reduced CotC amounts.	CotE	–	Most Bacillaceae, some *Clostridium* species	Eichenberger *et al.*, 2004; Henriques *et al.*, 1997; Henriques and Moran, 2007; McKenney and Eichenberger, 2012; McKenney *et al.*, 2010
CotO/ YjbX	25	σ^E	II	- Altered coat.	CotE	- Morphogenetic protein essential for coat formation and coat surface topology.	Most Bacillaceae	Henriques and Moran, 2007; McKenney and Eichenberger, 2012; McKenney *et al.*, 2010; McPherson *et al.*, 2005; Steil *et al.*, 2005
YknT/ Cse15	37	σ^E, SpoIIID	II	–	CotE	–	Some Bacillaceae	Henriques and Moran, 2007; McKenney and Eichenberger, 2012; Steil *et al.*, 2005
YncD	43	σ^E	II	–	CotE	- Alanine racemase.	All endospore formers	McKenney *et al.*, 2013; McKenney and Eichenberger, 2012; Pierce *et al.*, 2008; Steil *et al.*, 2005
CotA	58	σ^K, GerE(-)	V	- Pigmentation defect.	CotE	- Laccase; - Controls pigmentation; - UV resistance.	Most Bacillaceae and some *Clostridium* species	Eichenberger *et al.*, 2004; Henriques and Moran, 2007; Hullo *et al.*, 2001; McKenney and Eichenberger, 2012; McKenney *et al.*, 2010
CotB	43	σ^E, σ^K, GerE, GerR	V	–	CotE, CotG, CotH	–	Some Bacillaceae	Henriques and Moran, 2007; McKenney and Eichenberger, 2012; Steil *et al.*, 2005; Zilhao *et al.*, 2004
CotQ/ YvdP	49	σ^E, σ^K, GerE	V	–	CotE, CotG, CotH	–	Some Bacillaceae	Henriques and Moran, 2007; Kim *et al.*, 2006a; McKenney and Eichenberger, 2012; Steil *et al.*, 2005

Table A1: list of known spore coat proteins in *B. subtilis* (cont.)

	MW (kDa)	Transcriptional regulation	Class	Null mutant relevant phenotype	Assembly requirements	Relevant features	Conservation	Refs.
YlbD	15	σ^K, GerE	V	–	CotE	–	Most Bacillaceae	Henriques and Moran, 2007; McKenney and Eichenberger, 2012; Steil *et al.*, 2005
YtxO	16	σ^K, GerE	V	–	CotE	–	Only *B. subtilis*	Henriques and Moran, 2007; Imamura *et al.*, 2010; McKenney and Eichenberger, 2012; McKenney *et al.*, 2010; Steil *et al.*, 2005
CotU	11	σ^K, GerE, GerR(-)	VI	–	CotE, CotH, CotC, CotG	- Morphogenetic protein.	Only *B. subtilis*	Henriques and Moran, 2007; Isticato *et al.*, 2008; McKenney and Eichenberger, 2012
CotC	14	σ^K, GerE, SpoIIID(-)	–	–	CotE, CotH, CotU	–	Only *B. subtilis*	Henriques and Moran, 2007; Ichikawa and Kroos, 2000; Imamura *et al.*, 2010; Isticato *et al.*, 2008
SpsB	54	σ^K, GerE	–	–	CotE	- Involved in spore coat polysaccharide synthesis.	Some Bacillaceae	Cangiano *et al.*, 2014
Crust proteins								
CotX	18	σ^K, GerE, SpoIIID(-)	–	- Absence of crust; - Faster germination.	–	- Morphogenetic protein essential for the formation of the crust.	Most Bacillaceae	Henriques and Moran, 2007; McKenney *et al.*, 2010; Zhang *et al.*, 1994
CotY	17	σ^K, GerE, GerR	–	- Absence of crust; - Faster germination.	CotZ	- Morphogenetic protein essential for the formation of the crust.	Most Bacillaceae	Henriques and Moran, 2007; Imamura *et al.*, 2011; McKenney *et al.*, 2010; Zhang *et al.*, 1994
CotZ	16	σ^E, σ^K, GerE	III	- Absence of crust; - Faster germination.	CotE, CotH	- Morphogenetic protein essential for the formation of the crust.	Most Bacillaceae	Henriques and Moran, 2007; McKenney and Eichenberger, 2012; McKenney *et al.*, 2010; Zhang *et al.*, 1994
CotG	23	σ^E, σ^K, GerE	V	–	CotE, CotH	–	Only *B. subtilis*	Henriques and Moran, 2007; McKenney and Eichenberger, 2012; McKenney *et al.*, 2010; Steil *et al.*, 2005; Zilhao *et al.*, 2004

Table A1: list of known spore coat proteins in *B. subtilis* (cont.)

	MW (kDa)	Transcriptional regulation	Class	Null mutant relevant phenotype	Assembly requirements	Relevant features	Conservation	Refs.
CotW	12	σ^E, SpoIIID, σ^K, GerE	V	–	CotE, CotX, CotY, CotZ	–	Some Bacillaceae	Henriques and Moran, 2007; McKenney and Eichenberger, 2012; McKenney *et al.*, 2010; Zhang *et al.*, 1994
CotV	14	σ^K, GerE	–	–	CotW, CotX	–	Some Bacillaceae	Henriques and Moran, 2007; Imamura *et al.*, 2011; Zhang *et al.*, 1994
CgeA	14	σ^K, GerE	–	–	CotX	- Crust maturation.	Some Bacillaceae	Imamura *et al.*, 2011; Roels and Losick, 1995
Non-assigned coat proteins								
CgeB	36	σ^K, GerE	–			- Maturation of the crust.	Some Bacillaceae	Roels and Losick, 1995
CgeC	11	σ^K, GerE	–			- Maturation of the crust.	Some Bacillaceae	Roels and Losick, 1995
CgeD	49	σ^K, GerE	–			- Maturation of the crust; - Putative glycosyltransferase.	Some Bacillaceae	Roels and Losick, 1995
CgeE	29	σ^K, GerE	–			- Maturation of the crust; - Putative N-acetyltransferase.	Some Bacillaceae	Roels and Losick, 1995
CmpA	5	σ^E, SpoIIID	–	- Faster sporulation.	SpoVM	- Cortex morphogenetic protein.	All endospore formers	Ebmeier *et al.*, 2012
CotI/ YtaA	41	σ^K	–	- Altered coat.	CotE	- Putative kinase.	All endospore formers	Henriques and Moran, 2007; Scheeff *et al.*, 2010; Steil *et al.*, 2005
CotR/ YvdO	35	σ^K	–	–	CotE	- Lipolytic enzyme.	Only *B. subtilis*	Henriques and Moran, 2007; Kato *et al.*, 2010; Steil *et al.*, 2005

Table A1: list of known spore coat proteins in *B. subtilis* (cont.)

	MW (kDa)	Transcriptional regulation	Class	Null mutant relevant phenotype	Assembly requirements	Relevant features	Conservation	Refs.
CotSA/ YtxN	42	σ^K	–	–	CotE, CotH, CotS	- Putative glycosyltransferase,	All endospore formers	Henriques and Moran, 2007; Steil *et al.*, 2005
GerT	18	σ^K, GerE(-)	–	- Deficient germination.	CotE	- Involved in spore germination	Most Bacillaceae	Ferguson *et al.*, 2007
YabG	33	σ^K	–	- Altered coat.	SpoIVA	- Protease involved in maturation of coat proteins (SpoIVA, SafA and GerQ); - May associate transiently with the forespore coat.	All endospore formers	Henriques and Moran, 2007; Takamatsu *et al.*, 2000a; Takamatsu *et al.*, 2000b
YabQ	24	σ^E	–	- Absence of cortex; - Altered coat; - Heat, lysozyme and chloroform sensitivity.	–	– May localize in the outer forespore membrane	Most Bacillaceae and *Clostridium* species	Asai *et al.*, 2001; Henriques and Moran, 2007
YckK/ TcyA	29	–	–	–	–	- Component of cysteine ABC transporters.	All endospore formers	Henriques and Moran, 2007; Zilhao *et al.*, 2005
YdhD	48	σ^E	–	–	–	- Putative peptidoglycan hydrolase; - Contains a LysM domain, thus probably localizes in the inner layers.	All Bacillaceae and most *Clostridium* species	Henriques and Moran, 2007; Kodama *et al.*, 2000
YgaK	40	–	–	–	–	- Putative oxidoreductase.	Some Bacillaceae	–
YhbA	48	–	–	–	–	- Putative oxidoreductase.	Most Bacillaceae and *Clostridium* species	Henriques and Moran, 2007; Lai *et al.*, 2003
YhbB	35	–	–	–	–	–	Some Bacillaceae	–
YheC	41	σ^E	–	–	–	- Similar to YheD.	Some Bacillaceae	–

Table A1: list of known spore coat proteins in *B. subtilis* (cont.)

	MW (kDa)	Transcriptional regulation	Class	Null mutant relevant phenotype	Assembly requirements	Relevant features	Conservation	Refs.
YisJ	35	–	–	–	–	–	Only *B. subtilis*	–
YirY/ SbcC	128	–	–	–	–	- DNA exonuclease.	All endospore formers	Henriques and Moran, 2007; Lai *et al.*, 2003
YjdH	15	σ^E	–	–	–	–	Only *B. subtilis*	Henriques and Moran, 2007; Lai *et al.*, 2003; Steil *et al.*, 2005
YkuD/ Ldt	17	σ^K	–	–	–	- L,D-transpeptidase involved in cell wall synthesis; - Contains a LysM domain, thus probably localizes in the inner layers.	Most Bacillaceae and *Clostridium* species	Henriques and Moran, 2007; Kodama *et al.*, 2000
YkvP	46	σ^K, GerE	–	–	–	- Contains a LysM domain, thus probably localizes in the inner layers.	Some Bacillaceae and *Clostridium* species	Henriques and Moran, 2007; Kodama *et al.*, 2000
YobN	50	–	–	–	–	- Putative amine oxidase.	Some Bacillaceae and *Clostridium* species	Kim *et al.*, 2006a
YodI	9	σ^K	–	–	–	–	Some Bacillaceae	Henriques and Moran, 2007; Kim *et al.*, 2006a; Lai *et al.*, 2003; Steil *et al.*, 2005
YopQ	53	–	–	–	–	- Prophage derivative.	Only *B .subtilis*	Henriques and Moran, 2007; Lai *et al.*, 2003
YpeP	26	–	–	–	–	–	Most Bacillaceae	Henriques and Moran, 2007; Lai *et al.*, 2003
YpzA	9	σ^G	–	–	–	–	Most Bacillaceae	Henriques and Moran, 2007; Steil *et al.*, 2005

Table A1: list of known spore coat proteins in *B. subtilis* (cont.)

	MW (kDa)	Transcriptional regulation	Class	Null mutant relevant phenotype	Assembly requirements	Relevant features	Conservation	Refs.
YusA	30	–	–	–	CotE, CotH	- Component of a methionine ABC transporter.	Most Bacillaceae and some *Clostridium* species	Henriques and Moran, 2007; Kim *et al.*, 2006a
YwqH	15	–	–	–	–	–	Some Bacillaceae	Henriques and Moran, 2007; Lai *et al.*, 2003
SodA	22	σ^B	–	- Altered coat.	–	- Superoxide dismutase; - Oxidative stress resistance.	All endospore formers	Henriques *et al.*, 1998; Henriques and Moran, 2007
TasA/ CotN/ YqfT	30	σ^H, Spo0A	–	- Altered coat; - Asymmetrical spores.	–	- Morphogenetic protein; - Biofilm formation; - Contains a signal peptide for secretion.	Some Bacillaceae	Henriques and Moran, 2007; Serrano *et al.*, 1999; Stover and Driks, 1999

BL: basal layer; IC: inner coat; OC: outer coat; (-): negative regulation

Table A2: List of vectors used in Chapter 2

Number	Primers or source	Cloning vector
pKW50	Wang *et al.*, 2009	
amy-spoVID$_{L125A}$-cfp	MHC001 and MHC002	pKW50
amy-spoVID$_{I127A}$-cfp	MHC003 and MHC004	"
amy-spoVID$_{D130A}$-cfp	MHC007 and MHC008	"
amy-spoVID$_{L131A}$-cfp	MHC009 and MHC010	"
amy-spoVID$_{I133A}$-cfp	MHC011 and MHC012	"
pET21b-*spoVID-his*	MAD37 and MAD38	pET21b
pET21b-*cotE-STOP*	MAD39 and MAD96	"
pET21b-*spoVID$_{\Delta 125-136}$-his*	KW206 and KW207	pET21b-*spoVID-his*
pET21b-*spoVID$_{L125A}$-his*	MHC001 and MHC002	"
pET21b-*spoVID$_{I127A}$-his*	MHC003 and MHC004	"
pET21b-*spoVID$_{D130A}$-his*	MHC007 and MHC008	"
pET21b-*spoVID$_{L131A}$-his*	MHC009 and MHC010	"
pET21b-*spoVID$_{I133A}$-his*	MHC011 and MHC012	"
p*cotE$_{1-158}$-AD*	CotE F1 and CotE R1	pDEST-AD
p*spoVID$_{1-144}$-BD*	SpoVID F1 and SpoVID R1	pDEST-BD
p*spoVID$_{1-144\ (L131A)}$-BD*	SpoVID F1 and SpoVID R1	"
p*spoVID$_{1-144\ (I133A)}$-BD*	SpoVID F1 and SpoVID R1	"
pTC37	spoVID189D and spoVID1952R	pET16b
pFN30	VIDC16ADir and VIDC16ARev	pTC37
pFN31	VIDC90ADir and VIDC90ARev	"
pFN32	VIDC90ADir and VIDC90ARev	pFN30
pFN97	VIDStopDir and VIDStopRev	pTC37
pFN98	VIDC16ADir and VIDC16ARev	pFN97
pFN99	VIDC90ADir and VIDC90ARev	"
pFN100	VIDC90ADir and VIDC90ARev	pFN98

Table A3: List of oligonucleotides used in Chapter 2

Primer	Nucleotide sequence (5' – 3')
MHC001	CAATTGACGGATTCGCGCATTGCTACAATTCAAGCTGATTTAGCG
MHC002	CGCTAAATCAGCTTGAATTGTAGCAATGCGCGAATCCGTCAATTG
MHC003	CGGATTCGCGCATTTTAACAGCTCAAGCTGATTTAGCGATCG
MHC004	CGATCGCTAAATCAGCTTGAGCTGTTAAAATGCGCGAATCCG
MHC007	CGCATTTTAACAATTCAAGCTGCTTTAGCGATCGAAGGGCTTTTG
MHC008	CAAAAGCCCTTCGATCGCTAAAGCAGCTTGAATTGTTAAAATGCG
MHC009	GCATTTTAACAATTCAAGCTGATGCTGCGATCGAAGGGCTTTTGG
MHC010	CCAAAAGCCCTTCGATCGCAGCATCAGCTTGAATTGTTAAAATGC
MHC011	CAATTCAAGCTGATTTAGCGGCTGAAGGGCTTTTGGACGATACG
MHC012	CGTATCGTCCAAAAGCCCTTCAGCCGCTAAATCAGCTTGAATTC
MAD37	GCGCCATATGCCGCAAAATCATGCATTGCAATTTTC
MAD38	GCGCCTCGAGCGCATGGCTATTTTTATATTGAGGAATATAGAGAATCTGTCCTGC
MAD39	GCGCCATATGTCTGAATACAGGGAAATTATTACGAAGGC
MAD96	GCGCCTCGAGTTATTATTCTTCAGGATCTCCCACTAAAAACTCCG
KW206	TTGACGGATTCGCGCATTTTGGACGATACGCAAGACAAAG
KW207	CTTTGTCTTGCGTATCGTCCAAAATGCGCGAATCCGTCAA
CotEF1	GGGGACAACTTTGTACAAAAAAGTTGGCTCTGAATACAGGGAAATTATTACGAAG
CotER1	GGGGACAACTTTGTACAAGAAAGTTAATCTTCCTCGTCATCCTCTTC
SpoVIDF1	GGGGACAACTTTGTACAAAAAAGTTGGCCCGCAAAATCATCGATTG
SpoVIDR1	GGGGACAACTTTGTACAAGAAAGTTACTCTTTGTCTTGCGTATCGTCC
spoVID189D	GAGGATATGCATATGCCGCAAAATCATCGATTG
spoVID1952R	CCACATTTTCGGATCCCTTACGGTTTACGC
VIDStopDir	GGCATTCAGGGAGGAAGAGTAATAAGAGCCGCCGGCAC
VIDStopRev	GTGCCGGCGGCTCTTATTACTCTTCCTCCCTGATAGCC
VIDC16ADir	CTGTAGAAAGAATCGATCGCTTTCCAAAAAGGACAGG
VIDC16ARev	CCTGTCCTTTTTGGAAAGCGATCGATTCTTCTACAG
VIDC90ADir	GCGGAACTGACTCACGCTTTTCCTGTGGATATTACC
VIDC90ARev	GGTAATATCCACAGGAAAAGCGTGAGTCAGTTCCGC

Table A4: List of vectors used in Chapter 3

Number	Relevant features	Source
pTC55	pGEX-4T3 derivative for GST overexpression	Costa *et al.*, 2006
pOZ169	pGEX-4T3 derivative for GST-SpoVID overexpression	"
pFN86	pGEX-4T2 derivative for GST-SpoVID$_{\Delta E}$ overexpression	This study
pFN88	pGEX-4T2 derivative for GST-SpoVID$_{L125A}$ overexpression	"
pFN89	pGEX-4T2 derivative for GST-SpoVID$_{T126A}$ overexpression	"
pFN90	pGEX-4T2 derivative for GST-SpoVID$_{I127A}$ overexpression	"
pFN91	pGEX-4T2 derivative for GST-SpoVID$_{Q128A}$ overexpression	"
pFN92	pGEX-4T2 derivative for GST-SpoVID$_{D130A}$ overexpression	"
pFN85	pGEX-4T2 derivative for GST-SpoVID$_{L131A}$ overexpression	"
pFN93	pGEX-4T2 derivative for GST-SpoVID$_{I133A}$ overexpression	"
pFN94	pGEX-4T2 derivative for GST-SpoVID$_{E134A}$ overexpression	"
pFN95	pGEX-4T2 derivative for GST-SpoVID$_{G135A}$ overexpression	"
pFN96	pGEX-4T2 derivative for GST-SpoVID$_{L136A}$ overexpression	"
pFN76	pACYCDuet-1 derivative for SafA overexpression	"
pET21b-*cotE-STOP*	pET21b derivative for CotE overexpression	de Francesco *et al.*, 2012
pFN115	pMAD derivative to perform an *in frame* deletion in *safA*	This study
pCF149	pMLK83 derivative for insertion of *safA-yfp* at *amyE* locus	"
pFN87	pMAD derivative to perform an *in frame* deletion of *spoVID*	"
pFN116	pMAD derivative for deletion of region E in *spoVID*	"
pFN117	pMAD derivative for substitution L125A in *spoVID*	"
pFN118	pMAD derivative for substitution T126A in *spoVID*	"
pFN119	pMAD derivative for substitution I127A in *spoVID*	"
pFN120	pMAD derivative for substitution Q128A in *spoVID*	"
pFN121	pMAD derivative for substitution D130A in *spoVID*	"
pFN122	pMAD derivative for substitution L131A in *spoVID*	"
pFN123	pMAD derivative for substitution I133A in *spoVID*	"
pFN124	pMAD derivative for substitution E134A in *spoVID*	"
pFN125	pMAD derivative for substitution G135A in *spoVID*	"
pFN126	pMAD derivative for substitution L136A in *spoVID*	"
pFN101	pMLK83 derivative for insertion of *spoVID* at *amyE* locus	"
pFN102	pMLK83 derivative for insertion of *spoVID$_{\Delta E}$* at *amyE* locus	"
pFN103	pMLK83 derivative for insertion of *spoVID$_{L125A}$* at *amyE* locus	"
pFN107	pMLK83 derivative for insertion of *spoVID$_{T126A}$* at *amyE* locus	"
pFN104	pMLK83 derivative for insertion of *spoVID$_{I127A}$* at *amyE* locus	"
pFN105	pMLK83 derivative for insertion of *spoVID$_{L131A}$* at *amyE* locus	"
pFN110	pMLK83 derivative for insertion of *spoVID$_{I133A}$* at *amyE* locus	"
pFN111	pMLK83 derivative for insertion of *spoVID$_{E134A}$* at *amyE* locus	"

Table A5: List of oligonucleotides used in Chapter 3

Primer	Nucleotide sequence (5' – 3')	Cloning vector
VIDBamHID	CCGCGTGGATCCTTGCCGCAAAATCATCG	pFN86-96
VIDFLXhoIR	CGGCCGCTCGAGTTACGCATGGCTATTTTTATATTGAGG	"
VIDDel125-136Dir	GACTATCAATTGACGGATTCGCGCATTTTGGACGATACGC AAGACAAAGAGCCG	pFN86, pFN102
VIDDel125-136Rev	CCGGCTCTTTGTCTTGCGTATCGTCCAAAATGCGCGAATC CGTCAATTGATAGT	"
VID-L125ADir	CAATTGACGGATTCGCGCATTGCAACAATTCAAGCTGATT TAGC	pFN88, pFN103
VID-L125ARev	CGCTAAATCAGCTTGAATTGTTGCAATGCGCGAATCCGTC AATTG	"
VID-T126ADir	GACGGATTCGCGCATTTTAGCAATTCAAGCTGATTTAGCG	pFN89, pFN107
VID-T126ARev	CGCTAAATCAGCTTGAATTGCTAAAATGCGCGAATCCGTC	"
VID-I127ADir	CGGATTCGCGCATTTTAACAGCTCAAGCTGATTTAGCGAT CG	pFN90, pFN104
VID-I127ARev	CGATCGCTAAATCAGCTTGAGCTGTTAAAATGCGCGAATC CG	"
VID-Q128ADir	CGCGCATTTTAACAATTGCAGCTGATTTAGCGATCG	pFN91
VID-Q128ARev	CGATCGCTAAATCGACTGCAATTGTTAAAATGCGCG	"
VID-D130ADir	GCATTTTAACAATTCAAGCTGCTTTAGCGATCGAAGGGC	pFN92
VID-D130ARev	GCCCTTCGATCGCTAAAGCAGCTTGAATTGTTAAAATGC	"
VID-L131ADir	CGCGCATTTTAACAATTCAAGCTGATGCTGCGATCGAAGG GCTTTTGGACGATACGC	pFN85, pFN105
VID-L131ARev	GCGTATCGTCCAAAAGCCCTTCGATCGCAGCATCAGCTTG AATTGTTAAAATGCGCG	"
VID-I133ADir	CAAGCTGATTTAGCGGCCGAAGGGCTTTTGGACG	pFN93, pFN110
VID-I133ARev	CGTCCAAAAGCCCTTCGGCCGCTAAATCAGCTTG	"
VID-E134ADir	CAAGCTGATTTAGCGATCGCAGGGCTTTTGGACGATACG	pFN94, pFN111
VID-E134ARev	CGTATCGTCCAAAAGCCCTGCGATCGCTAAATCAGCTTG	"
VID-G135ADir	GCTGATTTAGCGATCGAAGCGCTTTTGGACGATACGC	pFN95
VID-G135ARev	GCGTATCGTCCAAAAGCGCTTCGATCGCTAAATCAGC	"
VID-L136ADir	GATTTAGCGATCGAAGGGGCTTTGGACGATACGCAAGAC	pFN96
VID-L136ARev	GTCTTGCGTATCGTCCAAAGCCCCTTCGATCGCTAAATC	"
SafA201Dir	GGGGAAAACCATGGCGAAAATCCATATCG	pFN76
SafA1364R	CGTTCGGATCCATCACTCATTTTCTTC	"
safA-364D	GCAAGTCGACAATCGGGACAGAAATGAATCTTG	pFN115
safA+135R	CCCGGGTCATACTGAGGCGATACTATTTTCATTCCAGGCA TGATTAAGTC	"
safA+748D	CATGCCTGGAATGAAAATAGTATCGCCTCAGTATGACCCG GGTTATG	"
safA+1250R	GGGAATTCTAAGCGTGTCAGTTCTCTCCATTTG	"

Table A5: List of oligonucleotides used in Chapter 3 (cont.)

Primer	Nucleotide sequence (5' – 3')	Cloning vector
safA-fl3D	CCGTCCGGAAGAAGAAAATGAGCTGGGCGGAGGCGGATCAGGCGGAGG	pCF149
fl3-yfpD	CTGCGGCAAGTAAAGGAGAAGAACTTTTCACTG	"
fl3-yfpR	GTTCTTCTCCTTTACTTGCCGCAGCTGATCCGCCTCCGCCAG	"
yfp-TsafAR	GATTTACATCGTTCCGAACGATCATTTGTATAGTTCATCCATGCCATGTG	"
VID-UP385Dir	CCGCATACCTTTAACCGTGCAGG	pFN87
VID-294Rev	CCAAGGCTAAAGAATTCATCCTGACCTGAACCCTAATATCAGGAT	"
VID-1846Dir	TCAGGATGAATTCTTTAGCCTTGG	"
VID-2290Rev	CGGTTCTCTCGTGAAGACGGGC	"
spoVID-17D	GAAAACAGATCTCAGGCAGCTGAGAAAG	pFN116-126
spoVID24D	CAATCTAGACAGCTGAGAAAG	pFN101-107, pFN110-111
spoVID-1952R	CCACATTTTCGGATCCCTTACGGTTTACGC	pFN101-107, pFN110-111, pFN116-126

Table A6: List of vectors used in Chapter 4

Number	Relevant features	Source
pFP2	pBEST501 derivative for insertion of *safA* at *safA* locus	This study
pFP3	pBEST501 derivative for insertion of $safA_{D10A}$ at *safA* locus	"
pFP4	pBEST501 derivative for insertion of $safA_{S11A}$ at *safA* locus	"
pFP5	pBEST501 derivative for insertion of $safA_{L12A}$ at *safA* locus	"
pFP6	pBEST501 derivative for insertion of $safA_{N30A}$ at *safA* locus	"
pFP7	pBEST501 derivative for insertion of $safA_{I39A}$ at *safA* locus	"
pCF72	pUC18 derivative to perform an *in frame* deletion in *safA*	"
pDG364	Integrative vector to insert *cat at amyE* locus	Cutting and Vander Horn, 1990
pCF75	pMLK83 derivative for insertion of *safA* at *amyE* locus	Fernandes, C.
pCF181	pMLK83 derivative for insertion of $safA_{D10A}$ at *amyE* locus	This study
pCF182	pMLK83 derivative for insertion of $safA_{S11A}$ at *amyE* locus	"
pCF183	pMLK83 derivative for insertion of $safA_{L12A}$ at *amyE* locus	"
pCF184	pMLK83 derivative for insertion of $safA_{I39A}$ at *amyE* locus	"
pCF185	pMLK83 derivative for insertion of $safA_{N30A}$ at *amyE* locus	"
pCF149	pMLK83 derivative for insertion of *safA-yfp* at *amyE* locus	Chapter 3
pCF186	pMLK83 derivative for insertion of $safA_{D10A}$-*yfp* at *amyE* locus	This study
pCF187	pMLK83 derivative for insertion of $safA_{S11A}$-*yfp* at *amyE* locus	"
pCF188	pMLK83 derivative for insertion of $safA_{L12A}$-*yfp* at *amyE* locus	"
pCF189	pMLK83 derivative for insertion of $safA_{I39A}$-*yfp* at *amyE* locus	"
pCF190	pMLK83 derivative for insertion of $safA_{N30A}$-*yfp* at *amyE* locus	"
pFP8	pLitmus28 derivative to switch Sp^r to Cm^r in *B. subtilis*	"
pTC178	pASK-IBA3 derivative for $LysM^{SafA}$-StrepTagII overproduction	"
pTC182	pASK-IBA3 derivative for $LysM^{SafA}$-GFP-StrepTagII overproduction	"
pAI1	pASK-IBA3 derivative for $LysM^{SafA}$ S11A-GFP-StrepTagII overproduction	"
pAI2	pASK-IBA3 derivative for $LysM^{SafA}$ L12A-GFP-StrepTagII overproduction	"
pAI3	pASK-IBA3 derivative for $LysM^{SafA}$ I39A-GFP-StrepTagII overproduction	"
pAI4	pASK-IBA3 derivative for $LysM^{SafA}$ D10A-GFP-StrepTagII overproduction	"
pAI5	pASK-IBA3 derivative for $LysM^{SafA}$ N30A-GFP-StrepTagII overproduction	"
pAI12	pASK-IBA3 derivative for GFP-StrepTagII overproduction	"
pFN45	pASK-IBA3 derivative for $LysM^{SpoVID}$-StrepTagII overproduction	"

Table A7: List of oligonucleotides used in Chapter 4

Primer	Nucleotide sequence (5' – 3')	Cloning vector
safA 677D	GGCTATGTTAACTATGGAAAATGCAAATTATCCG	pTC207
safA-gfpR	CTCCAGTGAAAAGTTCTTCTCCTTTACTCTCATTTTCTTCTTCCGGACGGCC	"
gfp30D	AGTAAAGGAGAAGAACTTTTCACTGGAG	"
gfpmut2-749R	GATCCTCGAGGAATTCTTATTTGTATAGTTCATCC	"
safAD10A-d	GAAAATCCATATCGTTCAAAAAGGCGCTTCGCTCTGGAAAATAGCTG	pFP3,pCF181, pAI4
safAD10A-r	CAGCTATTTTCCAGAGCGAAGCGCCTTTTTGAACGATATGGATTTTC	"
safAS11A-d	GAAAATCCATATCGTTCAAAAAGGCGATGCGCTCTGGAAAATAGCTGAAAAGTAC	pFP4, pCF182, pAI1
safAS11A-r	GTACTTTTCAGCTATTTTCCAGAGCGCATCGCCTTTTTGAACGATATGGATTTTC	"
safAL12A-d	CCATATCGTTCAAAAAGGCGATTCGGCCTGGAAAATAGCTGAAAAGTACGG	pFP5, pCF183, pAI2
safAL12A-r	CCGTACTTTTCAGCTATTTTCCAGGCCGAATCGCCTTTTTGAACGATATGG	"
safAN30A-d	GATGTTGAGGAAGTGAAAAAACTCGCTACACAGCTTAGCAATCCAGAC	pFP6, pCF185, pAI5
safAN30A-r	GTCTGGATTGCTAAGCTGTGTAGCGAGTTTTTTCACTTCCTCAACATC	"
safAI39A-d	GTCTGGATTGCTAAGCTGTGTAGCGAGTTTTTTCACTTCCTCAACATC	pFP7, pCF184, pAI3
safAI39A-r	CAGCTTAGCAATCCAGACTTAGCCATGCCTGGAATGAAAATAAAAGTGCCG	"
safA-364D	GCAAGTCGACAATCGGGACAGAAATGAATCTTG	pCF72
safA+135R	CCCGGGTCATACTGAGGCGATACTATTTTCATTCCAGGCATGATTAAGTC	"
safA+748D	CATGCCTGGAATGAAAATAGTATCGCCTCAGTATGACCCGGGTTATG	"
safA+1250R	GGGAATTCTAAGCGTGTCAGTTCTCTCCATTTG	"
safA-IBA3d	CAAAAATCTAGATAACGAGGGCAAAAAATGAAAATCCATATCGTTCAAAAAGGCG	pTC178
safA-IBA3r	CTGAGACCATGGACGTCTCCTTCTGACGGCACTTTTATTTTCATTCC	"
gfpmut2+4D	CCGACGTCAGTAAAGGAGAAGAAC	pTC182
gfpmut2+714R	CCGACGTCTTTGTATAGTTCATCC	"
gfpinpASKDir	CAAAAATCTAGATAACGAGGGCAAAAAATGAGTAAAGGAGAAGAACTTTTCACTGGAG	pAI12
gfpinpASKRev	TGCCAGCGCTTTTGTATAGTTCATCCATGCCATGTG	"
VID-LysM1761Dir	GCTCTAGATAACGAGGGCAAAAAATGAAAATTTGTATTGTGCAGCAGG	pFN45
VID-LysM1928Rev	GCCCATGGACGTCCGCATGGCTATTTTTATATTGAGG	"

Figure S1A

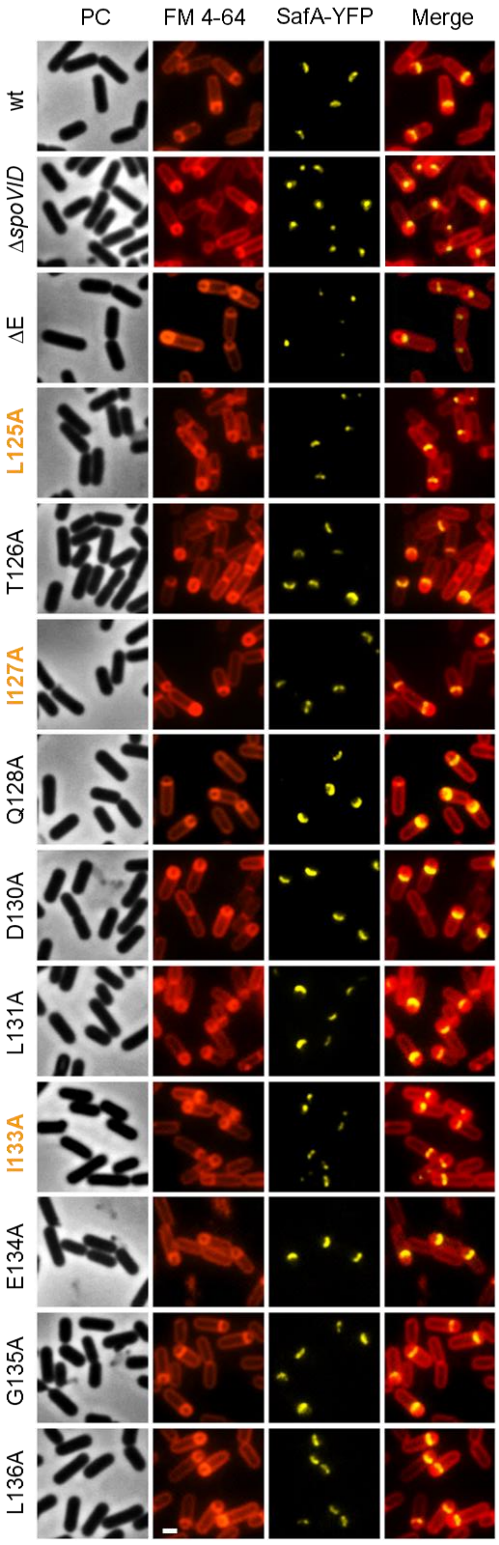
PC
FM 4-64
SafA-YFP
Merge
wt
ΔspoVID
ΔE
L125A
T126A
I127A
Q128A
D130A
L131A
I133A
E134A
G135A
L136A

Figure S1B

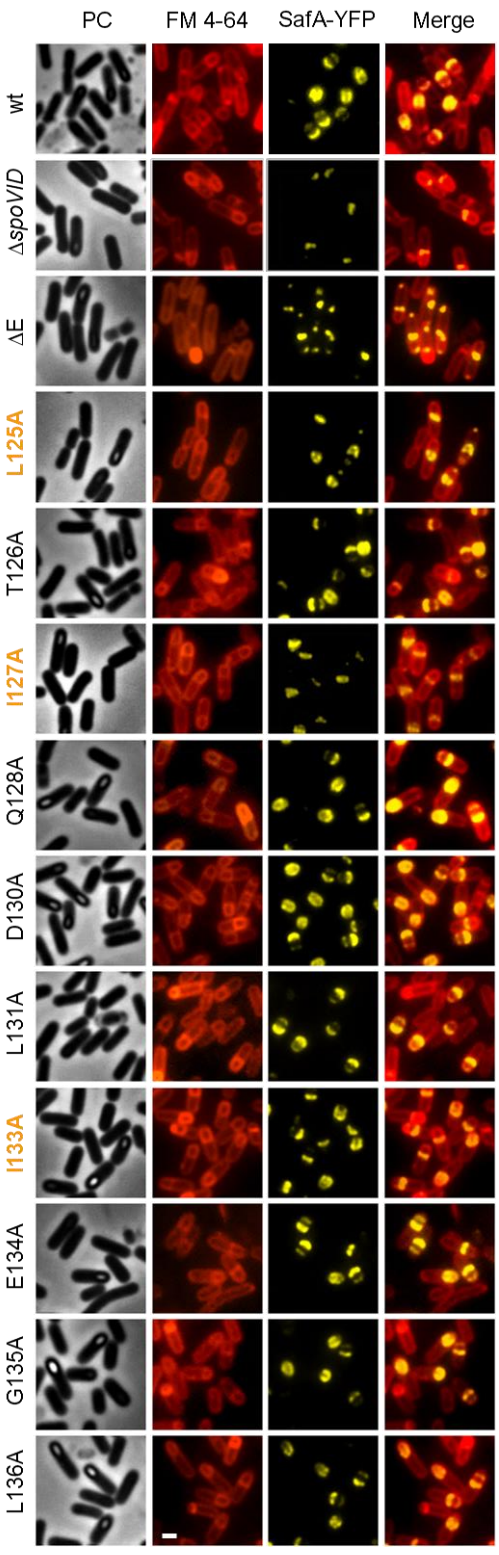
PC
FM 4-64
SafA-YFP
Merge
wt
ΔspoVID
ΔE
L125A
T126A
I127A
Q128A
D130A
L131A
I133A
E134A
G135A
L136A

Figure S1C

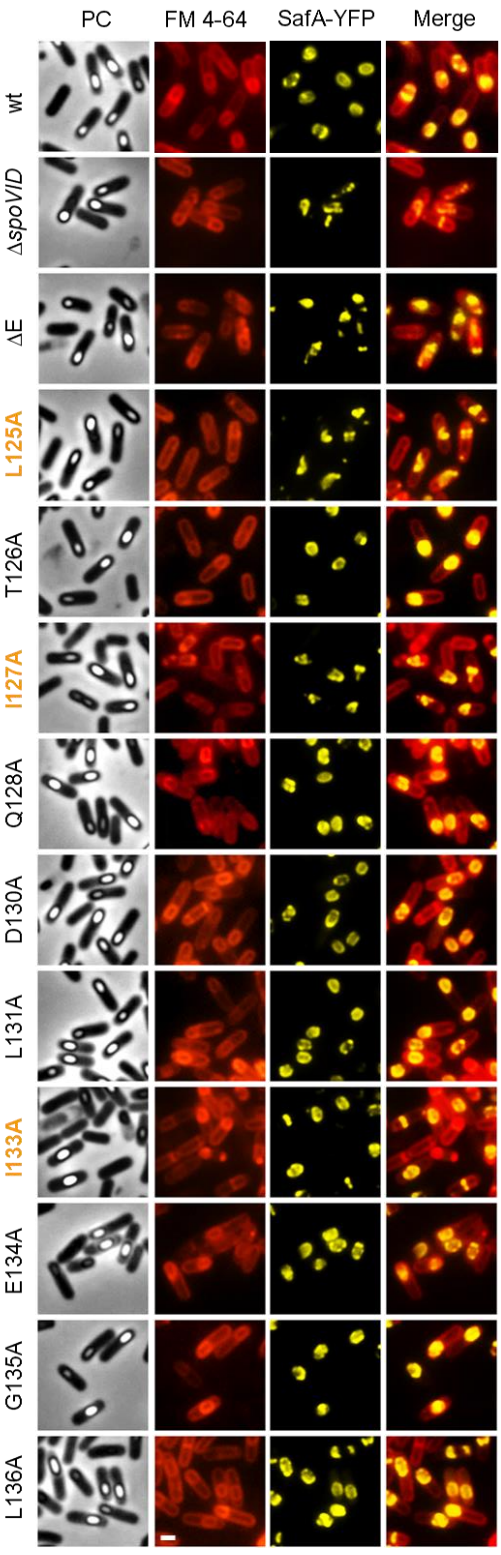
PC
FM 4-64
SafA-YFP
Merge
wt
ΔspoVID
ΔE
L125A
T126A
I127A
Q128A
D130A
L131A
I133A
E134A
G135A
L136A

Figure S2A

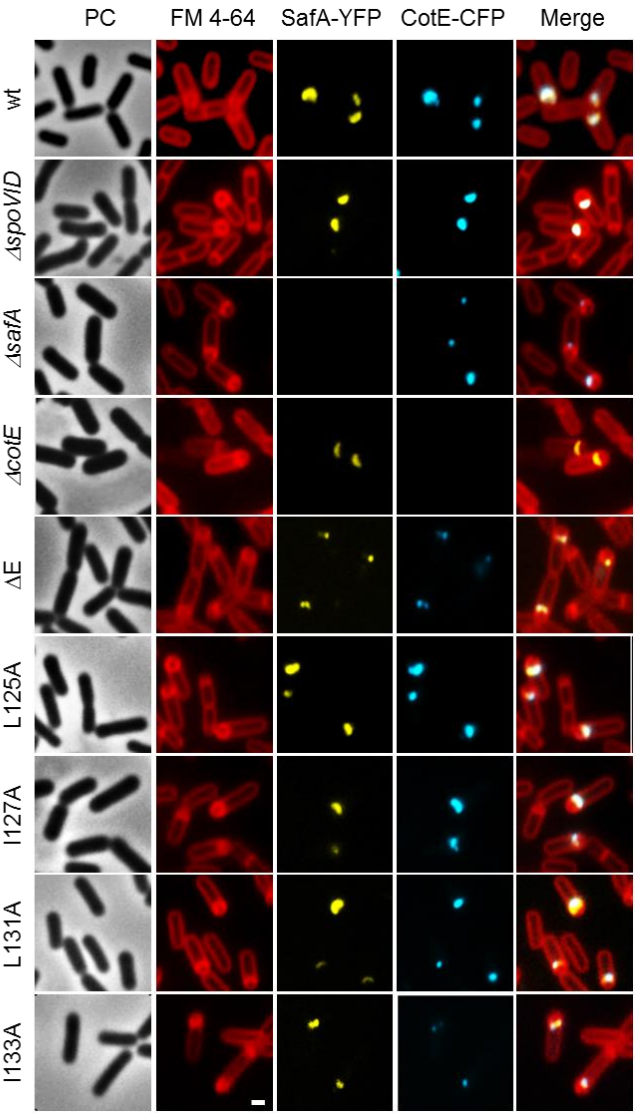
PC
FM 4-64
SafA-YFP
CotE-CFP
Merge
wt
ΔspoVID
ΔsafA
ΔcotE
ΔE
L125A
I127A
L131A
I133A

Figure S2B

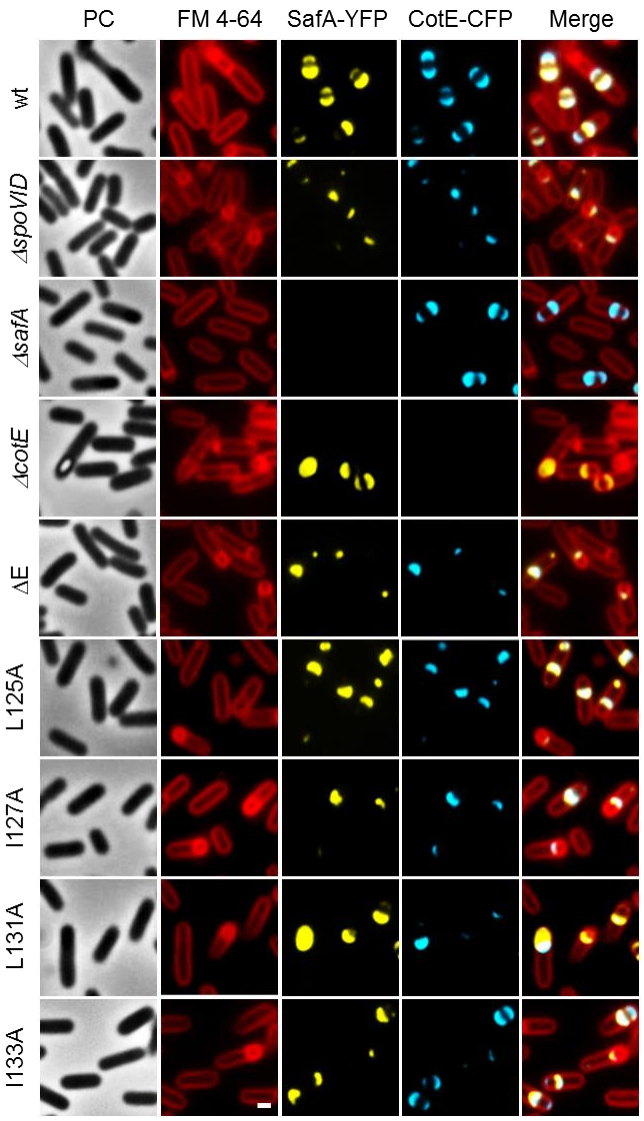
PC
FM 4-64
SafA-YFP
CotE-CFP
Merge
wt
ΔspoVID
ΔsafA
ΔcotE
ΔE
L125A
I127A
L131A
I133A

Figure S2C

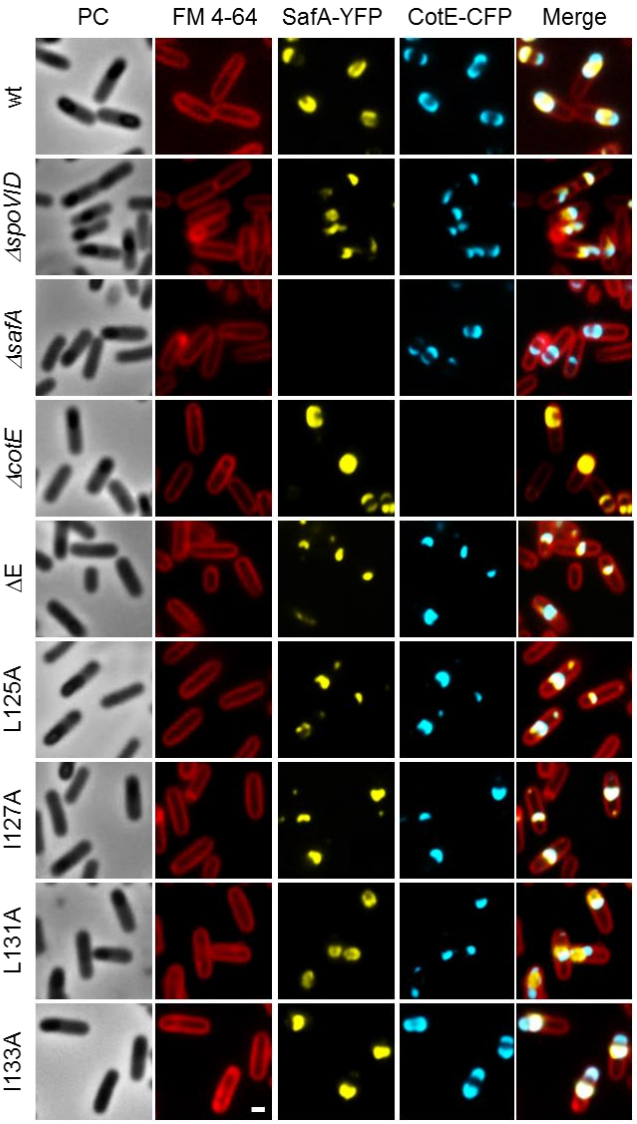
PC
FM 4-64
SafA-YFP
CotE-CFP
Merge
wt
ΔspoVID
ΔsafA
ΔcotE
ΔE
L125A
I127A
L131A
I133A

Figure S2D

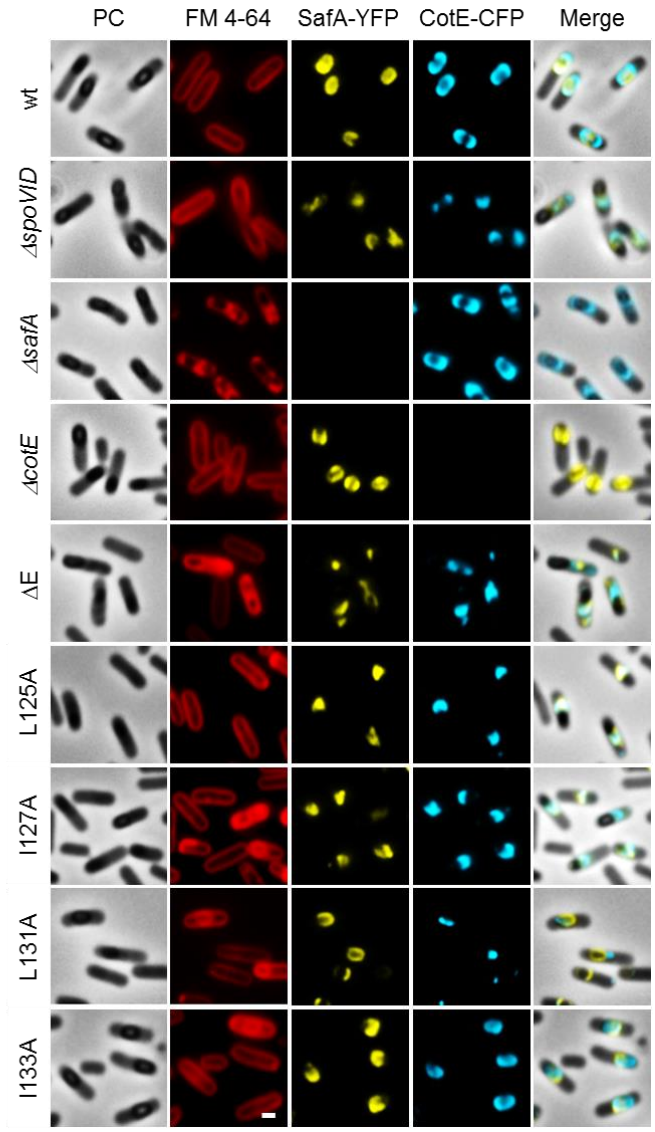
PC
FM 4-64
SafA-YFP
CotE-CFP
Merge
wt
ΔspoVID
ΔsafA
ΔcotE
ΔE
L125A
I127A
L131A
I133A

Figure S3A

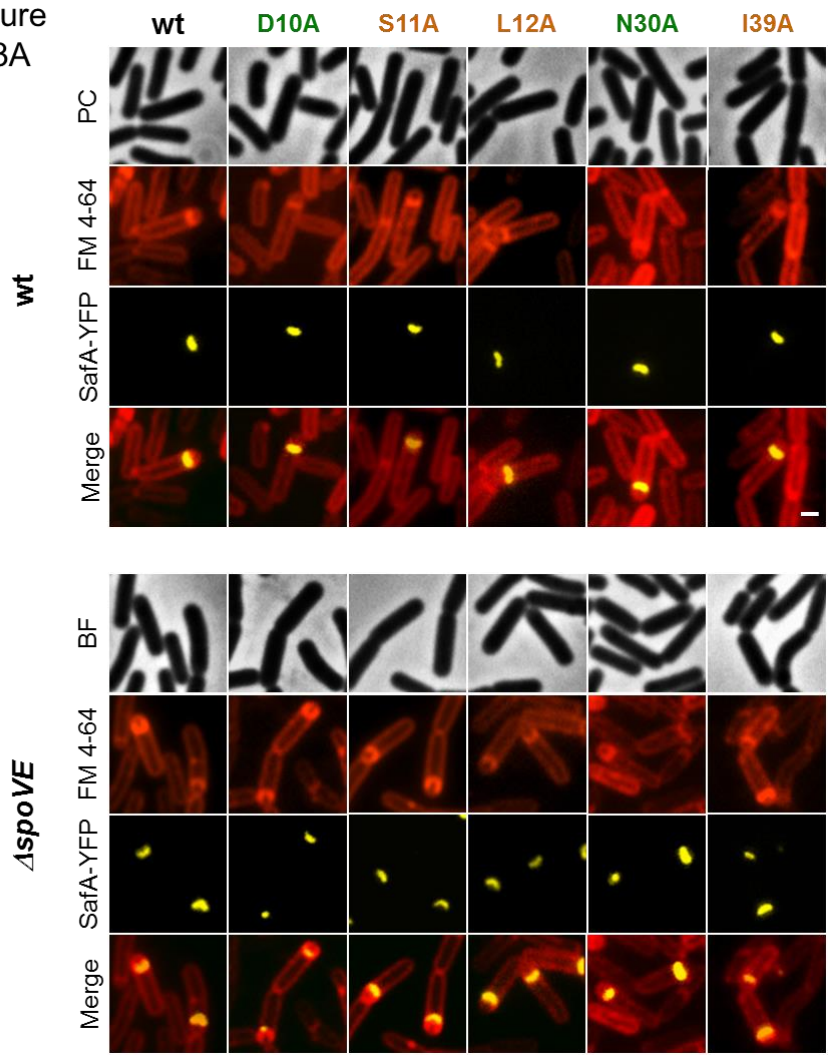
wt
D10A
S11A
L12A
N30A
I39A
wt
PC
FM 4-64
SafA-YFP
Merge
ΔspoVE
BF
FM 4-64
SafA-YFP
Merge

Figure S3B

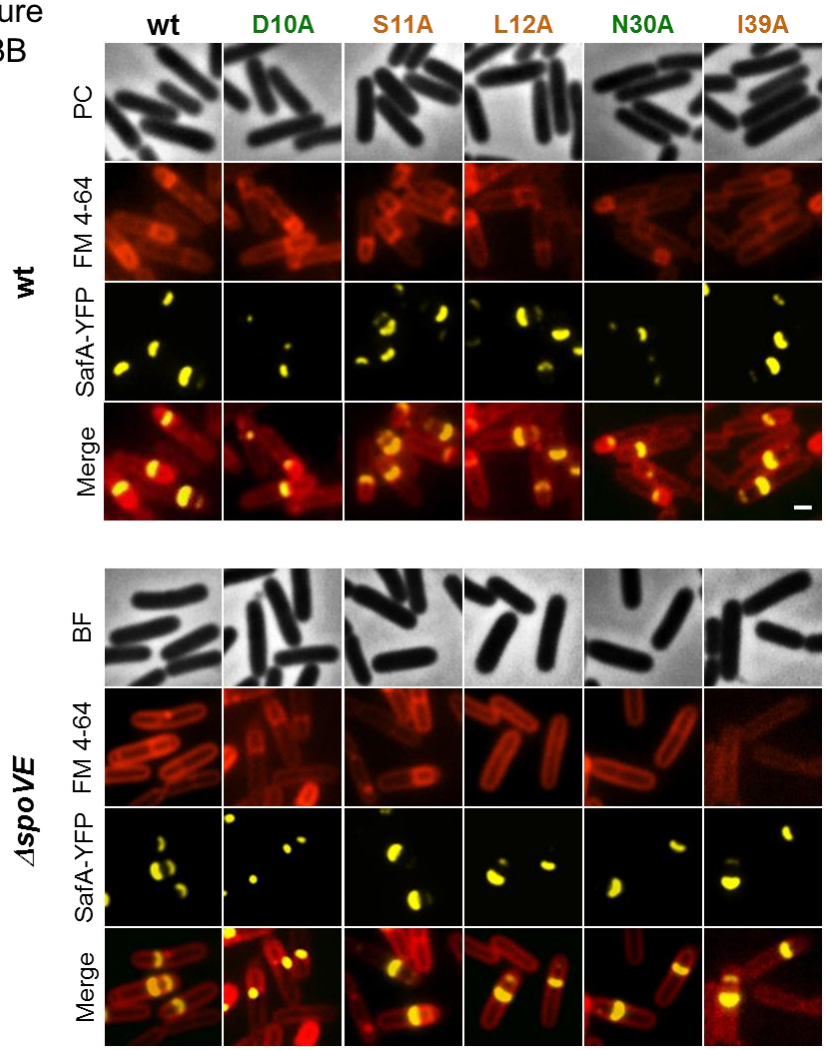
wt
D10A
S11A
L12A
N30A
I39A
wt
PC
FM 4-64
SafA-YFP
Merge
ΔspoVE
BF
FM 4-64
SafA-YFP
Merge

Figure S3C

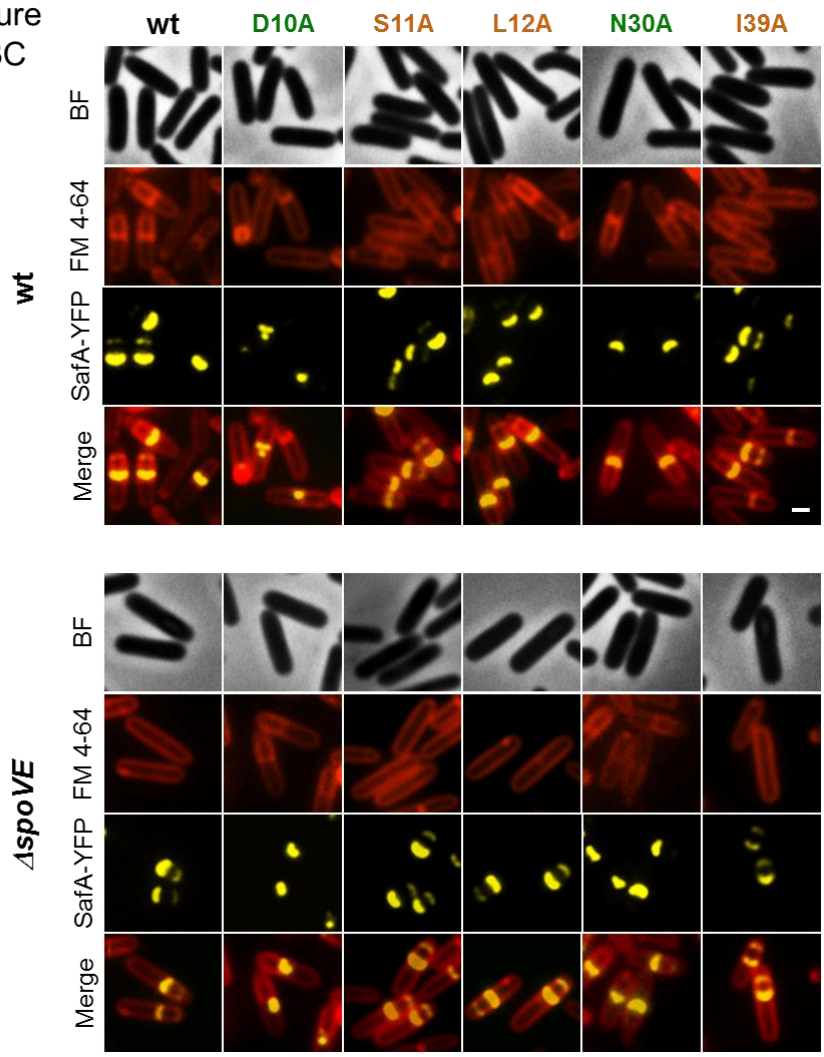

Figure S3D

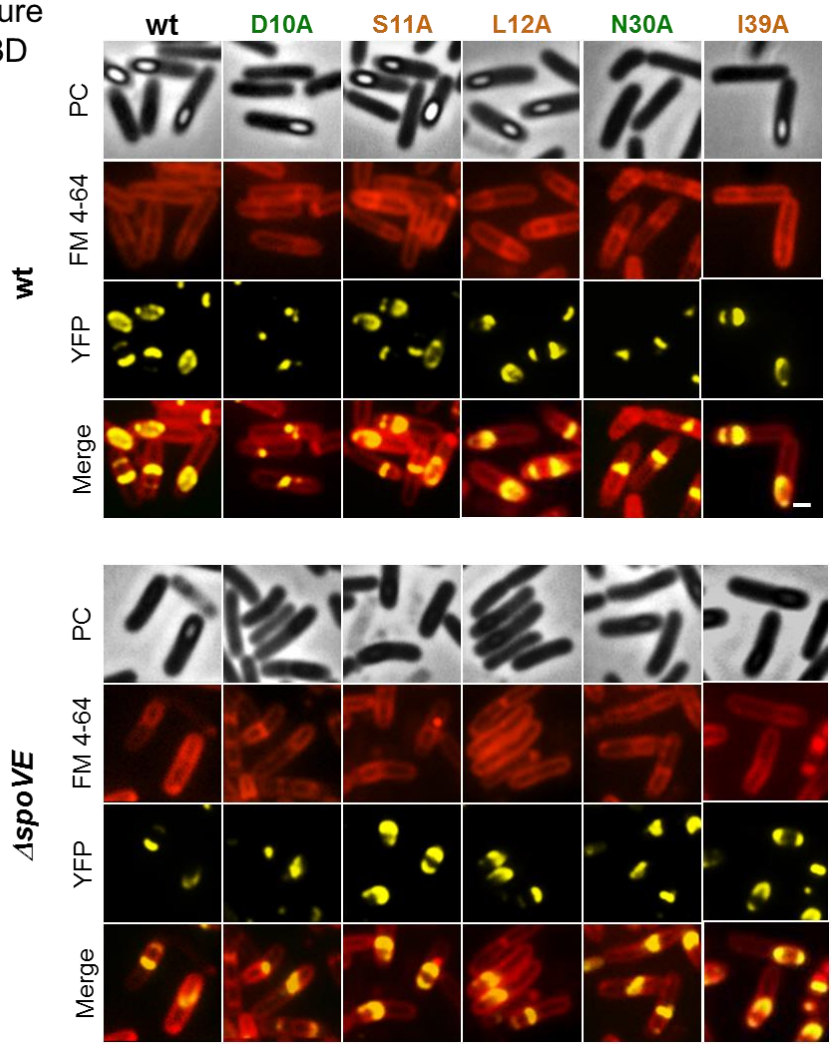

Figure S1: Subcellular localization of SafA-YFP in cells missing SpoVID or expressing SpoVID variants with alanine substitutions in region E residues. Strains were grown in sporulation media and samples were taken at 2, 4 and 6 hours after ressuspension (**A**, **B** and **C**, respectively). Cells were stained with FM 4-64 and analysed by fluorescence microscopy for the localization of SafA-YFP. A few representative cells are shown for each strain. 1st lane: phase-contrast; 2nd lane: stained membranes signal; 3rd lane: SafA-YFP signal; 4th lane: merge of the stained membranes and the YFP signals. Scale bar: 1 µm. The percentages of cells exhibiting each localization pattern of SafA-YFP are listed in Table 3.2, in Chapter 3.

Figure S2: Subcellular localization of SafA-YFP and CotE-YFP in mutant strains. Cells were grown in sporulation media and saples were taken at 2, 4, 6 and 8 hours after ressuspension (**A**, **B**, **C** and **D,** respectively). After staining membranes with FM 4-64, cells were analysed by fluorescence microscopy for the localization of SafA-YFP and CotE-CFP. A few representative cells are shown for each strain. 1st lane: phase-contrast; 2nd lane: stained membranes signal; 3rd lane: SafA-YFP signal; 4th lane: CotE-GFP signal; 5th lane: merge of the phase-contrast or the membranes signal with the YFP and CFP signals. Scale bar: 1 µm. The percentages of cells exhibiting each localization pattern of SafA-YFP and CotE-CFP are listed in Tables 3.6 and 3.7, in Chapter 3.

Figure S3: Subcellular localization of SafA-YFP variants with alanine substitutions in residues of the LysM motif, in wild type (top panel) and *spoVE* null mutant (bottom panel) backgrounds. Sporulating cells were stained with FM 4-64 and imaged by fluorescence microscopy at 2, 4, 6 and 8 hours after ressuspension (**A**, **B, C** and **D**, respectively). A few representative cells are shown for each strain. 1st row: phase-contrast; 2nd row: stained membranes signal; 3rd row: SafA-YFP signal; 4th row: merge of the membranes and the YFP signals. Scale bar: 1 µm. The percentages of all localization patterns of SafA-YFP are shown in Table 4.2, in Chapter 4.

REFERENCES

Asai, K., Takamatsu, H., Iwano, M., Kodama, T., Watabe, K., Ogasawara, N., 2001. The Bacillus subtilis yabQ gene is essential for formation of the spore cortex. Microbiology 147, 919-927.

Beall, B., Driks, A., Losick, R., Moran, C.P., Jr., 1993. Cloning and characterization of a gene required for assembly of the Bacillus subtilis spore coat. Journal of Bacteriology 175, 1705-1716.

Bourne, N., FitzJames, P.C., Aronson, A.I., 1991. Structural and germination defects of Bacillus subtilis spores with altered contents of a spore coat protein. Journal of Bacteriology 173, 6618-6625.

Buist, G., Steen, A., Kok, J., Kuipers, O.P., 2008. LysM, a widely distributed protein motif for binding to (peptido)glycans. Molecular Microbiology 68, 838-847.

Cangiano, G., Sirec, T., Panarella, C., Isticato, R., Baccigalupi, L., De Felice, M., Ricca, E., 2014. The sps gene products affect germination, hydrophobicity and protein adsorption of Bacillus subtilis spores. Applied and Environmental Microbiology 80, 7293-7302.

Costa, T., Isidro, A.L., Moran, C.P., Jr., Henriques, A.O., 2006. Interaction between coat morphogenetic proteins SafA and SpoVID. Journal of Bacteriology 188, 7731-7741.

Costa, T., Serrano, M., Steil, L., Volker, U., Moran, C.P., Jr., Henriques, A.O., 2007. The timing of cotE expression affects Bacillus subtilis spore coat morphology but not lysozyme resistance. Journal of Bacteriology 189, 2401-2410.

Costa, T., Steil, L., Martins, L.O., Volker, U., Henriques, A.O., 2004. Assembly of an oxalate decarboxylase produced under sigmaK control into the Bacillus subtilis spore coat. Journal of Bacteriology 186, 1462-1474.

Cutting, S.M., Vander Horn, P.B., 1990. Genetic Analysis. In: Harwood, C.R., Cutting, S.M. (Eds.), Molecular Biological Methods for Bacillus. John Wiley & Sons, Chichester, pp. 27-74.

Ebmeier, S.E., Tan, I.S., Clapham, K.R., Ramamurthi, K.S., 2012. Small proteins link coat and cortex assembly during sporulation in Bacillus subtilis. Molecular Microbiology 84, 682-696.

Eichenberger, P., Fujita, M., Jensen, S.T., Conlon, E.M., Rudner, D.Z., Wang, S.T.,

Ferguson, C., Haga, K., Sato, T., Liu, J.S., Losick, R., 2004. The program of gene transcription for a single differentiating cell type during sporulation in Bacillus subtilis. PLOS Biology 2, e328.

Ferguson, C.C., Camp, A.H., Losick, R., 2007. gerT, a newly discovered germination gene under the control of the sporulation transcription factor sigmaK in Bacillus subtilis. Journal of Bacteriology 189, 7681-7689.

Henriques, A.O., Beall, B.W., Moran, C.P., Jr., 1997. CotM of Bacillus subtilis, a member of the alpha-crystallin family of stress proteins, is induced during development and participates in spore outer coat formation. Journal of Bacteriology 179, 1887-1897.

Henriques, A.O., Beall, B.W., Roland, K., Moran, C.P., Jr., 1995. Characterization of cotJ, a sigma E-controlled operon affecting the polypeptide composition of the coat of Bacillus subtilis spores. Journal of Bacteriology 177, 3394-3406.

Henriques, A.O., Melsen, L.R., Moran, C.P., Jr., 1998. Involvement of superoxide dismutase in spore coat assembly in Bacillus subtilis. Journal of Bacteriology 180, 2285-2291.

Henriques, A.O., Moran, C.P., Jr., 2007. Structure, assembly, and function of the spore surface layers. Annual Review of Microbiology 61, 555-588.

Hullo, M.F., Moszer, I., Danchin, A., Martin-Verstraete, I., 2001. CotA of Bacillus subtilis is a copper-dependent laccase. Journal of Bacteriology 183, 5426-5430.

Ichikawa, H., Kroos, L., 2000. Combined action of two transcription factors regulates genes encoding spore coat proteins of Bacillus subtilis. The Journal of Biological Chemistry 275, 13849-13855.

Imamura, D., Kuwana, R., Takamatsu, H., Watabe, K., 2010. Localization of proteins to different layers and regions of Bacillus subtilis spore coats. Journal of Bacteriology 192, 518-524.

Imamura, D., Kuwana, R., Takamatsu, H., Watabe, K., 2011. Proteins involved in formation of the outermost layer of Bacillus subtilis spores. Journal of Bacteriology 193, 4075-4080.

Isticato, R., Pelosi, A., Zilhao, R., Baccigalupi, L., Henriques, A.O., De Felice, M., Ricca, E., 2008. CotC-CotU heterodimerization during assembly of the Bacillus subtilis spore coat. Journal of Bacteriology 190, 1267-1275.

Kato, S., Yoshimura, T., Hemmi, H., Moriyama, R., 2010. Biochemical analysis of a novel lipolytic enzyme YvdO from Bacillus subtilis 168. Bioscience,

Biotechnology, and Biochemistry 74, 701-706.

Kim, H., Hahn, M., Grabowski, P., McPherson, D.C., Otte, M.M., Wang, R., Ferguson, C.C., Eichenberger, P., Driks, A., 2006. The Bacillus subtilis spore coat protein interaction network. Molecular Microbiology 59, 487-502.

Kodama, T., Takamatsu, H., Asai, K., Ogasawara, N., Sadaie, Y., Watabe, K., 2000. Synthesis and characterization of the spore proteins of Bacillus subtilis YdhD, YkuD, and YkvP, which carry a motif conserved among cell wall binding proteins. Journal of Biochemistry 128, 655-663.

Kuwana, R., Takamatsu, H., Watabe, K., 2007. Expression, localization and modification of YxeE spore coat protein in Bacillus subtilis. Journal of Biochemistry 142, 681-689.

Lai, E.M., Phadke, N.D., Kachman, M.T., Giorno, R., Vazquez, S., Vazquez, J.A., Maddock, J.R., Driks, A., 2003. Proteomic analysis of the spore coats of Bacillus subtilis and Bacillus anthracis. Journal of Bacteriology 185, 1443-1454.

Levin, P.A., Fan, N., Ricca, E., Driks, A., Losick, R., Cutting, S.M., 1993. An unusually small gene required for sporulation by Bacillus subtilis. Molecular Microbiology 9, 761-771.

Little, S., Driks, A., 2001. Functional analysis of the Bacillus subtilis morphogenetic spore coat protein CotE. Molecular Microbiology 42, 1107-1120.

Masayama, A., Kuwana, R., Takamatsu, H., Hemmi, H., Yoshimura, T., Watabe, K., Moriyama, R., 2007. A novel lipolytic enzyme, YcsK (LipC), located in the spore coat of Bacillus subtilis, is involved in spore germination. Journal of Bacteriology 189, 2369-2375.

McKenney, P.T., Driks, A., Eichenberger, P., 2013. The Bacillus subtilis endospore: assembly and functions of the multilayered coat. Nature Reviews Microbiology 11, 33-44.

McKenney, P.T., Driks, A., Eskandarian, H.A., Grabowski, P., Guberman, J., Wang, K.H., Gitai, Z., Eichenberger, P., 2010. A distance-weighted interaction map reveals a previously uncharacterized layer of the Bacillus subtilis spore coat. Current Biology 20, 934-938.

McKenney, P.T., Eichenberger, P., 2012. Dynamics of spore coat morphogenesis in Bacillus subtilis. Molecular Microbiology 83, 245-260.

McPherson, D.C., Kim, H., Hahn, M., Wang, R., Grabowski, P., Eichenberger, P.,

Driks, A., 2005. Characterization of the Bacillus subtilis spore morphogenetic coat protein CotO. Journal of Bacteriology 187, 8278-8290.

Pierce, K.J., Salifu, S.P., Tangney, M., 2008. Gene cloning and characterization of a second alanine racemase from Bacillus subtilis encoded by yncD. FEMS Microbiology Letters 283, 69-74.

Qiao, H., Krajcikova, D., Xing, C., Lu, B., Hao, J., Ke, X., Wang, H., Barak, I., Tang, J., 2013. Study of the interactions between the key spore coat morphogenetic proteins CotE and SpoVID. Journal of Structural Biology 181, 128-135.

Ragkousi, K., Eichenberger, P., van Ooij, C., Setlow, P., 2003. Identification of a new gene essential for germination of Bacillus subtilis spores with Ca2+-dipicolinate. Journal of Bacteriology 185, 2315-2329.

Ramamurthi, K.S., Lecuyer, S., Stone, H.A., Losick, R., 2009. Geometric cue for protein localization in a bacterium. Science 323, 1354-1357.

Roels, S., Driks, A., Losick, R., 1992. Characterization of spoIVA, a sporulation gene involved in coat morphogenesis in Bacillus subtilis. Journal of Bacteriology 174, 575-585.

Roels, S., Losick, R., 1995. Adjacent and divergently oriented operons under the control of the sporulation regulatory protein GerE in Bacillus subtilis. Journal of Bacteriology 177, 6263-6275.

Scheeff, E.D., Axelrod, H.L., Miller, M.D., Chiu, H.J., Deacon, A.M., Wilson, I.A., Manning, G., 2010. Genomics, evolution, and crystal structure of a new family of bacterial spore kinases. Proteins 78, 1470-1482.

Serrano, M., Zilhao, R., Ricca, E., Ozin, A.J., Moran, C.P., Jr., Henriques, A.O., 1999. A Bacillus subtilis secreted protein with a role in endospore coat assembly and function. Journal of Bacteriology 181, 3632-3643.

Seyler, R.W., Jr., Henriques, A.O., Ozin, A.J., Moran, C.P., Jr., 1997. Assembly and interactions of cotJ-encoded proteins, constituents of the inner layers of the Bacillus subtilis spore coat. Molecular Microbiology 25, 955-966.

Steil, L., Serrano, M., Henriques, A.O., Volker, U., 2005. Genome-wide analysis of temporally regulated and compartment-specific gene expression in sporulating cells of Bacillus subtilis. Microbiology 151, 399-420.

Stover, A.G., Driks, A., 1999. Secretion, localization, and antibacterial activity of TasA, a Bacillus subtilis spore-associated protein. Journal of Bacteriology 181, 1664-1672.

Takamatsu, H., Chikahiro, Y., Kodama, T., Koide, H., Kozuka, S., Tochikubo, K., Watabe, K., 1998. A spore coat protein, CotS, of Bacillus subtilis is synthesized under the regulation of sigmaK and GerE during development and is located in the inner coat layer of spores. Journal of Bacteriology 180, 2968-2974.

Takamatsu, H., Imamura, A., Kodama, T., Asai, K., Ogasawara, N., Watabe, K., 2000a. The yabG gene of Bacillus subtilis encodes a sporulation specific protease which is involved in the processing of several spore coat proteins. FEMS Microbiology Letters 192, 33-38.

Takamatsu, H., Imamura, D., Kuwana, R., Watabe, K., 2009. Expression of yeeK during Bacillus subtilis sporulation and localization of YeeK to the inner spore coat using fluorescence microscopy. Journal of Bacteriology 191, 1220-1229.

Takamatsu, H., Kodama, T., Imamura, A., Asai, K., Kobayashi, K., Nakayama, T., Ogasawara, N., Watabe, K., 2000b. The Bacillus subtilis yabG gene is transcribed by SigK RNA polymerase during sporulation, and yabG mutant spores have altered coat protein composition. Journal of Bacteriology 182, 1883-1888.

Takamatsu, H., Kodama, T., Nakayama, T., Watabe, K., 1999. Characterization of the yrbA gene of Bacillus subtilis, involved in resistance and germination of spores. Journal of Bacteriology 181, 4986-4994.

Wang, K.H., Isidro, A.L., Domingues, L., Eskandarian, H.A., McKenney, P.T., Drew, K., Grabowski, P., Chua, M.H., Barry, S.N., Guan, M., Bonneau, R., Henriques, A.O., Eichenberger, P., 2009. The coat morphogenetic protein SpoVID is necessary for spore encasement in Bacillus subtilis. Molecular Microbiology 74, 634-649.

Zhang, J., Ichikawa, H., Halberg, R., Kroos, L., Aronson, A.I., 1994. Regulation of the transcription of a cluster of Bacillus subtilis spore coat genes. Journal of Molecular Biology 240, 405-415.

Zheng, L.B., Donovan, W.P., Fitz-James, P.C., Losick, R., 1988. Gene encoding a morphogenic protein required in the assembly of the outer coat of the Bacillus subtilis endospore. Genes & Development 2, 1047-1054.

Zilhao, R., Isticato, R., Martins, L.O., Steil, L., Volker, U., Ricca, E., Moran, C.P., Jr., Henriques, A.O., 2005. Assembly and function of a spore coat-associated transglutaminase of Bacillus subtilis. Journal of Bacteriology 187, 7753-7764.

Zilhao, R., Naclerio, G., Henriques, A.O., Baccigalupi, L., Moran, C.P., Jr., Ricca,

E., 1999. Assembly requirements and role of CotH during spore coat formation in Bacillus subtilis. Journal of Bacteriology 181, 2631-2633.

Zilhao, R., Serrano, M., Isticato, R., Ricca, E., Moran, C.P., Jr., Henriques, A.O., 2004. Interactions among CotB, CotG, and CotH during assembly of the Bacillus subtilis spore coat. Journal of Bacteriology 186, 1110-1119.

ITQB-UNL | Av. da República, 2780-157 Oeiras, Portugal
Tel (+351) 214 469 100 | Fax (+351) 214 411 277

www.itqb.unl.pt